Tectono-magmatic evolution of the younger Gardar southern rift, South Greenland

Brian G.J. Upton

Geological Survey of Denmark and Greenland Bulletin 29

Cover illustration
View east-north-east from the Tugtutôq central complex to the Ilímaussaq and Narssaq complexes. The Igdlerfigssalik complex is visible in the far right distance. The lake (Store Pilesø) stretching away from the viewer overlies a sector of the Older giant dyke.

Frontispiece: facing page
View towards the Igdlerfigssalik complex with fresh autumn snow from Kongevejen near Igaliku, displaying its characteristic, dull grey appearance and magmatic layering. Photo:A.A. Garde.

Citation of the name of this series
It is recommended that the name of this series is cited in full, viz. *Geological Survey of Denmark and Greenland Bulletin*.
If abbreviation of this volume is necessary, the following form is suggested: *Geol. Surv. Den. Green. Bull.* 29, 124 pp.

Contents

Abstract

Upton, B.G.J. 2013: Tectono-magmatic evolution of the younger Gardar southern rift, South Greenland.
Geological Survey of Denmark and Greenland Bulletin 29, 124 pp.

The 1300–1140 Ma Gardar period in South Greenland involved continental rifting, sedimentation and alkaline magmatism. The latest magmatism was located along two parallel rift zones, Isortoq–Nunarsuit in the north and the Tuttutooq–Ilimmaasaq–Narsarsuaq zone in the south addressed here. The intrusive rocks crystallised at a depth of <4 km and are essentially undisturbed by later events. Magmatism in the southern zone began with the emplacement of two giant, ≤800 m wide dykes and involved intrusion of transitional olivine basaltic, high Al/Ca magmas crystallising to troctolitic gabbros. These relatively reduced magmas evolved through marked iron enrichment to alkaline salic differentiates. In the Older giant dyke complex, undersaturated augite syenites grade into sodalite foyaite. The larger, *c.* 1163 Ma Younger giant dyke complex (YGDC) mainly consists of structureless troctolite with localised developments of layered cumulates. A layered pluton (Klokken) is considered to be coeval and presumably comagmatic with the YGDC. At the unconformity between the Ketilidian basement and Gardar rift deposits, the YGDC expanded into a gabbroic lopolith. Its magma may represent a sample from a great, underplated mafic magma reservoir, parental to all the salic alkaline rocks in the southern rift. The bulk of these are silica undersaturated; oversaturated differentiates are probably products of combined fractional crystallisation and crustal assimilation.

A major dyke swarm 1–15 km broad was intruded during declining crustal extension, with decreasing dyke widths and increasing differentiation over time. Intersection of the dyke swarm and E–W-trending sinistral faults controlled the emplacement of at least three central complexes (Narssaq, South Qôroq and early Igdlerfigssalik). Three post-extensional complexes (Tugtutôq, Ilímaussaq and late Igdlerfigssalik) along the former rift mark the end of magmatism at *c.* 1140 Ma. The latter two complexes have oblate plans reflecting ductile, fault-related strain. The Tugtutôq complex comprises quartz syenites and alkali granites. The Ilímaussaq complex mainly consists of nepheline syenite crystallised from highly reduced, Fe-rich phonolitic peralkaline (agpaitic) magma, and resulted in rocks with very high incompatible element concentrations.

Abundant anorthositic xenoliths in the mafic and intermediate intrusions point to a large anorthosite protolith at depth which is considered of critical importance in the petrogenesis of the salic rocks. Small intrusions of aillikite and carbonatite may represent remobilised mantle metasomites. The petrological similarity between Older and Younger Gardar suites implies strong lithospheric control of their petrogenesis. The parental magmas are inferred to have been derived from restitic Ketilidian lithospheric mantle, metasomatised by melts from subducting Ketilidian oceanic crust and by small-scale melt fractions associated with Gardar rifting.

There are numerous analogies between the southern Gardar rift and the Palaeogene East African rift.

Author's address

University of Edinburgh, School of Geosciences, Grant Institute, The King's Buildings, West Mains Road, Edinburgh EH9 3JW, UK.
E-mail: *brian.upton@ed.ac.uk*

Fig. 1. Overview map showing important place names (given in 'new spelling') used in the text, and locations of detail maps with figure numbers.

Introduction

Uniqueness of the southern branch of the Gardar rift

The concept of 'the Gardar rift' is sometimes spoken of. No such single 'Gardar rift' exists, but continental rifting certainly affected part of what is now southern Greenland. The rifting affected a stretch of the crust that embraced the southern margins of the Archaean craton and the adjacent regions of younger rocks that lie to its south. In the Mesoproterozoic, which encompasses the Gardar period between about 1300 and 1100 million years ago, Greenland was a component part of the Columbia supercontinent (Rogers & Santosh 2002) that lasted from *c.* 1800 million years (Ma) until *c.*1100 Ma. The affected crust was clearly a zone of mechanical weakness, vulnerable to repeated fracturing in response to stresses induced by the slow but steady flowage of hot mantle rocks deep beneath it. Crustal fracturing and pull-apart caused the pressure on the underlying mantle rocks (peridotites) to be locally reduced, with the result that the mantle underwent partial melting. Thus rifting was inevitably accompanied by magmatism which, in turn, caused volcanic activity at the surface. These processes were fundamentally the same as those operating within the Paleogene East African Rift system.

This bulletin attempts to describe and interpret the faulting and associated magmatism that defined the more southerly of the two rift zones, generated in the later part of the Gardar history, between 1180 and 1140 Ma. What we can now study in the field are rocks that then lay at estimated depths of 3–4 km below their contemporary land surface but which were subsequently uplifted and eroded to their present positions. To the question "What makes these riftzones so interesting?" there are several answers. First of all, the late Gardar southern rift may be globally unique in that nowhere else has an ancient rift been so dissected by erosion to reveal its deep anatomy. This alone accords it inestimable scientific interest. Furthermore, it may be inferred that immense volumes of magma were generated, the greater part of which was retained deep in the crust to undergo slow cooling and chemical maturation. Most of the latter took place via the process of fractional crystallisation by which the component elements (virtually all of the 92 elements that occur in nature) underwent selective redistribution.

Some of the latest melt fractions within the Ilímaussaq complex crystallised to rocks of extreme compositions. The latter contain high concentrations of many of the planet's rarest elements, including uranium, thorium, tin, niobium, beryllium, zirconium and the so-called 'rare-earth elements'. Consequently Ilímaussaq has exercised a strong attraction for, not only petrologists, mineralogists and geochemists, but also mining prospectors and engineers.

The igneous intrusions of the younger Gardar southern rift were studied by the Geological Survey of Greenland during its regional 1:20 000 geological mapping programme, 1956–1962. The mapping was followed by a large number of publications and unpublished PhD theses. A hundred years have now passed since the publication of Ussing's very perceptive memoir on Ilímaussaq (Ussing 1912), and the current economic interest in South Greenland offers an appropriate opportunity to collate the information gathered on this remarkable younger Gardar southern rift. This has a generalised width of between 10 and 15 km and transects the Ketilidian granitic Julianehåb batholith which it post-dates by *c.* 700 Ma (Figs 1, 2).

Of the ultimate causes of the lithospheric extension that marked the early stages of rifting and the left-lateral faulting that essentially ended it, we remain ignorant. This memoir merely describes and interprets the attendant tectono-magmatic phenomena while leaving these fundamental questions unresolved. The growth of the whole great volcanic system, which undoubtedly spanned many millions of years, was followed by over 1100 Ma of nearly unbroken quiescence.

This extraordinary region has a character that should allow it to be granted World Heritage status as a 'Geopark'. Quite apart from all it offers, scientifically and potentially commercially, it is undoubtedly a region of great natural beauty, as yet virtually unspoiled.
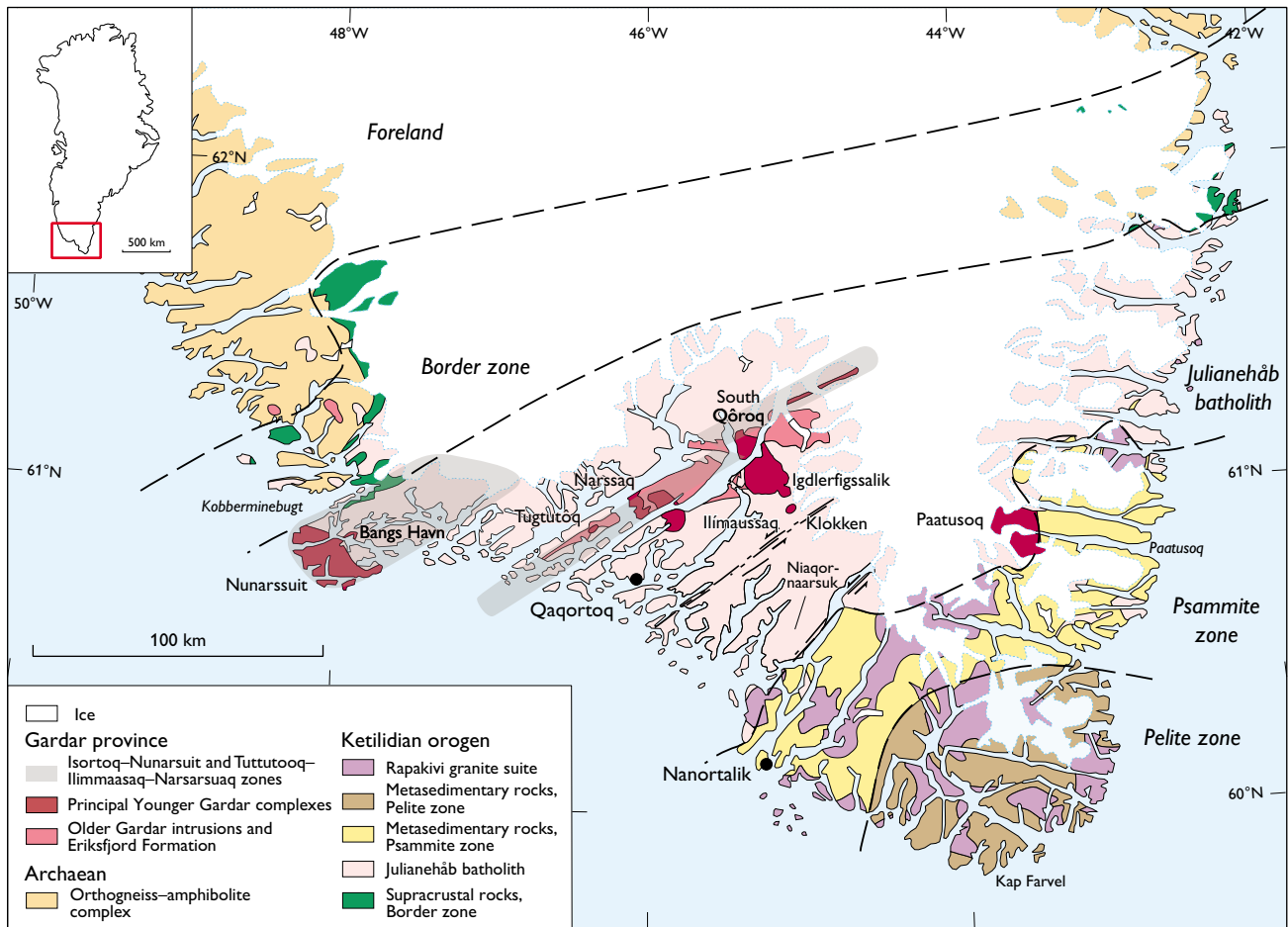
Fig. 2. General geological map of South Greenland with the Mesoproterozoic Gardar province within the Palaeoproterozoic Ketilidian orogen. Note the Isortoq–Nunarsuit and Tuttutooq–Ilimmaasaq–Narsarsuaq magmatic zones (rifts) comprising the labelled Younger Gardar complexes and the approximate extent of associated dyke swarms. The Gardar intrusions have mainly been emplaced into the Ketilidian Julianehåb batholith. The Ketilidian Border zone comprises clastic and chemical sedimentary rocks deposited on an Archaean basement, overlain in the west by a thrust sheet of metabasaltic and related rocks. Modified from Garde *et al.* (2002, fig. 1).

Nomenclature of place names

Throughout this bulletin place names are written with modern Greenlandic spelling. Most of the Gardar igneous complexes were named before the spelling reform in 1973, and because of the conventions for naming geological units the names of these geological features have not been changed. Thus, Ilimmaasaq denotes the mountain whereas Ilímaussaq is the intrusion. Accordingly, referring to the geographical features, the rift system described here will appear as the Tuttutooq–Ilimmaasaq–Narsarsuaq system.

General geological overview

Wegmann (1938) divided the geology of southern Greenland into 'an old basement' and younger formations. The former comprises Archaean gneisses whilst Wegmann subdivided the latter into the Ketilides and the Gardar Formation.

The Palaeoproterozoic Ketilidian rocks (*c.* 1800 Ma) are bounded to the north by the Archaean (>2800 Ma) craton. Emplacement of the 'Andean type' Julianehåb batholith marked the peak of Ketilidian orogenic activity (Garde *et al.* 2002). The batholith growth commenced at *c.* 1855 Ma and was finished at *c.* 1795 Ma, succeeded by fore-arc deposition, deformation, metamorphism and emplacement of the 1755–1723 Ma rapakivi suite (Garde *et al.* 2002). Over the next *c.* 500 Ma, the resultant Co-

Table 1. Radiometric age determinations from Gardar igneous rocks

Intrusion or locality	Rock unit	Material	Age (Ma)	± (Ma)	Reference
U-Pb zircon, baddeleyite and Pb-Pb pyrochlore age data					
Paatusoq	Syenite pluton	Zircon	1144.1	1.1	M. Hamilton (unp.)
Østfjordsdal	Syenite pegmatite	Zircon	1147.5	3.2	Salmon (2013)
Tugtutôq	Granite pluton	Zircon	1156	1.1	L. Heaman (unp.)
Ilímaussaq	Agpaite cumulate	Baddeleyite	1160	5	Waight *et al.* (2002)
Ilímaussaq	Agpaite cumulate	Baddeleyite	1160	2.3	Krumrei *et al.* (2007)
Tugtutôq	Younger giant dyke	Baddeleyite	1163	2	M. Hamilton (unp.)
Tugtutôq	Younger giant dyke	Baddeleyite	1165.7	1.2	L. Heaman (unp.)
Klokken	Syenite	Zircon	1166	3	Harper (1988)
Nunarssuit	Syenite pegmatite	Zircon	1171	5	Finch *et al.* (2001a)
Tugtutôq	Older giant dyke	Baddeleyite	1184	5	L. Heaman (unp.)
North Motzfeldt	Nepheline syenite	Zircon	1257.4	6.7	Salmon (2013)
Motzfeldt	Nepheline syenite	Zircon, pyrochlore	1273	6	McCreath *et al.* (2012)
Kûngnât	Gabbro ring dyke	Baddeleyite	1275.2	1.8	L. Heaman (unp.)
Motzfeldt	Syenite pegmatite	Zircon	1275.3	1.1	Salmon (2013)
Tugtutôq	BD dyke	Baddeleyite	1279	1.3	L. Heaman (unp.)
Kangerluarsuk	BD dyke	Baddeleyite	1280	3	L. Heaman (unp.)
Qaqortoq	BD dyke	Baddeleyite	1284	3	L. Heaman (unp.)
Rb-Sr whole-rock and mineral age data[†]					
Nunarssuit	Quartz syenites, granites[§]	Whole-rock	1130	14	Blaxland *et al.* (1978)
Ilímaussaq, late dyke, Kvanefjeld	Monchiquite	Phlogopite	1134	17	Larsen (2006)
Klokken	Gabbros, syenites	Whole-rock	1135	11	Blaxland *et al.* (1978)
Igdlerfigssalik 'late complex'	Gabbros, syenites, nepheline syenites	Whole-rock	1142	15	Blaxland *et al.* (1978)
Tugtutôq central complex	Quartz syenites, granites	Whole-rock	1143	36	Blaxland *et al.* (1978)
Ilímaussaq	Agpaites, syenites, granites	Whole-rock	1143	21	Blaxland *et al.* (1978)
Tugtutôq Older giant dyke	Gabbros, syenites, nepheline	Whole-rock	1150	9	Blaxland *et al.* (1978)
South Qôroq	Syenites, nepheline syenites	Whole-rock	1160	8	Blaxland *et al.* (1978)
Ilímaussaq	Agpaite	Alkali feldspar, eudialyte	1160	2.3	Waight *et al.* (2002)
Bangs Havn	Gabbros, syenites	Whole-rock	1185	22	Engell & Pedersen (1974)
Qassiarsuk	Trachytes, carbonatites	Whole-rock, min. sep.	1205	12	Andersen (1997)
Kûngnât	Gabbro, syenites	Whole-rock	1219	16	Blaxland *et al.* (1978)
Ivigtût	Alkali granite, cryolite body	Whole-rock	1222	24	Blaxland *et al.* (1978)
North Motzfeldt	Nepheline syenites	Whole-rock, min. sep.	1226	27	Finch *et al.* (2001)
Ivittuut region	Lamprophyres, dolerites	Biotite	1250	18	Patchett *et al.* (1978)
North Qôroq	Nepheline syenites, lujavrite	Biotite	1268	60	Blaxland *et al.* (1978)
Early Motzfeldt complex	Gabbro, nepheline syenite, lujavrite	Biotite	1282	30	Blaxland *et al.* (1978)
Grønnedal–Íka	Nepheline syenites, carbonatite	Biotite	1299	17	Blaxland *et al.* (1978)

Errors are quoted at the 2σ level.

[†] Rb-Sr data are presented as simple regressions, recalculated for the decay constant of Steiger & Jäger (1977)

[§] L. Heaman provided regressions for four units of the Nunarssuit complex. They all lie within error of the value for the Nunarssuit syenite quoted here.

unp.: unpublished data; min. sep.: mineral separates.

lumbia supercontinent experienced equilibration, uplift and erosion culminating in a long sequence of rifting events involving faulting and magmatism. The latter gave rise to the Gardar Igneous Province in which suites of (mostly) genetically related alkaline rocks were emplaced. The spatial relationship of the Mesoproterozoic Gardar alkaline rocks to the Palaeoproterozoic and Archaean formations are shown in Fig. 2 and radiometric age data are given in Table 1.

The earliest rocks that were ascribed to the Gardar period by Wegmann (1938) are the terrestrial sandstones and lavas composing the Eriksfjord Formation that un-conformably overlie the Julianehåb batholith. Isotopic dating of the lavas by Paslick *et al.* (1993), using the Sm-Nd mineral and whole-rock method, gave ages of *c.* 1170 ± 30 Ma and 1120 ± 30 Ma. The Qassiarsuk carbonatite–alkaline silicate volcanic complex, correlated with the Mussartût lavas close to the base of the Eriksfjord Formation, is dated at *c.* 1200 Ma (Rb-Sr and Pb-Pb; Andersen 1997). The formation is, however, clearly cut by the Motzfeldt pluton which has yielded ages of 1273 ± 6 Ma (U-Pb zircon; McCreath *et al.* 2012), 1282 ± 30 Ma (Blaxland *et al.* 1978) and 1226 ± 27 Ma (Finch *et al.* 2001b) (both Rb-Sr mineral & whole-rock analyses).

It is also cut by the North Qôroq pluton (Rb-Sr age 1268 ± 60 Ma; Blaxland *et al.* 1978) (Table 1). Accordingly whilst parts of the Eriksfjord Formation appear to be older than 1270 Ma, the principal outcrop farther to the west-south-west may be substantially younger (Paslick *et al.* 1993) although it predates the Younger Gardar dyke complex and the Narssaq and Ilímaussaq complexes.

Other Gardar intrusions that give relatively old ages include the Grønnedal–Íka complex (1299 ± 17 Ma, Rb/Sr dating; Blaxland *et al.* 1978) and three early alkali olivine dolerite dykes (the BD_0 dykes of the Geological Survey of Greenland) which yield U-Pb baddeleyite dates of 1284 ± 3 Ma, 1280 ± 3 Ma and 1279 ± 1.3 Ma (Table 1). Although neither Grønnedal–Íka nor the BD_0 dykes have contact relationships with the Eriksfjord Formation, the fact that each is believed to be related to alkaline magmatism in rifting environments lends support to the concept that the Eriksfjord Formation may be distinctly older than the dates indicated by the Sm-Nd method (Table 1; Fig. 3)

The Julianehåb batholith has a pronounced syn-magmatic foliation that was exploited in younger Gardar time by shearing and dyke intrusion, both along the northern margin of the batholith in the Nunarsuit–Isortoq region (bounded in the north by the Kobberminebugt and and in the south by Sermilik fjord), and more centrally in the batholith, embracing the Tuttutooq archipelago, the Ilimmaasaq–Qassiarsuk peninsula, the Narsarsuaq area and the nunataks north of Motzfeldt Sø. The latter region houses the southern rift with the Tuttutooq–Ilimmaasaq–Narsarsuaq magmatic system (Fig. 2). Most of the late Gardar intrusions lie within these two ENE-oriented zones and the two jointly compose a dissected, asymmetric rift zone, approximately 70 km wide. Whilst most of the intrusions in the southern rift (Tuttutooq–Ilimmaasaq–Narsarsuaq) are concentrated within a narrow zone (*c.* 15 km wide), its northern neighbour (Nunarsuit–Isortoq) is over twice as wide. Isotopic evidence suggests that Archaean crust underlies both rift zones (Halama *et al.* 2004; Krumrei *et al.* 2006). Although the northern rift possesses great intrinsic interest, description of it is beyond the scope of this bulletin.

There is very considerable geographic overlap between the igneous rocks of the Younger Gardar intrusions and those of the Older Gardar (Fig. 2). The latter date principally from 1280 to 1250 Ma (Table 1; Fig. 2) and are also not considered in any detail in this publication. That the Julianehåb batholith is bounded to north and south by Ketilidian metasedimentary and volcanic formations (Fig. 2) suggests the possibility that it marked the site

of a pre-Gardar dome. It is postulated that lithospheric weakness beneath the two Gardar rift zones permitted attenuation, fissuring and admission of mantle melts, producing parallel volcanic grabens from which several kilometres of cover have been removed by erosion (Upton & Blundell 1978; fig. 1a). The crustal extension across each of the two zones, indicated by their dyke swarms, was approximately 1.5 km. Hence the total dilation across *c.* 70 km was *c.* 3 km or *c.* 4.3%. A large positive Bouguer gravity anomaly, attributed to gabbroic rocks at shallow depths, characterises the southern rift system (Blundell 1978; Fig. 4), although no such gravity high is known from the Nunarsuit–Isortoq zone. Comparable gravity highs are associated with the East African Rift system and the Oslo Rift. The lack of an anomaly beneath the Nunarsuit–Isortoq zone is explicable if it was a more diffuse zone of attenuation, preventing large bodies of mafic magma from attaining shallow levels (Upton & Blundell 1978).

In Iceland, fissure eruption is commonly a prelude to increasing localisation of magma ascent and generation of a central-type volcano. It was recognised that these features represent consecutive parts of a single 'magmatic system', a concept elaborated by Walker (1993). By analogy with these Icelandic phenomena, the whole suite of intrusions along the younger Gardar southern rift (*c.* 1160–1140 Ma) is interpreted as a coherent, large-scale magmatic system. This unified system marked a tectono-magmatic event in which strain energy release, after rising to a maximum, was followed by an extended period of relaxation. This bulletin is based on the contention that the Ilímaussaq complex is among the youngest components of a great tectono-magmatic system that accompanied continental rifting. In its more mature stages, this system underwent gradual change from fissuring and dyke emplacement towards emplacement of stocks and ring-dykes as extensional stresses diminished.

Although the two Gardar rift zones share many features in common, there is a clear petrological difference in that the absence of phonolitic/foyaitic and subordinate ultramafic lamprophyre/carbonatite rocks in the northern rift zone contrasts with their importance in the Tuttutooq–Ilimmaasaq–Narsarsuaq zone to the south. Two specific foci of lithospheric weakness in the southern rift were provided by the intersection of the batholithic foliation and a set of transcurrent sinistral faults trending WNW–ESE to W–E. Apart from radiometric dating and intersections among the larger intrusions, two features invaluable for establishing the chronology within the system are the Main dyke swarm and the sinistral
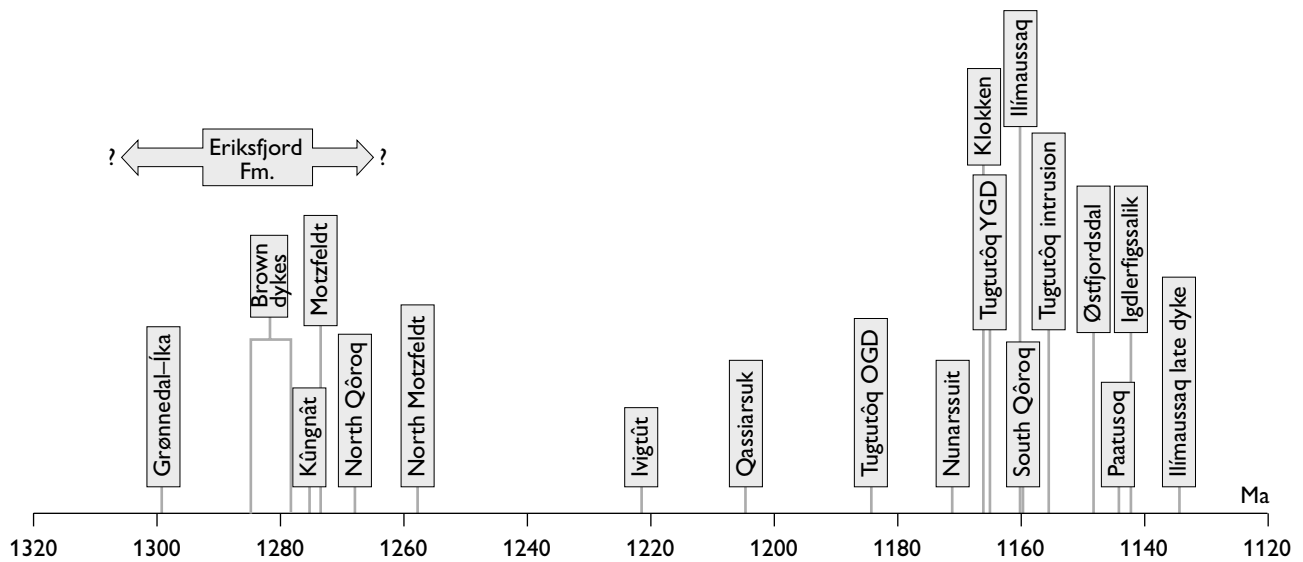
Fig. 3. Age distribution of Rb-Sr and U-Pb age determinations of Gardar intrusions from various sources (see Table 1). OGD: Older giant dykes. YGD: Younger giant dykes. Original drawing with courtesy of A. Bartels.

faults. Figuratively, the entire Tuttutooq–Ilimmaasaq–Narsarsuaq magmatic system may be compared to a symphonic work in several movements. An abrupt introduction that rose to a crescendo in the first movement gave way to a relatively quiescent ending with emplacement of the central Tugtutôq, Ilímaussaq and Igdlerfigssalik igneous complexes. Accordingly two principal stages are recognisable. The first was characterised by extension and dyke intrusion, brought to an end by transcurrent faulting, whereas the second stage saw the passive ascent of mainly salic magmas. During this post-faulting stage further extension was negligible.

The Gardar Province lay north of the Grenville Front and so avoided tectonic deformation in the Grenvillian Orogeny. Since the Mesoproterozoic, it has remained remarkably unscathed and the overall state of preservation of the Gardar plutons is excellent. Evidence for this stability is provided by e.g. miarolitic cavities in pegmatites of the (Older Gardar) Kûngnât complex that appear never to have been occupied or mineralised since their initial crystallisation, and by delicate acicular aegirine crystals in pegmatite geodes in the Ilímaussaq complex, highly susceptible to seismic damage, that remain unbroken. Some feldspars in the Klokken complex remain sufficiently unaltered to allow the oldest age dating by the Ar-Ar method concordant with U/Pb dating (Parsons *et al.* 1988). Crustal uplift in the Mesozoic/Cenozoic was followed by extensive erosion by the Pleistocene ice sheets. Retreat of these over the past few thousand

years has revealed the Gardar igneous rocks as superlative 'time-capsules'. Among the approximately one dozen central-type plutons, the Ilímaussaq complex is by far the best known because it hosts an extraordinary large-scale concentration of rare minerals and their component rare elements. The rare mineral assemblages are contained in highly peralkaline (agpaitic) rocks that were the youngest products of the complex. The most enriched part of the complex (Kvanefjeld) is now believed to contain the world's second largest deposit of rare-earth elements and its sixth largest uranium deposit (Parsons 2012). Research into Ilímaussaq has currently resulted in over two-hundred and thirty scientific publications.

In this bulletin an attempt is made to describe the various features of the tectono-magmatic system (intrusions and fault movements) in chronological order. This encounters some problems, e.g. faults can be re-activated on numerous occasions, some igneous units are undated or imprecisely dated, and the anorthosite body that from xenolith evidence inferentially underlies the entire province cannot be meaningfully discussed before description of the igneous rocks that host the xenoliths. Nonetheless this is the broad outline followed here.

History of exploration

The following notes are culled from Sørensen (1967) "On the history of exploration of the Ilímaussaq Intrusion, South Greenland" and supplementary notes in Sørensen (2001). The earliest significant investigations of the mineralogy of southern Greenland were those of K.L. Giesecke in the course of an expedition from 1806 to 1813. During this time he made two visits (1806 and 1809) to the Ilimmaasaq area (Giesecke 1910). His resultant collections were intercepted at sea during the Napoleonic Wars by the British Navy and landed at Leith. However, most of his specimens eventually arrived in Copenhagen and other European cities. Amongst the new minerals described were arfvedsonite, eudialyte and sodalite. In the course of K.J.V. Steenstrup's expeditions (1874–1890) the Ilimmaasaq area was visited in 1874, 1876 and 1877. Steenstrup was accompanied by G. Holm and A. Kornerup (Steenstrup 1910; Steenstrup & Kornerup 1881) and from their work in the Julianehåb district, a map of the Ilimmaasaq area was published in 1881. A collection of rocks and minerals was made by Flink in 1883 and some of the new minerals were described by Bøggild & Winther (1899). The commission for the Geological and Geographical Exploration of Greenland was continued in 1903 by N.V. Ussing (in the company of O.B. Bøggild) who mapped the intrusions around the Ilimmaasaq area and Igaliku. He also investigated Nunarsuit, Grønnedal and Ivittuut. Following his revisit to the Ilimmaasaq area in 1908, Ussing published his seminal work on the area in 1912. He recognised the principal rock types in Ilímaussaq as augite syenite, alkali granite, pulaskite, foyaite, sodalite foyaite and the poikilitic sodalite syenite that he was to name naujaite. He also described 'banded eudialyte nepheline syenites', to which he bestowed the name kakortokites, and fine-grained nepheline syenites (lujavrites). For the exotic eudialyte-bearing syenites Ussing coined the collective name 'agpaites'. Ussing also recorded the essexites, nordmarkites and alkali granites in the vicinity of Narsaq. Although there were some further studies of the Ilimmaasaq area by S.G. Gordon (published in 1924) and R. Bøgvad who visited it in 1939 on behalf of the company Kryolitselskabet Øresund, virtually no serious geological investigations were made into the igneous rocks of the area until after World War II when the Geological Survey of Greenland (GGU) became established in 1946.

Nonetheless, C.E. Wegmann made very significant geological advances in the region in 1936 when he established the basis for a chronology, introducing the term Gardar Period, named after the Norse archbishopric of Gardar established in what was then called Eriksfjord (Wegmann 1938). All the igneous activity described in this bulletin falls into his Gardar Period. After the war, reconnaisance work was undertaken by A. Noe-Nygaard, K. Ellitsgaard-Rasmussen, R. Bøgvad and H. Sørensen and, subsequently, J. Bondam and H. Pauly. In 1955, after the Danish government decided to investigate the potential uranium resources of the Ilímaussaq complex, a systematic geological mapping programme was initiated that was completed in 1962. Recognition of the ENE-trending zone of faulting, dyke intrusion and emplacement of salic complexes around Tunulliarfik was first mentioned by Berthelsen & Noe-Nygaard (1965).

In the southern rift zone, dykes of exceptional width ('giant dykes') reaching from 500 to 800 m width have few or no Phanerozoic counterparts. They exhibit the remarkable localised 'ballooning' and enigmatic changes, which suggests that the stress fields, lithospheric thicknesses and/or the thermal state of the lithosphere were dissimilar in the Mesoproterozoic and Phanerozoic. The giant dykes were initiated in the Tuttutooq–Ilimmaasaq–Narsarsuaq rift by the most primitive basaltic magmas in the Gardar Province. The largest of these intrusions is the Younger giant dyke complex or YGDC.

Gravity map

A Bouguer gravity map of the eastern Gardar Province around Narsaq and Julianehåb (Fig. 4), contoured at 50 gravity unit intervals, was produced by Blundell (1978). All its values are negative relative to the International Geodetic Reference Field. The contours are broadly parallel to the coast line and indicate a regional gradient with values from –200 gravity units near the coast to –700 gravity units close to the Inland Ice.

Superimposed on this regional pattern is a linear gravity high some 50 km long, centred on Tuttutooq and Tunulliarfik. Fortunately, the trend of this high is almost perpendicular to the regional gradient so that the two anomalies can be distinguished; but unfortunately, the gravity survey did not extend far enough inland to effect complete separation. The gravity high, though not as great as e.g. the North American Gravity High (Chase & Gilmer 1973) or that of the Kenya rift (Fairhead 1976), is clearly distinct from the regional field and cannot be accounted for by the exposed Gardar intrusions. It was interpreted as due to an underlying mass of dense mate-
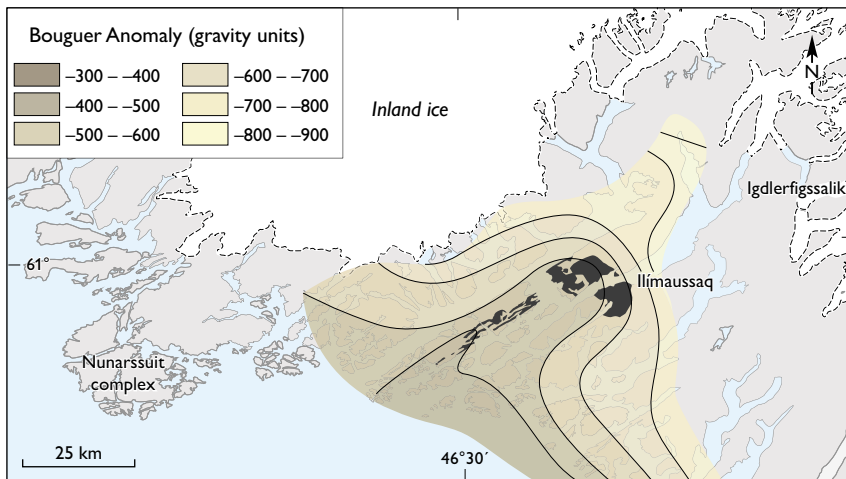
Fig. 4. Gravity map around the younger Gardar Tugtutôq, Narssaq and Ilímaussaq complexes, contoured at 100 gravity unit intervals. Simplified from Blundell (1978, fig. 2).

rial, deduced to be mostly at a depth of 3 to 5 km below the present surface. The anomaly broadens and decreases in magnitude westwards but reaches its highest structural levels in the vicinity of Narsaq. Beneath Tuttutooq it may represent the merging at depth of the giant dykes. The axis of the gravity high lies 3–5 km south of, but parallel to, the giant dykes. The intrusion responsible for the high underlies Tuttutooq at relatively shallow depths and is manifest at the surface as the Narsaq gabbro. Blundell (1978) concluded that it extends down to a depth somewhere between 10 and 40 km. Depending on the model chosen it is between 10 and 25 km wide, the latter representing the full width of the rift. The intrusion was inferred to include gabbro as a major component although, in view of the studies of the YGDC, peridotite cumulates probably play a large role.

The character of the linear gravity high is consistent with those of other continental rifts (e.g. the Oslo gra-

ben; Ramberg 1972), adding weight to the view that the Tugtutôq complex is an eroded continental rift (Upton & Blundell 1978). It also accords with the interpretation of the North American 'mid-continent high' in terms of a rift structure in which gabbroic intrusion is the major cause (Ocola & Meyer 1973). In view of the congruence between the linear gravity high and the YGDC outcrops in Tuttutooq, it may be anticipated that a recurrence of a gravity high would be found corresponding to the YGDC extensions up to the Inland Ice (discussed below) but, because of logistical problems, no data are available for that region. Nonetheless, the field evidence for large-scale emplacement of mafic magma early in the Younger Gardar episode together with the geophysical data clearly indicate that the giant dykes and their subsurface extensions reflect a very major magmatic event.

The Older giant dyke complex, Tuttutooq

The Older giant dyke complex (OGDC) is a massive, parallel-sided dyke, 500–600 m wide, with an undulating course traceable for *c.* 20 km through the island of Tuttutooq (Fig. 5; Upton 1962; 1964c; Upton *et al.* 1985). Whilst its chilled marginal facies show that it commenced with intrusion of hawaiitic magma, notably enriched in incompatible elements, the intrusion as a whole comprises a wide array of alkaline rocks. Although intrusion of the Younger giant dyke complex, described

below, is regarded as the major tectono-magmatic event in the development of the southern rift, emplacement of its closely related predecessor, the OGDC, is taken as the event that heralded rifting. U-Pb baddeleyite dating on the OGDC has yielded an age of 1184 ± 5 Ma whereas Rb-Sr age determinations gave 1154 ±16 Ma and 1150 ± 9 Ma (Table 1). The U-Pb baddeleyite date is accepted as the best age for the OGDC, also because the clearly younger YGDC has a U-Pb baddeleyite age close to 1163
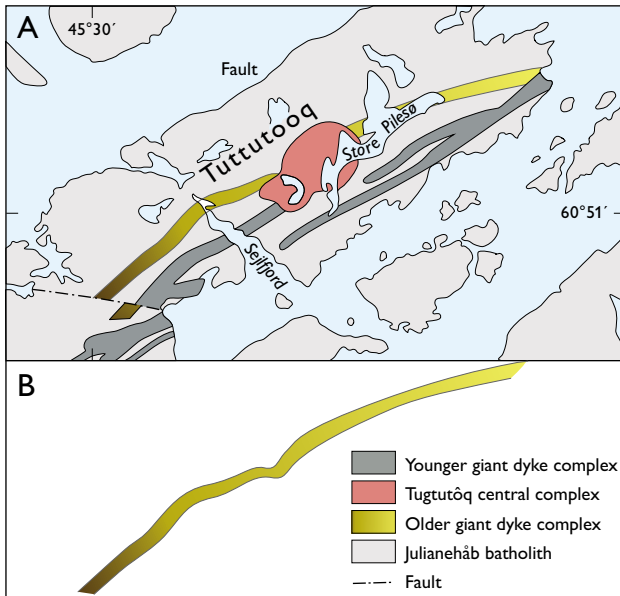
Fig. 5. **A**: Geological map of the giant dyke complexes on Tuttutooq and relationship to the younger central intrusions. **B**: Reconstructed form of the OGDC before the later intrusions and faulting. Dark brown: augite syenite. Lighter brown: pulaskite. Yellow: foyaite. Gradual transition from north-west to south-east.

Ma (Table 1). Thus, the beginning of the southern rift will be taken as 1184 Ma.

Marginal sheaths or 'border groups' up to 100 m wide, consisting of gabbroic to ferro-syenogabbroic rocks, enclose a 300 m wide axial zone of salic rocks that grade from augite syenite in its western parts, through pulaskite and foyaite to peralkaline sodalite foyaite in the easternmost outcrop. The salic rocks in the centre of the intrusion may represent a continuous sequence of cumulates (Upton *et al.* 1996) although a previous interpretation had suggested that the syenites crystallised *in situ* from a compositionally stratified magma body (Upton *et al.* 1985). Cryptic and phase layering phenomena within the salic rocks suggest a 'way up' from west to east and it is inferred that the intrusion was tectonically tilted (during late Gardar block-faulting?) about an axis normal to its length so that after uplift and erosion a deeper section is exposed at the western end than in the east (Upton 1962). The estimated difference in structural ('stratigraphic') levels is 2 to 3 km.

Marginal facies

The symmetrically graded marginal facies varies in width from *c.* 50 m to 100 m along most of the intrusion but appears to be absent over a short distance to the east of the cross-cutting Tugtutôq central complex. The rusty-brown weathering mafic rocks had greater erosional resistance than the central facies and consequently tend to form upstanding ledges on either side of the intrusion. Contacts against the Julianehåb granite are sharply defined and well chilled and are best exposed in the coastal section provided by a fjord (Sejlfjord) that bisects it approximately at right angles (Figs 5, 6). Away from the contact zones the rocks are subophitic and layering features are absent or very weakly developed.

The feldspars are strongly zoned plagioclases surrounded by perthitic calcic anorthoclase and grading to cryptoperthite outermost zones, lacking discernible exsolution features. Within these syenogabbroic rocks the feldspars exhibit a continuum from An_{63} via potassic oligoclase (An_{22}) and calcic anorthoclase into Ca-Na-sanidine (Upton *et al.* 1985), whilst the olivines show a range of Fo_{53-16}. Figure 7 shows the compositional range of olivines and pyroxenes. Transition from mafic marginal facies to the felsic central facies occurs over a width of 1–2 m and involves a complex mélange of the two rock types with the felsic rocks forming an irregular network pattern that may have originated from sidewall ascent of buoyant felsic magma interacting with incompletely crystallised syenogabbro (Fig. 8).

Central facies

Throughout its westernmost 12 km the central facies consists of mesocratic augite syenite although outcrops are sparse. The augite syenite is, however, splendidly exposed on either side of Sejlfjord. Preferential glacial excavation of the syenites left a broad flat valley and its light colouration gave rise to the term 'the White Valley' or 'Hviddal'.

The augite syenites contain perthitic feldspars up to 10 mm in size, with turbid (altered) interstitial nephelines. The ferromagnesian minerals are fayalitic olivine (largely replaced by iddingsite) with a compositional range of Fo_{10-4}, and idiomorphic clinopyroxene zoned from pinkish-grey centres to pale green rims that are typically surrounded by amphibole (brown, zoning out to blue-green) reaction rims. Titanomagnetite with biotite

Fig. 6. View east across Sejlfjord showing a section across the southern half of the OGDC. The low-lying area in the foreground and middle distance is underlain by the OGDC. The whitish parts of the low cliff across the fjord consist of augite syenite, whilst the brown-weathering rocks farther to the right are syenogabbros of the southern border group. The ridge in the middle distance behind the low cliffs consists of Julianehåb batholith rocks. The high cliff in the far left distance consists of syenites of the Tugtutôq central complex.

reaction fringes and fluor-apatite are minor components. The amphibole and biotite are probably subsolidus reaction products (Powell 1978).

East of the Tugtutôq central complex, the OGDC is seen only in scattered outcrops along the coasts of Store Pilesø and the small islands within it. The syenites in this sector have experienced substantial hydrothermal alteration, with development of epidote. The nepheline content is markedly higher (15–20% modally) than in the western syenites, and farther east the nepheline becomes increasingly idiomorphic. Analyses of separated feldspars show them to be essentially Ca-free, close to the Ab–Or join between Or_{40} and Or_{55} and straddling the Na-sanidine/sanidine fields (Upton 1964c). Feldspars from the most easterly outcrops are the most potassic whereas the host rocks become increasingly sodic. These compositions do not precisely lie on the extrapolated trend from the marginal zone, suggesting some discontinuity between the marginal series and the central series.

Barium contents in the feldspars peak at *c*. 1.6 wt% Ba within the Na–Ca-anorthoclase field, corresponding to *c*. 2.8 mol% celsian.

The OGDC presents a near-complete spectrum of rocks from gabbroic to foyaitic that are, inferentially, products of a suite of magmas that graded from the initial hawaiitic magma through ferro-mugearitic, nepheline-benmoreitic, nepheline-trachytic to peralkaline phonolitic. Analyses of the central series show negative Eu anomalies but these are absent in the marginal series, implying that any calcic feldspar fractionation commenced relatively late in the evolution of the suite (Upton *et al.* 1985).

As the rocks are apparently devoid of lamination or modal layering that might be ascribed to crystal settling, the question as to whether or not they should be regarded as a cumulate sequence is open to debate. The alternative hypothesis is that the sequence composing the central zone developed from a stratified magma chamber
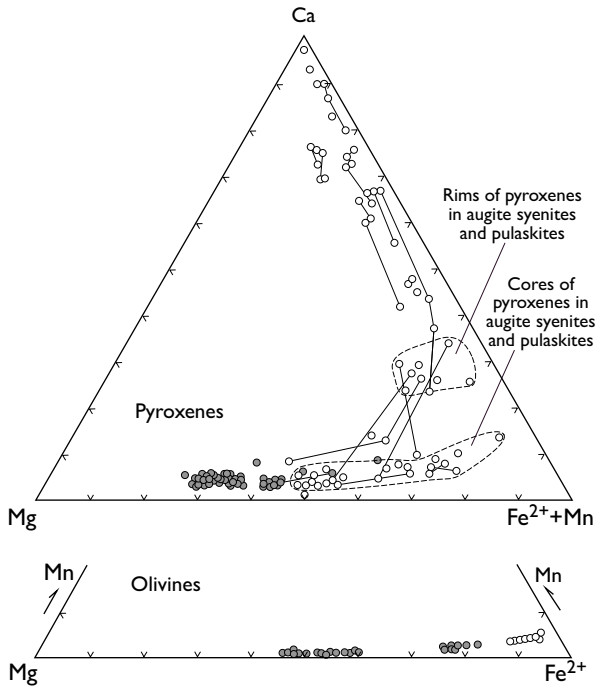
Fig. 7. Pyroxene and olivine compositions in the OGDC plotted in terms of Mg–(Fe^{2+} +Mn)–Ca and Mg–Fe^{2+}–Mn respectively. Modified from Upton *et al.* (1985).

that crystallised from below upwards with whole-rock compositions approximating to those of melts. As will be described below, there is evidence that compositionally stratified chambers played an important role elsewhere in the Gardar Province.

It is a matter of speculation as to whether continuation of the differentiation trend in the hidden uppermost facies of the intrusion (below Narsaq Sund) led to more extreme agpaitic fractionates. A schematic vertical section of the OGDC is presented in Fig. 9. Thus, from the start of the evolution of the Tuttutooq–Ilimmaasaq–Narsarsuaq lineament, the OGDC provides evidence bearing on the probable evolution of the peralkaline Ilímaussaq suite.

Fig. 8. Transition between the syenogabbroic marginal zone (brown) and augite syenite of the central zone (white) in the OGDC. The crudely vertical elongation of the syenite facies may denote channelways within the thermal boundary layer through which low-density, residual trachytic melts ascended.
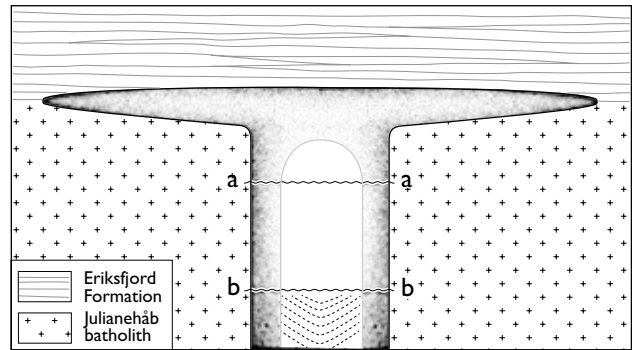
Fig. 9. Schematic vertical section of the OGDC at Tuttutooq (Upton *et al.* 1990). The marginal gabbroic rocks are indicated in close stipple ornament whilst the syenites of the central zone are shown in light stipple. The sill-like expansion of the OGDC at the unconformity in the host rocks is hypothetical, as is the synformal layering in the deeper parts of the central zone. The wavy horizontal lines 'a-a' and 'b-b' diagrammatically indicate the different erosion levels at the shallowest (easternmost) and deepest (westernmost) outcrops, respectively. The width of the giant dyke is 0.5 km. The height difference between 'a-a' and 'b-b' is estimated at 2–3 km.

The Younger giant dyke complex

This massive gabbroic intrusion, intruded at *c.* 1163 Ma (Table 1), has the form of a bifurcating suite of giant dykes (Upton 1962, 1964a, 1987; Upton & Thomas 1980). It crosscuts the OGDC and the time lapse separating these two intrusions probably amounted to around 20 million years. A change in trend between the two suggests a slight anticlockwise reorientation of the regional stress field. Palaeomagnetic data show an apparent polar movement of *c.* 10° to the east between the two so that significant plate movement may have intervened (Piper 1976).

The Younger giant dyke complex (YGDC) can be followed for *c.* 140 km from the Labrador Sea to the Inland Ice (Figs 10–12). Above the unconformity separating the batholith and the Eriksfjord Formation the dyke morphology switched to lopolithic much in the same manner as the Muskox Intrusion in arctic Canada (Irvine & Baragar 1972). The branching pattern of the YGDC on the Tuttutooq archipelago west of Ilimmaasaq and the generalised attenuation of its branches from east-north-east to west-south-west suggest lateral flow of magma from a focus to the east-north-east. That this focus lay in the region of Illimmaasaq is also indicated by the gravity map (Fig. 4). However, both the giant dykes and the succeeding Main swarm of the more fractionated post-YGDC dykes are traceable with undiminished intensity east-north-east of Illimmaasaq to where they pass beneath the Inland Ice. At their maximum the dykes attain widths of 800 m although more generally they are 300 to 500 m broad.

The entire intrusion of basaltic magma is deduced to have taken place during a single dramatic, large-scale, trans-tensional event. The mean initial magma composition, as indicated by analyses of what appear to be the least contaminated of the medium-grained doleritic marginal samples of the giant dyke branches close to the Inland Ice, closely matches that gained from study of the giant dykes on Tuttutooq (Upton & Fitton 1985). This observation supports the hypothesis that intrusion of all of the YGDC occurred simultaneously and involved a very large and homogeneous magma batch.

Heat loss is assumed to have taken place principally through the walls. The magma crystallised as a closed system although late-stage generation of silica oversaturated salic magma in eastern Tuttutooq probably involved crustal assimilation. Although the dykes are dominantly composed of troctolite, syenogabbros, ferrosyenites and syenites (both silica oversaturated and undersaturated) occur in localised differentiated facies. Plots showing compositional data on the YGDC olivines, feldspars and pyroxenes are presented in Fig. 13.

Although the cooling of the YGDC magma was sufficiently slow for most of it to crystallise as coarse-grained troctolite, it was sufficiently rapid to inhibit migration of intercumulus melts, thus preventing the textural and/or chemical re-equilibration of the high-temperature prod-

Table 2. Giant dyke compositions

	1	2	3
Major elements (wt.%)			
SiO_2	43.47	46.00	46.06
Al_2O_3	15.65	16.71	17.13
$Fe_2O_3{}^\dagger$	15.57	14.91	14.21
MgO	4.76	5.93	6.12
CaO	7.70	7.78	7.96
Na_2O	3.45	3.55	3.43
K_2O	1.81	1.45	1.41
TiO_2	4.40	2.63	2.51
MnO	0.19	0.19	0.18
P_2O_5	1.95	0.86	0.83
Total	98.95	100.01	99.84
Trace elements (ppm)			
Ni	22	52	63
Cr	5	30	42
V	138	160	168
Sc	16	17	17
Cu	40	39	44
Zn	81	91	90
Sr	1039	901	921
Rb	39	23	25
Zr	162	150	141
Nb	31	22	21
Ba	1669	1120	1052
La	47	44	27
Ce	103	64	63
Nd	57	34	32
Y	35	27	26
FeO*/(FeO* + MgO) wt.%	0.75	0.69	0.68
Al_2O_3/CaO	2.03	12.15	2.15
K/Rb	385	522	468
Ba/Sr	1.651	1.24	1.14
Zr/Nb	5.2	6.8	6.7
La/Y	1.34	1.63	1.04

1. Older giant dyke, Tugtutôq (chilled facies). n = 3.[§]
2. Younger giant dyke, Tugtutôq (chilled facies). n = 9.
3. Giant dykes, Nunatak region and north-east of Motzfeldt. n = 9.

[†]total iron as Fe_2O_3 or FeO.
[§]n = Number of analyses.

ucts that adds complexity to many 'classic' layered intrusions. Consequently, the troctolites and their associates are typical orthocumulates in which melt trapped within the interstices underwent extended *in situ* crystallisation. This yielded discrete intercumulus minerals and added zonal increments to the cumulus until the solidus was reached (Wager *et al.* 1960). Some subsolidus migration of aqueous fluids is also inferred.

Composition of the magma

The mean compositions of the chilled marginal facies of the YGDC on Tugtutoq and in the more easterly giant dyke branches, and the chilled marginal composition of the OGDC, are shown in Table 2. The initial magmas of the YGDC and its OGDC predecessor are inferred to have been closely related. Both had compositions close to 'the critical plane of undersaturation' (Yoder & Tilley 1962) but the YGDC magma had higher alkalis and mar-

Fig. 10. Distribution of the Younger giant dykes in the east-north-east of the Gardar system, extending (left to right) from Kangerlua to G.F. Holm Nunatak, and from the outer islands of the Tuttutooq archipelago to Narsaq Sund and their higher-level representatives around Narssaq and the Ilímaussaq complex. Narrow extensions of the YGDC continue 15 km south-west of the map boundary.

Despite these overall undersaturated characteristics, silica-oversaturated rocks occur in eastern Tugtutôq in the vicinity of Asorutit (see below). These may represent a local anomaly due to crustal assimilation. A photomicrograph of a chilled YGDC marginal sample is presented in Fig. 14.

Nd- and Sr-isotopic features are close to bulk Earth values (Upton *et al.* 2003). $^{87}Sr/^{86}Sr_{1163}$ values for the YGDC troctolites range from 0.70279–0.70321, suggesting insignificant crustal contamination (Mingard 1990). $\delta^{18}O_{smow}$ values for feldspars from the troctolites are +5.0 to +6.5‰; troctolitic and peridotitic whole-rocks give $\delta^{18}O_{smow}$ values of +4.0 to +5.4‰ and +4.4 to +6.9‰, respectively. Feldspars from the Assorutit quartz syenite have $\delta^{18}O_{smow}$ of +6.5 to +6.8‰ and the values for the corresponding whole-rocks range from +4.2 to +5.9‰. The oxygen isotope values for the troctolites are slightly lower than those of fresh Skaergaard gabbros (Taylor & Forrester 1979) where the feldspars have $\delta^{18}O_{smow}$ +7.6 to +8.7‰ and whole-rocks +7.2 to +8.2‰. Mingard (1990) considered that the low YGDC values (<+5‰) could be due to localised interaction between magma and meteoric water but noted that assimilation of low-$\delta^{18}O$ lower crust could not be excluded.

Crystallisation sequence

Melting experiments at 1 kb suggest that the magma was intruded at 1140° ± 10°C, in equilibrium with olivine and plagioclase, whilst the solidus was at *c.* 980°C (Upton 1971). Petrographic evidence indicates delayed crystallisation of augite and experimental (1 kb) work indicates that the olivine–plagioclase–clinopyroxene–liquid cotectic was not attained until 1060°C ± 15°C. The layered cumulates in the YGDC indicate that crystallisation of Fe-Ti-oxides and apatite preceded clinopyroxene. Studies on associated fine-grained dykes (the Main swarm described below) suggest that Fe-Ti-oxides and apatite joined the assemblage when MgO in the liquid had fallen to *c.* 3.75 wt% whereas pyroxene phenocrysts did not appear until this value had been reduced to *c.* 3.25 wt% (Upton & Thomas 1980; Martin 1985). Such relatively delayed crystallisation of pyroxene is unusual in basaltic systems. Crystallisation of Fe-Ti-oxides and apatite appears to have taken place within a very narrow temperature interval. The YGDC magma was relatively reduced with an oxygen fugacity lying between the QFM and IW buffers (Upton & Thomas 1980).

ginally lower K_2O/Na_2O (0.41 as opposed to 0.48). Its notably high K_2O content (1.43 wt %) is regarded as a primary characteristic, unrelated to crustal assimilation. The YGDC magma had lower CaO, Al_2O_3, TiO_2 and P_2O_5 contents than the initial OGDC magma and was also poorer in incompatible trace elements, especially Ba and Sr. The F content was approximately half that of the OGDC magma (Upton & Thomas 1980; Köhler *et al.* 2009). The YGDC magma was relatively poor in normative diopside and consequently crystallised to troctolitic rocks (Upton & Thomas 1980; Upton 1996). It was marginally silica undersaturated (*c.* 2% normative nepheline); residual veinlets of nepheline syenite are known from several localities at Tuttutooq, and a substantial body of nepheline syenite is present within the most easterly YGDC extensions in the nunatak region (described below).

Fig. 11. View towards east-north-east along the northern branch of the YGDC in western Tuttutooq, showing typical hummocky topography. The high ground to either side and in the distance is underlain by the Julianehåb batholith.

Fig. 12. Oblique aerial photograph along the YGDC, looking east-north-east along Tuttutooq. The northern part of the Ilímaussaq complex (with ice) is seen in the far distance. The valley to the right is excavated from YGDC gabbro. The parallel grooves in the foreground denote weathering of Main swarm dykes and shear zones in the Julianehåb batholith. Pale-coloured outcrops on the ridge in the middle distance are due to fast-weathering, crumbly outcrops of the YGDC.
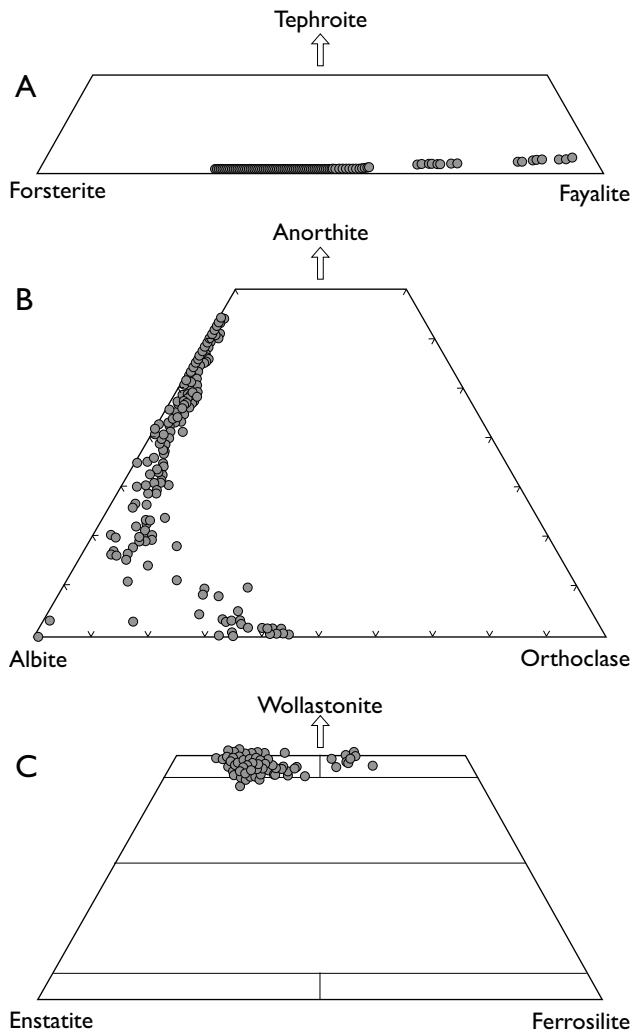
Fig. 13 (Modified from Mingard 1990). **A**: Olivine compositions in the Younger giant dyke complex, shown in the Fo–Fa–Tp ternary diagram, from Fo_{68} to near-end-member fayalite but with a small late-stage increase in Tp. **B**: Feldspar compositions in the Ab–An–Or ternary, extending from An_{65} through more sodic plagioclases and ternary compositions to alkali feldspar close to the minimum melting composition on the Ab–Or join. **C**: Clinopyroxenes in the system En–Fs–Wo, grading from salite to ferrosalite. In syenitic differentiates more extreme compositions (not shown) extend to ferro-hedenbergite and aegirine-augite.

Internal structures

Although the greater part of the intrusion consists of homogeneous troctolite, layered cumulates and/or differentiated rocks appear at irregular intervals along the dyke branches. Layering features define synformal structures which dip symmetrically inwards from the sides to horizontality along the dyke axes. Where closure can be discerned the layering has a canoe-like morphology, dipping inwards from the ends as well as from the sides (Fig. 15). The layered parts of the dyke may be described as nodes or pods inferred to mark sites, commonly only a few hundred metres long but which can be up to 3 km, where convection cells developed. The observation that the layering varies from barely visible to strongly accentuated may relate to the vigour of convection. The relatively abrupt changes along the intrusion from isotropic troctolite to the dozen or more layered nodes imply that the factors dictating the change from the one to the other were critically poised. These factors are presumed to have included the rate of heat loss, the local morphology of the intrusion, melt composition, and possibly structural depth in the intrusion (Irvine 1987). The presence or absence of cumulate layering was not simply governed by dyke width as there are broad sectors lacking cumulate features and narrow sectors in which layering is strongly developed. An astonishing variety of layering styles is exhibited, including feldspar lamination alone, normally-graded rhythmic layering, isomodal layering, micro-rhythmic layering, diffuse modal layering and graded rhythmic layers alternating with uniform 'standard' rock.

The YGDC in the Tuttutooq archipelago

In view of the spectrum of phenomena relating to fluid dynamics in the convecting cells in the magma chamber, the key localities along the Tugtutôq dyke branches are here described below from east-north-east to west-south-west. The descriptions are mainly based on Upton (1964b, 1987), Upton & Thomas (1980), and Upton *et al.* (1996), and some observations have not been published before. Figure 16 shows a series of schematic cross-sections along the YGDC.

Fig. 14. Photomicrograph of the chilled margin of the YGDC against Julianehåb granite. The opaque, flow-banded, chilled zone inferentially reflects a vitric facies subsequently recrystallised and oxidised. Pale spots in the lower part of the image are presumed spherulites. The original texture of the granodioritic country-rock has been profoundly modified by partial melting and recrystallisation. Two-way element exchange is assumed, involving entry of K and other mobile elements from the country-rock into the hot, chilled gabbro. Back-veining from the host rock has not occurred. Horizontal field of view 30 mm.
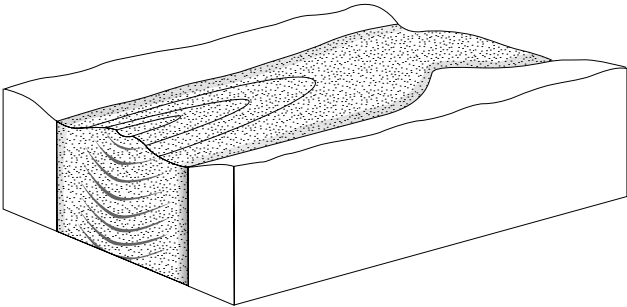
15. Schematic sketch of a layered synform in the YGDC. Increasing thickness of ferromagnesian cumulate towards the centre is indicated diagrammatically.

Sissarluttooq

The southern branch of the YGDC reaches its greatest observable thickness (*c.* 800 m) at the extreme east-south-east corner of Tuttuooq, on the Sissarluttooq peninsula (Fig. 17). However, the divergence of contacts towards the ENE implies its further widening beneath the waters of Narsaq Sund. A coastal section on its northern side reveals the chilled marginal zone transecting the OGDC whereas the southern margin is unexposed. The principal feature of interest at Sissarluttooq lies in the well-developed lamination due to parallel orientation of idiomorphic plagioclase crystals 2–3 mm across, tabular parallel to the (010) faces. Olivine is the second-most abundant component (up to 1 mm diameter) whilst idiomorphic apatite and titanomagnetite crystals are also cumulus components. Although modal layering is ab-
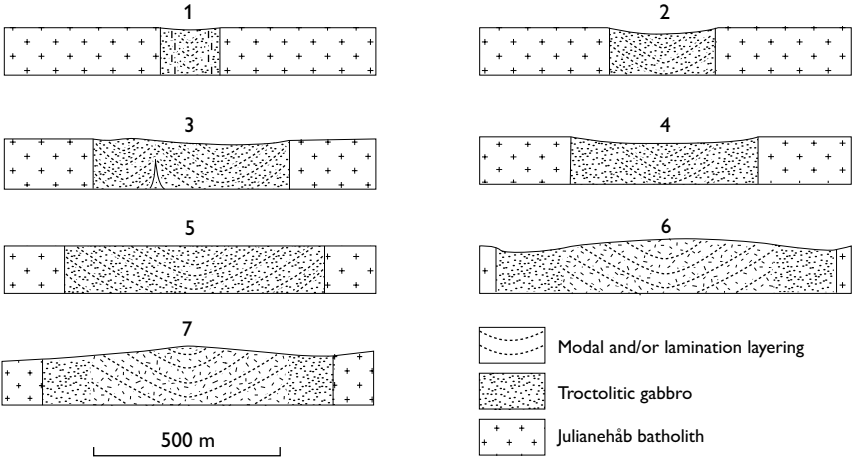
Fig. 16. Cross-sections through the Younger giant dyke at seven localities. **1**: Itillinguujuk. **2**: Tripyramidal peak west-south-west of Itillip Saqqaa. **3**: Itillip Saqqaa. **4**: Marraat. **5**: Sissarluttooq. **6**: Krydssø. **7**: Syenitknold. Locations: **1–6** on Tuttutooq and its western islands; **7** on nunatak north of Motzfeldt Sø, see Fig. 10.

Modal and/or lamination layering

Troctolitic gabbro
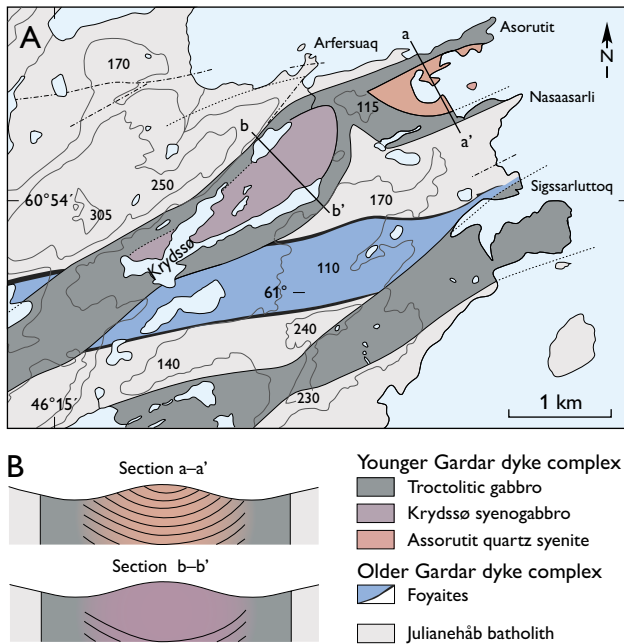
Julianehåb batholith

500 m

Fig. 17 (Modified from Upton 1962, 1964a). **A**: Geological map of the south-eastern coast of Tuttutooq, showing two YGDC branches cutting across the OGDC. The narrowing of the southern branch between the 230 and 240 m spot-heights reflects upward narrowing of the intrusion and is topographically controlled; this is not the case for the narrowing of the northern branch between Krydssø and Asorutit. The central, differentiated facies in the Asorutit area is composed of quartz syenite, separated from the marginal troctolitic gabbro by narrow syenogabbroic margins. The central, differentiated rocks at Krydssø comprise synformally layered syenogabbros grading up into augite syenite. Little or no layering is visible. **B**: Enlarged, schematic cross-sections of the differentiated facies at Asorutit and Krydssø. The synformal layering at Asorutit is hypothetical.

Fig. 18. Glomeroporphyritic clusters of plagioclase and olivine at Marraat, composing 'snowflake' textures. Pocket knife 10 cm long.

sent, the lamination in the central part of the intrusion (50–100 m from the contacts) defines synformal layering with inward dips of *c.* 40°, decreasing axially. The structure, however, is not that of a simple single basin as there appear to be several foci at which the lamination attains horizontality. The total length of the laminated pod is *c.* 1 km.

West-south-west of Sissarluttooq, the southern branch reverts to homogeneous troctolitic gabbro, but at a distance of *c.* 4 km it subdivides into a layered northern sub-branch and a homogeneous southern sub-branch. In the former, layering is shown by feldspar lamination that dips inwards at *c.* 30° before shallowing symmetrically to zero along the axis. This synformal structure persists for about 1 km before the gabbro dyke resumes homogeneity.

Marraat

Two kilometres west-south-west Sissarluttooq in the southern sub-branch, the coastal section at Marraat provides excellent exposures across the 500 m wide dyke. For the first few metres in from the contacts, thin vertical mafic layers occur parallel to the contacts with planar alignment of plagioclases. It is within these border-group rocks that the phenomenon of 'snowflake' plagioclase glomerocrysts occurs (Fig. 18). In the axial 300 m of the dyke, modal layering with feldspar lamination becomes more strongly developed with inward dipping layers at increasingly low angles to the central horizontal zone. Mafic layers up to 10 cm thick are due to concentrations of olivine, titanomagnetite and apatite; indications of normal grading and some cross-bedding are indicative of magma flow.

Asorutit

The northern branch of the YGDC crops out between the Nasaasarli and Asorutit headlands (Fig. 17). Like its southern counterpart, this branch is *c.* 800 m broad but the contact zones are now parallel, rather than divergent as in the former. Apparently homogeneous gabbros form 200 m thick marginal border groups that grade, through a few metres of iron-rich syenogabbro, into a vertical zone several metres broad, displaying a spectacular array of directionally oriented, branching, clinopyroxene

Fig. 19. Dendritic clinopyroxene prisms in the syenogabbroic zones separating the Asorutit quartz syenite from the border-group gabbros. Distance across the outcrop left to right is *c.* 75 cm.

Fig. 20. Coarse-grained quartz syenite at Asorutit. The interstices between idiomorphic perthitic alkali feldspar crystals mostly contain sodic amphibole, quartz and calcite. Diameter of coin 2.5 cm.

dendrites up to 50 cm long (Fig. 19). It is deduced that inward crystallisation of the giant dyke enclosed residual magma in which the pyroxene components became increasingly concentrated until a critical degree of supersaturation was reached, when nucleation of the dendritic crystals was triggered to form these remarkable crescumulate zones, symmetrically developed on either side of the intrusion. Sandwiched between these transitional syenogabbro border zones is a central body of syenite. In plan, this wedges out sharply as traced westwards, terminating shortly before the dyke narrows to a 'wasp waist' less than 250 m broad (Fig. 17).

The eastern outcrop of the syenite disappears beneath sea-level but, by analogy with salic cores elsewhere in the giant dykes both in the Tuttutooq–Ilimmaasaq–Narsarsuaq system and in the Isortoq region, the syenite is probably a localised lenticular development less than 2 km long. There are no clear indications of any layering features other than localised ferromagnesian-rich schlieren. The texture, however, suggests that the syenite is an orthocumulate (Fig. 20) and it is speculated that the visible rocks are underlain by layered cumulates comparable to those of Krydssø (described below).

The syenite is hypidiomorphic granular, composed *c.* 80% modally of squat rectilinear alkali feldspars 7–8 mm long. Cryptoperthitic cores grade out to more coarsely exsolved antiperthites, surrounded by clear outer zones of albite. Other early phases are ferroaugite, fayalitic olivine, titanomagnetite and apatite. Colourless to grey clinopyroxene cores zone out to pale green and, locally, to deeper green aegirine-augite. The olivine ($Fo_{5-2.5}$) contains exsolved parallel plates of Fe-oxide with variable re-

placement by iddingsite. Reaction fringes of blue-green alkaline amphibole grading sharply out into arfvedsonite surround the pyroxenes and olivines. This discontinous reaction series culminates in biotite, zoned from strongly pleochroic to colourless, as the youngest ferromagnesian mineral. The latest (intercumulus) components are quartz and calcite. Whereas the Asorutit syenite and the more primitive syenites of the OGDC share many petrographic affinities, the development of the albite coronae around the perthites and the intercumulus quartz and calcite distinguish it from its silica undersaturated OGDC predecessors. The youngest components of the YGDC suite at Asorutit are localised patches of granite pegmatite in the syenite. Veins of this coarse alkali granite (perthite, quartz, arfvedsonite and accessory zircon) are prominent over a distance of *c.* 2 km along the northern YGDC branch and are regarded as filter-pressed residues from the latter.

Krydssø

On the western side of the northern branch constriction, the giant dyke again appears composite but now with a core of syenogabbro/ferrosyenite (the Krydssø body) rather than a leucocratic syenite (Fig. 17). The core is lenticular in plan, *c.* 3 km long and, like the Assorutit syenite, it is ensheathed by troctolitic border groups. There is a degree of symmetry in plan between the Krydssø and the Asorutit bodies: in the central part of the giant dyke at Krydssø the rocks pass upwards from syenogabbro with

Fig. 21. Normally graded modal layering in ferro-syenogabbro, Krydssø. Scale is 50 cm long.

Fig. 22. View towards east-north-east beside Krydssø along the axial plane of the layered synform. Ferro-syenogabbros in the foreground dip NNW, while those in the distance dip SSE (white lines).

anhedral, intercumulus, pyroxene to syenites containing idiomorphic prismatic augite. It is the only place in the YGDC where phase layering has been observed rather than inferred. Whilst its crystallisation may have been coeval with that of the Asorutit syenite, the Krydssø syenogabbro/ferrosyenite body is transected by some of the residual alkali granite veins. Contact relations between the iron-rich core and the sheath of enveloping gabbro are unexposed. Modal layering in the syenogabbro dips inwards around the body so that any one layer thus defines a boat-like morphology. The modal layering involves alternation of melanocratic and mesocratic layers on a decametre scale, both with and without normal grading (Fig. 21). The Krydssø syenogabbros present one of the few opportunities along the YGDC to observe the axis of the synformal layered structure (Fig. 22).

Modal layering appears in otherwise homogeneous troctolite along the southern coast of Store Pilesø as 'inch-scale layering' i.e. micro-rhythmic isomodal alternation of mafic and felsic layers, each only 2–3 cm thick, presenting a unique layering style in the intrusion. Beyond this, as traced west-south-west, the northern branch is devoid of cumulate layering for nearly 16 km; this homogeneity persists until just west of the dislocation of the northern branch by one of the left-lateral faults that cut the southern rift. In the offset intrusion,
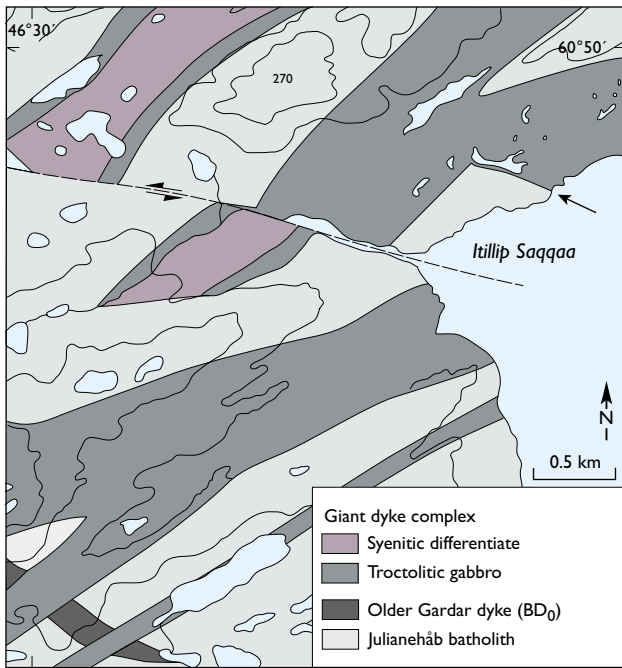
Fig. 23. Geological map of giant-dyke relationships at Itillip Saqqaa on central Tuttutooq, showing members of the OGDC, YGDC and an older Gardar dyke (BD_0) in the south-west. The WNW–ESE-trending contact of an offshoot from the YGDC (marked by an arrow) is parallel to the fault at Itillip Saqqaa and is inferred to have been controlled by a pre-existing shear zone.

Fig. 24. Intermittent spacing of thin black peridotitic layers in grey troctolites (Itillip Saqqaa). Scale is 50 cm long.

Fig. 25. 'Snowflake' glomerocrysts in a small (*c.* 2 m wide) dyke. Small island off the south-east coast of Tuttutooq. Scale is 50 cm long.

south of the fault at Itillip Saqqaa, the most striking layering phenomena appear in a style that is unique within the Gardar Province.

Itillip Saqqaa

The YGDC northern branch has been displaced 1300 m sinistrally by the fault; the gabbros on the immediate southern side of the fault are below sea-level so that the nearest outcrops for study are from 250 to 800 m distant from the fault plane on the Itillip Saqqaa coast (Fig. 23).

Although the transcurrent fault at Itillip Saqqaa has clearly displaced the giant dyke, marked contrasts in the dyke features on either side of the fault strongly suggest that some pre-existing structural element affected crystallisation prior to the main left-lateral movement. North-east of the fault plane the troctolite gabbro is homogeneous, contrasting with distinct heterogeneity imposed by modal layering on its south-western side. Evidence for convection, high-temperature faulting and

Fig. 26. White dendritic plagioclase grown upward from and within peridotite layers in the YGDC west-south-west of Itillip Saqqaa. Sections on scale are 5 cm long.

gravity slumping, present on the south-west side of the fault, is lacking to the north-east and there are no indications of the dyke parting into two branches. The possibility of major vertical displacement along the fault cannot be discounted. If so, downthrow to the north might be inferred, with the giant dyke outcrops to the south representing deeper structural levels. It is suggested that a plane of weakness, pre-dating the sinistral displacement, was already extant.

Prominent layering in the troctolites south of the fault typically consists of: (a) whitish-grey mesocratic troctolites with c. 70% (modal) plagioclase and c. 30% olivine (less than 10% interstitial augite and titanomagnetite), and (b) nearly black feldspathic peridotite consisting of >80% olivine (Fig. 24). The mesocratic rocks are considered to represent products of crystallisation along an olivine-plagioclase-liquid cotectic, with c. 30% olivine and c. 70% plagioclase. Typically there are sharp contacts between the contrasting pale and black layers. In some places the peridotite layers display irregular bases, attributed to differential loading by dense layers of olivine cumulus overlying readily deformable feldspar-rich layers. The black colouration of the peridotites is due to microscopic opaque inclusions in the olivines.

The magma is inferred to have reached a shallow crustal level whilst supersaturated with respect to plagioclase. Reduction in pressure on ascent is inferred to have stimulated plagioclase nucleation. The plagioclase grew rapidly, commonly from olivine nuclei, to form radiating 'snowflake' glomerocrysts (Berg 1980). The resultant troctolites lack plagioclase lamination and are inferred to be wholly composed of polymineralic 'snowflakes' that accumulated as cumulus. It is, however, only in chilled marginal facies that the 'snowflake' morphology becomes apparent. Well-developed large-scale 'snowflake' clusters are shown in a related dyke rock, outside the YGDC (Fig. 25).

The occurrence of dendritic plagioclase growth normal to peridotite layers can be seen in this part of the YGDC (Fig. 26). As with the growth of 'snowflake' clusters, it provides evidence that episodic supersaturation of the magma with respect to plagioclase was relieved by rapid growth of feldspar from a boundary layer to form a perpendicular feldspar crescumulate (Wager et al. 1960). Accumulation of the 'snowflake' glomerocrysts produced the troctolitic layers, the fabric of which consequently differs from that of the well-laminated troctolites (e.g. as seen at Sissarluttooq). Intermittently plagioclase failed to nucleate, leaving olivine crystallising alone to form the peridotites. Thus the bimodal layering resulted from whether or not plagioclase was crystallising. The peridotitic layers are also characterised by a characteristic jointing that is either normal to the layering or at a high angle to it.

Two parallel synforms are present in the YGDC cross section at Itillip Saqqaa. In the narrower and steeper southern synform, cross-lamination as well as some degree of normal grading between troctolite and peridotite is present. These features are attributed to erosion and deposition, together with crystal winnowing, resulting from vigorous downflow of magma adjacent to the southern contact of the giant dyke (Fig. 27). More

Fig. 27. Normally-graded and cross-bedded layers in the southern part of the paired synform at Itillip Saqqaa. The dark unit (*c.* 2 m thick) behind the person in the right is massive peridotite.

Fig. 28. Five peridotite layers in troctolite that have undergone ductile deformation in a normal fault with downthrow towards the layered synform axis. Itillip Saqqaa. Scale is 50 cm long.

tranquil deposition of olivine and olivine + plagioclase clusters appears to have typified the broader northern synform.

Peridotite layers tend to thicken down-dip. Older (lower) layers dip more steeply than stratigraphically younger layers in the southern synform. This structure exhibits a miniature equivalent to oceanic dipping reflectors in which the oldest units have the steepest dip towards the volcanic zone whilst younger units have progressively lower dips; the processes occurring in the two scenarios are thought to have been comparable: As crustal

extension persisted in the dilating dyke fissure, the earlier layers rotated downwards to be progressively overlain unconformably by younger layers. Normal faults developed at high temperatures (above 600°C?) when the cumulates acquired a capacity for brittle fracture. The faults throw down towards the synform axis so that the central zone was undergoing 'graben' subsidence (Fig. 28).

Whereas opening of the giant dyke fissures took place sufficiently fast to form deep, steep-walled magma chambers, this feature demonstrates that dilation of the dyke was still taking place while cumulates were being deposit-

Fig. 29. YGDC outcrop close to Itillip Saqqaa showing thin peridotite layers within troctolite towards the margin of northern synform. Height of outcrop *c.* 3 m.

Fig. 30. Synform axis, Itillip Saqqaa. In contrast to Fig. 29, this outcrop displays thick peridotite layers, separated by thinner troctolite layers more resistant to weathering. Scale bar is 0.5 m long.

ed. Thus the extensional stresses were still being exerted, not only during the deposition of the cumulates but also during the subsequent cooling history of the intrusion. In the northern synform the thickness ratio of troctolitic versus peridotitic layers decreases from flanks to centre, i.e. the marginal parts of the synform are predominantly mesocratic (Fig. 29) whilst those of the axial region are dominantly melanocratic (Fig. 30). Comparable down-dip thickening of mafic/ultramafic layers occurs in other Gardar cumulate bodies, e.g. within the Kûngnât Fjeld syenites (Upton *et al.* 2013). There is a notably inequi-

granular (i.e. non-equilibrated) texture shown in the peridotites (Fig. 31).

Near the northern synform axis a slump breccia occurs, comprising clasts of peridotite up to half a metre across, enveloped in a troctolitic matrix (Fig. 32). Some of the clasts show layering, and the angular discordances from clast to clast clearly indicate their rotation during slumping. Deformed layering in the surrounding matrix points to it having been highly ductile or mushy, contrasting with the coherent clasts. The form of many of the peridotitic clasts is defined by roughly planar surfac-
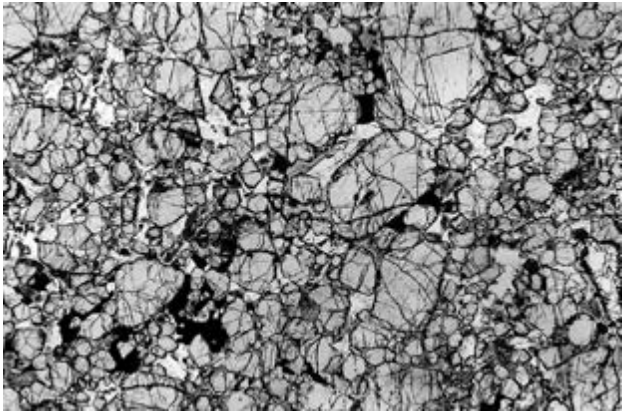
Fig. 31. Photomicrograph (plane polarised light) of typical peridotite from Itillip Saqqaa. Note the un-equilibrated texture and the large inequality of sizes of the olivine cumulus. Intercumulus minerals are plagioclase, magnetite and scarce augite. Olivine crystals are up to 2 mm across.

Fig. 32. Slump breccia of peridotite clasts in troctolite matrix. Itillip Saqqaa. Hammer length *c*. 26 cm.

Fig. 33. **A**: Lenticular-section of a peridotite unit in the western YGDC. The peridotite is abruptly defined between troctolite above and below, and displays characteristic jointing transverse to cooling surfaces. Scale-bar (centre, against peridotite) is 50 cm long. **B**: Sketch showing joints in the peridotite ('troll's smile').

es, suggesting that a joint system had already developed at the time of their disruption, and it is presumed that this corresponds to the jointing seen in the peridotite layers. Hence the peridotites had already achieved a state capable of brittle fracture while the troctolites were still readily deformable. The situation mirrors that shown by ultramafic and feldspathic material in syenite cumulates at the Nunarssuit and Kûngnât complexes (Upton *et al*. 1996). The slump breccia at Itillip Saqqaa is deduced to have formed when steeply dipping (jointed) peridotite layers in the synform limbs became gravitationally unstable and collapsed, yielding a chaotic breccia in the synform hinge-zone.

Remarkable features, specific to the giant dyke between the coast at Itillip Saqqaa and the tripyramidal peak 3 km farther west-south-west, were given the field-name the 'troll's smile'. These features comprise crescent-shaped peridotite bodies between 5 and 10 m long and up to 3 m thick, concave-up (as seen in dyke-parallel exposures) within the pale-coloured troctolites. The crescents exhibit a crude columnar jointing, normal to their margins, which gives the fanciful appearance of a smiling mouth whilst the jointing gives the impression of irregular teeth (Fig. 33). These features are interpreted to be cross-sections of fan-like olivine-rich bodies that propagated downwards and inwards from the dyke side-walls at *c*. 90° to their strike. To explain the 'troll's smile' phenomenon it is proposed that snowflake cumulus cascaded continuously down the thermal boundary layers to accumulate on pre-existing crystallising cumulus, to form a 'sedimentary' pediment sloping down to the median axis. This process would have been unsuspected had it not been for the sidewall foci where plagioclase nucleation failed, leaving olivine to crystallise and sink alone. Steep localised channels leading down normal to the dyke walls can be inferred, down which dense slurries of melt + olivine crystals would have flowed. The slurries initially excavated troughs in unconsolidated cumulus be-
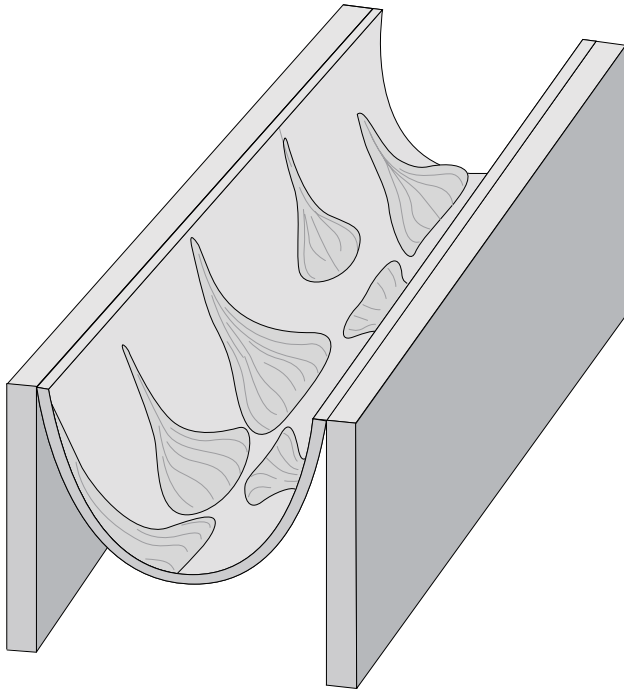
Fig. 34. Schematic section of the giant dyke illustrating the concept of localised 'sedimentary fans' descending from the side walls to spread out as they approach the synform axis.

Tripyramidal peak west-south-west of Itillip Saqqaa

Three kilometres west-south-west of Itillip Saqqaa, the northerly YGDC sub-branch underwent localised expansion ('ballooning') before abruptly narrowing to a third of its thickness (Fig. 10). The expanded section is less than 1 km long and gives rise to a characteristic tripyramidal peak. The reason for the thickness change is unknown; whereas the expanded section is composed of homogeneous troctolite, the thinned section west of it is strongly layered, exhibiting the same style of layering as at Itillip Saqqaa. In this section the limbs of a layered synform contains jointed peridotite layers that thicken down-dip (Fig. 35). This phenomenon is attributed to gravitational creep or saltation ('jumping') of cumulus olivines.

Itillinnuujuk

The northern sub-branch of the northern YGDC branch has a wedge-shaped termination a few kilometres farther west but then reappears on the island of Itillinnguujuk, where it is reduced to a width of 200 m (Fig. 10). The locality is of interest in showing a repetition, albeit in a narrower dyke section, of the features seen at Marraat. As at the latter, synformally layered gabbro (defined by modal layering) forms the central third of the dyke with the enclosing border groups composing the other two thirds. The radial growth ('snowflake' texture) of plagioclase

fore depositing their load of olivine crystals as velocities decreased. This formed peridotitic deposits that widened outwards toward the dyke axis. Morphologically such features may be compared to sedimentary alluvial fans (Fig. 34). Although no size analyses of the olivines have been made, the mean size of the crystals may be expected to increase downslope towards the axis.

Fig. 35. Peridotite layer with oblique jointing, exhibiting characteristic down-dip thickening towards the synform axis.

Fig. 36. Typical small homogeneous dyke of dolerite. Nasaasarli, east coast, Tuttutooq.

(<5 m) dolerite dykes that can be traced for several tens of kilometres. Macdonald *et al.* (2010) presented an argument for some of the large Palaeogene dykes in southern Scotland having been arrested at fault planes that were acting as aquifers. Following the same line of reasoning it is suggested that, assuming the giant dyke branch was being propagated with a strong west-south-westerly component, the halting of the bulk of the magma resulted from water-cooling at the crush zone. A portion of the magma, however, was able to penetrate beyond it, forming the dyke swarm.

around olivine nuclei is again well shown. The locality is the most extreme westerly one at which a synformally layered 'pod' is developed within the YGDC.

Figure 16 shows the variability in the cross-sections of the YGDC along its outcrop.

Minor offshoots from the giant dykes

There are many smaller basaltic dykes parallel to the YGDC that are regarded as offshoots from it (Fig. 36). A notable example is seen where the magma of the southern sub-branch of the southern YGDC branch, inferred to have been propagating in a westerly direction, encountered a crush zone in the Julianehåb granite. Here it was not completely stopped but continued westwards beyond the crush as a comb-like swarm of a dozen or more small

Narsaq gabbro and lopolithic relicts

The mildly alkaline gabbros cropping out at Narsaq and along the Nuugaarmiut peninsula to its north were referred to as essexites by Ussing (1912) and as essexite gabbros by Wegmann (1938). The outcrop has a generalised NW–SE trend for some 3 km from the tip of the Nuugaarmiut peninsula to Fabriksbugt (Fig. 37). The petrography and internal structures have such close affinity with those of the Tugtutôq giant dykes (*c.* 5 km to the WSW) as to remove doubt that these gabbros are integral components of the Younger giant dyke complex. To the west, the gabbro is bounded by the waters of the Narsaq Sund while to the east, it is truncated by the Narssaq syenite (Fig. 37).

Critical information on the relationship of the intrusion to older formations comes from two exposures on both sides of Niaqornaarsuk. The vertical contact between gabbro and Julianehåb granite (Fig. 38) does not have the regional ENE–WSW trend but is oriented be-
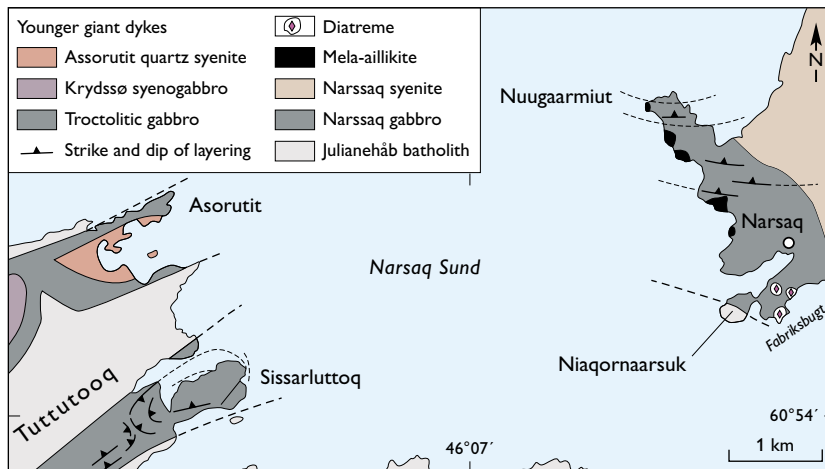

Fig. 37. Geological sketch map showing relationship of the giant dykes on eastern Tuttutooq to the gabbro outcrop around Narsaq and Nuugaarmiut.

Fig. 38. Vertical contact between gabbro (left) and granite (right of shadow in centre of image). West coast of Niaqornaarsuk near Narsaq. For location see Fig. 37.

tween ESE–WNW and E–W. It presents a well-chilled, fine-grained marginal facies with small subhorizontal pegmatitic segregations persisting for several metres from the contact. This contact is correlated with the southern contact of the YGDC on Sissarluttooq, described above.

At Fabriksbugt a contrasting exposure reveals a chilled contact of the gabbro dipping at a low angle against quartzite strata of the Eriksfjord Formation (Fig. 39). The fine-grained gabbro is crowded with plagioclase megacrysts and small xenoliths of anorthosite. Over the unexposed 1200 m between these two exposures the geometry of the YGDC clearly changed from that of a vertical dyke in the Julianehåb granite to a subhorizontal sill or lopolith at the unconformity between the granite

and the Eriksfjord Formation. In the vicinity of Narsaq, away from the contact zones described above, the gabbro is coarse (*c*. 1 cm) and mainly structureless, lacking lamination or modal layering. Anorthosite xenoliths, mostly <1 m, occur plentifully together with plagioclase megacrysts several centimetres across (Fig. 40). Many of the critical outcrops on glaciated slabs have later been covered by buildings as the town expanded.

The gabbro in and around the oldest part of Narsaq has been pervasively affected by hydrothermal alteration that caused sericitisation of the feldspars and replacement of the olivines, pyroxenes and biotites by chlorite and epidote. The alteration is ascribed to low-temperature fluids exuded during crystallisation of the cross-cutting

Fig. 39. Chilled margin of the Narssaq gabbro, crowded with plagioclase megacrysts and scarcer anorthositic xenoliths up to 5 cm large. Fabriksbugt, Narsaq.

Fig. 40. Anorthosite xenolith (*c*. 25 cm across) and plagioclase megacrysts, Narsaq township.

Narssaq syenite (described below). Traced north-westward into the Nuugaarmiut peninsula the alteration, and also the anorthositic xenoliths and associated megacrysts, disappear and the gabbros acquire a layered structure shown by plagioclase lamination and conformable, but discontinuous, mafic layers. The layers consist of concentrations of olivine, apatite and magnetite: in one such layer the mode was 12.5% plagioclase, 50% olivine, 30% titanomagnetite and 7.5% apatite. Plagioclase within these mafic layers shows a higher degree of lamination than those in the average gabbro suggesting that density winnowing by flowing magma was responsible both for the concentration of heavy minerals and the lamination (Upton 1961). Sharp changes in dip and strike of the layering features and the truncation of the mafic layers by shear zones reflect penecontemporaneous tectonic or gravitational instabilities within incompletely solidified cumulates. The layering strikes approximately E–W with dips to the north of between 10° and 40° (Fig. 37). Assuming a generalised dip of 25°, the total stratigraphic thickness of these cumulates is roughly 530 m. Whilst the more southerly, unlayered gabbros, with their content of anorthosite xenoliths and plagioclase megacrysts, are inferred to lie close to the intrusion roof, it is only at deeper levels, i.e. in the more northerly outcrops, that modal layering developed.

Between Narsaq and the Ilímaussaq intrusion there are several gabbroic masses which are inferred to be xenolithic relics of former easterly extensions of the Narssaq gabbro. The largest of these are on the 681 m mountain (Qaqqarsuaq), to the east of the town and on the Talut ridge close the western contact of the Ilímaussaq intru-
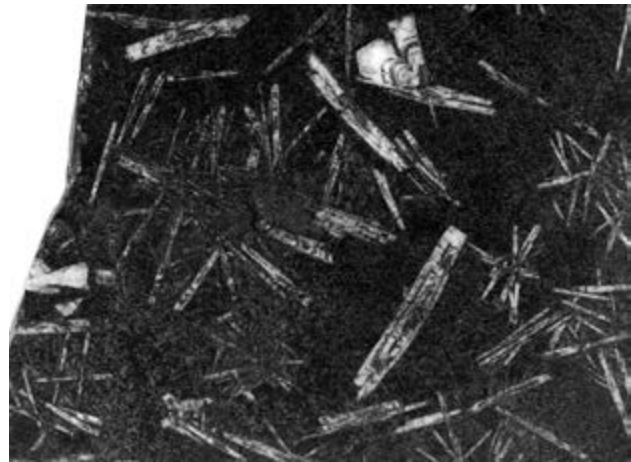
Fig. 41. Polished slab 6.5 cm wide of rapidly cooled dolerite at Qaqqarsuaq with quenched, skeletal and concentrically zoned plagioclase megacrysts and phenocrysts. Some of the latter occur as 'snowflake' glomerocrysts.

sion. These are interpreted as part of one or more sheets, at least 100 m thick, the tops of which have been eroded (Bridgwater & Harry 1968 and references therein). Fast-chilled facies contain skeletal plagioclase phenocrysts, some as 'snowflake' aggregates (Fig. 41).

Anorthosite, gabbro-anorthosite xenoliths and plagioclase megacrysts also occur as inclusions in the intrusions younger than the YGDC. Some 8 km north-east of Narsaq gabbroic anorthosite containing abundant feldspar megacrysts occurs as rafts in the Ilímaussaq lujavrite on Kvanefjeld, and isolated fragments of anorthosite and laminated gabbro are known from the Ilímaussaq augite
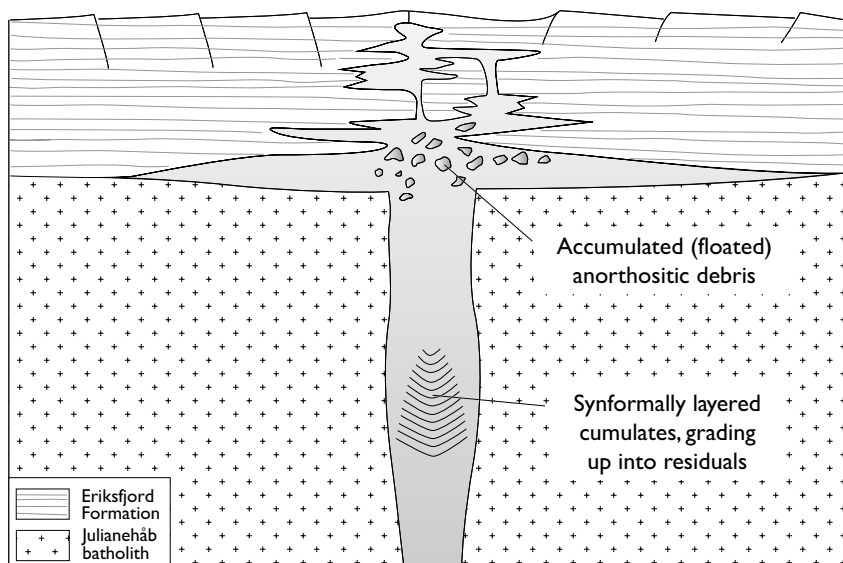
Fig. 42. Hypothetical cross section of the giant dyke and overlying intrusions. Not to scale.

syenite (Hamilton 1964; Sørensen 2006). The quantities of anorthosite xenoliths and plagioclase megacrysts in these occurrences support other observations that they came from high structural levels in the gabbro and had been concentrated as a result of flotation. Whereas the great bulk of the original gabbroic intrusion, of which they are considered to have been a part, was engulfed by younger, syenitic and granitic magmas, these relatively low-density roofing facies containing feldspathic rocks failed to sink. Figure 42 presents a hypothetical cross section, showing a giant dyke expanding into a lopolith at the Julianehåb granite–Eriksfjord Formation unconformity, with overlying 'cedar-tree' laccolithic extensions into the overlying supra-crustal strata. Whilst the original extent of this lopolith is a matter for speculation, the relics in the Narssaq and Ilímaussaq intrusions suggest that it may have measured some 10 km north-west–south-east and extended a similar distance north-eastwards.

Younger giant dyke extensions west and north of Motzfeldt Sø

Gabbroic giant dykes crop out from 25 to 60 km east-north-east of Qassiarsuk in Mellemlandet and the nuna-taks west and north of the Motzfeldt complex (Fig. 10). The widths, courses, compositions (Table 2) and internal structures of these so closely resemble those on Tuttutooq as to leave no doubt that they are easterly components of the same intrusion.

These giant dyke extensions are, however, sinistrally offset (c. 20 km) from the Tugtutôq dykes by faulting. Two approximately E–W-trending, left-lateral faults, or fault systems, were responsible. The southernmost of these faults across the Ilímaussaq peninsula controlled the emplacement of the Narssaq complex described in a later section. Displacement along this fault is inferred to have shifted the YGDC intrusion some 10 km to the west so that its outcrop is now almost wholly concealed by the waters of the Bredefjord. This section of the YGDC would remain wholly hypothetical if it was not for a short section of gabbroic dyke cropping out a few kilometres west of Qassiarssuk at Kangerlua (Fig. 10).

Another c. 10 km of translation to the west was probably brought about by a more northerly fault system that traverses the Qassiarsuk and South Qooroq areas (Fig. 10). On the eastern side of northern Tunulliarfik there is a deep gorge, co-linear with the giant dykes to the east-north-east in Johan Dahl Land (Walton 1965),

the outflow from which contains troctolitic boulders. Consequently the continuation of one of the giant dyke branches is inferred in this sector.

Three giant dyke branches traverse G.F. Holm Nunatak but only the southern branch of these is continuous south of Nordtop from Sydtungegletscher to Syenitknold. From its absence on Mellemlandet (to the WSW), this branch is presumed to pinch out beneath the Qooqqup Sermia glacier. The middle branch on G.F. Holm Nunatak is absent on the Nordtop nunatak, having terminated to the west-south-west of G.F. Holm Nunatak. The northern branch is presumed to underlie the ice just north of Nordtop, traversing the northern part of Mellemlandet (Fig. 10) to the WSW and on through much of Johan Dahl Land, but failing to reach the fjord section north of Narsarssuaq.

The east-north-east extensions of the YGDC have vertical, typically parallel sides and maintain more-or-less constant widths of 300 to 600 m. They can, however, attenuate to zero thickness over a distance of one or two kilometres as exemplified by the southern dyke branch on Mellemlandet (Fig. 10). Internal differentiates are restricted to the southern dyke branch between Sydtungegletscher and Syenitknold where there are two remarkable developments ('pods') of layered cumulates in the axial part of the intrusion, comparable to those described above from Tuttutooq.

The giant dykes close to the Inland Ice appear to be simple dilational dykes. The combined thickness of the three giant dyke branches at their east-north-eastern-most outcrops is closely similar to that of the two branches at the east-north-east end of Tuttutooq and it is probable that the branches continue, beneath the Inland Ice, to the east coast of Greenland. Their marginal facies (2–5 m wide) have been generally affected by back-veining from re-melted country-rock granitoids and granitic gneisses with considerable evidence of hybridisation. Otherwise, within 10 m of their contacts they tend to be chilled to homogeneous medium-grained dolerites, grading inwards to coarse-grained mesocratic troctolite (Fig. 43).

Plagioclase lamination and modal layering within the coarser-grained axial parts define symmetrically developed synclinal structures in which the dips vary from steep at the margins to horizontal along the dyke axis, much as described by Walton (1965) for the giant dyke in Johan Dahl Land. Figure 44 shows parallel modal layering in the southern branch across Mellemlandet whilst textures in the laminated gabbro are shown in Fig. 45.
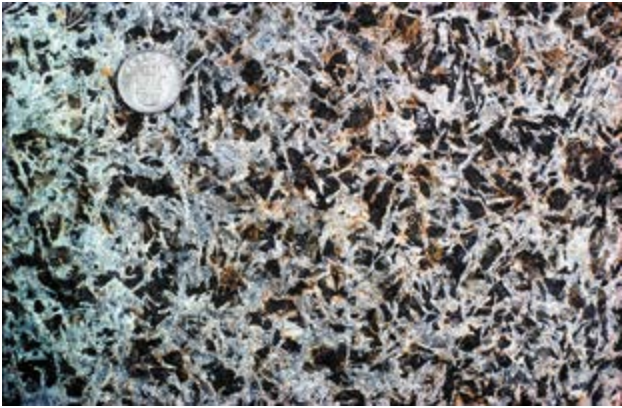
Fig. 43. Coarse troctolite, Syenitknold. Diameter of coin 2.5 cm.

Sydtungegletscher and Syenitknold

In the southern giant dyke branch, at the Sydtungegletscher, well-layered syenogabbros form an axial pod, distinguished from the troctolitic host by their dark colour (due to high content of magnetite) and the presence of prismatic clinopyroxenes. Modal layering shows normal grading with erosional troughs filled with mafic cumulates, providing evidence for vigorous magma flow, reminiscent of features at Itillip Saqqaa on Tuttutooq.

Approximately 3 km to the west-south-west at Syenitknold, immediately east of Qooqqup Sermia, is one of the most remarkable occurrences of differentiated rocks within the YGDC. The course of the dyke makes an abrupt change so that the outcrop on the map resembles a duck's head pointing into the glacier. On this analogy, the 'head' and 'body' of 'the duck' are 600 m wide. Sym-metrical border zones of troctolite, carrying plagioclase megacrysts, enclose a central 300 m of mesocratic augite syenite that is traceable east-north-east to the 'neck' for *c.* 1 km. The Syenitknold occurrence has much in common with that at Asorutit on Tuttutooq. However, at the latter the syenite is silica oversaturated, with filter-pressed, pegmatitic alkali granite residuals whereas the Syenitknold syenite contains intercumulus nepheline. Coarse-grained veins of nepheline syenite, containing aegirine, late-stage fluorite and calcite, intruding the adjacent troctolite, are undersaturated counterparts to the granites in and around Asorutit. The syenite is separated from the troctolite by a rusty-weathering zone several metres broad of ferro-syenogabbro grading to ferrosyenite, the colour being due to the high content of magnetite and fayalitic olivine. Although these differ texturally from the iron-rich syenogabbroic zones that separate troctolite from syenite at Asorutit, (e.g. in lacking dendritic pyroxenes) they represent analogous phenomena.

Modal layering in the augite syenite dips symmetrically in towards the axial plane; the layering involves rhythmically developed normally-graded units, 10–15 cm thick, in which the bases are defined by melanocratic layers rich in ferromagnesian minerals, passing up into more leucocratic tops. These graded layers are separated by homogeneous layers *c.* 0.5–1 m thick (Fig. 46). Although the Gardar intrusions as a whole display a wide variety of layering styles, this style is unique to the Syenitknold syenite and closely resembles that of the Upper Zone ferrogabbros of the Skaergaard Intrusion (Wager & Deer 1939).

Fig. 44. Parallel layering in the southern branch of the giant dyke in Mellemlandet.

Fig. 45. Lamination in a polished slice of gabbro from Mellemlandet. Traces of 'snowflake' plagioclase growth are discernible in some areas. Width of sample 8 cm.

facies of the giant dyke that detached along a subhorizontal joint before collapsing into the underlying residual magma. The latter, which from the mineralogy of the syenite is inferred to have had a benmoreitic to trachytic composition, would have had a density lower than its already crystallised gabbroic roof. A slab of this is inferred to have peeled loose and sunk, finally coming to rest on the upgrowing syenite cumulus. The situation envisaged is shown diagrammatically in Fig. 48. The situation described here is reminiscent of that described from the Poe Mountain anorthosite, Labrador, where anorthositic/leucogabbroic blocks that may have come from a now-eroded roof zone sank through resident magma to be arrested on the upgrowing cumulus floor (Scoates 2000).

A significant feature at Syenitknold is the presence, more or less centrally within the syenite, of a crudely tabular, gabbro inclusion estimated to be 50 m thick and 100 m across (Fig. 47). Although the upper contact has been eroded, it is surmised that this slab was formerly overlain by the syenite and that it composes a large autolithic inclusion of a distinctive gabbro facies. It differs from the host gabbro in being highly feldspathic, containing an abundance of large (up to 20 cm) anhedral plagioclases surrounded by darker olivines.

The gabbroic slab is texturally similar to the roofing facies of the gabbro at Narsaq (described above) and is accordingly presumed to have been part of the roofing

Fig. 46. Layering in the Syenitknold syenite. The thin layers, differentiated into melanocratic bases and leucocratic tops, are separated at regular intervals by thicker layers of typical unsorted syenite.

Fig. 47. Conformable gabbroic layer within layered syenite at Syenitknold forms the prominent dark unit in the middle distance.
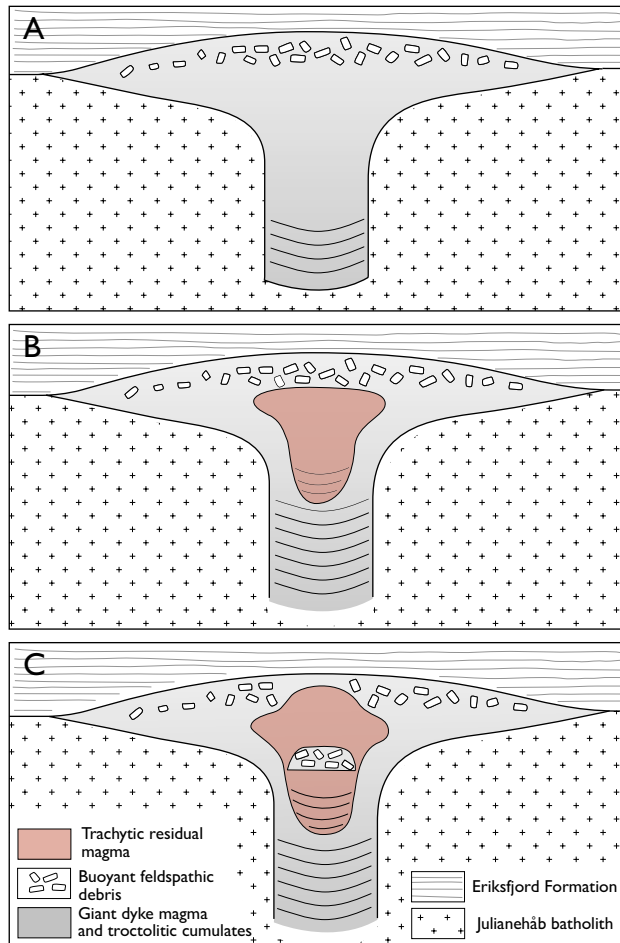
Fig. 48. Interpretive sections of the geological evolution at Syenitknold. **A**: The giant dyke spread out into a laccolithic or lopolithic body at the unconformity between the Julianehåb batholith and the overlying Eriksfjord Formation. Buoyant feldspathic debris from a deep-lying anorthositic protolith accumulated close to the roof. **B**: The dyke cooled from the sidewalls, while layered synforms grew up from the floor, eventually yielding a trachytic residual magma towards its apex. **C**: The density of the residual magma was now less than that of the crystallised roof, a portion of which detached to become embedded within upgrowing syenite cumulus.

Central complexes and late dykes

Klokken complex

The Klokken complex is a stock, approximately oval in plan, (4 km west-north-west–east-south-east × 3 km north-north-west–south-south-east), aligned transverse to the Tuttutooq–Ilimmaasaq–Narsarsuaq lineament and in an isolated position (Fig. 49; Blaxland & Parsons 1975; Parsons 1979). It has been U-Pb dated at 1166 ± 1.2 Ma (Table 1), and has a $^{87}Sr/^{86}Sr_i$ of 0.7031 ± 0.0003 (Blaxland *et al*. 1978). The complex has a concentric tripartite structure, the three parts crystallising in sequence inwards. It comprises an outer zone of gabbro (incomplete at the present level of exposure) up to 400 m broad, partially surrounding a broader zone (up to 900 m) of unlaminated syenite. The circular core (*c*. 2.5 km diameter) of the complex consists of strikingly layered syenites (Fig. 50) penetrated in the focal area by a small intrusion of quartz-bearing biotite syenodiorite.

Fig. 49. Geological map of the Klokken complex. Modified from Parsons (1979).

Marginal gabbro

A cross-section and partial cross-section of Klokken are shown in Fig. 51. The gabbro has near-vertical chilled contacts against the granite-gneiss country rocks. Some assimilation between the gabbro and its wall rocks, however, precludes analysis of chilled marginal samples to give approximations of the initial magma composition. Evidence from wall-rock pendants suggests that the gabbro body narrows upwards, as depicted in the cross-section that also supposes the complex to be subvolcanic (Fig. 51A).

The mechanism of emplacement remains enigmatic; xenoliths of gneiss do not accord with ring-faulting and caldera collapse but suggest a process more akin to stoping. Apart from gneiss xenoliths the gabbros contain plagioclase megacrysts (high-pressure phenocrysts?) and anorthosite xenoliths that will be described in a later section. Within the chilled zone Parsons (1979) described development of a wavy pyroxene facies resembling that in the marginal border group of the Skaergaard intrusion (Wager & Deer 1939). The latter facies has recently been interpreted by Humphreys & Holness (2010) as formed by partial gravitational collapse of crystallising border group cumulates. There are also some subvertical layer-

ing features, similar to those of channel-fill structures in sedimentary rocks, indicative of magma flow parallel to the sidewalls together with inward crystallisation. The gabbro, where unaffected by hybridisation, is characterised by stellate clusters ('snowflakes') of plagioclase. This feature, very similar to that seen in the YGDC on Tuttutooq, is indicative of rapid growth of plagioclase from a melt super-saturated with respect to plagioclase. Like the YGDC gabbros, those of Klokken are troctolitic, with late and subordinate crystallisation of augitic pyroxene.

Syenogabbro and unlaminated syenite

At high structural levels the marginal gabbro grades into syenogabbro and unlaminated syenite whereas at lower levels there is a distinct break (Parsons & Brown 1988). Modal layering features within it are scarce but those that do occur strike parallel to the contact and are vertical or outward-dipping in the outer section but inward-

Fig. 50. Oblique aerial photograph of the central part of the Klokken complex. The steep escarpments are formed by granular syenite, separated by crumbling, rusty-weathered, laminated syenite.
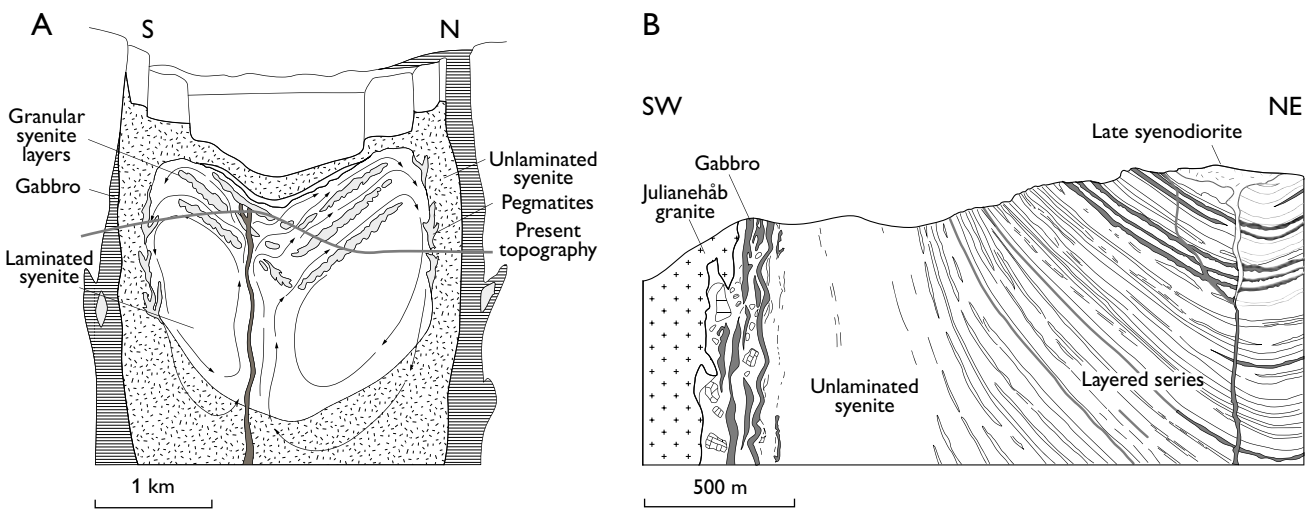
Fig. 51. **A:** Cross-section of the Klokken complex, postulating an overlying caldera. Arrowed flowlines indicate inferred late-stage convection of hydrothermal fluids. Modified from Parsons & Becker (1986). **B:** More detailed partial section illustrating relationships between country rocks, gabbro, unlaminated syenite and the layered syenites of the central region. Modified from Parsons & Brown (1988).

dipping farther in. The unlaminated syenite grades, over 30–100 m, into the central layered series. There is, however, strong cryptic variation within the unlaminated syenites; the Fe/Mg ratio of the ferromagnesian minerals increases and the feldspars become increasingly Ca-poor and K-rich. The compositions indicate that these progressed in growth from plagioclase through ternary feldspar to sanidine, with subsequent development of exsolution lamellae. Feldspar pairs indicate temperature decreases from 950°C in the outer syenogabbros through 910°C in intermediate syenodiorites to 900°C or less in the syenites (Parsons & Brown 1988).

The significance of the break from marginal gabbro to the unlaminated syenite remains debateable. Whereas there is no obvious evidence for influx of a more evolved magma, variation in the width of the gabbro sheath and its absence from the southern perimeter suggests that the gabbro underwent thermal or mechanical erosion by new magma. Comparable unexplained relationships have been noted above for the OGDC. By contrast, the unlaminated, granular and laminated syenites are all considered to have grown from a single magma chamber. The transition from unlaminated syenite to the central strongly layered syenites is interpreted as marking the change from sidewall cumulate ('marginal border group') to lower-angled, centrally directed layered rocks and is analogous to the relationships within parts of the YGDC (e.g. Syenitknold). Studies of intrusions in which both 'marginal border group' and inward-dipping layered cumulates occur, e.g. Skaergaard (Wager & Deer 1939; Wager & Brown 1968) and parts of the the YGDC, lead to the conclusion that two processes occurred more or less concurrently. Crystallisation against the sidewall thermal boundary layer dominated the early stages when heat-loss was higher, and 'sedimentary' upgrowth of cumulus talus, descending gravitationally alongside the boundary layer, occurred when thermal insulation was well established. In the first, the growing crystals remained attached to the sidewall whereas in the latter, they were carried down in relatively dense crystal-melt slurries to accumulate above the hypothetical hidden series.

At Klokken, as in the YGDC and several other Gardar cumulate sequences, the factors controlling the relative thicknesses of marginal border groups and central layered series are unknown. Extremes range from those that lack any discernible marginal border group (e.g. Itillip Saqqaa, Tuttutooq (Upton 1987) and the western stock of the Kûngnât complex (Upton *et al.* 2013) to cases where marginal border groups are well developed (e.g. Asorutit, Krydssø and Itillip Saqqaa).

Central layered series

The core of the Klokken complex is characterised by a layered sequence dipping 30–50° towards a central focus, providing a 650 m thick stratigraphic succession. What makes the central layered series outstanding among all the layered Gardar intrusions is the intercalation of more weathering-resistant layers of granular syenite with less resistant and coarser laminated syenites that compose *c.* 15% of the series (Figs 50–52).

The laminated syenites show extreme modal layering with inverse grading. Here, felsic layers grade upwards into nearly monomineralic pyroxenite layers composed of hedenbergite (up to 90% modal hedenbergite) with interstitial alkali feldspar and titanomagnetite (Parsons 1979; Fig. 53). Furthermore, in places the top (<10 cm) of these inversely graded layers consists almost wholly of fayalite with minor hedenbergite and with interstitial magnetite, amphibole, biotite and alkali feldspar. This rhythm is only completely developed at certain horizons. The mafic/ultramafic upper parts of these layers are orthocumulates in which there is contrast in crystal size between the large tablets of alkali feldspar and the smaller pyroxenes (*c.* 5 × 1 × 1 mm) and the still smaller fayalites (approximately isometric at *c.* 1 mm). A further notable feature is the high degree of modal sorting. Some pyroxene layers contain >90% hedenbergite but no olivine whereas the olivine-rich layers may contain >90% fayalite.

In the inversely graded layers the cumulus phases have slightly more evolved compositions than the same phases in either normal rock or when present as an intercumulus phase in adjacent parts of layers. The layering is attrib-

Fig. 52. Polished surface (width 10 cm) of laminated syenite from the Klokken layered series.
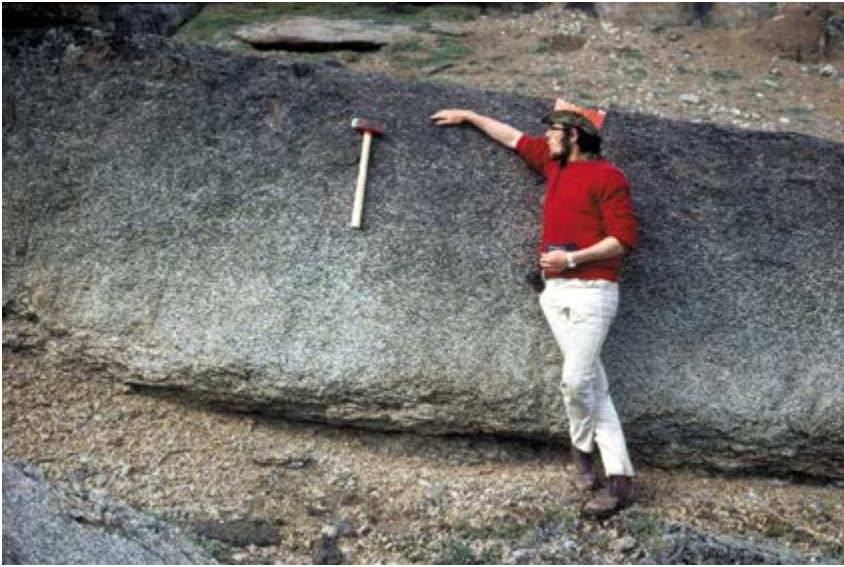
Fig. 53. Layer in the laminated series, central Klokken complex, showing inverse grading from feldspathic base to fayalite-rich top.

uted to varying degrees of undercooling in a magma in which all phases exhibit a narrow crystallisation interval, and which was subject to rhythmic build-up of pressure followed by sudden pressure releases. Crystal accumulation took place under near-stagnant conditions in a thin chamber immediately beneath the roof of the intrusion (Parsons 1979).

The granular syenites contain sparse phenocrysts of alkali feldspar and the individual units tend to become coarser down the sequence. Although there is some feldspar lamination in the lowest units, the granular syenites remain distinct from the enclosing laminated syenite. In the uppermost 100 m of the section, the granular units dominate over the intervening laminated syenites. Compositionally, they become increasingly evolved from the highest to the lowest units, showing a regular cryptic variation downwards from more primitive to most evolved while also showing an increase in grain size. The units are interpreted as successive slices of roofing cumulates (i.e. an 'upper border group'), and the latest (highest) unit may represent a reasonably close approximation to a chilled facies beneath a roof. Slabs or slices of units are presumed to have detached serially as planar joints developed during crystallisation, and sank, while retaining mechanical coherence, to become enveloped in the upgrowing cumulus pile that gave rise to the laminated syenites (Parsons 1979).

In contrast to the strong fractional crystallisation reflected in the granular roofing cumulates, there is only slight cryptic layering in the laminated syenites. It is presumed that there was a sandwich horizon at which well-equilibrated downward- and upward-growing roof and floor sequences met. A hidden layered sequence underlying the lowest laminated syenites is inferred. Thus the alternating sheets of the two contrasted syenite types composing the layered central series may be likened to two packs of cards interleaved by a dealer. The granular syenite units were repetitively detached from downgrowing roofing cumulates, whilst the laminated syenites were upgrowing floor cumulates onto which the granular syenite slices came to rest. It may be assumed that the density of the resident magma in the central chamber decreased with time, whereas the density of the roofing rocks with which it was in contact, increased as more and more primitive layers were exposed to it as the detachment continued. That the evolving laminated syenite cumulus remained ductile (or mushy) as the granular syenite slabs settled into it is shown by the development of load structures beneath them (Fig. 54). The repetitive detachment and settling of roof cumulates evidenced in the Klokken core syenites illustrates the same process described above for the detached roofing block at Syenitknold. And, as will be described below, a precisely similar phenomenon took place in the Ilímaussaq agpaites.

Feldspar studies indicate a cooling rate for the syenites of 600 to 500°C in 10^4 years (Brown et al. 1983). Although the laminated syenites are deduced to have generally formed as a result of crystals settling in near-tranquil magma, evidence that there were sometimes disturbances is provided by some erosional 'trough and fill' features and cross-bedding. Rare, normally graded layers are believed to have originated from gravity sorting

Fig. 54. Load-balls of granular syenite surrounded or penetrated by 'flames' from unconsolidated laminated syenite. Central Klokken complex. Hammer *c.* 30 cm long.

through current flow. The Klokken pyroxenes exhibit a continuum from relatively diopside-rich augites in the gabbros to sodic hedenbergites in the more evolved syenites. The colours change from purplish-brown (in gabbros and unlaminated syenites) to greenish-brown (in upper granulated syenites), apple green (in hedenbergite-rich laminated syenites), to deep green sodic hedenbergites (in the lower section of the laminated syenites) and pale green in the late quartz syenites. The more evolved rocks show enrichment in acmite, and in quartz-bearing aplites the pyroxene compositions lie close to end-member acmite (Fig. 55).

That so many features of Klokken are replicated in the YGDC leads to the conclusion that the two intrusions were probably both coeval (Table 1) and comagmatic. The principal difference lies in their geometry: the YGDC involved narrow, elongate (dyke-type) magma chambers whereas that at Klokken was cylindrical. The compositional ranges, reflected in their respective mineralogies, in both are near-identical. However, whilst the Klokken syenites are almost critically saturated with respect to silica (although terminating in silica-oversaturated products), those of the YGDC vary from over- to undersaturated in silica. The chronological successions, from chilled gabbros sharing textural and petrographic features, via intermediate rock types within vertically layered border groups to syenite cumulates displaying inwardly dipping layering, are very similar at Klokken, Krydssø and Syenitknold described above. By analogy with evidence from the YGDC, the presence of anorthositic xenoliths in the Klokken gabbros may denote proximity to a roof zone in the gabbro.
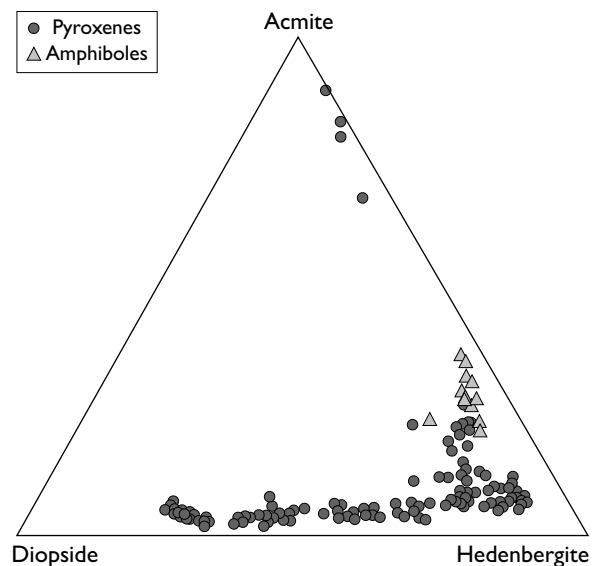

Fig. 55. Pyroxene and amphibole compositions in the Klokken complex shown in the acmite–diopside–hedenbergite ternary diagram. Modified from Parsons (1979).

Anorthosite xenoliths and plagioclase megacrysts in the YGDC and Klokken gabbros

Anorthositic xenoliths and plagioclase megacrysts occur in the troctolitic gabbros of both the YGDC and Klokken. At Syenitknold and Asorutit in the YGDC and also at Klokken (Fig. 56) they are restricted to the outer sheaths of gabbro but are absent from the syenites. At Asorutit the gabbro on the north side of the giant dyke contains a crowded array of anorthosite xenoliths up to 100 m across, essentially occupying the full width of the gabbro outcrop (Figs 57, 58). The xenolith-bearing gabbro has an apparently fault-bounded contact with the adjacent syenite and it is speculated that this fault downthrows to the NNW, bringing a distinctly high level of the gabbro into juxtaposition with the syenite. This hypothesis would explain the exceptional abundance of anorthositic material, if it is accepted that it is a near-roof facies of the gabbro, crowded with low-density plagioclase-rich material that has floated into place.

With increasing distance to the west-south-west along the northern branch of the YGDC on Tuttutooq, anorthosite xenoliths and plagioclase megacrysts become scarcer and are absent beyond Store Pilesø (Fig. 5), consistent with the conclusion reached on other grounds that the 'Tugtutôq block' has been tectonically tilted down towards the ENE so that, after erosion, shallower structural levels are seen in the east-north-east and deeper ones in the west-south-west. Thus, at both the Klokken and Tugtutôq complexes, it is concluded

Fig. 57. Laminated anorthosite xenolith on the Asorutit peninsula, eastern Tuttutooq. The dark intercumulus material is predominantly olivine. Sections on scale are 5 cm long.

Fig. 58. Photomicrograph (crossed nicols) of laminated anorthosite from Asorutit. It is an orthocumulate comprising cumulus labradorite and intercumulus material mainly consisting of poikilitic olivine. Plagioclase crystals up to 12 mm long.

Fig. 56. Anorthosite xenolith in the marginal gabbro of the Klokken complex, showing anhedral plagioclase, typically with hydrothermally altered mafic minerals in the interstices. Pocket knife 10 cm long.

that the anorthosite-bearing facies were concentrated towards the top of the intrusion. The anorthositic xenoliths commonly occur together with discrete plagioclase megacrysts up to 0.5 m long. The megacrysts are divisible into cleavage fragments presumed xenocrystal from disintegration of anorthositic autoliths, and subhedral crystals regarded as high-pressure phenocrysts. In the outcrops on the south-eastern side of Fabriksbugt at Narsaq, the marginal facies of the gabbro at Narsaq contains abundant fragments of plagioclase together with some anorthosite xenoliths; similar material is well exposed in road-cuts in the vicinity. Anorthosite xenoliths (Fig. 40) are abundant around Fabriksbugt and extend northwards in decreasing amounts past Narsaq and are

absent on the Nuugaarmiut peninsula. These observations lead to the conclusion that the xenoliths and megacrysts arrived at their present position through flotation in the troctolitic magma (Bridgwater 1967; Bridgwater & Harry 1968).

As related above in the section dealing with giant dykes north of Motzfeldt Sø, the large gabbroic autolith crammed full of feldspathic debris that occurs centrally within the syenites of the Syenitknold is interpreted as derived from a roofing facies within which low-density anorthositic material had accumulated. By the time that a residual low-density body of trachytic magma had been generated beneath the roof, a slab of the roof detached and sank to be arrested within the accreting syenite cumulates. At each of these three localities, the plagioclase-rich fragments occur in close proximity to syenite. As the fragments are regarded as indicative of shallow levels in the intrusions, their occurrence is compatible with the conclusion that the syenites were themselves late-stage, shallow-level products generated above upward-grown sequences of gabbroic cumulates.

shown sympathetic downflow. In more evolved melts, in which magnetite had joined the cumulus assemblage, the residual melt would have been more buoyant than the bulk magma and the two effects would then have been antipathetic. However, the evidence throughout all facies of the dyke points to sidewall, two-phase convection in which the crystal-melt slurries were driven by the relatively high modal contents of iron-rich olivines as illustrated diagrammatically in Fig. 34. Whereas the giant dyke chambers commenced with a tabular, deep and narrow morphology, their geometry would have changed continuously until, in the latest stages (as exemplified by the Syenitknold syenites) the residual chamber would have become broad and shallow (Fig. 59). Similarly (e.g. at Klokken), a magma chamber that initially approximated to a deep cylinder with a relatively small diameter would have evolved to a disc-shaped chamber with a quite different aspect ratio. There are indications of a similar morphological evolution of chamber floors at the Igdlerfigssalik complex (see below), an evolution that has relevance also at the Ilímaussaq complex.

Origin of synformal layering in the Younger giant dyke complex

The layered pods along the YGDC branches exhibit a remarkable variety of layering styles. Using an estimated density of 2.8 g/cm³ and a viscosity of 150 poise (g/cm⁻¹/sec⁻¹) for the initial YGDC magma, Mingard (1990) calculated a Rayleigh number of c. 10^{16} and concluded that convection would have been turbulent. However, many of the features observed are best interpreted as products of two-phase (i.e. crystals + melt) convection and, in the more primitive western parts of the intrusion, thermal and compositional convection would have been complementary. Why vigorous two-phase convection occurred only at highly localised nodes along the dyke branches remains enigmatic. Slurries of crystals + melt, generated in the vicinity of the dyke walls, are postulated to have descended towards a central 'valley' within the relatively narrow, deep and elongate magma chambers, the crystals being progressively deposited as slurry velocities decreased. A comparable process is thought to have operated depositing the coarse laminated syenites at Klokken. In the more primitive YGDC facies, as seen in western Tuttutooq, the relatively Fe-rich melt residual from olivine + plagioclase crystallisation would have been denser than the main magma body and would have
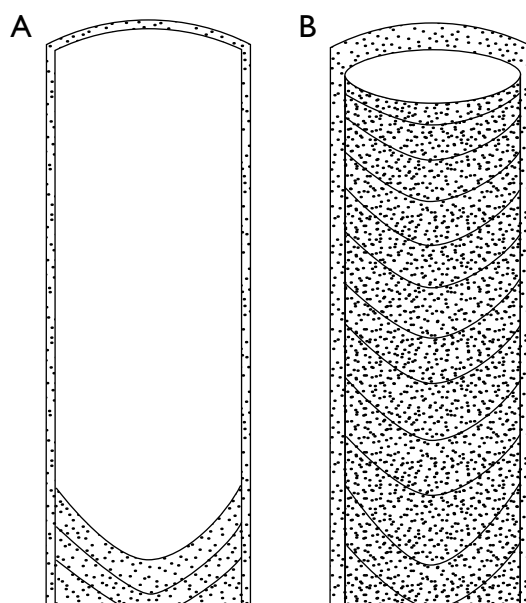

Fig. 59. Evolving cumulate morphology in a giant dyke or stock-like intrusion.

Mela-aillikites, carbonate-silicate rocks and carbonatites

Magmatism of an alien character, strongly contrasting with the more voluminous feldspathic Gardar igneous suites, occurred intermittently along the southern rift zone and involved ultramafic lamprophyre, carbonatite and carbonate-silicate magmas. Such magmas appear to have played a minor role at various times through Gardar evolution, and it is postulated that their sporadic recurrence was related to episodic replenishment events as new basaltic magma was introduced into the deep lithosphere, mobilising readily fusible metasomites (Upton *et al.* 2006). These aberrant low-silica magmas gave rise to small hypabyssal intrusions (dykes, sills and plugs) and explosive diatremes. The aillikites contain 20–34 wt% SiO_2 whilst the more carbonate-rich rocks contain *c.* 2–10 wt% SiO_2. This has led to doubt as to whether there is a compositional discontinuity or a continuum, possibly reflecting variable degrees of melting in mantle metasomites (Upton & Fitton 1985).

There are several lines of evidence pointing to a genetic relationship between the ultramafic lamprophyre and carbonate-rich rocks in the Gardar Province in general, and specifically demonstrated by Stewart (1970) and Andersen (1997, 2008) for the Qassiarsuk volcanic complex. The latter took part in the Older Gardar activity and has been correlated with the lowest lava member (Mussartût Member) by Andersen (1997). Ultramafic aillikitic lavas and sills occur at several horizons within the Eriksfjord Formation (J.G. Larsen 1977; Upton *et al.* 2006).

Although it is commonly impossible to ascertain their precise chronology, some of the ultramafic magmas appear to have been closely associated with the activity along the younger Gardar southern rift. Some ultramafic lamprophyre dykes on Mellemlandet and in the vicinity of Syenitknold cut benmoreite and trachyte dykes, thus establishing their Younger Gardar provenance. However, other similar dykes north of Narsarsuaq in west-south-west Mellemlandet are cut by Younger Gardar doleritic and trachytic dykes confirming the conclusion that such silica-deficient magmas were capable of intrusion over a considerable time period (Upton & Fitton 1985). The observation that ultramafic dykes are present as integral components of the Younger Gardar Main dyke swarm is itself strongly suggestive that they are all of Younger Gardar provenance.

The age of many of these dykes relative to other Gardar intrusions is unknown but their trend and presence within the Main and Igaliko dyke swarms makes a Late Gardar age probable. Moreover, small carbonatite dykes cut even the youngest parts of the Igdlerfigssalik complex which is among the latest major intrusions in the Gardar Province (Table 1). Accordingly, as was noted by Emeleus & Harry (1970), carbonatites occurred throughout a very wide span of Gardar time.

Mela-aillikite intrusions in the Narsaq area and on Tuttutooq

Several small intrusions near Narsaq comprise ultramafic, silica-deficient alkaline rocks that fall under the definition of ultramafic lamprophyre (Rock 1991). They contain >80% (modal) of ferromagnesian silicates and oxides, conferring a colour index of >90. Earlier literature referred to them as jacupirangites (Ussing 1912) or biotite pyroxenites (Upton 1966; Upton & Thomas 1973) but here, following Rock (1986, 1991, 1997) and Tappe *et al.* (2005) they will be described as mela-aillikites, i.e. ultra-potassic (K_2O/Na_2O >3) ultramafic lamprophyres. The field relationships of the mela-aillikites described below leaves little doubt for considering them as post-dating YGDC but pre-dating the Main dyke swarm.

The mela-aillikites are anomalous texturally, mineralogically and geochemically with respect to the majority of Gardar igneous rocks. Typically they are very fine-grained (50–500 μm) and petrographically very fresh. There are five outcrops of these ultramafic rocks along the west-facing coast of the Nugaarmiut peninsula, from the extreme north-west end of the peninsula to *c.* 1 km from the centre of Narsaq (Fig. 37). As all five lie approximately at the same stratigraphic level in the host layered gabbros, they may represent protrusions of a conformable, though somewhat irregular, sill-like body (Upton & Thomas 1973; Upton *et al.* 2006). Another, poorly exposed, mela-aillikite occurs on the east side of Narsaq township at the water tower. Here the mela-aillikite is adjacent to a diatreme containing angular clasts of quartzite (presumed Eriksfjord Formation) and black mafic rock (possibly recrystallised basalt?). Yet another (unstudied) occurrence lies on the coast of Tunulliarfik, a few kilometres south-east of Narsaq.

Silica activities were too low for feldspars to crystallise whereas perovskite is a common accessory. Crystallisation occurred under oxidising conditions ranging from close to the quartz-fayalite-magnetite (QFM) buffer to just below the hematite-magnetite (HM) buffer. In the most highly oxidised facies the clinopyroxenes are bright
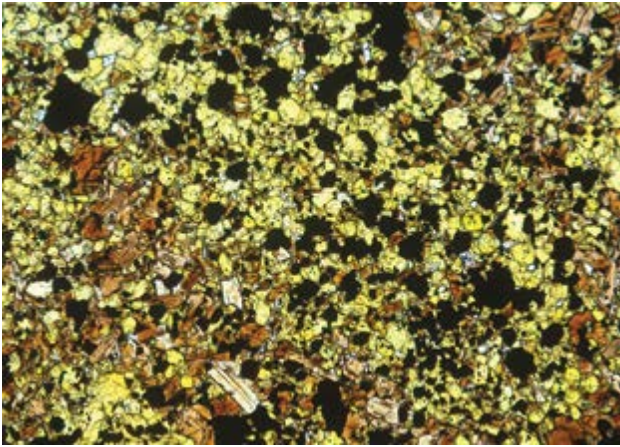
Fig. 60. Photomicrograph of a highly oxidised pyroxenitic facies in the mela-aillikites. Yellow: ferrian diopside. Brown to pale brown: phlogopite. Black: opaque oxides. Colourless: olivine and apatite. Field width 2.5 cm.

yellow, pleochroic ferri-diopsides (Fig. 60), and compositions of the accompanying olivines approach pure forsterite (up to Fo_{99}). Apart from other extreme compositions of otherwise common mineral species (very

Fig. 61. Complex, bilaterally symmetrical veins in mela-aillikite on Nuugaarmiut peninsula. Diameter of coin 2.5 cm.

Ba-Ti-rich biotites and Sr-rich kaersutites), the rocks also contain unusual igneous minerals including cuspidine and monticellite. Although the principal mineral assemblages appear stable at high temperatures (>600°C), the presence of serpentine, vesuvianite, epidote, chlorite and hydro-garnet indicates that crystallisation persisted to below 400°C (Craven 1985; Upton *et al.* 2006).

Compositionally, the rocks combine high contents of compatible elements (11–24 wt% MgO, 300–1000 ppm Ni and 100–1000 ppm Cr) with high contents of incompatible elements (Craven 1985). Such combination of compatible and incompatible elements is a characteristic of other similar rocks such as potassic ultramafic lavas and kimberlites.

Veining is a characteristic of the mela-aillikites. Complexly zoned veins showing bilateral symmetry, up to 10 cm wide, describe curviplanar courses commonly with intersecting flamboyant patterns. The forms of these veins indicate that they were emplaced at relatively high temperatures when their sidewalls were still ductile (Fig. 61). It is inferred that the veins mark former conduits for Ca-, Ba-, Sr-, F- and CO_2-rich fluids expelled from volatile-rich magmas during their terminal crystallisation.

Mela-aillikites are known from two localities on Tuttutooq. One is a vertical plug about 80 m in diameter that was intruded up the southern margin of the YGDC, where the latter narrows between the two differentiated pods at Asorutit and Krydssø (Fig. 16). Although itself very fine-grained, the mela-aillikite contains corroded olivine megacrysts and small peridotitic xenoliths. Meandering late veins, very similar to those of the Nûgârmiut intrusions, traverse the plug. The plug has largely obliterated an earlier diatreme containing clasts of partially melted Julianehåb granite, quartzite and black mafic or ultramafic rock. These relationships imply that an initial energetic release of gas preceded the ascent of the magma itself. The plug may represent a former conduit supplying a small monogenetic volcano.

The other Tuttutooq occurrence is a small body of indeterminate size and shape at the intersection of the OGDC and the northern branch of the YGDC. It contains olivine megacrysts, pegmatitic segregations and sparse veins rich in ferrian diopside and phlogopite (Craven 1985; Upton *et al.* 2006). At both occurrences, the spatial relationships of the mela-aillikites and the giant dykes suggest that the latter were already in place before the mela-aillikites were intruded.

Fig. 62. Altered mantle xenoliths in ultra-mafic lamprophyre host, Illutalik. Hammer *c*. 35 cm long

Mantle xenoliths

A dyke-like body of aillikitic ultramafic rock, cutting granites on Illutalik Island *c*. 7 km south-west of Narsaq, is noteworthy for its abundance of ultramafic nodules, interpreted as recrystallised mantle xenoliths (Upton 1991; Fig. 62). They are rounded, up to 40 cm in diameter, and are almost wholly composed of tremolite and chlorite but with scarce olivine ($Fo_{91.5}$) and chrome-spinels. Whilst still identifiable as former peridotites the intense recrystallisation, attributed to deuteric re-equilibration within volatile-rich magma, makes the original petrography debatable. Despite the fact that these rocks have been extremely altered they contain cross-cutting veins of glimmerite that may be relatively unchanged.

These are principally composed of phlogopite but with small quantities of calcite, apatite, zircon and titanite. They are regarded as providing evidence for K-rich metasomatism that had affected the peridotites prior to their entrainment.

Diatremes

The above-mentioned occurrences in Narsaq township and near Krydssø on Tuttutooq provide evidence for the spatial association of gas-drilled pipes, filled with material that collapsed inwards after venting, and magmatic mela-aillikites. Several other diatremes on Tuttutooq

Fig. 63. Diatreme at Narsaq. The larger clasts are quartzite (white) and metabasalt (black). Height of outcrop *c*. 1 m.

and Illutalik are also surmised to be due to degassing of mela-aillkite magmas as are three diatremes that cut the gabbro at Narsaq (Fig. 37). Since these diatremes lie approximately on strike with the five mela-aillikite outcrops at Nuugaarmiut, they are also suspected products of mela-aillikite magma degassing. Each diatreme is less than 100 m in diameter and is filled with an unsorted assemblage of angular quartzite and metabasalt clasts, presumably derived from formerly overlying Eriksfjord Formation strata (Fig. 63). Interstices between the clasts contain calcite, fluorite and gypsum providing support for the concept that the diatremes were generated by highly oxidised, halogen-rich and reactive CO_2-rich gases or super-critical fluids (Upton *et al.* 2006).

Several other isolated diatremes in eastern Tuttutooq and Illutalik may also relate to this phase of magmatism. A diatreme with a carbonated ultramafic matrix cutting the South Qôroq complex must be considered as Younger Gardar (Emeleus & Harry 1970).

Other aillikite, carbonate-silicate and carbonatite dykes

Small (<2 m wide) ENE–WSW-trending ultramafic dykes occur in south-eastern Tuttutooq and Illutalik. The extreme alteration in these is ascribed to volatile-rich, low-temperature residual fluids (Martin 1985).

The lamprophyre dykes in Mellemlandet and nunataks to the east-north-east are typically much altered; they are principally composed of fine-grained aggre-

gates of opaque oxides, biotite, carbonate and what may be olivine and pyroxene pseudomorphs. It is likely that late-stage deuteric reactions in the volatile-rich magmas have largely erased early-formed ferromagnesian phases. A swarm of related dykes, trending ENE–WSW and exposed along the eastern coast of Tunlliarfik fjord north of Narsarsuaq, is characterised by very nodular weathering surfaces. The nodules may represent relics of former olivine-rich xenoliths that underwent extensive deuteric recrystallisation.

Ultramafic lamprophyre dykes with up to 20 wt% MgO are early components of the Igaliko dyke swarm (Pearce & Leng 1996). They consist of approximately equal amounts of diopside and phlogopite, accompanied by opaque oxides, calcite and ferroan pargasite. Calcite ocelli occur and one dyke comprises two distinct (streaky) facies, one composed of calcite and the other of carbonate-rich ultramafic lamprophyre with phlogopite and perovskite. A comparable silico-carbonatite dyke composed of alternating streaky layers of calcite and ultramafic rock occurs in the Main dyke swarm close to the inland ice (Fig. 64). Flow-differentiation of materials with contrasted ductility was suggested for the latter (Upton *et al.* 2006).

Carbonatite (sövite), aillikite and carbonate-silicate dykes occur sparingly among the Main dyke swarm east-north-east of Ilimmaasaq (Martin 1985; Upton & Fitton 1985) but are relatively abundant in the Igaliko dyke swarm. These two dyke swarms are described in a later section. The carbonatite dykes, which are restricted to the vicinity of the Igaliko syenites, play only a very minor role. Whilst the principal carbonate is calcite, other com-

Fig. 64. Carbonate-silicate dyke east-north-east of Narsarsuaq. White layers are calcitic; dark layers are rich in opaque oxides and silicates. Diameter of coin 2.8 cm.

ponents are salite/ferrosalite, phlogopite, apatite, olivine, albite, andradite, perovskite, allanite, bastnaesite, pyrochlore, fluorite and secondary chlorite (Pearce 1988). Exceptionally, fluorite can compose up to 50% (modal) of the dykes. Sr, Ba and LREE commonly reach wt% concentrations whilst Y, Nb, Zn and Th also occur in abundance. Fenitisation of their wall-rocks demonstrates alkali loss during their crystallisation (Pearce 1988; Pearce & Leng 1996; Coulson *et al*. 2003).

Genesis of the ultramafic rocks

The case for a genetic relationship between the mela-aillikites and carbonatites was made by Coulson *et al*. (2003) and Upton *et al*. (2006), based on a synthesis of Sr, Nd, C and O isotopic data for these and other Gardar carbonatites and lamprophyres (Coulson *et al*. 2003). These authors found no evidence for a compositional gap between the two and concluded that they represent different degrees of melting from the same source. Small-fraction, volatile-rich partial melts rising from the asthenosphere became frozen in as lithospheric metasomites before being remobilised during Gardar rifting. That a continuum existed from ultramafic aillikites through silico-carbonatites to carbonatites was also suggested for the Main swarm dykes in the nunatak regions (Up-

ton & Fitton 1985). An alternative genetic scheme that the ultramafic lamprophyres and carbonatites are related through liquid immiscibility has been proposed by Pearce & Leng (1996) as also by Andersen (2008) in the case of the Older Gardar Qassiarsuk rocks.

The observation that the mela-aillikites at Narsaq and on Tuttutooq are closely associated with the YGDC invites the suggestion that thermal energy from the latter was responsible for remobilisation of metasomite bodies in the lithospheric mantle, generating the mela-aillikite magmas (Martin 1985). The Younger Gardar aillikite–carbonatite events are inferred to have been short-lived and localised. Although they are probably petrogenetically irrelevant to the principal story of the southern rift magmatic system, they afford some insights into the nature of the contemporary lithosphere (Coulson *et al*. 2003; Upton *et al*. 2006). As stated earlier, these ultramafic occurrences have no counterparts in the northern (Nunarsuit–Isortoq) rift zone.

Narssaq complex

The Narssaq complex transects the Narssaq gabbro but is cut by the Ilímaussaq complex on its eastern flank so that it was intruded during the interval between *c*. 1163 and *c*. 1160 Ma (Table 1). Although disturbed by faulting, it
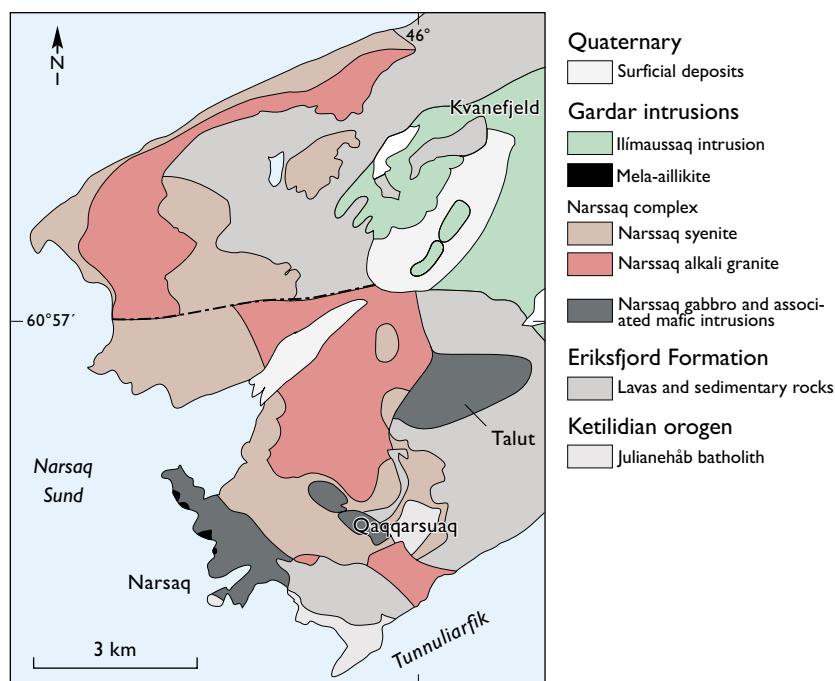

Fig. 65. Distribution of syenites and alkali granites of the Narssaq complex. Note also the intrusions at Talut and Qaqqarsuaq, which are presumed shallow-level extensions from the Narssaq complex.

Fig. 66. View east from Narsaq to Qaqqar-suaq mountain (685 m). Gabbro underlies the foreground and town of Narsaq. The Qaqqarsuaq mountain is dominantly composed of Narssaq syenite and alkali granite, with doleritic sheets.

may initially have had an ovoid plan with a diameter of some 10 km (Fig. 65). Although Fig. 65 shows the complex as consisting of two units only: a) quartz syenite and porphyritic pyroxene syenite, and b) alkali granite, this apparent simplicity belies the truth. Through a combination of relatively poor outcrop, topographic difficulties and apparent lack of economic resources the Narssaq complex has been neglected in comparison with the Ilímaussaq complex, its younger neighbour to the east. The bulk of the syenite was presumably emplaced through foundering of the gabbroic lopolith (described above as part of the YGDC) and its overlying cover of Eriksfjord Formation strata.

Originally mapped for GGU by J.W. Stewart in the 1950s (Stewart 1964) and the northern part subsequently mapped in detail by Olsen (1977, 1982), the maps and descriptions have not been published. Considerable complexity was revealed by Olsen's detailed studies and unpublished map. Five intrusive units are distinguished, each with feldspar-phyric margins chilled against the preceding unit. Augite syenite I is silica oversaturated. A fine-grained variant contains abundant anorthoclase phenocrysts while another variant is labelled as a black, larvikitic type. Augite syenite II has augite zoned by aegirine-augite and mainly lacks the anorthoclase phenocrysts of augite syenite I. It also contains widespread pegmatites. Olsen additionally notes mafic syenite, syenogabbro, leuco-syenodiorite, leucogabbro with anorthosite (presumably as xenoliths) and plagioclase megacrysts. The mountain behind Narsaq (Qaqqarsuaq; Fig. 66) is largely composed of the syenite but is capped by dolerite regarded as part of the former Narssaq lopolith.

Amongst the granite varieties, Olsen (1977, 1982) lists microgranite, rhyolite and alkali granite with alkali am-phibole. From the author's own observations some contain aegirine-augite. Some mafic layering is described, dipping steeply to ENE. In the north-east, low-angled sheets of syenite transgress the metavolcanic and sedimentary strata of the Eriksfjord Formation which form roof pendants to the intrusion. The present level of dissection is probably close to the roof zone of the complex (Emeleus & Upton 1976). Heterogeneous (streaky) rhyolite crops out on the north-east side of Qaqqarsuaq (author's unpublished field notes) and I. Gibson (personal communication, 1974) suggested that this rhyolite could be a caldera-ponded parataxitic ignimbrite. Dating of this rhyolite would be desirable to ascertain whether it is part of the Narssaq complex or an aberrant component of the Eriksfjord Formation lavas. On the assumption that it is part of the Narssaq complex it would strengthen the case for it all comprising very shallow-level intrusions retaining as well as some extrusive rocks.

Hydrothermal alteration, pervasive throughout the Narssaq complex rocks, may be attributed to fluids expelled during cooling of the Ilímaussaq complex that lies 2–3 km to the east.

The initial geometry of the complex has been significantly modified by transcurrent faulting. An approximately E–W-trending, left-lateral, transcurrent fault bisects the complex. On the assumption that the fault displaced the YGDC dykes westwards from their position as seen on Tuttutooq (at Narsaq) to sites now beneath the waters of Bredefjord, it is necessary to postulate a displacement of 6–7 km. However, judging from the mapped contacts of the granite (the youngest component of the complex), the movement was much less, possibly only half that distance. Accordingly, one may infer that the complex was intruded during an interval of active faulting. The fault

Fig. 67. Geological map showing the relationships between the South Qôroq, Igdlerfigssalik, Østfjordsdal, North Qôroq, Motzfeldt complexes and satellite intrusions. Modified from Emeleus & Harry (1970) and Stephenson (1976a), with abbreviated labelling.
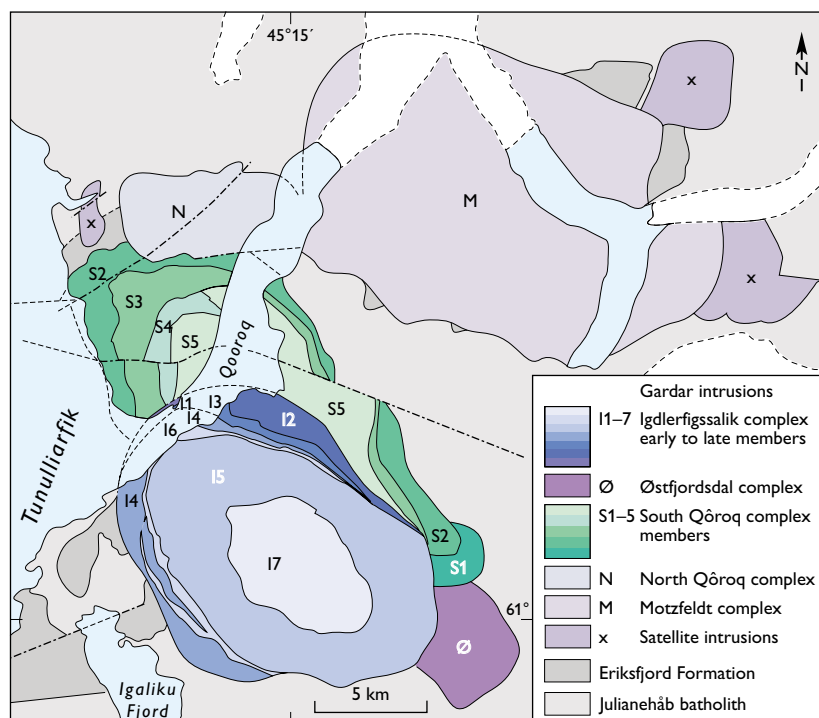
is likely to have played a significant role in localising the ascent of the Narssaq magmas as well as having some influence on the younger Ilímaussaq complex to its east.

The Ilímaussaq complex, described in detail below, contrasts with the Narssaq complex in being almost entirely composed of silica-undersaturated syenites. It contains, however, an early intrusion of quartz syenite and highly evolved alkali granite. Whereas these oversaturated magmas could have arisen from batches intimately associated with the undersaturated Ilímaussaq magmas that had experienced substantial crustal contamination, it may alternatively be speculated that they were residual from the Narssaq complex. Examples of batches retained within the plumbing systems and making late appearance are known from basaltic volcanoes (e.g. on Hawaii) so that the concept of 'left-over' Narssaq magmas subsequently re-appearing a few kilometres to the east as components in the neighbouring Ilímaussaq complex is not wholly inconceivable.

South Qôroq complex

Figure 67 is a geological map showing the South Qôroq complex adjacent to the North Qôroq and Igdlerfigssalik complexes. South Qôroq is a part of the Igaliko Syenites that collectively constitute one of the Earth's largest agglomerations of nepheline syenites. Rb-Sr dating gives South Qôroq an age of 1160 ± 8 Ma (Table 1). It was emplaced across a zone of active faulting and pre-dates the Main dyke swarm (described below), sharing these features with the Narssaq complex. The South Qôroq and Narssaq complexes, both emplaced at shallow crustal levels, may possibly mark the sites of two contemporaneous volcanoes, approximately 50 km apart.

Whereas the Narssaq complex transects the lopolithic portion of the YGDC, the South Qôroq complex lies several kilometres to the south-east of the giant dykes. It lies across the ESE-trending zone of sinistral faults to the north of that affecting the Narssaq complex (Figs 10, 65). The South Qôroq complex, which is partly obscured by the Qooroq fjord, was initially mapped by Emeleus & Harry (1970) and subsequently studied in detail by Stephenson (1972, 1974, 1976a).

Cutting into the Eriksfjord Formation supracrustal strata, the South Qôroq complex reached into the shallow crust and, crystallising largely from low-density phonolitic magmas, it may be a subvolcanic complex. The

Fig. 68. Nepheline syenite of the South Qôroq complex, viewed across Tunulliarfik. Main swarm dykes are prominent in the middle distance, trending upper right to lower left.

South Qôroq magmas rose through weakened lithosphere adjacent to the Older Gardar nepheline syenite complexes of Motzfeldt and North Qôroq (ages in Table 1). The close association of all the Igaliko syenite complexes is attributed to a lithospheric 'weak spot' focussed by the intersection of sinistral faulting and the ENE–WSW rifting. The age data in Table 1 suggest that a time gap of roughly 100 Ma separated the Older and Younger Igaliko complexes during which vigorous plate motion is indicated by palaeomagnetic data (Piper 1992, 1995). In view of the close affinities between the Older and Younger complexes over such a long interval, it is concluded that all shared a similar petrogenesis, presumably from lithospheric rather than asthenospheric sources.

Although the complex measures 26 km west-north-west – east-south-east and 10 km north-north-east – south-south-west on the geological map it may originally have had a nearly circular plan with a diameter of *c*. 10 km (Stephenson 1976b). According to Stephenson (1976b) the crudely elliptical plan can be explained by ductile deformation of the intrusions while they were still hot, by

large-scale simple shear. The complex is cut by alkaline dykes of the Main swarm (Fig. 68), considered in a later section. Intrusion of some of these dykes may also have overlapped with episodes of fault motion (Stephenson 1976a).

The South Qôroq complex is predominantly composed of foyaites. The first intrusion (S1 in Fig. 67) occupies a small crescentic area in the far south-east. This was followed by three concentric bodies of foyaite (S2, S3 and S5 in Figs 68, 69) inferred to have been sequential stocks with steep outward-dipping contacts. Emplacement was by ring-faulting and central subsidence, with younger units engulfing most of their predecessor(s). Diffuse or gradational contacts between the three intrusions imply rapid emplacement one after the other. The foci of the successive South Qôroq intrusions went through a generalised migration towards the south-east.

In view of the high structural level of the complex, an attendant sequence of nested calderas within an overlying volcano may be envisaged. The foyaites are layered cumulates possessing feldspar lamination and modal lay-
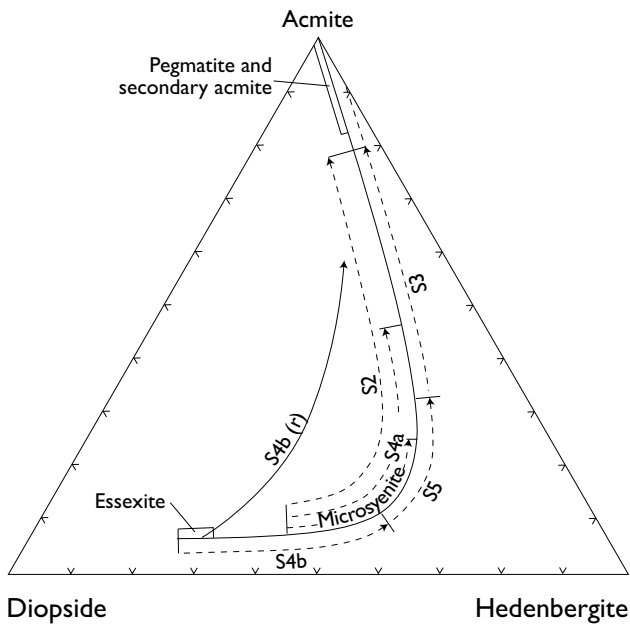
Fig. 69. Compositional variations in clinopyroxene in different intrusive members of the South Qôroq complex. Modified from Stephenson (1972) where the prefix 'SS' was used instead of 'S'.
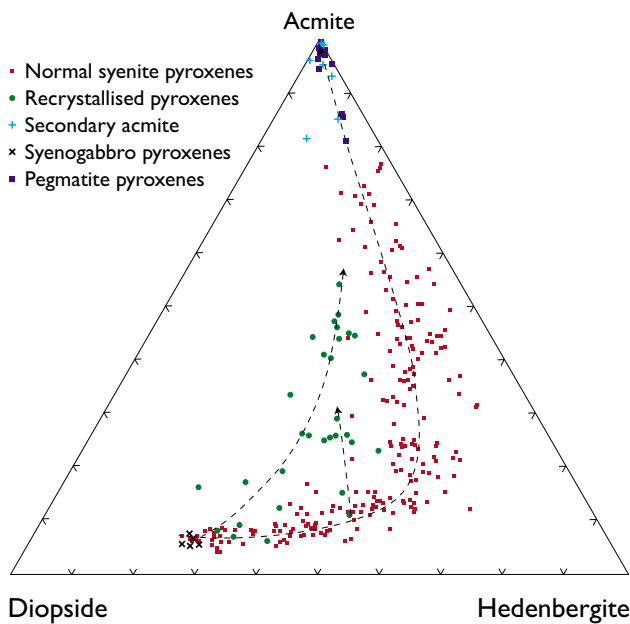

Fig. 70. Pyroxene compositions in the South Qôroq complex. Modified from Stephenson (1972).

ering with inwardly directed dips. The foyaites were cut by a ring dyke of layered augite syenite (S4), introduced in two pulses, which was itself intruded by a short length of a broad (100 m) syenogabbroic dyke. Stephenson

(1976a) gives the latter the more precise name of analcime nepheline monzonite. There are also four satellitic intrusions with petrographic characters that encompass most of those forming the main South Qôroq complex but which, however, appear to be older than the latter. In view of their high structural level there is the possibility that small phonolitic volcanic cones developed at an early stage, predating growth of the main edifice.

The sequence of intrusion S1-S2-S3-S4-S5 deduced by Emeleus & Harry (1970) was changed to S1-S2-S3-S5-S4b by Stephenson (1976a). Figures 69 and 70 show pyroxene compositions from the South Qôroq complex. Pyroxenes from S3 are more evolved than those from S5 that, in turn, are more evolved than those from S4b.

The olivines in the South Qôroq complex are noteworthy for their enhanced Ca and Mn contents (Stephenson 1974). Thus their CaO contents lie in the 0.2 to 0.4 wt% range, considerably higher than the normal contents for plutonic olivines. As with Ca, the Mn content of the olivines is abnormally high, averaging 5 wt% MnO but with values up to 8.6 wt% MnO. The Mn concentration increased steadily with fractionation until, in the augite syenite and the foyaites, it became the principal fractionating element in the olivine while Fe^{2+} decreased. The observed olivine range is from $Fo_{36}Fa_{62}Te_2$ to $Fo_2Fa_{82}Te_{16}$. The appropriate annite-alkali feldspar-magnetite buffer curve cuts across the fayalite-magnetite-quartz (FMQ) curve so that, in the later stages, the magma following this curve had a f_{O_2} greater than that for FMQ at any given temperature. When the two curves crossed, the olivine became unstable and disappeared (Stephenson 1974).

The successive intrusive units show a compositional trend towards increasingly less evolved compositions. This is regarded as indicative of their having been tapped from progressively deeper levels of a compositionally stratified magma chamber (Stephenson 1976a). Accordingly, a magma chamber may be envisaged in which highly fractionated phonolitic magma at the top was underlain by silica-undersaturated benmoreitic magma passing down to mugearitic to hawaiitic magma at still lower levels.

Fig. 71. Map of the post-YGDC Main dyke swarm on Tuttutooq (dark grey). The Tugtutôq central complex is shown in red.
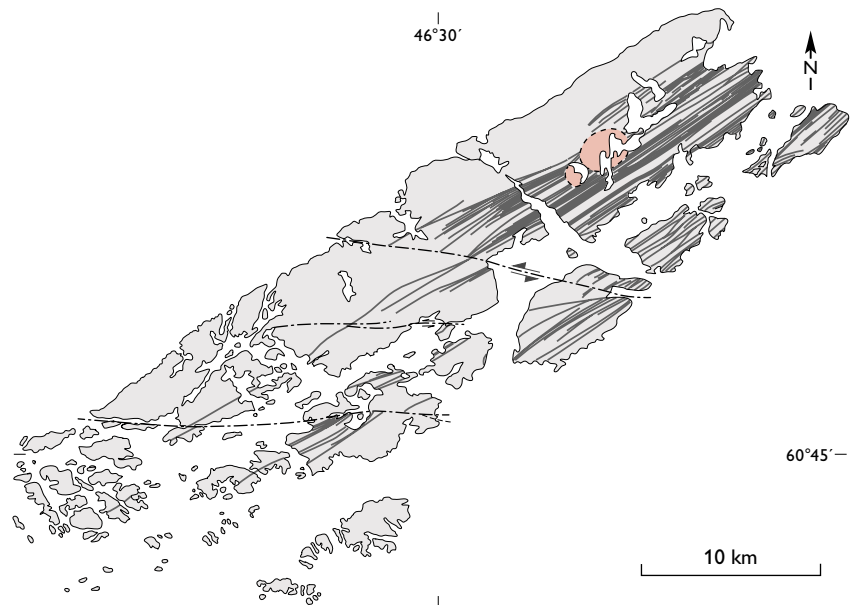
Post-YGDC dyke swarms

Main dyke swarm

The lithospheric extension, and presumed attenuation, along the younger Gardar southern rift persisted without abeyance beyond the YGDC event, but at a decreasing rate. The evidence is provided by a remarkable dyke swarm. This, the Main dyke swarm, is concentrated along an ENE–WSW-trending zone, approximately 10 km wide, that can be traced more than 120 km from the Inland Ice into the Tuttutooq archipelago. Although the component dykes never attained widths comparable to those of their giant dyke predecessors, some are up to 30 m wide. There is, however, a generalised decrease in size with increasing youth while the dyke compositions tended to become increasingly more evolved with time (Martin 1985; Upton *et al*. 1990).

West of Ilimmaasaq the swarm exhibits a compositional spectrum from trachybasaltic (hawaiitic/mugearitic) via benmoreitic/trachytic to quartz trachytic, comenditic and (rarely) phonolitic (Upton 1964a; Macdonald 1969; Martin 1985; Upton *et al*. 1990; Pearce 1988). Throughout the Tuttutooq region both the abundance of dykes and their widths diminish notably in the westernmost half of the archipelago (Fig. 71), suggesting that their magma sources lay towards the east-northeast. The swarm occupies more or less the same zone as that occupied by the giant dykes and is inferred to have been intruded along the axial part of the southern rift.

Whereas the giant dykes are unique in size, morphology and composition, the Main dyke swarm also represents an outstanding phenomenon lacking any obvious analogue. It has no counterpart in the Younger Gardar of the Nunarsuit–Isortoq region and although there are alkaline dykes in the Older Gardar e.g. in the Grønnedal-Íka district (Emeleus 1964), these compare neither in width nor extent with the Main swarm dykes nor with its compositional range.

Whilst there are many narrow dykes, broader ones with widths >5 m are common, some up to 30 m. Distinctive individuals can be followed laterally for up to 40 km. In brief, whilst less spectacular than the Gardar plutons and giant dykes, the Main dyke swarm represents a major, voluminous, influx of alkaline magmas and, bearing in mind the relatively shallow depth of erosion, it may be suspected that it includes dykes that fed fissure eruptions. Some seventy Main swarm dykes were recorded in a traverse across the swarm along the east coast of Tuttutooq. Together with the four giant dyke branches (aggregate width *c*. 1500 m) and assuming only a 2 m average for the Main swarm dykes, this indicates a total *c*. 1650 m of dyke within a *c*. 7500 m traverse i.e. a basement dilation here of *c*. 28%.

Most of the Main swarm dykes are silica saturated to oversaturated and only a small proportion are silica undersaturated (Macdonald 1969, 1970; Martin 1985; Winther 1992). The wide compositional spectrum is ascribed to fractional crystallisation of feldspar, olivine, clinopyroxene ± titanomagnetite and apatite. With evo-
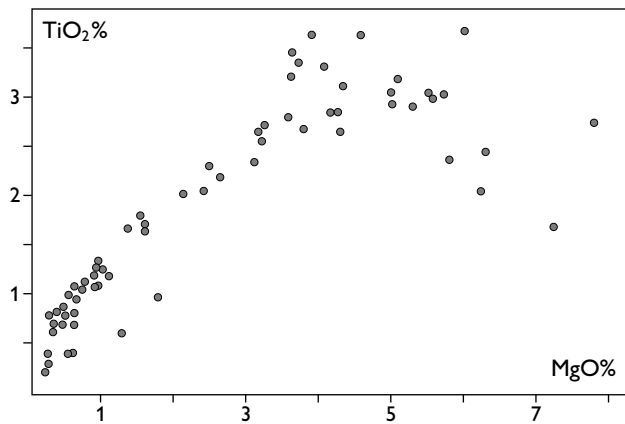
57

Fig. 72. Whole-rock TiO_2 vs. MgO in dykes from the nunatak area north-east of Motzfeldt Sø.

lution from hawaiite to mugearite, the residual magmas were increasingly directed into a residual system, attaining the composition of trachyte approximating to the low-temperature minimum on the Albite–Orthoclase join. From there the typical trend was towards the alkali rhyolite cotectic and, as emphasized by Macdonald (1969), a bundle of affiliated lines of descent was involved rather than a single liquid line of descent. The dyke rocks are typically fine- to medium-grained so that whole-rock analyses are taken to approximate the magma compositions. However, with rising silica contents, devitrification textures become increasingly common, and it is known that devitrification of alkali rhyolite glass is accompanied by significant loss of alkalis (especially Na) and trace elements. Consequently the measured whole-rock compositions, particularly of the quartz trachytes/microsyenites and rhyolites/microgranites, must deviate significantly from the original melt compositions (Macdonald 1969; Macdonald & Edge 1970). The dominance of plagioclase fractionation in the more primitive magmas resulted in Fe- and Ti-enrichment, peaking at the stage when MgO had fallen to c. 4 wt% (Fig. 72). Total Fe (as Fe_2O_3) declined from c. 17 wt% in the hawaiites to c. 4.5 wt% in the rhyolites (Martin 1985). Phosphorus reached a maximum (c. 2.5 wt% P_2O_5) at the same stage as TiO_2, reinforcing the conclusion from YGDC studies that titanomagnetite and apatite commenced crystallisation at essentially the same temperature. The highest concentration of Ba was reached when MgO had been reduced to c. 2 MgO wt%, approximately at the stage when plagioclase gave way to monoclinic (high-temperature) ternary feldspar.

Whilst silica-oversaturated (micro-quartz syenitic) dykes extend through the whole length of the southern rift system, rhyolitic dykes are principally confined to the Narsaq–Tuttutooq sector. Conversely, whereas phonolitic dykes are very scarce in the latter, they play a major role in the Igaliko dyke swarm further south and east (see below), in the vicinity of the Igaliko syenites.

Big feldspar dykes

Very distinctive dykes were intruded early in the history of the Main dyke swarm. These dykes, which also participate in the Igaliko swarm (described below), are characterised by their content of large feldspars (megacrysts) and anorthositic xenoliths (Fig. 73). Such dykes, known as 'big feldspar dykes' (BFDs), are not confined to the southern rift but are also widely distributed across the northern (Isortoq–Nunarsuit) rift as well as still further north into the border zone of the Archaean craton. The megacrysts are rarely greater than 50 cm in length, but typically are <10 cm. Allaart (1969), however, quotes a size up to 2 m for feldspars from a BFD south-east of the Ilímaussaq complex. Megacryst compositions range from labradorite to calcic oligoclase and anorthoclase (Bridgwater 1967; Allaart 1969; Winther 1992).

BFDs commonly exceed 5 m in width and can reach 30 m. Since individual dykes can be traced for tens of kilometres, the volume of magma involved was very substantial. These dykes were described in detail by Bridgwater (1967), Bridgwater & Harry (1968) and Winther (1992). More recently, detailed investigations were made into BFDs of the Isortoq area by Halama et al. (2002).
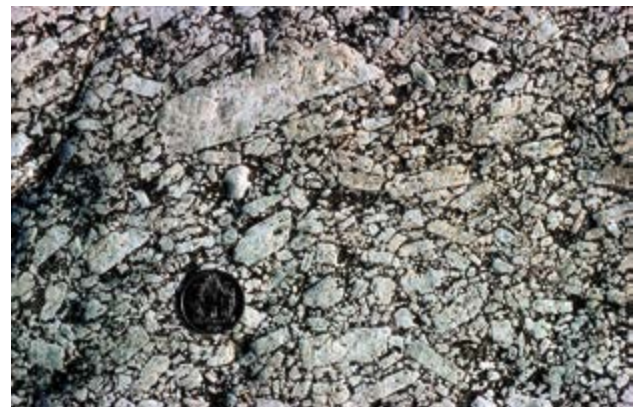

Fig. 73. Big feldspar dyke; Main swarm. Island south-east of Tuttutooq. Diameter of coin 2.5 cm.

The morphology of the feldspar megacrysts is variable: some are interpreted as corroded high-pressure phenocrysts whereas others are angular cleavage fragments presumed to be derivatives of disintegrating anorthosite masses (Bridgwater & Harry 1968; Halama *et al.* 2002; Fig. 73). The megacrysts and xenoliths are typically confined to the central parts of the dykes, with the outer zones free from, or poor in, megacrystic material.

Although the relatively fine-grained matrices of the central (inclusion-rich) parts are hawaiitic to mugearitic (containing 55 ± 5 wt% SiO_2), the marginal facies are distinctly more evolved (benmoreitic to trachytic) and the rocks are described as trachydoleritic and quartz microsyenitic, respectively (Bridgwater 1967; Bridgwater & Harry 1968). However, the terms tephrite, shoshonite and latite are employed by Winther (1992) for some of the dykes, emphasising their potassic nature. The margins contain alkali feldspar phenocrysts but are typically devoid of both megacrysts and xenoliths (Fig. 74).

The phenocryst assemblage in the trachydoleritic central facies comprises plagioclase, olivine (usually pseudomorphed), magnetite and apatite. Augite phenocrysts first appear in the mugearite range when the MgO content is down to between 3.5 and 3.0 wt%. From experimental studies on chilled Younger giant dyke rocks, the liquid-olivine-plagioclase-clinopyroxene cotectic corresponding with this petrography is attained at a temperature of 1060 ± 15°C at 1kb (Upton 1971). The trachydolerite matrices consist of feldspar (zoned from oligoclase to microperthitic alkali feldspar), olivine, magnetite, clinopyroxene, apatite ± hornblende. S and Cu reach maxima at *c.* 4 wt% MgO, inferred to mark the stage
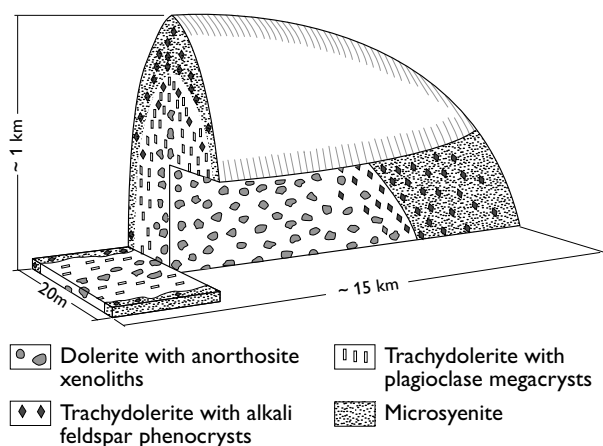

Fig. 74. Schematic relationships within a big feldspar dyke. Modified from Bridgwater & Harry (1968).

at which an immiscible Cu-bearing sulphide separated (Martin 1985).

The widths of evolved marginal facies relative to the more primitive central facies can vary along a single dyke. In the case of one exceptionally wide (20 m) dyke traceable from west-south-west to east-north-east through most of the Tuttutooq archipelago, the marginal facies (porphyritic trachyte) expands, from *c.* 1 m, at the expense of the big-feldspar-bearing trachydoleritic centre, until it occupies the entire width of the dyke. Although there is commonly gradation between the two facies, the compositional distinction is abrupt in some instances. Thus, in some dykes veinlets of trachydolerite transgress the microsyenite indicating that the latter was solid when the trachydolerite magma remained fluid.

The microsyenitic and trachydoleritic facies of the BFDs are regarded as cogenetic and their relationship is taken as indicative that they were derived from a compositionally stratified parental magma body in which the more evolved magma overlay the less evolved. During crustal dilation, the benmoreitic-trachytic magma (yielding microsyenite) ascended first, followed, after a variable time interval, by the mugearitic-hawaiitic magma (yielding trachydolerite) that exploited the mechanically weak, still hot, median plane of its predecessor as dilation progressed. The observation that the central facies is generally many times broader than the sum of the border facies may imply that fissure opening began slowly but accelerated as the hotter, inclusion-rich, mafic magma intruded.

The BFDs contributed to both the Main and Igaliko dyke swarms and their widespread and highly distinctive characters are suggestive of intrusive phases occurring at a time when very similar compositionally stratified parental magmas bodies existed at depth. Whilst it is not claimed that all BFDs were synchronous, their features are so idiosyncratic as to make it likely that they were products of a single phase in Gardar magmatism. Whether or not the hypothesised stratified chambers extended over a great area embracing both the northern (Nunarsuit–Isortoq) and the southern rift zones remains a moot point. The fact that they brought up copious quantities of xenolithic anorthosite and feldspar megacrysts shows that, like the Younger giant dyke magma, the BFD magmas ascended from beneath a solid anorthositic protolith as well as from beneath a level at which large feldspars were growing.

Study of the megacrysts points to their having experienced complex histories prior to entrainment (Winther 1992). The interpretation of some as high-pressure phe-
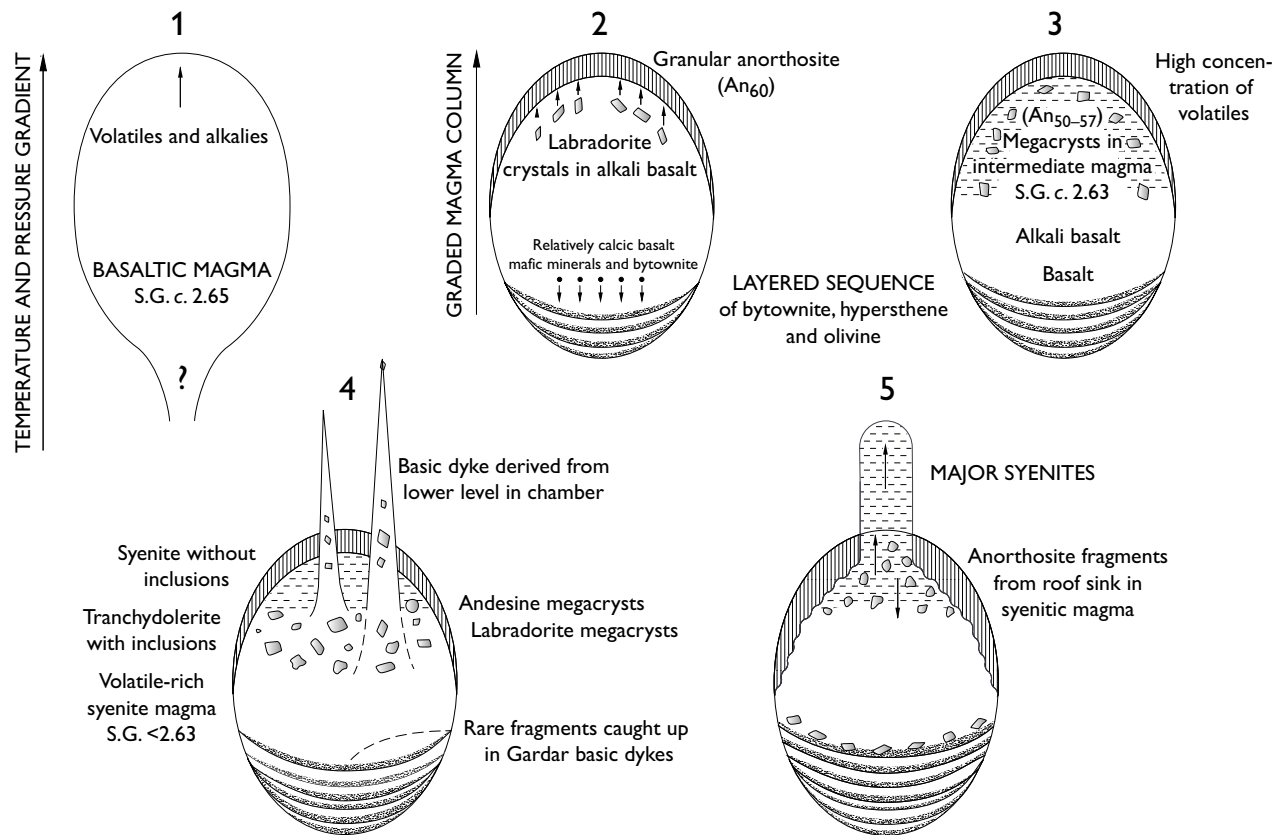
Fig. 75. Stages of magmatic evolution in the Gardar province, modified from Bridgwater (1967). **1**: A magma chamber forms. **2**: The chamber produces layered floor cumulates and plagioclase flotation cumulates (An$_{60}$). **3**: Density of magma lowers and more sodic plagioclase crystallises. **4**: Compositional stratification forms in in the main magma chamber. The uppermost, more buoyant magma breaks through the anorthositic flotation cumulate. **5**: Larger volumes of low-density magma (interpreted in the present text to be benmoreitic) ascend to initiate the large Gardar alkaline centres. **S.G.** = Specific gravity.

nocrysts augments the conclusions that the anorthosite was comagmatic with the dyke magmas, and that large feldspars were still crystallising at the time that BFDs were being emplaced. It is of particular interest that the megacryst population includes not only labradorites but, as noted above, also more sodic plagioclases and anorthoclases (Allaart 1969; Winther 1992). Since no xenoliths composed of such more evolved feldspars have been described, this implies that the latter were high-pressure phenocrysts or primocrysts that became entrained by hawaiitic-mugearitic magma as it ascended rapidly through relatively evolved crystal-melt slurries or mushes which themselves underlay consolidated anorthosite.

The rarity of xenoliths and megacrysts in the initial differentiated magma fractions suggests that their densities were greater than that of the magma and inhibited their entrainment. The case has previously been made in the earlier section discussing the more primitive YGDC

initial magma, that the feldspathic cargo was buoyant and, hence, capable of flotation. The remarkable abundance of xenoliths + megacrysts (up to 80% (modal); Bridgwater & Harry 1968) in the BFD trachydolerites may be construed as evidence that there was broad equivalence between the densities of the host trachydolerite (hawaiite/mugearite) magma and its xenolith/megacryst inclusions.

It is of interest that granitoid country-rock xenoliths occur in neither facies, probably as a result of being too dense. The impression gained from these remarkable BFDs is that even small density differences between melts on the one hand and solid materials (megacrysts and xenoliths) on the other could be of critical importance in controlling whether the latter were entrained or not. Such discrimination may also provide further evidence for the low viscosities of the melts. The fact that the magmas could acquire such large quantities of solid

detritus and still be capable of intrusion is itself suggestive of low viscosities.

Bridgwater (1967) proposed that the underlying stratified magma was generated through a process of liquid fractionation in which alkalis and volatiles migrated to and accumulated at the top of the magma chamber. His genetic model is encapsulated in a cartoon, which in principle remains acceptable (Fig. 75).

The development of stratified magma chambers, analogous to that postulated to explain the relationships in the BFDs, is thought to have been responsible for the sequence of intrusions in the South Qôroq complex (see above). Such stratified magmas may have been generated repeatedly throughout Gardar times as exemplified by the Kûngnât complex in the Older Gardar (Upton *et al*. 2013). It is probable that, with passage of time, the volume and depth of the salic upper component progressively increased, thereby reducing the chances for the underlying mafic magma to ascend.

Salic dykes of the Main dyke swarm

The differentiated dykes of the Main dyke swarm are generally younger than the BFDs and most of the cross-cutting dykes are more evolved than those they cut, pointing to the probability that parental magma chambers at depth were undergoing progressive fractional crystallisation (Martin 1985; Upton *et al*. 1990). Benmoreite dykes, although typically <15 m wide, can attain widths up to 25 m. They are compositionally so similar to the marginal facies of the BFDs that they probably arose through the subsequent selective tapping of the uppermost layer of the hypothesised stratified magma body, a layer that may well have grown in volume with the passage of time. Feldspar phenocrysts, generally displaying strong zonation, in the benmoreitic dykes have the rhomboid morphology of ternary feldspars and in some instances exhibit the characteristic (100) cross-hatched polysynthetic twinning of anorthoclase (Bondam 1955; Upton 1964a; Fig. 76). Phenocrysts of (pseudomorphed) olivine, ferrosalite, magnetite and apatite are typically present.

There is close compositional correspondence between the benmoreitic dykes (54–56 wt % SiO_2 and 1.4–1.7 wt% MgO) and the chilled marginal facies of the Ilímaussaq augite syenite (Upton & Emeleus 1987). However, while the latter is just silica undersaturated, the majority of the benmoreitic dykes are silica oversaturated.
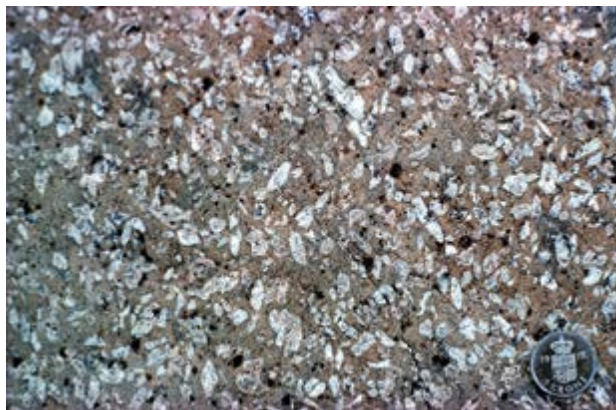

Fig. 76. Rhomb-porphyry-textured benmoreite dyke, eastern Tuttutooq. Polished slab. Diameter of coin 2.5 cm.

Magmas crystallising to the quartz trachytes and alkali rhyolites are inferred to have been intimately related to the parent magmas for the Assorutit syenite, the Narssaq complex and the Tugtutôq central complex (described below). The microperthitic, tabular, alkali feldspar phenocrysts of the trachytes and quartz trachytes are presumed to have crystallised as sanidines that subsequently underwent ordering and exsolution. The matrices, often showing well-defined trachytoid textures, comprise alkali feldspar, quartz, biotite, amphibole, aegirine-augite, haematite and primary calcite. With increasing differentiation the amphiboles vary from hastingsite to arfvedsonite. Aegirine-augite is present in the more evolved trachytes, as is calcite.

Whereas devitrification textures are seen only in the fast-chilled margins of the benmoreite and trachyte dykes, the majority of the rhyolitic (comendite or 'quartz-feldspar porphyry') dykes represent devitrified glasses (Figs 77, 78). The devitrification products are spherical or polygonal spherulites, but in some dykes devitrification led to patchy or finely laminated (flow-banded) rocks coloured deep blue or green according to whether the ferromagnesian component is arfvedsonite or aegirine (Fig. 78). Buff colours may signify crystalline cores in some dykes.

Most of the rhyolitic dykes are <5 m wide. Phenocrysts in these dykes are hedenbergite, low-quartz paramorphs after high-quartz, and former sanidine, commonly partially exsolved. Other components include arfvedsonite, aegirine, astrophyllite, zircon and fluorite (Macdonald 1969; Martin 1985). The strongly alkaline character of these silicic dykes is typical of comendites. They are rich in incompatible trace elements and Zr increases in the Main dyke swarm from <200 ppm in the trachydoler-

Fig. 77. Comendite dyke cutting OGDC foyaite, eastern Tuttutooq. Editor of this volume Lotte M. Larsen for scale.

ites to >3000 ppm in the comendites. Zr, unlike some of the other elements (e.g. Li and Ga), appears not to have been expelled during devitrification (Macdonald & Edge 1970; Macdonald & Parker 1970).

The compositions of the salic dykes plot to the per-alkaline side of the thermal divide in the system SiO_2–Al_2O_3–$(Na_2O + K_2O)$ (Macdonald 1969). There is a gradual increase in $Na_2O/(Na_2O + K_2O)$ from hastingsite microsyenites to the more evolved arfvedsonite microsyenites. Beyond that point, however, there is a regular decrease of alkalis in the more siliceous dykes, ascribed to preferential loss of Na_2O in a fugitive fluid phase rich in halides and water.

There are several occurrences of composite dykes with mafic margins and rhyolitic cores. It is speculated that these arose from underlying chambers in which rhyolite overlay mafic magma and that, as lithospheric pull-apart proceeded, the more mobile deeper magma was drawn up through the viscous rhyolite layer to intrude as a dyke in the overlying country rocks. The hot axial plane of this basaltic pathfinder then lubricated the previously passive rhyolitic magma to permit its intrusion as the younger

central component of the composite dyke (e.g. Meade *et al.* 2009; Macdonald *et al.* 2009, 2010). The widest (20–30 m) and most extensive composite dyke in the Tuttutooq region lies close to the northern giant dyke branch and can be traced for 40 km.

One of the most extreme compositions in the Main dyke swarm is a pantelleritic trachyte dyke on the island of Illutalik, off the south-eastern coast of Tuttutooq (Fig. 10). This 20 m wide, partially devitrified, dyke is remarkable for its conspicuous phenocrysts of narsarsukite (Fig. 79). The associated mineral assemblage includes albite, aegirine, zincian nordite, emeleusite, pectolite and unidentified REE-rich silicates (Upton *et al.* 1976, 1978). Geochemically the dyke is noteworthy for its low Zr/Nb ratio, 0.53 (500 ppm Zr and 940 ppm Nb).

Igaliko dyke swarm

Offset from the Main dyke swarm but adjacent to it on its southern side is the Igaliko dyke swarm (Pearce

Fig. 78. Polished surfaces of devitrified comendites from dykes on Tuttutooq. Phenocrysts consist of bipyramidal low-quartz (after high-quartz) and perthitic feldspars after sanidine. Blue and green colorations in the matrix reflect arfvedsonite and aegirine, respectively. Widths about 6 cm.
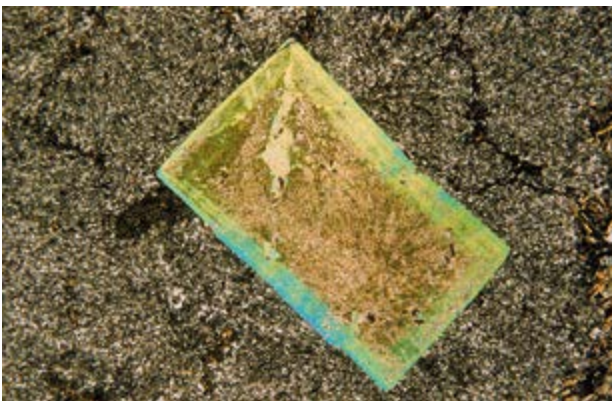

Fig. 79. Photomicrograph (crossed nicols) of zoned narsarsukite phenocryst in pantelleritic trachyte, Illutalik. Length of crystal *c.* 3 mm.

1988; Pearce & Leng 1996). Although this has also been termed the South-East swarm e.g. by Winther (1992), the name Igaliko dyke swarm will be used here. This swarm is geographically more restricted, coinciding approximately with the area occupied by the Igaliko syenites and traversing the peninsula to their west-south-west, between the Tunulliarfik and Igaliku fjords (Fig. 1). This region is intersected by the same *c.* E–W-sinistral fault that appears to have controlled intrusion of the Narssaq complex 20 to 30 km farther west (Figs 2, 80). The variable degrees of offset exhibited by the dykes show that the fault was active at the time the swarm was being emplaced (Allaart 1969). A small number of the dykes, however, post-date the faulting and include the remarkable 'micro-kakortokite' dyke that will be described in a later section.

Pearce (1988) pointed out that whereas the geometry of the YGDC branches can be related to shear zones with transtensional extension, the smaller dykes required only simple sinistral shear. The Igaliko dykes were emplaced as arrays of *en echelon* fissures in a sinistral shear regime and the dyke fractures are deduced to have propagated both vertically and horizontally from their source. Across a zone *c.* 15 km broad some 30 km west-south-west of the Igdlerfigssalik complex (Fig. 2), the abundance of dykes gave rise to a crustal extension of *c.* 4.5% (Allaart 1969).

The Igaliko swarm dykes cover a wide compositional range but are dominantly silica undersaturated and thus differ from the Main dyke swarm. Some of the mafic dykes were described by Pearce (1988) as lamprophyres; on the total alkali-silica (TAS) classification these fall into the fields of tephrites and basanites. Alkali lamprophyre (camptonite) dykes within the swarm are distinctive in carrying salite/diopside and kaersutite phenocrysts in a matrix of pyroxene, kaersutite, plagioclase, oxides and a feldspathoid. Some BFDs showing much the same characteristics as those of the Main dyke swarm are also present (Allaart 1969).

The majority of the dykes, however, are silica undersaturated trachytes and phonolites grading to peralkaline types, to which the mafic dyke magmas are regarded as parental (Pearce 1988). According to Pearce, up to 70% by volume of the Igaliko dyke swarm consists of phonolites with phenocrysts of anorthoclase or sodian sanidine, nepheline and rare salitic pyroxene. Research was carried out into the distribution of REE and some other trace elements between phenocrysts and matrices of some of these alkaline dykes to determine partion coefficients between crystals and coexisting liquids (Larsen 1979).
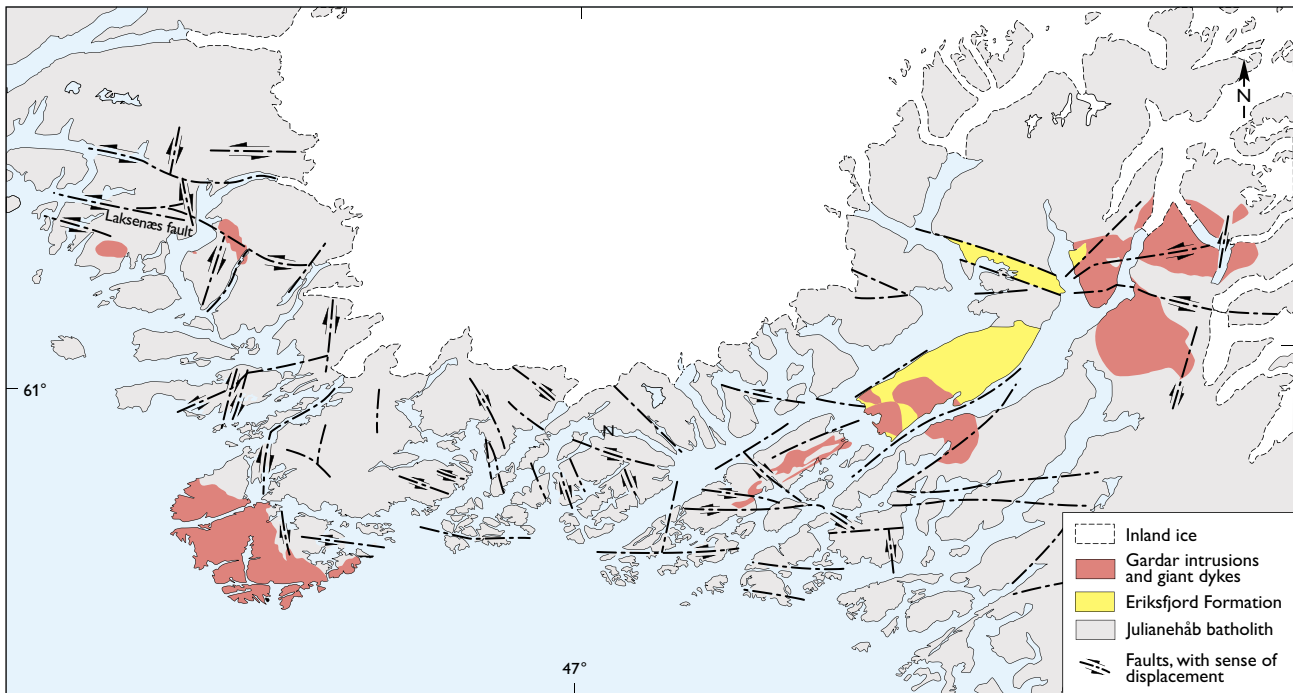
Fig. 80. Transcurrent faults in the Gardar province. Those trending E–W to WNW–ESE are invariably sinistral. The dextral faults have directions between NNW–SSE and NE–SW.

Pearce (1988) noted that Zr/Nb ratios of the mafic dykes provide a discriminant between the Main and Igaliko swarms: dykes of the former have higher values, averaging 6.4, contrasting with values averaging 3.9 for dykes of the Igaliko swarm. Thus a whole-rock Zr/Nb ratio of *c*. 5.2 effectively distinguishes the two swarms. Accordingly the Igaliko dyke swarm is relatively enriched in Nb and this, in conjunction with its generally more alkaline and silica-undersaturated nature, suggests that its primitive ancestral melts may have been derived from smaller degrees of source rock melting than those of the Main dyke swarm.

Tugtutôq central complex

The Tugtutôq central complex (TCC) is a small (4.5 × 2.5 km) central complex composed of syenites, quartz syenites and alkali granites (Upton 1962; 1964a; Upton *et al*. 1990). It lies astride the OGDC and YGDC and also intersects alkaline dykes of the Main dyke swarm (Fig. 81). Although it is cut by a few ENE-trending dykes, the Late basic dykes, (described in a subsequent section), it is clearly a very late feature of the southern rift magmatic

system, dated at 1156 ± 1.1 Ma (Table 1). There is, however, no evidence as to whether the complex pre- or post-dates the sinistral faulting that ended the main phase of dyke emplacement.

As described previously, the Main dyke swarm is considered to represent batches of magma that were episodically released from a deep crustal magma chamber that was undergoing prolonged fractional crystallisation. It is deduced that when extensional rifting was almost finished, a residual volume (>8 km^3) of buoyant salic magma ascended by stoping and/or cauldron subsidence. Figure 82 is a block diagram illustrating the complex and its principal components. The presence of numerous basalt and quartzite xenoliths within the TCC implies that the Eriksford Formation formerly extended westwards across Tuttutooq and suggests that the complex was emplaced at shallow crustal levels. Confirmation of low confining pressures comes from the miarolitic character of many of the TCC rocks.

The earliest intrusions of the complex took advantage of the course inflection of the Older giant dyke (Fig. 5) and gave rise to a small (*c*. 700 m) plug of porphyritic microsyenite (Unit 1a). Possibly at much the same time, another intrusion (Unit 1b) occurred at a second focal point, 2.5 km to the east-north-east, that transected both
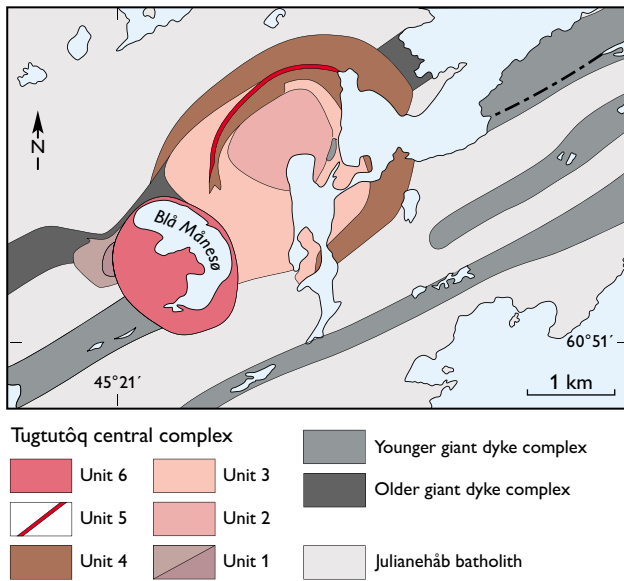
Fig. 81. Geological map of the Tugtutôq central complex. Simplified from Upton (1962). For location see Fig. 5.

Fig. 83. Map of the Unit 1 microsyenites in the Tugtutôq central complex. See Fig. 81 for location.
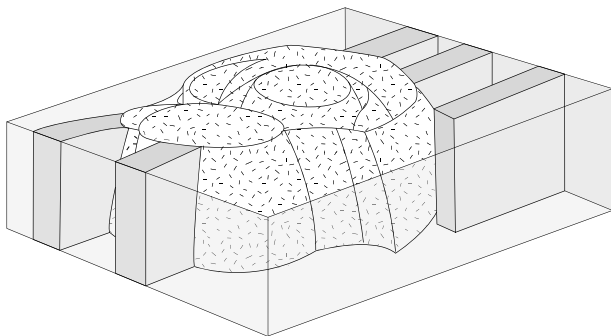

Fig. 82. Block diagram of the Tugtutôq central complex and its relationship to the OGDC and YGDC. The OGDC is farthest from the viewer. Modified from Upton *et al.* (1990)

the OGDC and the northern branch of the YGDC. This produced a larger body of very similar porphyritic microsyenite. The western microsyenite was apparently then invaded by a coarser syenite that divided the microsyenite into subrounded masses up to 2 m in diameter by a curviplanar network of syenite and quartz syenite veins. The contacts within the plug are diffuse and the veins were intruded when the microsyenite was still hot and ductile, probably above its solidus. The veined microsyenite surrounds a coarser core to this western intrusion. In the eastern centre the microsyenite is present as two annular, steeply dipping sheets (screens) up to 40 m thick that are approximately concentric with the younger components of the eastern centre (Fig. 83). The two

screens may have originally been contiguous, possibly forming a stock about 2 km across (i.e. over twice the size of that in the western centre). This was later split into the two screens by a ring dyke of alkali granite. As in the western centre, the microsyenite is pervaded by veins of coarser syenite that subdivide it into ovoid masses (Fig. 84). In both the western and eastern centres, the veining represents intimate penetration by late-stage fractions of the enclosing magma at temperatures above those permitting brittle fracture.

The inner of the two microsyenite screens hosts a large mass (400 × 200 m) of porphyritic country-rock granodiorite as well as smaller biotite-rich mafic xenoliths assumed to have been derived from the Eriksford Formation basalts and YGDC gabbro. The Unit 1 microsyenites are considered to represent magma that crystallised rapidly around the roof and walls of the respective intrusions as a result of loss of heat and volatiles. Accordingly they may be considered as analogues of the granular roofing syenites at the Klokken complex.

Four further episodes of roof failure and block subsidence then followed as the eastern centre expanded outwards by stoping and ring-faulting (Fig. 85). In so doing it evolved into an ovoid complex 3 km east-north-east–west-south-west and 2.3 km north-north-west–south-south-east.

Unit 2 (*c.* 1200 m diameter) is a heterogeneous quartz syenite that contains an abundance of xenoliths. These include: (a) gabbro from the YGDC, (b) basalt lava, ba-

Fig. 84. Relationship between syenite (pale cream) and microsyenite (dark) in the eastern centre (Unit 1) of the Tugtutôq central complex. Width of sample 12 cm.

saltic agglomerate and quartzite from the Eriksfjord Formation, (c) granitoids from the Julianehåb batholith, (d) clasts derived from the Unit 1 microsyenite and (e) clasts from the Main swarm dykes.

It is hypothesised that a raft of roofing rocks (reminiscent of features in the Grønnedal-Íka and Kûngnât complexes (Emeleus 1964; Upton *et al.* 2013) collapsed into the Unit 2 chamber. Whilst this raft, composed of rocks from above and below the Julianehåb granite/Eriksfjord Formation unconformity, underwent disintegration, it retained its overall stratigraphic integrity. The matrix containing the xenoliths is coarse-grained and, whilst lacking any regular layering features, contains concentrations of olivines and pyroxenes forming mafic/ultramafic schlieren (Fig. 86). Localised pegmatitic facies of quartz syenite grading to alkali granite add to the heterogeneity.

Unit 3 ranges from slightly feldspar-phyric quartz syenite to alkali granite and appears to have been intruded with minimal pause after Unit 2 as no chilled contacts separate them. Unit 3 is largely homogeneous apart from some mafic/ultramafic schlieren like those in Unit 2. Some schlieren are low-angled with a suggestion of gravity grading. The unit contains scarce clasts of Julianehåb granodiorite as well as one great mass (*c.* 300 × 100 m) of extensively metasomatised YGDC gabbro. Where Unit 3 is in contact with the Unit 1 microsyenite the contact is sharp and dips outwards at 20°.
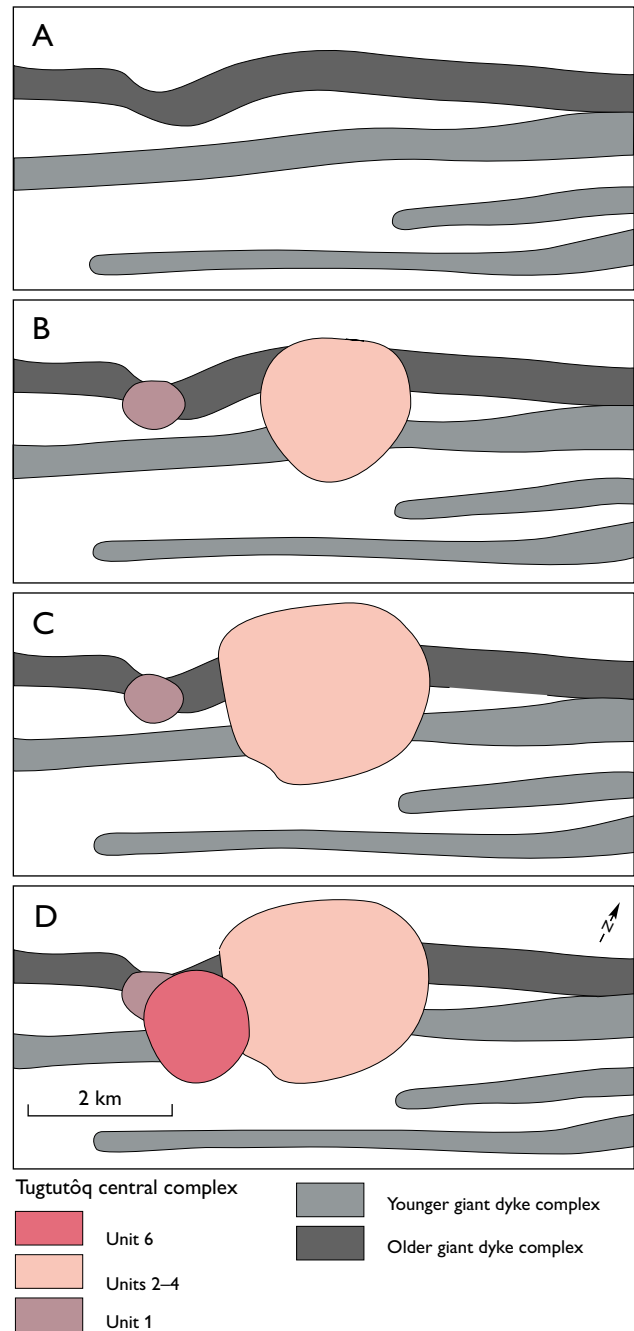

Fig. 85. The inferred intrusive sequence in the Tugtutôq central complex. **A**: Giant-dyke disposition predating the Tugtutôq central complex. **B**: Emplacement of Unit 1 and 2 microsyenites of the western and eastern centres. **C**: Expansion of the eastern centre by Units 3, 4 and 5. **D**: Emplacement of Unit 6. Modified from Upton *et al.* (1990).
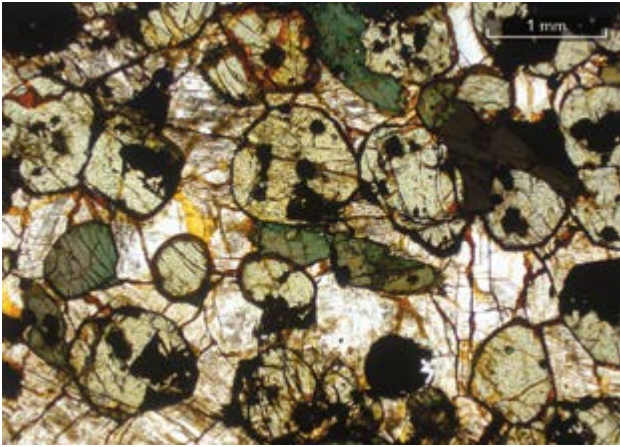
Fig. 86. Photomicrograph of fayalite-hedenbergite-magnetite-rich cumulate in Unit 3, Tugtutôq central complex. Olivine partially replaced by opaque oxides. Intercumulus alkali feldspar.

Unit 4 is a coarse-grained hornblende granite, distinguished (commonly with difficulty) from Unit 3 in having more quartz, lacking a porphyritic character and containing prominent amphibole. Its emplacement is presumed to have involved ring faulting and subsequent cauldron collapse together with the earlier units that are enclosed by it. It appears to form a broad branching sheath around Units 1, 2 and 3. Numerous thin alkali granite sheets within it dip outwards. Unit 4 is largely free from xenoliths but does contain some substantial quartzite xenoliths. Chilled margins are again absent and the outward dipping contact with Unit 3 is gradational over *c.* 10 cm suggesting that only a relatively short time interval separated the two magma influxes. External contacts with the Julianehåb granitoids are, however, sharp and dip outwards at *c.* 45°.

Unit 5 consists of a very narrow alkali granite ring dyke, only a few metres broad. It is traceable for *c.* 2 km through Units 3 and 4 and represents the final stage in the evolution of the eastern centre, possibly marking a culminating caldera collapse within a larger collapse structure associated with the Unit 4 emplacement. All four units of the eastern centre appear to have steep outward-dipping contacts as shown in Fig. 82.

Unit 6 is a subcylindrical stock with a diameter of *c.* 1.5 km that straddles both the OGDC and the northern branch of the YGDC and links the eastern and western centres. This intrusion is unique among the Gardar intrusions in consisting almost wholly of alkali feldspar (>95% modal) and can be termed a perthosite. From the roughly crescent-shaped lake (Blå Månesø; Fig. 81) that covers much of its outcrop, it was given the name Blå Månesø perthosite. Whilst the common rock is made up of idiomorphic feldspar crystals *c.* 2 cm across (Fig. 87), the feldspars in randomly distributed pegmatic patches are up to 15 cm long. Other finer-grained patches can be termed aplitic. In brief, the Unit 6 perthosites are texturally heterogeneous.

Mineralogy and geochemistry

The principal minerals in the TCC are alkali feldspar, quartz, olivine, clinopyroxene (ferrosalite to aegirine-augite and aegirine) and amphibole (ferrorichterite to arfvedsonite). Minor minerals include aenigmatite, biotite, ilmenite and magnetite. The olivine ranges from $Fo_9Fa_{88}Tp_3$ to $Fo_0Fa_{95}Tp_5$ (absent from Unit 6) whilst the pyroxenes extend from ferrosalite $Di_{35}Hd_{62}Ac_3$ to virtually pure aegirine. Hedenbergite contents reached Hd_{95} before there was any discernible Na enrichment (Upton *et al.* 1990). Pyroxene crystallisation was generally terminated by reaction to amphibole due to falling temperature and f_{O_2} and rising P_{H_2O} and/or P_F, although acmitic pyroxene post-dated the amphibole in some facies. The residual melts in Units 3 and 4 became highly peralkaline, and in Unit 6 aegirine is the sole pyroxene. Accessory minerals (Ridolfi *et al.* 2006a) include apatite, zircon, fluorite, thorite, sphalerite, pyrochlore, astrophyllite, Ce-chevkinite, yttro-pyrochlore, zirconolite, xenotime, ceriobetafite and ferropyrochlore. The different units of the TCC are principally distinguishable through their textural and modal differences.
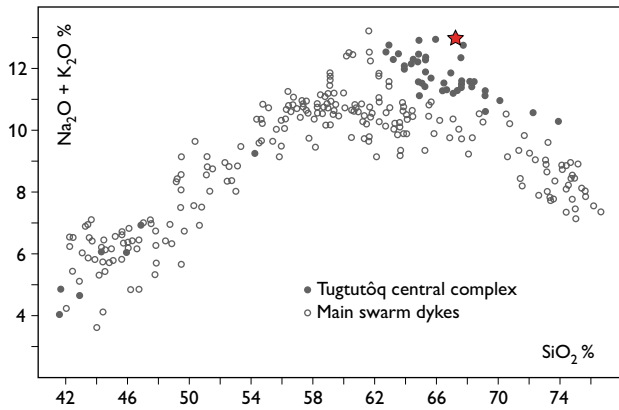

Fig. 87. Typical exposure of the Blå Månesø (Unit 6) perthosites. Hammer *c.* 40 cm long.

Fig. 88. Alkali/silica plot of samples from the Tugtutôq central complex and the Main swarm dykes. Star symbol at *c.* 67 wt.% SiO$_2$ represents minimum melting point composition on the Albite-Orthoclase join. Modified from Upton *et al.* (1990).

Cathodo-luminescence studies of the Blå Månesø feldspars demonstrated interconnected pores (a microporosity of 4.1%) that permitted passage of metasomatic fluids with consequent large-scale interaction. The fluids flowed along grain boundaries via the micro-pore network (Finch & Walker 1991). The relative abundance of fluorite in Units 2 to 6 points to concentration of fluorine in the magmas, and the marked metasomatism that affected the inclusions is attributed to the reactivity of halogenated melts or fluids. Na-rich aqueous fluids, inferred to have persisted to subsolidus temperatures, caused secondary alteration of the perthites to clays (Ridolfi *et al.* 2006a). Primary carbonate is only rarely seen, occurring interstitially in some syenites of the eastern centre (Upton 1964a). However, there is evidence that carbonatitic fluids, rich in F, Na, Ca, P and lanthanides, permeated the rocks, leaving their mark in the form of distinct post-magmatic textures and mineralogies. These fluids also generated albite, fluorite, Ce-monazite and almost pure Ce-bastnaesite within rock fractures and vugs. Evidence for selective interaction between the early mineral phases and late-stage LREE-rich fluids comes from the scattered patterns shown by whole-rock geochemical plots of Zr vs. lanthanides. The nature of the post-magmatic phases implies that the hydrothermal fluids were enriched in Na, Ca, P, LREE, F and CO$_2$. Fluid interaction took place at temperatures <550°C. Activity by CO$_2$-rich fluids followed and, at lower temperatures (150–250°C), by H$_2$O-rich fluids (Ridolfi *et al.* 2006a).

Whole-rock compositions from the TCC contrast with those of the Main swarm dykes with comparable silica contents (58–74 wt% SiO$_2$) in having more Al$_2$O$_3$, K$_2$O and Na$_2$O and less MgO, Fe$_2$O$_3$ (total iron), MnO and TiO$_2$ (Fig. 88). Whereas the compositions of the more rapidly crystallised Main swarm rocks may be taken to roughly equate with those of their magmas, the TCC rock compositions are believed to deviate significantly from their melts because of differential loss of high-density (Fe-rich) minerals that left the residual magma correspondingly richer in feldspar components. This process was most profound in the residual magmas of Unit 6. The consequent perthosites are therefore regarded not as alkali feldspar flotation cumulates, but as products of residual magma following gravitational depletion in ferromagnesian minerals. The composition of this residual magma approximated closely to the minimum melting point composition on the albite-orthoclase join (Upton *et al.* 1990). Lower Zr/Nb ratios in the TCC relative to Main swarm salic dykes may also be due to selective loss of zircon through crystal settling.

Petrogenesis

The earliest components of the TCC (Unit 1) appear to be more primitive (resembling the preceding benmoreite dykes) than those of Units 2, 3 and 4. The interstitial mineral assemblage of the Unit 6 perthosites demonstrates that the magma was more highly fractionated than those of the earlier TCC units and supports the thesis that the magmas became increasingly evolved with time. The conclusion is that benmoreitic magma at depth was steadily evolving towards a peralkaline quartz trachyte composition (Upton *et al.* 1990), i.e. essentially what was concluded in the case of the Main dyke swarm. Clearly it was not a continuation of the latter but rather that it was a localised repetition beyond the time when lithospheric attenuation had virtually ceased.

The Puklen complex in the northern (Nunarsuit-Isortoq) rift shares numerous features with the TCC. It is similar in size and was also intruded across a gabbroic giant dyke (Pulvertaft 1961, 1965; Parsons 1972). Both complexes consist of syenites, quartz syenites and peralkaline granites. An isotopic study of Puklen suggested that whereas the syenites may be regarded as mantle derivatives variously modified by assimilation of upper crustal materials, the O isotope data for the granites imply either a different source or a different crustal contaminant (Marks *et al.* 2003). These conclusions may also be applicable to the TCC.

Comparable phenomena to those of the TCC and Puklen are known from syenite autoliths within the Kilombe volcano in the Kenya rift. Kilombe may provide a modern analogue for the volcano inferred to have overlain the TCC. It was deduced from Kilombe that carbonatitic fluids rich in F, Na and REE percolated the subvolcanic system, interacting with the syenites at the thermal boundary layers of the magma chamber during and after their crystallisation (Ridolfi *et al*. 2006a, 2006b).

If the TCC was overlain by a central volcano comparable to Kilombe, this would have been largely composed of trachytic and comenditic extrusives. The western centre may have been crowned with a small trachytic cone whereas the eastern centre probably underlay a nested set of concentric calderas. The Unit 6 magmas may have underlain a culminating caldera, developed by late collapse of a peralkaline salic volcano. On the basis of Macdonald and Smith's (1968) hypothesis relating the area of calderas to the volume of extrusives, the TCC may have erupted <6 km³ of magma.

Late basic dykes

Whereas intrusion of the Main dyke swarm was essentially ended before the Tugtutôq central complex was emplaced, there was some small-scale revival of dyke activity in post-TCC times (Martin 1985) that produced sparse, thin (<2 m) dykes with the same regional ENE–WSW trend as the rift as a whole. A few are trachytic but other basic dykes are distinctive in that they are typically flow-banded and contain megacrysts and in some cases xenoliths and also generally contain ocelli (Fig. 89). The volatile-rich nature, ocelli, megacrysts and phenocrysts indicate a lamprophyric and, more specifically, a camptonitic character. Similar, strongly altered, camptonite dykes cut the Kvanefjeld area of the Ilímaussaq complex (Sørensen *et al*. 1974, Larsen 2006). The ENE–WSW trend of the camptonites strengthens the case for their acceptance as Gardar intrusions and they are provisionally accepted as of Younger Gardar age although they have not been dated. A very fresh, NNE-striking monchiquite dyke that cuts the Ilímaussaq intrusion on Kvanefjeld (Larsen 2006) has been Rb-Sr dated to 1134 ± 17 Ma (Table 1). The unaltered character of this dyke suggests it was emplaced after the alteration of the camptonites, also strengthening a Gardar age for these.

The camptonite dykes contain phenocrysts of plagioclase and titan-augite. The ocelli, generally occupied by chlorite and calcite ± albite and epidote, compose up to 15% by volume of the dykes. Single feldspar megacrysts (up to 5 cm large) occur as do composite aggregates comprising feldspar, magnetite and ferromagnesian minerals. The feldspars are normally-zoned, An_{66-33}. The megacryst assemblages include amphibole (potassian kaersutite) and titanium-rich biotite as well as clinopyroxene, magnetite and apatite. It is the concentration of megacrysts and phenocrysts into subparallel layers that gives rise to the flow-banding of the dykes.

Compositionally the Late basic dykes resemble the Main swarm hawaiites but differ in being olivine-free, more volatile-enriched and silica undersaturated. Major element ratios typifying both dyke sets are similar and both are typical of Gardar mafic rocks in general (i.e. with high Al/Ca and low Mg/Fe). These late dykes, however, have lower Al/Ca but significantly higher Mg/(Mg+Fe),

Fig. 89. Late basic dyke, Nasaasarli, Tuttutooq. Hammer *c.* 50 cm long.

Ni, Cr and V than the main swarm hawaiites. The chondrite-normalised incompatible element patterns of the late basic dykes are relatively smooth, much like those of the main swarm hawaiites. They lack any significant Eu anomaly and have La_N/Yb_N values between 12.8 and 17.5 (Martin 1985). However, relative to main swarm hawaiites, the late basic dykes are less enriched in REE. If they are late components of the southern rift (Tuttutooq–Ilimmaasaq–Narsarsuaq) magmatic system these dykes are important in signalling a renewed mantle melting episode, albeit on a minor scale.

Ilímaussaq complex

The original description of this extraordinary intrusion was given by N.V. Ussing (1912) and over the past forty years a plethora of publications has appeared adding much detailed information. General reviews have been presented by Ferguson (1964), Larsen & Sørensen (1987) and Sørensen (2001, 2006). The Ilímaussaq complex has long attracted attention for its exotic mineralogy and for the layered syenites. The petrogenesis of its rocks has long been debated and still remains contentious. In the 1950s and 1960s Ilímaussaq received close investigation because of its potential as a source of uranium. Subsequently its content of rare metals including zirconium, beryllium, niobium, and tantalum brought it to the attention of mining companies. Most recently the possibil-
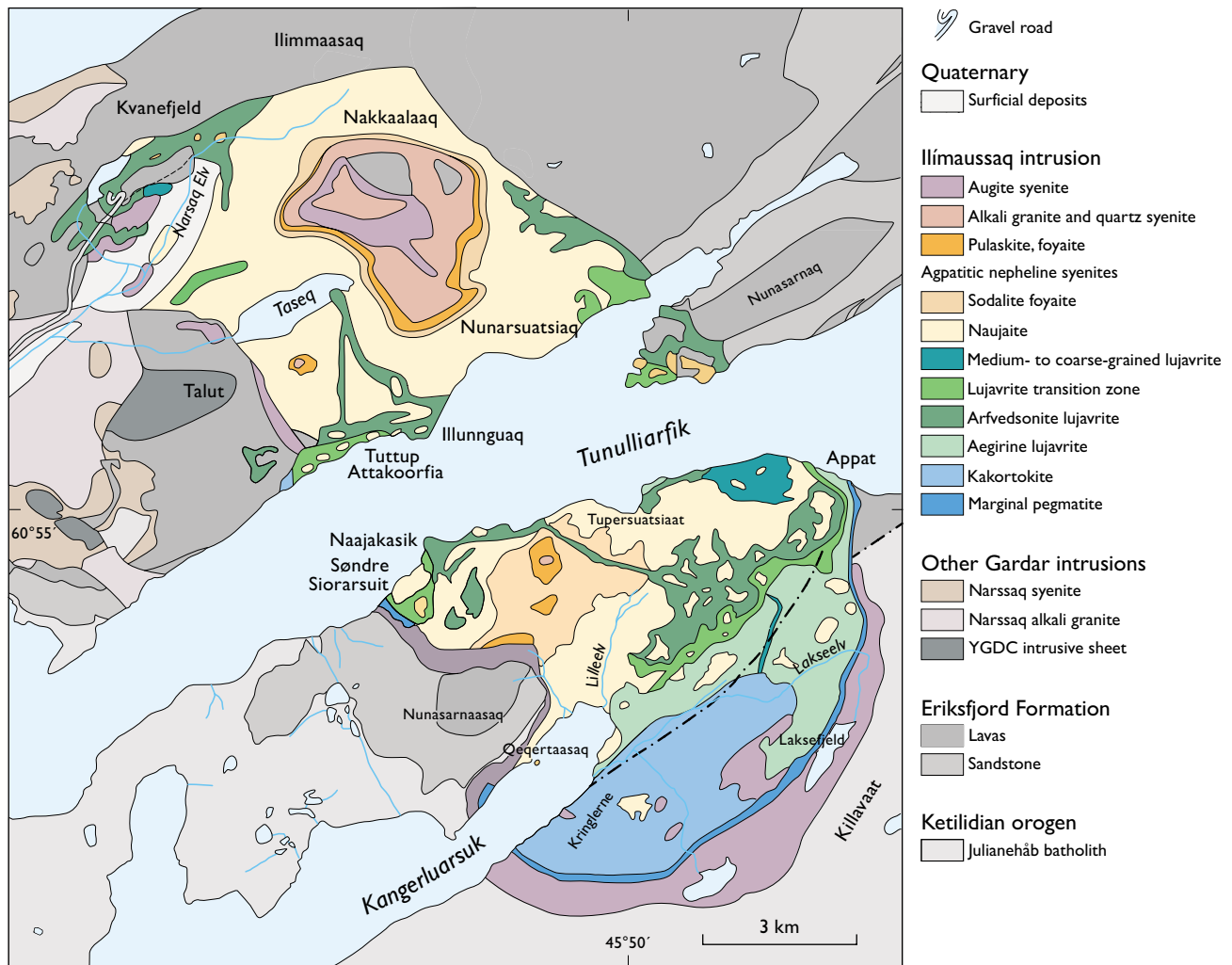

Fig. 90. Geological map of the Ilímaussaq complex. Modified from Ferguson (1964) north of Tunulliarfik, Andersen *et al.* (1988) south of Tunulliarfik, and Sørensen (2001).

Fig. 91. Northern part of the Ilímaussaq complex viewed across Tunulliarfik.

ity of exploiting different rock facies for rare-earth elements has kindled worldwide interest.

The complex has a crudely ovoid plan *c.* 18×8 km, elongate north-west–south-east, transverse to the southern rift zone (Figs 90, 91). It has been precisely dated at 1160 Ma (Table 1). Although intruded across the transcurrent fault that previously accompanied and displaced the Narssaq complex, it post-dated all significant movements along it. Nonetheless, the form of the intrusion appears to have been partially dictated by the fault, particularly the marginal embayment in its north-western sector. Stephenson (1976b) suggested that the overall elliptical outline of the complex was a product of strain when it was still ductile, as in the cases of the South Qôroq and Igdlerfigssalik complexes. Planar deformation flaser structures occur in the earliest component (augite syenite) beside Narsaq Elv (Narsaq River) close to the fault extrapolation (Hamilton 1964). A photograph in Ferguson (1964) portrays stretched naujaite (a rock type described below) that appears to have undergone ductile deformation. Although the precise locality is not given, it is from "N.W. of Taseq lake" which could put it close to the eastward extrapolation of the transcurrent fault. These deformations in the augite syenite and naujaite suggest that seismic stability had not been entirely achieved at the time the complex was emplaced. On the eastern slopes of Kvanefjeld (in the north-western part of the complex) the country rocks are fractured and sheared close to the contact. The volcanic roof in this locality dropped by 300 to 400 m through faulting prior to consolidation of the agpaitic rocks beneath (J.G. Larsen 1977). Some 12 km to the east-south-east, at Nunasarnaq on the north side of Tunulliarfik

fjord, the Eriksfjord Formation sandstones and lavas are strongly sheared (Sørensen 2006). Such shearing is atypical at the margins of the Gardar plutons; emplacement by stoping would not entail such deformation and the implication is that faulting had taken place prior to magma emplacement. As with the Narsaq complex, intersection of the transcurrent fault and rift axis fissuring is presumed to have provided the potential conduit that was exploited by buoyant magmas. The magmatic focus, however, had now relocated from the Narsaq area several kilometres eastwards along the fault zone.

A critical hinge-fault, traversing the southern part of the Ilímaussaq complex, can be traced east-north-eastwards from the Kangerluarsuk Fjord and along Lakseelv (Fig. 90). This fault divides the complex into a southern portion containing the lowest exposures and a larger northern portion that reveals shallower levels in the intrusion (Ferguson 1964; Bohse *et al*. 1971; Sørensen 2006). The downthrow on the northern side diminishes towards the east-north-east from at least 600 m in Kangerluarsuk towards zero as it reaches Appat on the southern coast of Tunulliafik. The northerly downthrow relates to two (and possibly three) successive movements: pre-Ilímaussaq, post-aegirine lujavrite, and possibly post-arfvedsonite lujavrite (Bohse *et al*. 1971; Sørensen 2006). In the structurally higher northern part the upper part of the complex is preserved, with Eriksfjord Formation strata as the principal country rocks. The exposures in the deeper southern part below the base of the Eriksford Formation show the Ilímaussaq augite syenite in contact with the Julianehåb batholith granitoids (Fig. 90).
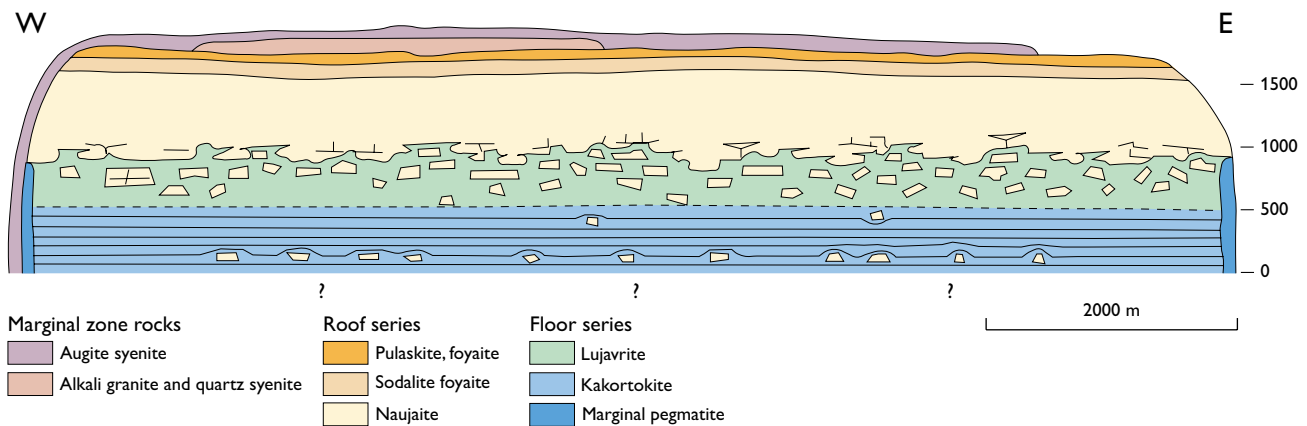
Fig. 92. Simplified section across the Ilímaussaq complex. From Andersen *et al.* (1981a).

Until recently there was general consensus that the complex formed through three successive intrusions but recent work (Sørensen *et al.* 2006) suggests that there were four or possibly more, each of which followed sufficiently quickly to preclude development of well-chilled internal contacts. Accordingly the entire Ilímaussaq assemblage would have cooled as a single thermal unit. All the components are believed to have originated from a single parental source, with fractional crystallisation governed by low water activity, low silica actvity and low f_{O_2} (Engell 1973; Larsen 1976, 1977; Larsen & Sørensen 1987; Marks & Markl 2001). Crystallisation of the entire complex took place over an extended temperature interval of at least 950–450°C (Larsen & Sørensen 1987) and possibly persisting down to 300°C (Marks *et al.* 2007) with the closing phases being marked by an abundance of pegmatites and hydrothermal veins (Engell *et al.* 1971).

In this account it will be assumed that there were three principal intrusions, yielding: 1) augite syenite, 2) alkali granite and quartz syenite, 3) agpaites, but bearing in mind that the actual number of agpaitic influxes remains controversial. Agpaite was the name bestowed by Ussing (1912, p. 341) on these highly peralkaline rocks. He defined them as follows: "Thus if *na*, *k* and *al* are the relative amounts of Na, K and Al atoms in the rock, the agpaites may be characterized by the equation $(na + k)/al \geq 1.2$, whereas in most ordinary nepheline syenites the ratio does not exceed 1.1". Ussing called this ratio the 'agpaitic index' but it is more correctly termed 'the peralkalinity index' (Sørensen 1997). Agpaites are peralkaline nepheline syenites containing aegirine, sodic amphibole and/or aenigmatite as well as complex Zr- and Ti-silicates. They are rich in F, Cl and H_2O (Sørensen 1960) and are characterised by exceptionally high con-

tents of Zr, Hf, Nb, REE, U and a host of other highly incompatible elements (Bailey *et al.* 2001). The Ilímaussaq agpaites are regarded as the products of extremely fractionated iron-rich phonolitic magmas and include some of the most evolved and incompatible-element-rich rocks on Earth. They comprise the rock types sodalite foyaite, naujaite, kakortokite and lujavrite.

For several decades after Ussing it was considered that a single agpaitic magma body had differentiated into a downgrown roof sequence, a complementary upgrown floor sequence of layered cumulates, and a trapped 'sandwich horizon' that crystallised between the two (Fig. 92). This hypothesis, proposed by Ussing (1912), that an initially homogeneous magma had crystallised as a closed system to produce the contrasting rock types was, for many years, generally accepted (e.g. Ferguson 1964, 1970a 1970b; Sørensen 1969; Engell 1973). Studies over the past thirty years, however, have shown that the closed system model for the agpaitic magma is too simplistic although it retains its adherents. Whilst belief in the ultimate consanguinity of the agpaitic rocks remains unshaken, at least two magma influxes of peralkaline composition are now proposed (Sørensen 2006) and the possibility of multiple replenishments is being considered.

There is general consensus that the rocks crystallised at a pressure of *c*. 1 kb, corresponding to a depth of 2–3 km (J.G. Larsen 1974; Konnerup Madsen *et al.* 1979; Krumrei *et al.* 2007). Heat-flow data suggest that the total thickness of the agpaitic rocks, with their high contents of radioactive elements, should be less than 1 km (Sass *et al.* 1972). Gravity and density data gave a best-fit model showing that a heavy body, with density of least 2.9 g/cm³ and vertical boundaries, underlies the complex

at a depth of 2–5 km (Forsberg & Rasmussen 1978). As emplacement of the complex must have involved foundering, not only of Julianehåb granitoids but of the basaltic Eriksfjord Formation lavas and gabbros of the YGDC lopolith, this heavy body is likely to include these pre-Ilímaussaq country rocks together with any cogenetic high-density cumulates.

Augite Syenite

Augite syenite is present as a partial shell around the western and southern sides of the complex. The augite syenite probably originally formed a single body almost all of which, except for the remnant shell, foundered within the younger agpaitic magma(s). The focus of the agpaitic activity migrated eastwards by <1 km in relation to its augite syenite predecessor. The augite syenite contacts vary from steep to vertical to outwardly dipping beneath quartzites and an intrusive sheet (Older Gardar) between Tunulliarfik and Kangerluarsuk fjords. In the northern part of the complex the augite syenite has a subhorizontal contact with Eriksford Formation trachytic lava (Ferguson 1964). Whereas there is consensus that the youngest agpaitic magmas crystallised essentially in a closed system beneath a more or less impervious capping, this is less certain in the case of the augite syenite.

The augite syenite is deduced to have been emplaced by block subsidence (Sørensen 1978; Nielsen & Steenfelt 1979). Evidence of some piecemeal stoping, however, is provided by clasts of quartzite up to 100 m across derived from the Eriksfjord Formation, that occur in the augite syenite on the southern shore of Kangerluarsuk fjord (Ussing 1912; Ferguson 1964). Since these quartzite xenoliths occur far below the Eriksfjord Formation – Julianehåb granite unconformity, their presence implies that the magma had both low density and low viscosity. The pattern for emplacement among several Gardar plutons involved repetitive collapses of slices or rafts of roof rocks (providing temporary 'floors' for cumulate deposition) and this process may also have characterised the augite syenite emplacement. On either side of Kangerluarsuk fjord the augite syenite has well-chilled margins against the country rock granitoids although on the northern coast there is notable rheomorphism. The augite syenite also shows signs of chilling against Eriksfjord Formation trachyte in the summit area north and north-east of Taseq (Fig. 90) where the roof zone is exposed (Ferguson 1964).

Strongly sheared augite syenite xenoliths are found at Kvanefjeld in the far north-west of the complex and within lujavrite in a contact breccia (mélange) at the western contact on the northern coast of Tunulliarfik. Augite syenite is also seen as large xenolithic masses in the kakortokites which, as described below, form the lowest exposed unit in the complex (Ferguson 1964; Sørensen 1978, 2006; Nielsen & Steenfelt 1979). Tilting of Eriksfjord Formation strata in towards the intrusion suggests that country rock engulfment during emplacement of the augite syenite and/or the agpaitic magma(s) was accompanied by down-drag of the adjacent crust. However, the inward dips may also relate to very late-stage downsagging of the central part of the complex (Ussing 1912; Sørensen 2006).

Fine-grained marginal facies of the augite syenite show the magma to have been a silica-undersaturated benmoreitic magma, closely related to the benmoreites of the Igaliko dyke swarm (Upton & Emeleus 1987). Apart from some relic oligoclase (Hamilton 1964; Larsen 1981), zonation in feldspars from the chilled marginal facies shows the rhomboidal form characteristic of early-formed anorthoclase (Upton 1964a; Larsen 1981). The chilled marginal feldspars are identical to those of the South Qôroq augite syenite S4 (Stephenson 1976a; Larsen 1981). The feldspars are mostly untwinned cryptoperthite to microperthite, with compositions $An_{20}Ab_{76}Or_4$ to $An_{3.5}Ab_{43.5}Or_{53}$ straddling the oligoclase – ternary feldspar (anorthoclase) – sodic sanidine range. Nepheline occurs interstitially. The early ferromagnesian minerals are ferrosalitic pyroxene (100 Mg/(Mg+Fe^{2+}+Mn) = 52–21) and olivine ($Fo_{17.3-4.0}$) closely mirroring compositions in the eastern stock at the Kûngnât complex (Larsen 1976; Stephenson & Upton 1982). These are accompanied by amphibole (titanian ferroan pargasitic hornblende), titan-biotite, nepheline, magnetite and apatite (Larsen 1976, 1981). The ternary feldspar crystallised at *c.* 1000°C and according to Marks & Markl (2001) and Markl *et al.* (2001) it was joined by magnetite, olivine and augite within the interval 800–650°C. However, on the presumption that the parental augite syenite magma was a younger batch from the same source as the preceding 'rhomb-porphyry' benmoreite dykes, it is more probable that it already contained phenocrysts of feldspar, olivine, augite, titanomagnetite and apatite at the time of intrusion.

In the deeper section of the complex, south of the Kangerluarsuk–Lakseelv fault, the augite syenite exhibits various forms of modal layering. Some gravity-stratified modal layering dips steeply inward (Fig. 93). This is

Fig. 94. Polished slab (11 cm wide) of the Ilímaussaq alkali granite. The green colouration is due to micro-inclusions of aegirine in the alkali feldspar. Grey areas are quartz; black is mainly arfvedsonite.

Fig. 93. Modal layering in augite syenite on the south coast of Kangerluarsuk. Hammer *c.* 40 cm long.

comparable to features in the Nunarssuit and Kûngnât syenites ascribed to marginal, downflowing slurries of melt and primocrysts that deposited their crystal component as the flow velocity diminished and the sidewalls graded into lower-angled chamber floors (Upton *et al.* 1996). However, repetitive inch-scale isomodal layering is also developed in these southernmost outcrops (Ferguson 1964). The inference is that the syenite formed a layered, stock-like body from a magma chamber in which two-phase (i.e. liquid+crystals) convection developed. The Older Gardar eastern stock of the Kûngnât complex appears to provide the closest analogue in the Gardar Province (Upton 1960; Upton *et al.* 2013).

Alkali granite and quartz syenite

Two silica-oversaturated sheets cut the augite syenite in the highest parts of the complex. The quartz syenite forms a layer above the pulaskite (described below) and is overlain by alkali granite (Ferguson 1964; Steenfelt 1981). The age relationships between the quartz syenite and granite are indeterminate and it has been suggested that the quartz syenites are products of interaction be-

tween the granite and nepheline syenite magma (Sørensen 2006).

The alkali granite (Fig. 94) is hypersolvus and comprises *c.* 54% perthite, *c.* 30% quartz, *c.* 15% aegirine+ arfvedsonite and *c.* 1% accessory minerals (Hamilton 1964). Early, untwinned, alkali feldspar is inferred to have been replaced by microcline perthite and later, granular albite. The feldspars contain a host of minute (<100 μ) aegirine prisms, possibly exsolution products, that confer a green colouration to the rock (Fig. 94). Arfvedsonite, with some relic aenigmatite cores (Larsen 1977) has rims partially replaced by aegirine. The granite magma was highly enriched in incompatible elements (Bailey *et al.* 2001) manifest in the presence of e.g. Na-Zr and Na-Be silicates (elpidite and epididymite). Other minor components include astrophyllite, pyrochlore, leucosphene, fluorite, calcite and zircon (Ussing 1912; Hamilton 1964). The La/Yb$_N$ ratio is 9–10 and there is a marked negative Eu anomaly. Crystallisation occurred at, or above, 750°C but the late growth of aegirine (at the expense of arfvedsonite) took place at, or below, 350°C (Markl *et al.* 2001).

Agpaitic syenites

The rocks crystallised from the agpaitic magma comprise a roof series of pulaskite, foyaite, sodalite foyaite and naujaite, a floor series of kakortokites and lujavrites, and a 'sandwich horizon' of lujavrites. The total thickness of agpaitic rocks is estimated at c. 1600 m (Andersen et al. 1981a; Krumrei et al. 2007). By the time the lowest exposed kakortokites were deposited, the roof series was already solidified and c. 800 m thick (Bohse & Andersen 1981) so that the naujaite had cooled to, or below, its solidus at c. 500°C (Andersen et al. 1981a; Konnerup-Madsen & Rose-Hansen 1982). Subsidence of the chamber floor probably occurred incrementally rather than in a single event while the floor cumulates were being deposited. The occurrence of naujaite and foyaite autoliths at various levels within the kakortokite-lujavrite succession suggests episodic roof instability. At Nunasarnaq (eastern contact, north coast of Tunulliarfik, Fig. 90) the magma chamber wall appears to have collapsed, with detachment of large xenoliths (some several hundred metres across) of naujaite and Eriksfjord Formation basalt into unconsolidated lujavrite (Sørensen 2006). And at the southern and eastern contacts vertical fractures present in the augite syenite and adjacent Julianehåb granitoids are thought to be related to the 'rafts' of these rocks that collapsed into the chamber during emplacement of the lujavrite. At Kvanefeld (at the north-west margin of the intrusion) xenoliths of basalt, gabbro, anorthosite, augite syenite, naujaite and alkali syenite lie within the lujavrite (Ferguson 1964; Sørensen 2006; Sørensen et al. 2011).

The agpaitic magmas are regarded as residual after very high degrees of fractional crystallisation from an augite syenite parental magma (Engell 1973; Bailey et al. 2001) and are inferred to have been highly fractionated, iron-rich phonolites. Their crystallisation was controlled by low activities of water and silica in conjunction with low oxygen and sulphur fugacities (Sørensen et al. 2006). The time span for fractionation within the agpaite magma has been shown by Ar data to have been not merely less than 5 Ma, but possibly much shorter, probably of the order of 500–800 ka (Krumrei et al. 2006).

Molecular CH_4 and other hydrocarbons present in fluid inclusions in the agpaites have generally been regarded as of magmatic origin (Konnerup-Madsen & Rose-Hansen 1982; Konnerup-Madsen et al. 1988; Konnerup-Madsen 2001). However, this has recently been challenged by Laier & Nytoft (1995, 2012) who argue that the hydrocarbons contain characteristic biomarkers and the carbon isotope signatures point to an organic origin, probably originating from downward percolation of fluids from much younger Mesozoic–Cenozoic sediments.

Although the great bulk of the agpaites consists of cumulates or pegmatites some rocks (e.g. the finer-grained facies of the marginal pegmatite and some of the final lujavrites and the micro-kakortokite dyke, each described below, have bulk compositions thought to approximate to those of melts (Larsen & Steenfelt 1974; Larsen & Sørensen 1987; Sørensen 2006).

Roof series

Pulaskite, foyaite, sodalite foyaite. Rocks constituting the roof series of the agpaitic part of the complex are preserved beneath a cover of augite syenite and/or Eriksfjord Formation lavas. Although Fig. 92 shows the agpaitic roof to be approximately horizontal, it is distinctly irregular (Sørensen 2006). The roof rocks are notably coarse-grained with much conformable pegmatite, attributable to accumulation of volatiles beneath an impermeable roof (Ferguson & Pulvertaft 1963; Ferguson 1964; Larsen & Sørensen 1987; Sørensen 2006). A downward accreting crystallisation front created a roof series comprising a four-member sequence (Ussing 1912; Ferguson 1964; Larsen & Sørensen 1987; Sørensen 2006). From the top down these are pulaskite, foyaite, sodalite foyaite and naujaite, produced successively from increasingly fractionated melts. Thus the sequence has some analogy with the Upper border group at Skaergaard (Wager & Brown 1968) as well as with the inferred roof series at Klokken. Although the pulaskite and foyaite do not themselves qualify as agpaites they are regarded as the earliest (roof) products from the magma body from which the true agpaites crystallised. The sodalite foyaite crops out over a wide area above the naujaite between the Tunulliarfik and Kangerluarsuk fjords. Engell (1973) considered the bulk composition of the sodalite foyaite to approximate that of the magma from which the agpaitic part of the Ilímaussaq complex formed. From Zr and Be data it was estimated that, in order to have progressed from the augite syenite stage to the sodalite foyaite stage, 80 to 95% crystallisation of augite syenite (or benmoreite) magma must have occurred and accordingly Engell postulated a very large underlying magma chamber.

The pulaskite, foyaite and sodalite foyaite units differ texturally as well as petrographically. The pulaskite is coarse-grained and essentially homogeneous, consisting of alkali feldspar, fayalite, hedenbergite, titanomagnetite and apatite with minor nepheline (Larsen 1976). In con-

Fig. 95. Layered foyaite overlying naujaite, between Tunulliarfik and Kangerluarsuk fjords.

trast, the foyaite (*c.* 20 m thick) is very heterogeneous and exhibits both modal and textural layering (Fig. 95). Layers of pegmatite, *c.* 1 m thick, occur at the tops of the layers, with crystals that have grown perpendicularly downwards. Each pegmatite then grades into normal coarse foyaite below (Ferguson 1964; Larsen & Sørensen 1987).

The underlying sodalite foyaite marks the onset of agpaite crystallisation. Because the composition of the sodalite foyaite is similar to that of the calculated average agpaite it may approximate to the magma composition (Ussing 1912; Sørensen 1958, 1969; Gerasimovsky & Kuznetsova 1967; Engell 1973). The sodalite foyaite is coarse but more evenly grained than the units above, with a poikilitic texture in its lower parts. The rock comprises alkali feldspar, nepheline, alkali pyroxene, alkali amphibole and sodalite, with minor early-formed hedenbergite, fayalite, titanomagnetite and apatite, and late analcime and natrolite; in addition the characteristic agpaitic phases eudialyte and rinkite are present (Ussing 1912; Ferguson 1964; Hamilton 1964; Larsen 1976). According to Hamilton (1964), the modal percentage of fayalite decreases downwards through the sodalite foyaite.

As the pulaskite-foyaite-sodalite foyaite succession accreted downwards, Mg in the melt decreased whilst Na and Zr concentrations increased (Larsen 1976). The temperature is estimated to have fallen from *c.* 900 to *c.* 800°C. Initially the magmas were in equilibrium with a H_2O-free high-temperature mineral assemblage (alkali feldspar, fayalite, hedenbergite, Ti-magnetite and apatite). The change from foyaite to sodalite foyaite involved an increase in nepheline as well as the appearance of so-

dalite. The latter signalled the stage at which the magma became saturated in chloride. When the temperature fell to *c.* 700°C, volatile saturation is thought to have been attained and exsolution of a fluid phase brought about reaction of the high temperature mafic minerals to alkali amphibole, aegirine, aenigmatite and eudialyte (Larsen & Sørensen 1987).

Naujaite. The sodalite foyaite is underlain by the remarkable rock type which Ussing (1912) called naujaite. Although the modal assemblage of the naujaite is essentially identical to that of the foregoing sodalite foyaite, the texture and mineral proportions are strikingly different. Naujaite, unique in composition and texture, contains sodalite as the dominant component. The sodalite is typically present up 40–50% modally but can vary from 20 to 75% (Sørensen 2006; Fig. 96). The crystals (2–3 mm large) appear in two distinct morphologies (Hamilton 1964; Larsen & Sørensen 1987), dodecahedra and hexagonal prisms. The latter, formerly thought to pseudomorph nepheline (Hamilton 1964), are more probably paramorphs after a high-pressure polymorph (A.A. Finch, personal communication, 2012).

Ussing (1912) recognised that the concentration of idiomorphic to euhedral sodalite must have been brought about through a flotation process, a conclusion accepted by all subsequent investigators. The density of sodalite (*c.* 2.29 g/cm³) is presumed to have been less than that of its host magma so that the sodalite primocrysts floated up and accumulated beneath the sodalite foyaite. Fayalite, hedenbergite, titanomagnetite and apatite are

Fig. 96. Naujaite outcrop showing one or more giant oikocrysts of eudialyte (reddish brown). Hammer shaft *c.* 50 cm long.

still present as early phases (primocrysts), but are only very minor components in the naujaite. Being dense phases the bulk of them may have sunk to contribute to an unseen complementary floor sequence of cumulates (Larsen 1976).

The naujaites are very loosely compacted cumulates with the intercumulus taking the place of the 30–60% contemporary melt. Most of the latter crystallised to alkali feldspar, nepheline, arfvedsonite and eudialyte oikocrysts up to 30 cm across (Fig. 96). Their large size is taken as further evidence that the melt had very low viscosity, providing exceptional ease for ionic migration. The feldspar is mainly microcline microperthite (with some cryptoperthite) marginally altered to analcime and natrolite. The thickness of the naujaite unit is estimated at some 600 m (Andersen *et al.* 1981a) but, as its lower levels have been magmatically eroded by later magma, the original thickness is inferred to have been significantly greater (Sørensen 2006; Sørensen *et al.* 2006). On the assumption that the naujaite extended across the whole agpaite complex, a volume of >60 km³ has been estimated (Sørensen 2006).

A large, convecting, slowly cooling magma chamber with crystallisation along its roof, walls and floor is envisaged (Larsen & Sørensen 1987). Sodalite crystallising at depth along the chamber walls may have ascended to contribute to the downgrowing roof cumulate. Furthermore, in order to account for the extraordinary quantity of sodalite in the naujaites, a parental magma chamber with a volume many times greater than that of the present volume of the complex is supposed (Larsen & Sørensen

1987; Rose-Hansen & Sørensen 2002). Such a chamber must have had a volume at least ten times greater than the estimated (minimum) 60 km³ of the naujaite.

Large-scale layering in the naujaite (Fig. 97) is due to the occurrence of conformable pegmatite horizons about 0.5 m thick (Ussing 1912; Larsen & Sørensen 1987), separated by 10–30 m of normal rock. In the pegmatite horizons the sodalite crystallised downwards from the contemporary roof as prismatic crystals. This, together with the pegmatites in the foyaite, affords a second example of inward-growing crescumulates, the development of which may have coincided with periods of tranquillity when convection in the underlying magma diminished, allowing volatile concentration beneath the chamber roof. Addition of volatiles is presumed to have lowered the melt density to less than that of sodalite, temporarily preventing further flotation of sodalite primocrysts, i.e. there were interludes when the normal process of accretion ceased and sodalite crescumulates developed *in situ*. Thus, the naujaite crystallisation front appears to have accreted downwards in a pulsatory fashion.

There is a generalised increase in the amount of pegmatite down-section, signifying concentration of volatiles in the diminishing host magma (Larsen & Sørensen 1987). Another form of layering in the naujaites noted by Hamilton (1964) is that in places mafic layers composed of arfvedsonite and aegirine "are not uncommon". Thin layers (*c.* 25 cm) of mafic rock containing concentrates of prismatic aegirine pass upwards into normal naujaite in which aegirine has poikilitic morphology. There are also unusual features in the naujaites of Narsaq Elv (north-

Fig. 97. Terracing in naujaite on the southern side of Tunulliarik fjord, caused by in-weathering of pegmatitic horizons.

west Ilimmaasaq, Fig. 90) in which masses of naujaite (up to 2 m) are enclosed in another naujaite facies (Hamilton 1964). Clearly there are some features within the naujaites suggestive of more complex marginal structures. Larsen & Sørensen (1987) mention discontinuous screens of naujaite within the younger pegmatite zone surrounding the kakortokites that may represent remnants of a former marginal facies to the naujaite body.

Geochemical changes in the upper roof sequence include marked differences in the Zr/U ratios through the pulaskite, foyaite, sodalite foyaite and higher parts of the naujaite, and a much lower concentration of U for any given Zr value in the lower naujaites (Bailey *et al.* 2001). Clearly naujaite growth was not a simple steady-state process but one of considerable complexity. In these sodalite-rich rocks, chlorine is a major rock-forming element; the naujaites typically contain 2–3.5 wt% Cl but the content can reach 4.6 wt% (Bailey *et al* 2001). Cryptic layering, previously noted in the pulaskite-foyaite-sodalite foyaite suite, persisted in the naujaites. Early sodalites are enriched in Br, I and B relative to later ones (Bailey 2006). Sulphur is also present in the sodalite as SO_4 (the sulphatic sodalite referred to as hackmanite) although

both sulphide and sulphate ions coexisted in the melt (Krumrei *et al.* 2007). The cores of the sodalite crystals contain minute aegirine prisms as well as hydrocarbon inclusions; study of the latter reveals that the host sodalites grew from a highly reduced, halogen-rich magma in equilibrium with CH_4 at *c.* 800°C. The sodalites are inferred to have acquired their aegirine and hydrocarbon inclusions in the course of their crystallisation during magma ascent. By contrast, their inclusion-free rims may represent crystallisation during emplacement (Krumrei *et al.* 2007).

Whereas the naujaites crystallised at a pressure of *c.* 1 kb, the fluid inclusions in the sodalites are deduced to have been trapped at pressures of up to 4 kb (Krumrei *et al.* 2007). On this basis, the depth of the magma in which the sodalites commenced growth could have been as much as 12 km. Accordingly, the crystals may have grown over a wide range of depths, either during passive ascent (flotation) or while they were entrained in rising magma. This conclusion necessitates a re-assessment of the hitherto accepted belief that the agpaitic rocks at Ilímaussaq have a total thickness barely exceeding 1 km (Sass *et al.* 1972). The conduit through which the nau-

Fig. 98. Layered kakortokites at Kringlerne, looking south across Kangerluarsuk fjord. The unlayered mass in the centre, immediately above a talus slope, is a large xenolith of naujaite. In the far distance are peaks of the Julianehåb batholith (Redekammen) behind the southern margin of the complex.

jaite magma ascended may have been restricted in size (dyke-like?), spreading laterally into a near-horizontal tabular body (*c*. 100 km², Sørensen 2006) at or near the Eriksfjord Formation basal unconformity, as is inferred for the giant dyke intrusions. Such a geometry may explain the discrepancy between a model demanding a very large volume of agpaitic magma crystallising at depth and the conclusion reached by Sass *et al*. (1972). However, the heat-flow measurements by Sass *et al*. (1972) were made at Kvanefjeld near the north-west margin of the complex; this opens the possibility that, had the measurements been taken at a more central locality, significantly higher values might have been obtained, more compatible with the concept of a much larger (deeper) phonolitic chamber capable of supplying the great quantity of sodalite requisite for naujaite formation. It would be of future interest to investigate fluid inclusions within the sodalites grown *in situ* in the pegmatitic layers in the naujaite.

Floor series

Accumulated on a hypothetical floor beneath the naujaites are the kakortokites that occur in an excellently exposed succession that must rank among the most astounding examples of layered cumulates on the planet. The kakortokites compose the lowest exposed 300 m of the succession and pass gradationally up into *c*. 400 m of lujavrites. The stratigraphy was established by Bohse *et al*. (1971) and reviewed by Bohse & Andersen (1981) and Andersen *et al*. 1981; Fig. 98).

Kakortokites. The kakortokites are generally separated from their wall rocks (augite syenite, Julianehåb granite and Eriksfjord Formation quartzites) by a steep pegmatitic zone, 25 to 100 m wide (Andersen *et al*. 1981a; Sørensen 2006) that is absent from most of the western, northern and eastern agpaite contacts and is essentially restricted to the lower part of the complex, adjacent to the kakortokite and aegirine lujavrite. The pegmatite zone is texturally heterogeneous, with fine-grained

Fig. 99. Graded units in kakortokite of the Ilímaussaq complex. Scale 50 cm.

foyaite intervening between abundant anastomosing veins of pegmatite. The former may provide insight into the nature of the magma from which the layered series crystallised (Sørensen et al. 2006; Sørensen 2006). The outer boundary of the marginal pegmatitic zone is sharp but the inner side (against the kakortokites) is more indistinct (Bohse & Andersen 1981). It would appear that a relatively finer-grained chilled facies was extensively modified by later migration of volatiles, down a temperature gradient, towards the chamber walls. Analogy may be drawn with the marginal border group of the eastern syenite at the Kûngnât complex (Upton et al. 2013) and comparison may also be made to the outflow of residual fluids from the Igdlerfigssalik syenites (see below).

The marginal zone surrounds twenty-nine well-defined layered units, dipping gently (c. 10°) towards the centre of the intrusion and making up the lower part of the exposed sequence. These units, composing the lower layered kakortokite series (Fig. 98), are numbered from −11 upwards to +17 and have thicknesses of 3.5–12.5 m with an average of c. 8 m (Bohse et al. 1971). The idealised unit is tripartite, commencing abruptly with an arfvedsonite-rich base of black kakortokite that grades up into increasingly eudialyte-rich red kakortokite succeeded in turn by white kakortokite in which feldspar and nepheline are the dominant components. However, in some units the red kakortokite facies is poorly developed or even absent. The normal grading in each unit (Fig. 99) has been accepted by most investigators as explicable in terms of gravitational sorting during crystal settling, reflecting the decreasing density in the sequence arfvedsonite, eudialyte, feldspar+nepheline.

The kakortokites are orthocumulates in which the principal cumulus components are alkali feldspar, nepheline, eudialyte and arfvedsonite. Fluorite and aenigmatite attain cumulus status in some units (L.M. Larsen 1977; Sørensen & Larsen 1987). Thus the kakortokite magma appears to have crystallised along a remarkable poly-component cotectic. Arfvedsonite as a cumulus phase is, however, restricted to the (black) basal layers and the mineral is only present as an intercumulus component in the red and white layers. There is a significant difference in the degree of compaction from bottom to top of the units, with close-packing of arfvedsonite in the basal portions grading to loose packing in the unlaminated white kakortokite tops (Upton 1961). From their thin tabular morphology the microcline microperthitic feldspars of the kakortokites inferentially crystallised as monoclinic sanidines. The transition from white tops of the units to the overlying black bases can take place over several centimetres or can be knife-sharp (Ferguson 1964).

Apart from localised thinnings (as beneath roof rock autoliths), the units tend to retain constant thickness and to be laterally continuous for distances of c. 5 km along strike. Although there are some indications of incipient trough erosion and deposition in the lower units there is generally very little evidence for convective flow of the magma. The passage upwards in each unit from well-laminated mafic or ultramafic bases to unlaminated leucocratic tops, attributed to progressively declining flow of magma currents by Upton (1961), more probably reflects close-packing of the dense arfvedsonites contrasting with low degree of packing in the felsic tops. The observations suggest that the kakortokite magma was remarkably tranquil and had low viscosity, thus permitting virtually complete settling of all arfvedsonite crystals as each unit commenced crystallisation. The agpaitic magmas are estimated to have been de-polymerised and at least as fluid as basaltic magmas despite their lower temperatures (Larsen & Sørensen 1987; Bailey et al. 2001). Accordingly they would have been capable of turbulent flow so that, initially, only a small percentage of the primocrysts (cumulus) could remain in suspension. Because eudialyte was part of the cumulus assemblage, Zr was a compatible element and the Zr content of the melt may have been consistently reduced from a maximum of c. 9000 ppm (Bailey et al. 2001).

The kakortokites (and the succeeding lujavrites) lack the fayalite, hedenbergite, titanomagnetite and apatite of the roof series, implying that the magmas from which the kakortokites and lujavrites crystallised were more

Fig. 100. Cross-section through the margin of the Ilímaussaq intrusion, showing steepening of kakortokite and lulavrite units against the marginal pegmatite. Inclusions of naujaite and augite syenite within the layered sequence are indicated diagrammatically. Modified from Bohse & Andersen (1981).
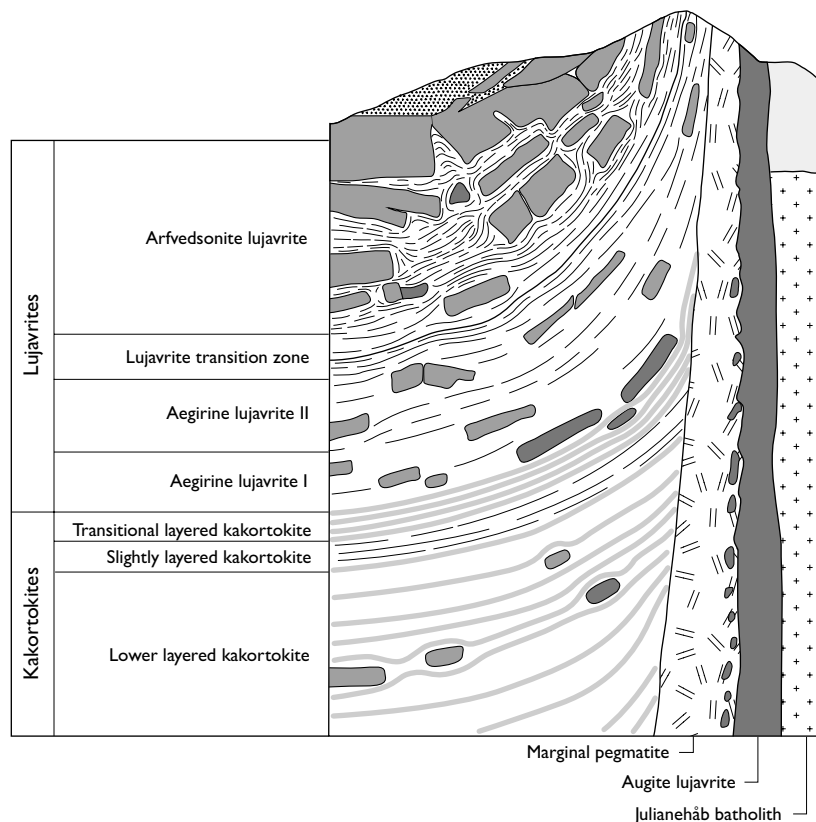
evolved than those that yielded the roof series (Larsen 1976; Bailey *et al.* 2001; Sørensen & Larsen 1987). By the time the lowest exposed kakortokite was crystallising, some 800 m of the roof series had already formed (Bohse & Andersen 1981). Although the amphiboles in the ka-kortokites are more magnesian and less calcic than those of the naujaites (Larsen 1976) and the floor series growth was separated from that of the roof series by a significant time lapse (Steenfelt & Bohse 1975; Sørensen *et al.* 2006) this does not necessarily imply that two distinct intru-sions were involved, merely that the temporal equivalents of the roof series in the floor series is well below unit −11.

The magma chamber is considered to have been tabu-lar with an estimated length and breadth of 17×8 km (Andersen *et al.* 1981a) and a relatively shallow depth variously estimated at >1 km (Bohse & Andersen 1981) to <1 km (Pfaff *et al.* 2008). Although visible only in the relatively uplifted southern part of the complex, the as-sumption is that the kakortokites extend right across the whole agpaitic complex. The low dips of the units steep-en close to the margins so that overall, the layering de-fines a wide basin-like geometry with upturned margins with dips up to 50°. Bohse & Andersen (1981) suggested that this form reflects an original sedimentary feature

(Fig. 100). From studies of other Gardar intrusions (cit-ed above and in Upton *et al.* 1996) this appears highly likely. Whereas the principal heat loss is assumed to have been through the roof (Larsen & Sørensen 1987; Krum-rei *et al.* 2006), some heat loss through steep sidewalls promoting crystallisation would have led to foot-wall cu-mulus deposition and accretion of inward-dipping crys-tal talus. This does not deny that some late-stage floor sagging may have contributed to the geometry (Ussing 1912; Bohse & Andersen 1981). Traced laterally, the ka-kortokite units grade into the marginal pegmatite, their regular black, red and white layers become thinned, bro-ken and folded as they merge into the matrix to the peg-matite zone. Within this matrix cross-bedding, graded bedding and wash-out channels are recorded (Sørensen 2006), with the implication that dynamic action was sufficient for magma flow to erode previously deposited cumulus and winnow the minerals.

Large autoliths of naujaite, up to several hundred metres across, accompanied by inclusions of augite sy-enite and foyaite, occur at one main horizon (unit +3) and are regarded as resulting from a major roof collapse (Ferguson 1964; Bohse *et al.* 1971; Sørensen 1978). They demonstrate that naujaite was already at or below its soli-

dus by the time the lower layered kakortokites were accumulating (Bohse & Andersen 1981). Whilst there are no impact structures beneath the autoliths, they were capable of compressing the underlying unit to about half its thickness (Ferguson 1964). The implication is that the unit under pressure was incompletely crystallised and that loading caused expulsion of *c.* 50% modal intercumulus melt. This is disputed by Bailey & Gwozdz (1994) who consider that the intercumulus melt content was as low as 15%. The tabular, slab-like form of the autoliths conforms to a pattern common for inclusions in a number of the Gardar plutons (e.g. Klokken and western Kûngnât complexes). They tend to form conformable horizons suggesting detachment along low-angled joints in the roof rocks, thus permitting magma to ascend to a higher level. Emplacement of the kakortokite-lujavite magma may have followed such a pattern.

Despite the low density of its sodalite component, the solidified naujaite must have had a density greater than that of the underlying kakortokite and lujavrite magmas for the autoliths to sink. There is a broad analogy with the situation at Syenitknold (see Fig. 48) where a roofing facies apparently generated by plagioclase flotation had, after reaching its solidus, acquired a whole-rock density greater than the evolved (trachytic) magma in the underlying chamber, permitting it to sink after breaking off. At a later stage in the magmatic evolution of Ilímaussaq the density of the iron-rich lujavrite magma is deduced to have increased to match that of the naujaite so that autoliths failed to sink but remained more or less static in the luvavrite. Autoliths of naujaite within the succession as a whole tend to increase in abundance upwards (Bohse & Andersen 1981; Fig. 100).

Slump structures in kakortokite units −6, −5 and −4 are probably products of gravitational sliding of unconsolidated mafic cumulus from steep sidewalls (Fig. 101). The slumps indicate the depth of unconsolidated cumulus to have been at least 20 m (Bohse & Andersen 1981). Relatively steep to very steep sidewall dips are seen in several other Gardar intrusions, e.g. the YGDC described above and the Kûngnât complex (Upton *et al.* 2013). Slumped cumulates are known from the YGDC and also from the Nunarssuit syenites (Upton *et a*l. 1996). By analogy the kakortokite slumps may also have originated from gravitational instabilities in steep sidewall cumulates.

Origin of the kakortokite layering. There have been numerous attempts to explain the layering in the kakortokites (e.g. Ussing 1912; Ferguson & Pulvertaft 1963;

Fig. 101. Slump structures in kakortokite close to the southern shore of Kangerluarsuk. Hammer *c.* 40 cm long.

Ferguson 1964, 1970a). One explanation, proposing repeated convective overturn of the magma (Bohse *et al.* 1971), was dismissed on the grounds that the thin tabular geometry of the chamber would not have supported such convection. Subsequently an elegant model was proposed involving double-diffusive convection and the upward crystallisation of a compositionally stratified magma (Larsen & Sørensen 1987; Sørensen & Larsen 1987). The model appeals to differences in nucleation and growth rates between different minerals. The mafic minerals nucleate and grow at lower degrees of undercooling than the felsic ones. The sharp unit boundaries may correspond to sudden increases of volatile pressure and/or increase in degree of undercooling triggering crystallisation in the overlying magma layer. Possibly the separation of large amounts of feldspar and nepheline led to increase in the vapour pressure, releasing heat that, in turn, increased the degree of undercooling. Thus crystallisation of successive stagnant bottom layers resulted from differing degrees of undercooling of the minerals in a multiply saturated magma (Sørensen & Larsen 1987; Larsen & Sørensen 1987). This successive layer by layer crystallisation in response to upward loss of heat (and some volatiles) was responsible for the overall uniformity of mineralogy and chemistry. Pfaff *et al.* (2008), however, considered that magma layering induced through double diffusion would have yielded only thin (centimetre-scale) layering.

Problems arise in explaining why the vapour pressure was increased and how the model accounts for the marginal steepening of the layers. The model also encounters difficulties in explaining the bowl-shaped disposition

of the layering and evidence for some magmatic flow as well as the gently undulatory form of the units and their draping over the naujaite autoliths. Another unanswered question is to what extent were the magma layers crystalline when they were generated. Were they aphyric or bearing only microcrysts?

A contrasted mechanism suggested by Pfaff *et al.* (2008) was based on the concept of geyser eruptions, namely that a gas phase separating from a magma in a closed system increased its hydrostatic pressure. When the latter exceeded the lithostatic pressure, volatiles were released and, as the vapour pressure fell, the lithostatic pressure promptly sealed the vent and closed the system. As crystallisation recommenced, vapour pressure increased and the process was repeated many times. This model is a refinement of earlier ideas on vapour pressure control to explain the repetitive layering in the kakortokites (Ussing 1912; Ferguson & Pulvertaft 1963). The most serious objection to these hypotheses is that volatile retention appears to have been complete up to the final stage of crystallisation of the agpaite magma.

Pfaff *et al.* (2008) proposed repeated influx (multiple replenishments) of new magma after each vapour release event, suggesting that the lower layered kakortokites crystallised not from a single overlying magma body but from numerous batches supplied from a large underlying chamber. An oscillation between closed and open system conditions is envisaged. In order to have produced the *c.* 8 m kakortokite units, it was deemed necessary to postulate a magma body *c.* 600 m deep. Lindhuber (2011), however, noted that, although at the base of unit +7 of Bohse *et al.* (1971) there is evidence for flow across an incompletely solidified surface (of unit +6), it is only at this horizon that there is clear evidence for the influx of new (slightly more primitive) magma. Because of this lack of evidence for replenishment at the bases of the other units, Lindhuber (2011) invoked the concept of 'mineral crowding' in which rapidly sinking arfvedsonite crystals catch up with smaller (slower) crystals beneath, generating amphibole-rich mats, a process that may have occurred simultaneously at different levels, forming distinct physical barriers. The amphiboles and eudialytes exhibit a sympathetic cyclicity of compositional change upwards through the stratigraphy. For the arfvedsonites, this is seen only in the black basal layers, the only part of each unit in which this mineral was cumulus. Fe^{2+}/ Mn in the eudialytes decreases from the bottom to top of each unit, indicating progressive fractionation in the magma in each unit. With the exception of units 0 and +7, the ratio is essentially constant in the black layers but

progressively decreases up through a unit's red and white layers (Lindhuber 2011). However, the lateral continuity of the units over long distances is difficult to reconcile with the crystal mat concept.

As not infrequently observed in science, an initially simple hypothesis (Ussing 1912) has been shown by subsequent research to be erroneous: as more data accrue, the more complex the phenomena appear. Despite now being in possession of far more detail on the field relationships, chronology, mineralogy and geochemistry, a satisfactory explanation for this fascinating cumulate succession that lacks significant cryptic layering and has such striking macro-rhythmic layering, is still awaited.

Kakortokite-lujavrite transition. The lower layered kakortokites are overlain by approximately 50 m of poorly exposed kakortokites. Although layering in these is indistinct, prominent modal layering reappears in the overlying *c.* 60 m of transitional layered kakortokites. The highest layered unit of these has an aegirine- rather than arfvedsonite-dominated base but, as this is overlain by 'red' and 'white' layers as in the lower layered series, it is still regarded as kakortokite. These transitional kakortokites pass conformably up into lujavrite cumulates.

Whereas in the lower layered kakortokites compositional changes in whole-rocks and minerals (specifically arfvedsonite and eudialyte) are small, such changes become much more pronounced in the overlying strata. This phenomenon had been noted with respect to the upward increase in U in the eudialytes (Bohse *et al.* 1974; Steenfelt & Bohse 1975) and Zr/Y ratios (Andersen *et al.* 1981b). More recent work has demonstrated an upward decrease in Ca/(Na+K) in the arfvedsonites and in Ca/ (REE+Y) in the eudialytes; these changes are much more accentuated in the lujavrites than in the kakortokites. There is a marked decrease in Fe_{tot}/Mn and in the range of compatible trace elements in the rocks, whilst the incompatible trace elements increase (Pfaff *et al.* 2008).

These phenomena reflect strong fractional crystallisation in a diminishing volume of magma at the latest stages of Ilímaussaq evolution. Chlorine, Br and I contents had become exhausted by persistent sodalite crystallisation in the first agpaite event but the F content reached a maximum in the kakortokite stage before decreasing during the lujavrite stages (Bailey *et al.* 2001). There is a continuum from the kakortokites up through the overlying series to the highest lujavrites beneath their naujaite roof (Rose-Hansen & Sørensen 2002 and references therein).

Lujavrites. The lujavrites are defined as melanocratic, eudialyte-bearing nepheline syenites and, whereas the

dominant ferromagnesian mineral in the kakortokites is arfvedsonite, aegirine is commonly dominant in the lujavrites. Despite having major minerals in common, the kakortokite and lujavrite suites differ in their minor mineral components and in grain-size and texture, the lujavrites being finer-grained and more fissile (Ferguson 1970c).

The lower part of the lujavrite sequence is aegirine-rich whereas arfvedsonite predominates in the upper parts (Bohse & Andersen 1981; Sørensen *et al.* 2006). The lujavrites differ from the kakortokites in that both albite and microcline co-existed as discrete phases (Ussing 1912), implying a change from hypersolvus conditions during kakortokite deposition to subsolvus conditions for the lujavrites, brought about by falling temperatures and rising vapour pressure, i.e. there was a significant change in the physical conditions of crystallisation. The thickness of the lujavrite sequence has been variously estimated from 300 m to >500 m (Sørensen 2006) and the measured thickness in the southern part of the complex is 485 m (Andersen *et al.* 1981a). The rocks possess a steep lamination close to the contacts but the lamination is approximately horizontal in the more central parts of the intrusion (Bohse & Andersen 1981). Although mainly trapped between the kakortokite and naujaite, the lujavrite transgresses its eastern and western contacts north of Tunulliarfik to intrude both the roof series and the Eriksfjord Formation lavas.

Aegirine lujavrites in the lower part of the sequence retain cumulate textures but these are less well-developed than in the lower layered kakortokites. Still younger lujavrites appear to represent very poorly compacted cumulates, the bulk composition of some being thought to converge with that of the melt. The principal components are aegirine, nepheline, microcline, albite, eudialyte and analcime so, as described above, transition from kakortokites to lujavrites involved change from hypersolvus to subsolvus crystallisation. The aegirine lujavrites have been subdivided into a lower group, 'aegirine lujavrite I', with grain-size decreasing upwards, and an upper group, 'aegirine lujavrite II', characterised by large arfvedsonite oikocrysts (Bohse & Andersen 1981). This is finer grained and lamination and fissility are less extreme than in aegirine lujavrite I. The faint layering in aegirine lujavrite I is absent in aegirine lujavrite II (Bohse & Andersen 1981).

A time gap between aegirine lujavrites I and II was marked by intrusion of quartz syenitic sheets that cut aegirine lujavrite but which are themselves cut by arfvedsonite lujavrite (Rose-Hansen & Sørensen 2001). This

Fig. 102. Alternating layers of dark arfvedsonite- and greenish grey aegirine-lujavrites. South-eastern Ilímaussaq complex. Hammer *c.* 50 cm long.

observation is of interest in demonstrating that at this late stage in the rift system, some silica oversaturated magma was still available.

A transitional succession (60 m thick) separates aegirine lujavrite II from the overlying main arfvedsonite lujavrite layer (150 m thick). Above the aegirine lujavrite II is a 20 m thick lujavrite unit characterised by centimetre-sized 'augen' of nepheline or eudialyte. Still higher in the succession, alternating layers of aegirine lujavrite and arfvedsonite lujavrite are common (Rose-Hansen & Sørensen 2002; Fig. 102). Sodalite, nepheline, albite, microcline, eudialyte and aegirine are present as cumulus phases in the transitional lujavrites, with arfvedsonite generally confined to the intercumulus.

According to Ferguson (1964, 1970c), some layers in both the black and green lujavrites display density stratification. In some places the green/black layers could be due to infiltration of arfvedsonite lujavrite along planes in the aegirine lujavrite, but elsewhere the transformation from one to the other was either gradational or episodic (Rose-Hansen & Sørensen 2002). The crystallisation of either aegirine or arfvedsonite was determined by the activities of water, silica and f_{O_2} (Larsen 1976; Markl *et al.* 2001), and the alternation between arfvedsonite- and aegirine-rich layers in the arfvedsonite lujavrites may at least partly be related to pressure relief caused by fracturing of the naujaite roof (Rose-Hansen & Sørensen 2002).

Micro-rhythmic layering in the lujavrites draped around naujaite autoliths (Fig. 103) commonly involves dark layers up to 15 cm thick alternating with thinner, lighter coloured layers. The dark layers are isomodal. The

Fig. 103. Autolithic slabs of pale naujaite enveloped by dark grey lujavrite. Note ductile deformation of foliated lujavrite between the slabs. North shore of Tunulliarfik.

lower parts of the lighter layers are enriched in nepheline and eudialyte whereas the upper parts are richer in analcime and REE phosphate minerals (Bailey *et al*. 2006). Spheroidal bodies up to 20 cm diameter occur locally in the arfvedsonite lujavrites. Their sharp, meniscus-like margins suggest that they originated through liquid immiscibility. Bulk compositions of the spheroids and their host are similar although H_2O contents are lower in the former. The spheroids have distinct rims and cores: the rims contain analcime, brown aegirine and K-feldspar (?adularia) whilst the cores are mainly of arfvedsonite and analcime. The internal differentiation of the spheroids is attributed to very late-stage migration of H_2O- and K-rich fluids from the interiors to the rims (Sørensen *et al*. 2003).

There is little stratigraphic variation of whole-rock Zr/U and Zr/Y ratios within the kakortokites, but these ratios illustrate a marked cryptic variation within the lujavrites (Andersen *et al*. 1981). In the lujavrites U rises steadily in relation to Zr and there is a lesser, but complimentary, behaviour of Y (Fig. 104). Overall the Zr/U

ratios decrease upwards from 1200 in the early black kakortokites to 9.2 in the final naujakasite lujavrites on Kvanefjeld. In detail, there are separate Zr-U trends in the lower layered (black) kakortokites and transitional layered kakortokites, whilst in aegirine lujavrite I the trends define well-defined stratigraphic intervals. Overall, Zr/Y ratios decrease from 18.2 in the black kakortokites to 2.8 in naujakasite lujavrite, and again there are distinct trends in individual rock types and stratigraphic intervals. Each trend is controlled by fixed contents of U and Y in their main host mineral, the cumulus (Na-Zr-bearing) eudialyte. The shifts in chemistry are attributed to the onset of crystallisation in a sequence of progressively less dense, liquid layers in the magma chamber (Andersen *et al*. 1981b; Bailey 1995; Bailey *et al*. 2001). It is notable that the shifts in magma chemistry within aegirine lujavrite I do not coincide with the macro-rhythmic units in this rock type (Bailey 1995).

It has long been accepted that the lujavrites represent a normal continuation of differentiation beyond the kakortokite stage (e.g. Bohse *et al*. 1971). Two recharge
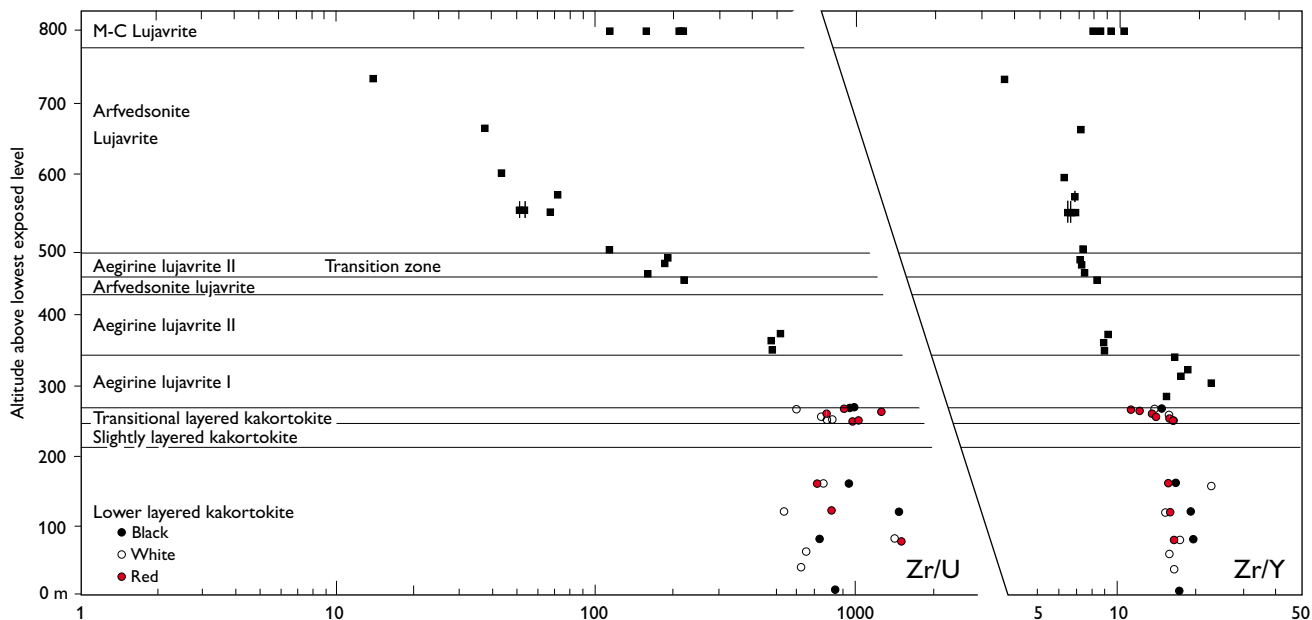
Fig. 104. Zr/U and Zr/Y (whole-rock data) vs. stratigraphic height in the southern Ilímaussaq complex. From Andersen *et al.* (1981).
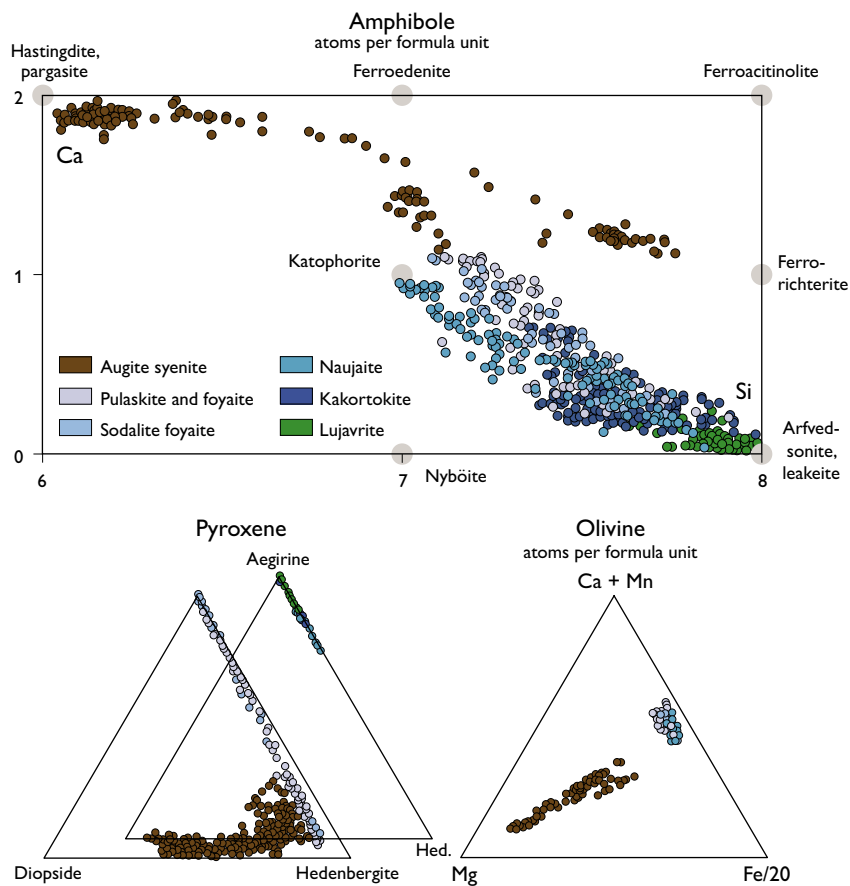

Fig. 105. Compositions of mafic minerals from Ilímaussaq augite syenite and agpaites. From Marks & Markl (in press).
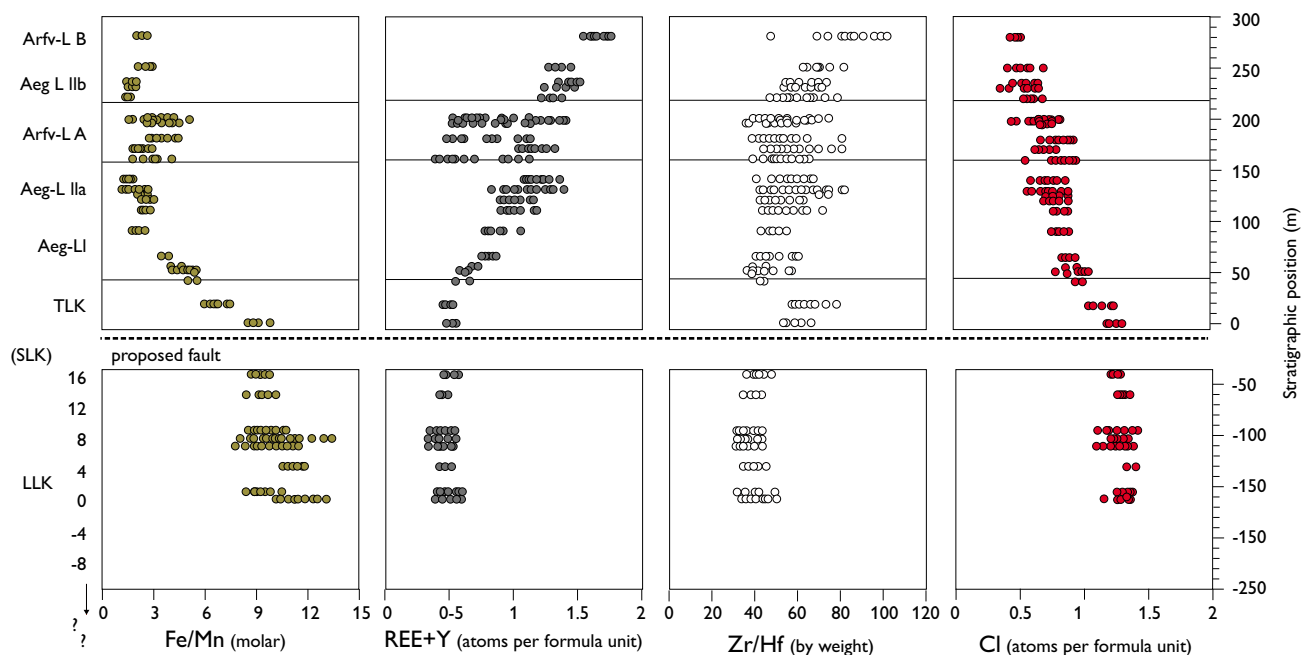
Fig. 106. Stratigraphic plot of Fe/Mn, REE+Y, Zr/Hf and Cl compositions of eudialytes from the 'floor series' agpaites of the southern Ilímaussaq complex. For the lower layered kakortokites (LLK) only (cumulus) eudialytes from the black layers are represented. As yet there are no data from the slightly layered kakortokites (SLK). Note: Marks & Markl (in press) postulate a fault separating the SLK from overlying transitional layered kakortokites (TLK). Data from Pfaff *et al.* (2008), Lindhuber (2011) and Ratschbacher (2011). From Marks & Markl (in press).

events, however, took place within the lujavrite sequence. The arfvedsonite lujavrites in the southern part of Ilímaussaq form a sill-like complex with a feeder zone at their base (Ratschbacher *et al.* 2011). Andersen *et al.* (1981a) and Rose-Hansen & Sørensen (2002) concluded that the lujavrites did not consolidate in one continuous chamber but rather in several shallow subchambers that are probably connected with each other.

Data collated on the mafic mineral chemistry of the augite syenites and agpaites (Marks & Markl in press) help to illuminate the question of separate magmatic influxes. Figure 105 shows the compositional trends of the olivines, pyroxenes and amphiboles. Whilst there is no question of the separateness of the augite syenite and agpaitic intrusions, the general conformity of the olivine and pyroxene trends harmonises with the conclusion that these magmas were closely related, although there is clearly a mismatch in their respective amphibole trends.

In Fig. 106 the generalised petrogenetic coherence of the agpaites is brought out by the composition of eudialytes from the floor sequence in southern Ilímaussaq (Marks & Markl in press). The Fe/Mn, REE+Y, Zr/Hf and Cl contents plotted against height may be taken as a crude reflection of the evolution of the post-naujaite magmas, e.g. in demonstrating their overall increase in

REE and decrease in Cl. The up-section decrease in Cl is caused by the compatibility of this element within the sodalite and eudialyte structures. The greater incompatibility of Mn^{2+} relative to Fe^{2+} in the cumulus assemblages is also emphasised. Zr/Hf values stayed rather constant until the crystallisation of the late lujavritic residues when the ratio increased. The discrepancies in these four sets of data in the lower part of the arfvedsonite lujavrite succession (Arfv-LA) might be ascribed to magma recharge from a deeper reservoir.

Hyperagpaites

The most extreme compositions, designated hyperagpaites, occur in the roof of the lujavritic body, particularly in the Kvanefjeld area in the north-western part of the complex. A steady stream of residual melts and volatiles towards the top is envisaged by Rose-Hansen & Sørensen (2002). These authors report that dykes and sheets of the uppermost lujavrites penetrate the naujaite. Intermittent emplacement of the lujavrite melts took place in vertical zones during several periods of deformation and faulting of the roof (augite syenite and lavas), producing an intrusion breccia (Sørensen *et al.* 1969, 1974; Nielsen

& Steenfelt 1979). The lujavrites in the Kvanefjeld area may represent an offshoot from the larger lujavrite body in the central area. Crystallisation of the Kvanefjeld lujavrites led to an explosive release of volatiles and forceful intrusion of volatile-rich magma into fractures where it crystallised as hyperagpaitic rocks such as naujakasite lujavrite (Sørensen *et al*. 2011).

The hyperagpaites possess a wealth of Na-rich minerals and, in the latest sodium-rich residua, nepheline became unstable and was eventually replaced by naujakasite, $Na_6(Fe,Mn)Al_4Si_8O_{26}$, which can form up to 75% (modal) of the rocks (Khomyakov *et al*. 2001; Sørensen & Larsen 2001; Andersen & Sørensen 2005; Sørensen *et al*. 2011). Villiaumite (NaF), in place of fluorite, is confined to the highest levels in the lujavrites and is a characteristic mineral of the hyperagpaites. A further reaction involved growth of steenstrupine, $Na_{14}(Ce,Th,U)_6Mn_2Fe_2Zr(PO_4)_7Si_{12}O_{36}(OH)_2\cdot3H_2O)$, at the expense of eudialyte. Uranium and Th ions that had formerly been preferentially accepted by eudialyte-series minerals were now accommodated in steenstrupine, denoting an increase in the stability of Th-U complex ions. The behaviour of U indicates that other processes such as formation of U complexes and volatile transfer probably operated (Bailey *et al*. 1981a; Rose-Hansen & Sørensen 2002). Thus the hyperagpaites are petrographically unique rocks comprising albite, naujakasite, steenstrupine and villiaumite (Fig. 107).

Fig. 107. Photomicrograph of hyperagpaitic lujavrite at Kvanefjeld. Albite (colourless), naujakasite (greenish-grey), steenstrupine (opaque) and villiaumite (orange).

Hidden layered series

The lowest unit accessible in the kakortokites is identified as unit −11 (Bohse *et al*. 1971). Without drill cores it is necessary to speculate on the nature of the underlying rocks. As noted above, the kakortokites and lujavrites crystallised from more evolved magmas than those of the roof series. The reasonable assumption is that an upgrowing layered cumulate suite grew concomitantly with the downgrowing roof series. Accordingly, strata in the hidden layered series contemporary with the sodalite foyaite and naujaite should contain a cumulus assemblage of alkali feldspar, nepheline, fayalite, hedenbergite, titanomagnetite and apatite (Larsen & Sørensen 1987; Sørensen *et al*. 2006). Sodalite, also co-crystallising, may have been selectively lost by flotation to contribute to the downgrowing flotation cumulate.

Because of the great volume of sodalite encapsulated within the >500 m thick naujaite, the agpaitic magma

body must, as emphasised earlier, have been many times greater. Consequently the corresponding floor cumulates should be several kilometres thick. Beneath these a downward progression of floor cumulates should be expected, equating to the pre-agpaitic foyaite and pulaskite stages. Pursuing this hypothesis, the foyaite and pulaskite cumulates should logically be underlain by a layered series, accumulated at >700°C, of augite syenite and thence syenogabbro as seen in the YGDC cumulate sequence.

It is tempting to equate the hidden layered series to the upgrown succession in the Older giant dyke (OGDC on Tuttutooq) which shows the sequence augite syenite – pulaskite – foyaite – sodalite foyaite. Although the OGDC is a much smaller and finer-grained intrusion than its Ilímaussaq counterpart, the affinity is obvious. Not inconceivably, a small-scale sodalite cumulate may be present in the hidden upper, peralkaline facies of the OGDC, beneath the waters of Narsaq Sund. In the naujaites, feldspar, nepheline, olivine, titanomagnetite and hedenbergite crystallised in equilibrium with the early sodalites and these minerals may well have been contributing to contemporary cumulates in the hypothesised hidden series of upgrowing cumulates on the floor of the early agpaitic magma chamber. It is noteworthy that, much earlier in the Older Gardar, a magmatic progression through augite syenite, pulaskite, foyaite to agpaite had come about in the Motzfeldt complex (Jones & Larsen 1985).

Ilímaussaq parental magma

As described earlier, the OGDC contains a succession grading up from augite syenite through pulaskite and foyaite to peralkaline sodalite foyaite. Although its uppermost facies must lie offshore and is unavailable for study, the sequence can be regarded as the approximate inverse of that seen in the downgrown roof of the Ilímaussaq agpaites. As the OGDC salic magmas were regarded as residual from fractional crystallisation of the basalt magma that initiated the younger Gardar southern rift system, it is deduced that the Ilímaussaq magmas were also products of a related basaltic parent magma (Upton *et al*. 1985).

The Ilímaussaq whole-rock compositions demonstrate a hundred-fold increase in U and Th from the initial augite syenite to the final lujavrite stages, requiring >99% crystallisation of the starting magma. Furthermore, a continuous fractionation process within a chamber below the present outcrop level is implied because the Th-U data show no gap between the augite syenite and the earliest nepheline syenite (pulaskite) (Bailey *et al*. 1981a). The whole complex is considered to be ultimately derived from a single basaltic parental magma fractionating in the deep crust but with the silica-oversaturated intrusive phase requiring crustal assimilation (Larsen & Sørensen 1987; Stevenson *et al*. 1997; Marks *et al*. 2004). Ilímaussaq εNd values range from −0.9 to −1.8 and oxygen $\delta^{18}O_{smow}$ is 5.2 to 5.7‰. These data are taken to indicate derivation from an isotopically homogeneous OIB-type mantle source, generally without indication of crustal contamination except for the alkali granite which has a lower εNd of −3.1, probably due to contamination in the lower crust. The mantle source is inferred to have been slightly enriched in ^{18}O but depleted in ^{147}Sm (Marks *et al*. 2004). The oxygen fugacities of the parental melt were below the FMQ buffer curve, resulting in highly reduced mineral assemblages (Karup Møller 1978; Konnerup-Madsen *et al*. 1979). Two immiscible fluids separated and were present through most of the crystallisation. One was a CH_4-dominated vapour and the other a highly saline aqueous fluid (Petersilie & Sørensen 1970; Konnerup-Madsen 2001; Krumrei *et al*. 2007). However, as mentioned above, the claim that the methane (and other hydrocarbons) are of mantle origin has been disputed by Laier & Nytoft (1995, 2012).

Micro-kakortokite dyke

A dyke immediately to the south of the Ilímaussaq complex provides unique insight into the nature of the magma(s) from which the agpaites grew. This ENE–WSW-trending, 10–30 m wide dyke, traceable for *c*. 18 km, transgresses the Ilímaussaq augite syenite at its southern extremity (Fig. 108; Larsen & Steenfelt 1974). Although it has been noted in earlier sections that the Late Gardar sinistral faulting coincided with the end of extensional rifting, this, together with the late basic dykes, shows that the cessation was not absolute. The dyke consists of porphyritic phonolite with tabular alkali feldspars, $An_{0.0}Ab_{53.4}Or_{46.6}$, (up to 7 cm large, and composing *c*. 10% (modal)), accompanied by nepheline,
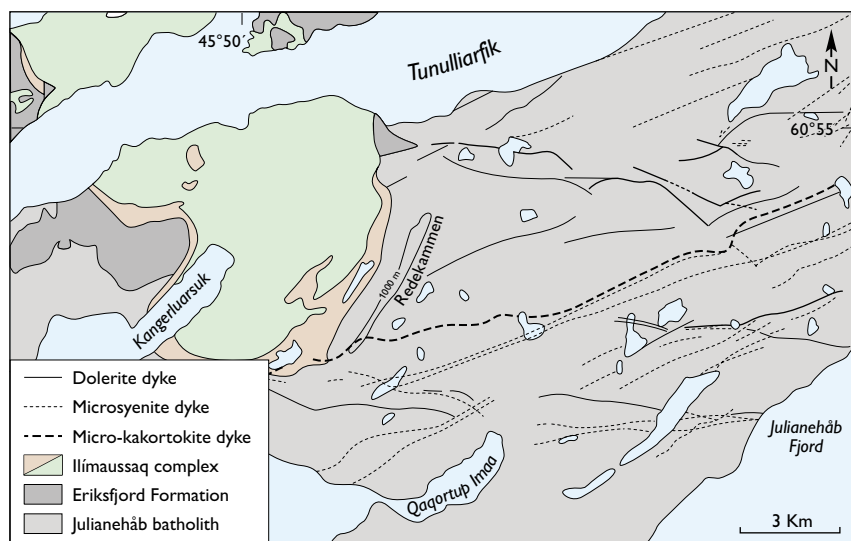

Fig. 108. Map showing the relationship between the southern part of the Ilímaussaq complex and the micro-kakortokite dyke (thick dashed line trending ENE–WSW). Modified from Allaart (1969) and Larsen & Steenfelt (1974).

hedenbergite and fayalite ($Fo_{0.8}Fa_{92.7}Te_{5.1}La_{1.4}$) and magnetite microphenocrysts.

Although it is considered that the dyke magma was initially homogeneous the dyke rocks exhibit two contrasting facies; *viz.* high alkali and low alkali. In the first, the matrix comprises microcline, albite, nepheline, sodalite and natrolite together with aegirine, arfvedsonite (grown around fayalite), aenigmatite (at the expense of magnetite), eudialyte and fluorite. Consequently, the petrography links it indelibly to that of the sodalite foyaites of the roof series, with which it was probably coeval. The affinity to Ilímaussaq is confirmed by its whole-rock composition which is very much the same as that of average kakortokite. Marks & Markl (2003) generally concur with these conclusions, noting that the micro-kakortokite magma separated at an early stage from the Ilímaussaq agpaite magma chamber.

The whole-rock content of alkalis (Na_2O+K_2O) is 13–15 wt% in the high alkali facies but 11–13 wt% in the low alkali facies. The latter is petrographically distinct, e.g. in being devoid of eudialyte (the Zr being accommodated in hiortdahlite and zircon) and is accordingly classified as miaskitic rather than agpaitic. The difference between the two facies is ascribed to alkali loss during emplacement and crystallisation (Larsen & Steenfelt 1974). The localised loss of Na_2O and H_2O as well as of F, Cl and some trace elements into the wall rocks in low-temperature fluids can be considered in the same light as that from comendite dykes (Tugtutôq), carbonatite dykes (with fenitised margins) in the nunatak region and, on a larger scale, the fluid loss from the Igdlerfigssalik syenites. The micro-kakortokite dyke magma had low f_{O_2} and it was concluded that, in order for undersaturated salic melts to generate a characteristic agpaitic mineral assemblage, they had to be iron-rich, strongly peralkaline and capable of retaining their alkalis (Larsen & Steenfelt 1974).

Østfjordsdal syenite and Igdlerfigssalik complex

Age relationships

The timing of the Østfjordsdal syenite and the Igdlerfigssalik complex presents a dilemma relative to the Tugtutôq and Ilímaussaq complexes. The Østfjordsdal syenite on the south-east side of the Igdlerfigssalik complex is clearly older than the latter (Fig. 67). Both the Østfjordsdal syenite and the younger components of the Igdlerfigssalik complex are intersected by members of the ENE-trending dyke swarm. The whole of the Igdlerfigssalik complex appears to have been emplaced before movements along the left-lateral *c.* E–W transcurrent faults ceased (Emeleus & Harry 1970). Although this *prima facie* evidence suggests a greater age for these two relative to the Tugtutôq and Ilímaussaq complexes, this is contradicted by the radiometric ages (Table 1) that indicate Rb-Sr ages of 1148 ± 3.6 and 1142 ± 15 Ma for Østfjordsdal and the late Igdlerfigssalik complex respectively. The Østfjordsdal Rb-Sr dating is supported by a U-Pb (zircon) age of 1147.5 ± 3.2 Ma (Table 1). Thus on the basis of the age determinations these two could be *c.* 10 Ma younger than Ilímaussaq and therefore among the youngest intrusions in the province, together with the recently discovered Paatusoq intrusion (1144.1 ± 1.1 Ma, Table 1) situated well outside the rift zone on the southern contact of the Julianehåb batholith, some 90 km east-south-east from Igdlerfigssalik.

Østfjordsdal syenite

Although truncated by one of the latest Igdlerfigssalik units, the Østfjordsdal syenite appears to have been a sub-cylindrical stock with a diameter of *c.* 5 km. It is largely composed of coarse-grained syenite consisting of alkali feldspar, nepheline and subordinate aegirine-augite and biotite. It is also cut by some trachyte and lamprophyre dykes whilst being younger than some phonolitic dykes (Emeleus & Harry 1970). So far very little has been published on the Østfjordsdal syenite.

Igdlerfigssalik complex

The Igdlerfigssalik complex, like its South Qôroq predecessor, has an elliptical plan (11 × 15 km), elongate south-east–north-west and, as at the South Qôroq complex, the faulting may have been responsible for this geometry, deforming the rocks while they were still hot and ductile (Stephenson 1976b). It is the southernmost major intrusive centre amongst the Igaliko syenites. The complex cross-cuts the South Qôroq syenites as well as the Østfjordsdal syenite that lies on its extreme south-east side (Fig. 67; Emeleus & Harry 1970).

Fig. 109. View east towards nepheline syenite mountain of the Igdlerfigssalik complex. In the foreground and middle distance Julianehåb batholith overlain by outliers of the Eriksfjord Formation, visible beyond the farm. See also Frontispiece.

Igdlerfigssalik, which reaches a height of 1752 m, is well-exposed with deep dissection (Fig. 109). The physical difficulties, however, imposed by the terrain are such as to leave much of this complex unstudied in detail (Emeleus & Harry 1970). The seven syenite intrusions that compose most of the complex are divisible into two groups, three older and four younger. Using the (modified) symbols for the intrusions as divided by Emeleus & Harry (1970), the first of these groups comprises I1, I2 and I3 which pre-dated the latest stages of the ENE dyke intrusion. Only a narrow strip of I1 remains, in the north-western part of the complex, and I2 is also fairly vestigial, seen as a strip on the northern side of the complex. The outcrop of I3 around the north side is less than 1 km wide but has a well-developed inward dipping lamination at 20–70°. The majority of each of these units has been obliterated by its successor. The second group of syenites comprises I4, I5, I6 and I7 and was emplaced after the intrusion of the Igaliko dyke swarm had come to an end, implying that the Igdlerfigssalik complex was

not complete until after the regional lithospheric extension ceased.

Eriksfjord Formation strata south-west of I4 (in the Tunulliarfik and Igaliku Fjord areas) are approximately horizontal up to a *c.* 1 km broad zone adjacent to the intrusion, in which the strata are flexed downwards at up to 60° towards the contact. This may reflect downsag (drag) towards the syenite that accompanied subsidence of an approximately cylindrical block of the country rocks as I4 was being emplaced.

Intrusion I4 crops out around the north, west and south sides of the complex, displaying contrasting facies. It is inferred to have been part of a steep-sided stock involving a marginal border group and an inner layered cumulate series subsequently largely replaced by I5, I6 and I7 (Emeleus & Harry 1970).

Amongst the several facies of I4, the 'dark layered syenite' is considered to have been part of a marginal border group. As implicit in its name, this shows prominent development of modal layering brought about by concentration of ferromagnesian minerals. The layering is

Fig. 110. Inward-dipping layers in syenite unit I4 of the Igdlerfigssalik complex exposed in the cliffs above Qooroq fjord.

steeply inclined with layers cut (eroded) by layers farther from the outer contact, providing good evidence for inward younging (Fig. 110). These rocks were compared by Emeleus & Harry (1970) to those of the Eastern border group at the Kûngnât complex (Upton *et al.* 2013) where the layering is ascribed to magma downflow alongside thermal boundary layers.

Well-laminated, concordant cumulates in I4 are relicts of the former layered series. This contains xenolithic masses of anorthositic gabbro. These, mantled by overlying syenite cumulates, generated impact disturbances in the underlying syenites. To find such rocks in the salic Gardar intrusives is unusual, the great majority being in mafic and intermediate hosts. As the protoliths are believed to be of lower or mid-crustal origin, their presence may indicate rapid uplift in an earlier magma batch before they collapsed into the upgrowing I4 cumulates. I4 is cut by sheets of syenitic and microsyenitic rocks which themselves contain xenoliths of both the I4 host syenite and anorthosite or gabbroic anorthosite.

A pegmatite close to Narsarsuk on the southern border of I4 and related to a porphyritic microsyenite sheet

has been a Mecca for mineralogists. One mineral among the assemblage, named from the locality, is narsarsukite, $Na_2(Ti,Fe)Si_4(O,F)_{11}$ (Flink 1901).

Intrusion I5 forms a broad annular outcrop (Fig. 67) accounting for most of the complex including the summit. It is a remarkably uniform, coarse-grained syenite but, where signs of layering appear, all dip towards the intrusion centre. I6 forms a virtually complete 360° ring dyke (*c.* 35 km circumference) mostly separating I4 from I5. It is ovoid, 15 × 10 km diameter with a long axis trending NW–SE, varying in width from 600 m to 30 m. The rock textures are highly variable from medium-grained to coarse-grained with pegmatitic patches. I7, the youngest of the syenitic units, is ovoid in plan (7 × 5 km) and lies entirely within I5. It is a steep-sided stock with contacts dipping outwards at 75–80°, consisting of a medium-grained leucocratic foyaite. Structurally it consists of thick layers stacked one on top of the other in a shallow saucer-like form with gently upturned margins. It presents a superb section across a layered intrusion, displaying conformable igneous lamination and small-scale

Fig. 111. Photo and sketch of layered structures in syenite unit I7 of the Igdlerfigssalik complex as seen from the south-eastern side of Qoororsuaq, looking west towards the complex. Sketch modified from Emeleus & Harry (1970).
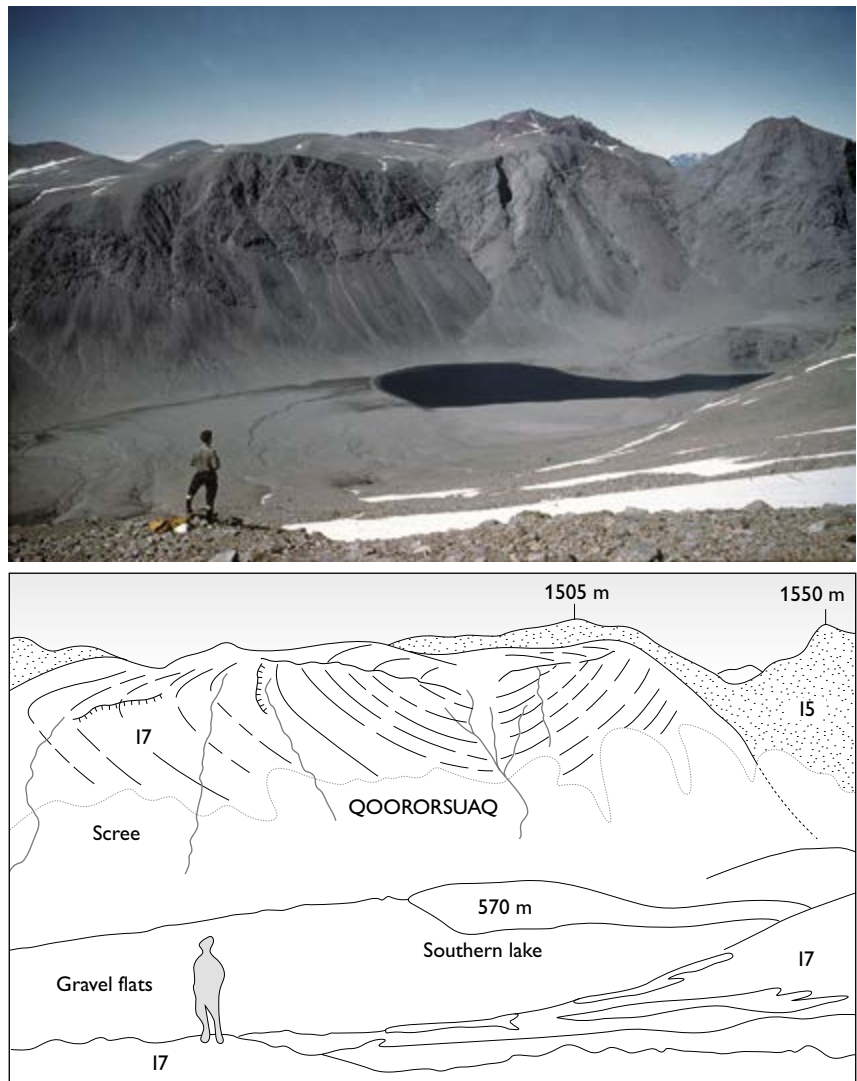
modal layering (Fig. 111). Thus I5 and I7 form a central downfaulted block bounded by the I6 ring-dyke.

Cumulus phases in the Igdlerfigssalik foyaites are alkali feldspar, clinopyroxene, apatite, magnetite ± olivine and nepheline; intercumulus phases include zonal overgrowths to the above, plus amphibole, biotite, aenigmatite, sodalite, nepheline, alkali feldspar, alkali pyroxene and magnetite. Additionally subsolidus phases were produced through the action of H_2O- and/or CO_2-rich fluids acting on the magmatically crystallised minerals. Subsolidus products include biotite (grown through alkali feldspar–magnetite–H_2O interaction), blue-green amphiboles around olivines, (silica and alkali rich relative to the browner intercumulus amphiboles), cancrinite through interaction of CO_2-rich fluid and nepheline, as well as gieseckite from nepheline and sericite from feldspar (Powell 1978).

Whilst the cumulus assemblages in the foyaitic rocks of the South Qôroq and Igdlerfigssalik complexes are more evolved and complex than those in the YGDC and the Klokken complex, very similar processes operated within the magma chambers. The rocks are dominantly poorly compacted orthocumulates reflecting the relatively rapid cooling of magmas at shallow depths. Olivine–clinopyroxene thermometry indicates crystallisation between 980° and 900°C, consistent with water-saturated liquidus temperatures at 1 kb (Powell 1978). The fluted sidewall cumulates in Igdlerfigssalik unit I4 point towards flowing magma currents with the capacity to thermally or mechanically erode previously formed layers (Fig. 112). In the Igdlerfigssalik magma chambers, as in those of several other Gardar plutons, it is probable that convection involved two-phase downflow driven by loading of high-density pyroxenes ± olivines. The in-

Fig. 112. Cut-and-fill cross-bedding in the Igdlerfigssalik syenite unit I4. Scale 1 m long.

ward inclination of the modal layering, most perfectly preserved in unit I7 of Igdlerfigssalik, can again be assigned to the accumulation of cumulus minerals deposited peripherally as crystal talus or pediment by crystal-rich slurries detaching from the thermal boundary layers before flowing radially towards the central part of the chamber floors. The high degree of parallelism widely observed in the tabular feldspar crystals of the laminated syenites is ascribed to orientation by flowing magma as it was in the YGDC gabbros. Whereas in the South Qôroq complex there was progressive evolution towards successively more primitive magma batches (Stephenson 1976a), there are, as yet, no data to discern any such pattern for the Igdlerfigssalik intrusions.

Late fluids expelled from the late Igdlerfigssalik intrusions migrated outwards to form an aureole *c*. 1 km wide. This transects the South Qôroq complex and is marked by a zone in which the South Qôroq ferromagnesian minerals are recrystallised (Stephenson 1976a). Finch (1995) demonstrated that the fluids emanating from the Igdlerfigssalik complex reacted with the biotites of neighbouring rocks, specifically affecting the octahedral sites and hydroxyl sites. The unaffected South Qôroq rocks contain biotite with a fluorine content reflecting that of the late-stage South Qôroq fluids. By contrast, in the recrystallised aureole, the F content of the biotite is distinct, inferentially closely related to that of the late-stage fluids expelled from Igdlerfigssalik. These fluids also modified the REE, Zr and Hf contents of the affected South Qôroq biotites. Exchange of late-stage fluids, exuded from younger intrusions, may be commonplace in alkaline igneous systems and the F content in the micas provides a sensitive indicator of this phenomenon (Finch 1995).

Eccentric to all of these salic components is a partial ring dyke of gabbro/syenogabbro that crosscuts the eastern side of the complex and transgresses the I5, I6 and I7 syenites as well as the Østfjordsdal syenite (Fig. 67). Consequently this can be compared to the very late intrusion of mafic magma (from a source below that of the syenitic magmas?) that occurred in the South Qôroq complex.

Because Igdlerfigssalik rises to >1.7 km above sea level and its lower outcrops cut the Eriksfjord Formation that was probably never more than 4 km thick, the uppermost parts of the complex clearly penetrated high in the Eriksfjord Formation. It would therefore be surprising if the Igdlerfigssalik complex did not have an extrusive expression. I6 may, for instance, have broached surface level to produce an eruptive curtain around the subsiding block of I5 and I7. The exposed syenites may have been components within a composite body that lay either within higher stratigraphic levels of the Eriksfjord Formation or possibly within the superstructure of a large overlying volcano. Assuming the forms of the annular syenites approximate to the sizes of calderas in a nested suite, such a volcano (built up largely of pyroclastic products?) may have had a diameter from 50 to 75 km. Possible modern analogues include Kilimanjaro in Tanzania and Cantal in Auvergne. Considered jointly, the South Qôroq and Igdlerfigssalik complexes may illustrate consecutive attempts to build a large salic volcano over an active tectonic zone. Products of the first attempt then experienced more or less concurrent faulting and dyke fissuring before being overgrown by the second (Igdlerfigssalik) volcano that was affected in its early phases by dyke intrusion as lithospheric extension reached its close, and which probably post-dated all but the very latest stages of the transcurrent faulting (Stephenson 1976b).

The role of anorthosite

Anorthosites of the Nain Province are major features in the Mesoproterozoic geology of Labrador, but do not outcrop east of the Labrador Sea. Nonetheless, the abundance of anorthositic xenoliths in Gardar intrusions leaves no doubt that an extensive anorthosite body underlies the province, constituting a petrological 'elephant in the room': obvious but rarely discussed. It is inferred to have accreted over the whole time-scale of Gardar magmatism and to have played a seminal role in their petrogenesis (Bridgwater 1967; Bridgwater & Harry 1968; Upton 1996, Halama *et al*. 2002).

The distribution of xenoliths suggests a parent body with estimated dimensions of 250–500 km by 50–100 km, i.e. comparable in size to the Angola and Nain (Labrador) anorthosites (Emslie 1977). Both the cryptic Gardar anorthosite and the mid-Proterozoic anorthosites of Labrador and Quebec lie close to a terrane boundary and were related to extensional tectonics and failed rifts (Morse 1982, 2006). There are numerous parallels between the Michikamau anorthosite of the Nain province and observed or inferred features for the sub-Gardar anorthosite. At Michikamau the succession entails anorthosite, ferrodiorite, ferromonzonite and ferroadamellite (Emslie 1965, 1970) whereas the deduced Gardar succession is anorthosite, ferro-syenogabbro, ferro-syenite, syenite (and thence foyaite or alkali granite). The principal differences between the Nain and Gardar provinces appear to be the much shallower level of erosion and the more alkalic characteristics of the latter.

The Gardar rocks overlie or intrude the Julianehåb batholith, but there are relatively few data regarding the make-up of the Archaean–Palaeoproterozoic lithosphere beneath the Gardar Province (see the discussion in Garde et al. 2002 and references therein). Seismic studies offshore South Greenland indicate a Moho depth of 30–35 km. Dahl-Jensen et al. (1998) interpreted seismic reflection data to suggest a thick wedge of Archaean continental crust under the eastern part of the batholith, whereas a Pb-Pb isotopic study in the west by Kalsbeek & Taylor (1985) showed that an Archaean lead isotopic signature at the north-western margin of the batholith quickly disappears towards the centre of the batholith. Garde et al. (2002) concluded that the bulk of the batholith (and hence also the deep crust of presumed mafic composition) consists of juvenile material that was accreted onto the southern margin of the Archaean craton. This leaves the depth of the presumed anorthositic Gardar cumulate open to interpretation.

Xenoliths of anorthosite and gabbroic anorthosite, together with plagioclase megacrysts, are especially abundant within the mafic and intermediate intrusions of the two Younger Gardar rift zones (Bridgwater & Harry 1968). Halama et al. (2002) conducted studies on isotope and trace element geochemistry of the megacrysts in the Isortoq district, confirming that most of the anorthosite xenoliths are alkaline and cognate with the Gardar magmatism. The maximum pressures deduced for these megacrysts are 10–12 kb. Others, however, may have crystallised higher in the crust, suggesting a polygenetic and polybaric history. In comparison, the Nain complex

in Labrador may consist of over 20 different plutons (Wiebe 1992).

Anorthosite formation may have taken place throughout most of the Gardar time. The Gardar anorthosite body is presumed to predate the giant dykes and the Main dyke swarm. Bridgwater (1967) and Bridgwater & Harry (1968) suggested that granular anorthosites (with a specific gravity of c. 2.63 g/cm³ at 1000°C), formed as flotation cumulates deep in the crust and acted as a trap for residual magmas (Fig. 75). The feldspars are extensively sericitised; this, and secondary oxidation of the oxides, was attributed to accumulation of water and other volatiles close to the anorthosite before entrainment. The granular anorthosites were thus thought to have formed a more or less impermeable cap above the differentiating alkaline magmas.

Generation of so large a body, with its restricted composition, must have involved repeated batches of relatively evolved magma. Given the sodic labradoritite composition and the overall alkaline nature of the xenoliths, the parental magmas would have had to be hawaiitic. Although plagioclase cumulates may have formed temporary chamber roofs that had some mechanical strength, it is probable that such low-density bodies at depth were unstable and occasionally were disrupted during tectonic disturbances, yielding crystal-liquid mushes. These would subsequently crystallise to coherent rocks capable of fragmentation and entrainment in basaltic to intermediate magmas.

Most of the granular xenoliths approximate to pure anorthosite of remarkably constant composition, with plagioclase of An_{61-56} (Bridgwater & Harry 1968). The feldspar crystals are typically equant, anhedral and randomly oriented. Crystal sizes are mainly from 3 to 5 cm but can exceed 20 cm. In order of decreasing modal importance, other phases are olivine (Fo_{73-60}), Fe-Ti oxides and pyroxene, typically augite. Blocks of texturally distinct granular anorthosite within host granular anorthosites points to a complex polycyclic origin for the protolith, with possible additional mixing from diapirism at depth. The earlier components may show some deformation, which is attributed to compaction rather than to tectonic deformation.

Laminated anorthosites

The laminated anorthosite autoliths are considered to be genetically distinct from the granular anorthosites

(Bridgwater 1967; Bridgwater & Harry 1968). They appear to be confined to the southern rift, principally in the YGDC and Klokken gabbros, and consequently are considered to have played an important role in the magma genesis of the system as a whole. The laminated anorthosites have a less complex history than the granular anorthosites and retain pristine and perfectly preserved cumulate textures (Fig. 58). Whilst there is superficial similarity between the granular and laminated anorthosites, their mode of formation was clearly contrasted. While the former probably accreted as flotation cumulates (see above), the latter are more likely to have grown as cumulates upwards from a magma chamber floor. By analogy with the Nain and Angola examples, the laminated type at Asorutit may represent a layered body that overlies granular anorthosites. The problem of accounting for both supposed floor and roof cumulates in the Nain anorthosite complex was called the 'feldspar/magma density paradox' (Morse 1973; Scoates 2000).

The laminated xenoliths in the YGDC at Asorutit have idiomorphic tabular plagioclase (An_{58-52}) enclosing intercumulus olivine (Fo_{71-69}), subordinate augite, ilmenite, biotite and apatite. The relatively small haematite component in the ilmenites (Upton & Thomas 1980) indicates a reduced state of oxidation whilst the lack of strong zonation in the plagioclases and their coarse grain-size relative to that of the troctolite host suggest that cooling was slow in comparison to that of the host magma. There is wide disparity in sizes of the plagioclase crystals, suggesting that nucleation occurred at different levels in the parent magma. The latter is inferred to have approximated to a plagioclase-olivine-melt composition.

Some of the xenoliths (up to 100 m across) show primary layering in which well-laminated layers alternate with poorly compacted layers with more randomly oriented plagioclases and correspondingly greater amounts of olivine. Consequently there is modal layering but it is solely due to textural changes; plagioclase remains the sole cumulus participant. The absence of cogenetic olivine+plagioclase and olivine floor cumulates is attributed to their greater density. Whereas the xenoliths with sufficiently high plagioclase content would float, the more mafic cumulates could not. Closely similar phenomena have been described from the Michikamau anorthosite, Labrador (Emslie 1970) and the Paul Island anorthosite, Labrador (Wiebe 1992). The anorthosites at Asorutit were interpreted as having originated as floor cumulates in which the degree of lamination was controlled by the rate of magma flow, good laminar orientation being related to flowage whereas the disorientated

layers were attributed to tranquil interludes (Upton 1961). The original attitude of the hypothetical chamber floor is, of course, unknowable. Scoates (2000), however, considers that sloping floors may be characteristic of all Proterozoic anorthosite complexes to allow downslope drainage of relatively high-density intercumulus melts. Since virtually all the floor cumulates exposed in the Gardar Province are inclined, a sloping floor for e.g. the Assorutit anorthosites, is an acceptable proposition.

Genesis of the anorthosites

Among basic igneous rocks, it is uncommon to find evidence for olivine crystallising late relative to plagioclase and, on the basis of behaviour in the An-Fo binary system (Osborn & Tait 1952), Upton (1961) proposed that a fall in P_{H_2O} had shifted the cotectic towards olivine, thus extending the plagioclase field. Consequently, plagioclase nucleated alone until fractionation brought the system back to the olivine-plagioclase-liquid cotectic when olivine precipitation commenced.

The relative compositions of plagioclase and olivine differ significantly from troctolite host to anorthosite xenoliths, i.e. from An_{65} and Fo_{68} in the former to An_{58} and Fo_{71} in the latter, possibly attributable to pressure differences pertaining at the different crystallisation depths. Furthermore, the whole-rock incompatible element ratios (assumed to reflect those of the melts for these orthocumulates) also differ. Thus P/Ti and P/Zr ratios of the anorthosites are notably higher than for the host troctolites. High whole-rock contents of Sr (1700–1800 ppm) suggest distinctly high Sr concentrations (and relatively low Ca/Sr) in the anorthosite parent magma. Chondrite-normalised REE patterns (Fig. 113) are generally similar to those of the initial YGDC and OGDC magmas but are more strongly fractionated, with La/Yb_N c. 18.1 in the laminated anorthosites versus c. 11.5 for the YGDC and c. 16.9 for the OGDC. It is of interest that the normalised patterns for the two Asorutit samples closely resemble those for Proterozoic orthopyroxene-bearing anorthosites (Wiebe 1992). From the plagioclase composition a hawaiitic parent magma is presumed, with high concentrations of LREE, P and Sr. Whilst the YGDC, OGDC and inferred anorthosite magmas were all cognate, they represented quite distinct magma batches.

Basaltic melts are more compressible than crystals at >6 kb, and plagioclase more sodic than An_{90} then has a density less than melt (Kushiro & Fuji 1977; Kushi-
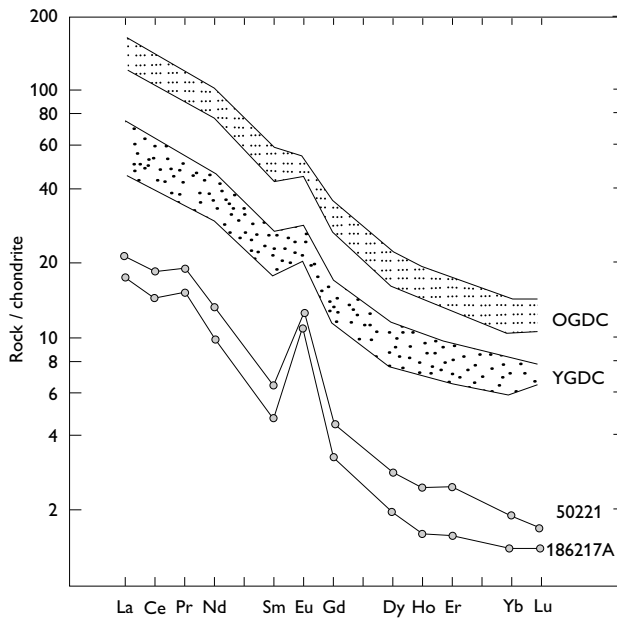
Fig. 113. Chondrite-normalised REE patterns for two anorthosite samples from Asorutit, compared to REE ranges from the YGDC and OGDC marginal facies (Upton 1996).

ro 1980). These authors concluded that, for polybaric crystallisation models, plagioclase may sink at low pressures but float at the higher pressures appropriate to the deeper crust, and the density difference will increase as Fe-contents rise from hawaiitic to mugearitic compositions. Bridgwater (1967) postulated that the Gardar anorthosites formed in the lower or middle crust. Experimental studies on YGDC intitial compositions (Upton & Thomas 1980) showed that the olivine-plagioclase-melt equilibrium did not persist above *c.* 6 kb, suggesting a maximum depth limit for anorthosite formation of approximately 20 km. Study of the Laramie (Wyoming) anorthosites led Mitchell *et al.* (1995) to conclude that fractionation of magmas in the upper mantle produced high-Al basic residues that gave rise to plagioclase-rich diapirs that ascended and crystallised at mid-crustal depths. However, data for plagioclase megacrysts from the Isortoq BFDs implied crystallisation near the crust-mantle boundary (Halama *et al.* 2002).

Scoates (2000) pointed out that there is little direct evidence for plagioclase flotation cumulates either in lay-

ered intrusions or in Proterozoic anorthosite complexes. However, evidence favouring flotation of plagioclase megacrysts and anorthosite xenoliths is apparent from the relationships described above from the Tugtutôq, Narsaq and Klokken complexes. Whereas the Assorutit occurrences are all of laminated anorthosite, both granular and laminated anorthosite inclusions occur in the Klokken complex.

It has been widely accepted that the Proterozoic anorthosites derive from partial melting of depleted upper mantle sources and that the melts pond at or near the crust/mantle boundary (Ashwal 1993). More recently a contrasted genetic hypothesis has gained support which proposes that the anorthosites came from reaction between underplating basalts and aluminous lower crust (Duchesne *et al.* 1999; Bédard 2001; Charlier *et al.* 2010). The Y-Yb-Lu data for the anorthositic Nain Plutonic Suite indicate residual garnet in garnet granulite source rocks (Bédard 2001). Light has been cast upon this petrogenetic dilemma by Gleissner *et al.* (2010) from studies on the Kunene anorthosite complex of Angola. This, one of the world's largest massif-type anorthosites, comprises two successive intrusions: an older one of pyroxene anorthosite and leuconorite, and a younger one dominated by olivine-bearing anorthosite. The conclusion reached is that the magma of the first was subject to crustal contamination whereas the second, with characteristics close to those inferred for the Gardar anorthosite protolith, experienced almost no contamination.

The Kunene and the inferred Gardar anorthosites are similar in size. With respect to Kunene, Gleissner *et al.* (2010) concluded that only partial melting of a mantle source could provide enough primary melt to give rise to so large an anorthosite body and that plume activity was probably involved. Moreover, extensive melting of the lower crust is unlikely to have been on such a scale as to produce the requisite vast amounts of almost homogeneous parental melts. Accordingly, the Kunene interpretation supports a simple mantle origin for the Gardar anorthosite and there appears no obvious reason to discard the more conventional Ashwal (1993) hypothesis. Furthermore, the alkaline nature of the Gardar anorthosite is not readily compatible with the AFC model involving garnet granulite.

Emplacement mechanisms and tectonics

Emplacement mechanism of the giant dykes

Big dykes with widths on the 100–1000 m scale are rarities in the Phanerozoic but are comparatively common in the Precambrian. Assuming that asthenospheric convection was more vigorous in the Precambrian, shear rates on overlying lithospheric plates were correspondingly greater. The greater stresses led to more dramatic failures than in Phanerozoic rifts and great volumes of basaltic melts, like those of the YGDC, could be concentrated and intruded rapidly as dykes with widths on the kilometre scale (Macdonald & Upton 1993).

The great majority of dykes in the region, both the early Gardar BD_0 dykes that long pre-date the younger Gardar southern rift and also those that post-date the giant dykes, were simple dilational intrusions. The OGDC has essentially parallel margins for its 20 km outcrop. Its broad bow-shaped (northwardly convex) plan (Fig. 5) presents some problem with respect to intrusive mechanism but this is dwarfed by the much more abrupt 'tight' bend, (concave to the north) developed about half-way along its trace. The western termination of the OGDC also merits attention. Despite poor outcrop, the western termination of the OGDC appears to be along an E–W-trending plane oblique to the dyke trend, suggesting that the plane had been a pre-existing shear zone in the granitoids that acted as a mini-transform fault during dilation of the dyke fissure. This hypothesis implies that the country rocks on the northern side of the fault were parted by a diagonal displacement of c. 3500 m during intrusion although the width of the dyke was only c. 500 m.

The absence of internal chills and typical lack of extensive wall-rock melting in the YGDC imply rapid intrusion and that, if there were any conduits for surface eruptions, these were highly localised. The giant dyke branches are considered to have crystallised as unitary cooling systems. However, the forms displayed on the geological map by the YGDC (Figs 5, 10) present a significant problem with regard to its emplacement. Field evidence shows that the YGDC branches were capable of expansion and contraction in both horizontal and vertical senses. In places the branches underwent a localised expansion for which the term 'ballooning' is appropriate. For example, the northern branch of YGDC on Tuttutooq, traced west from Narsaq Sund (Figs 10, 17) shows

a gradual constriction to a narrow 'waist' c. 400 m broad, with some ballooning on either side of this waist. A more pronounced instance of this behaviour is shown some 2 km west of Itillip Saqqaa where the northern YGDC branch subdivides (Fig. 23). The northernmost of the two sub-branches displays some remarkable features. In contrast to the approximately constant width of 500 m maintained for several kilometres to the east, it locally expands, over a distance of few tens of metres, to a width of c. 700 m. This width is maintained for a short distance (c. 1.25 km) before it narrows abruptly into a westward extension a mere 200 m wide. Still farther west this progressively diminishes to a few tens of metres before swelling once again before terminating against an approximately E–W shear zone, very much as exhibited by the OGDC. As with the OGDC terminus, this ending (and also that of a parallel giant dyke branch to its south-east), suggests that the shear zone acted as a mini-transform fault. The YGDC outcrops reappear east of Ilimaasaq at Kangerlua (Fig. 10) reaching their fuller expression on Mellemlandet and nunataks north of Motzfeldt Sø. In the nunatak region between Nordtop and Geologfjeld,
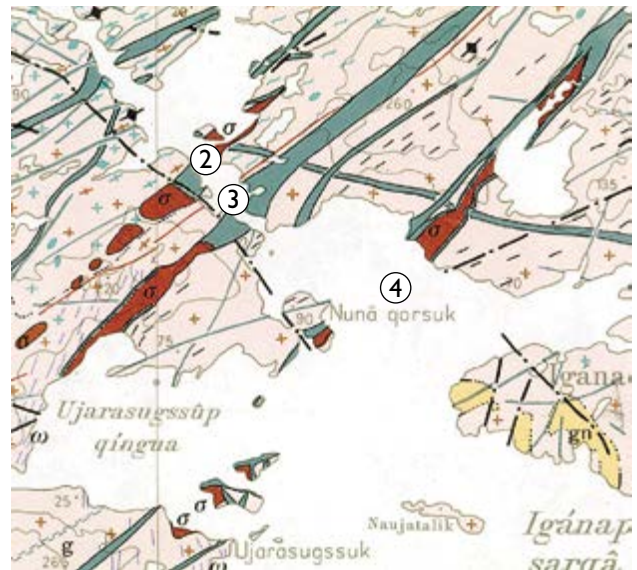

Fig. 114. Outcrop forms in giant dykes at Isortoq. Grey: mafic facies. Red-brown: salic facies. Extraction at 60°55′N, 47°30′W from Nunarssuit geological map at scale 1:100 000 (Pulvertaft 1967), with old spelling of place names. The circled dykes 2–4 refer to Bridgwater & Coe (1970).

Fig. 115. Anastomosing dykes and giant dykes north-east of the Bangs Havn intrusion, Nunarsuit–Isortoq Zone. Grey: mafic facies. Red-brown: salic facies. Extraction at 60°50′N, 47°53′W from Nunarssuit geological map, scale 1:100 000 (Pulvertaft 1967), with old spelling of place names.

two lenticular pods of differentiated rocks occur in the southern dyke branch between marginal sheaths of troctolitic gabbro. At Syenitknold (Fig. 10), the giant dyke made a remarkable shift of course, as if it had been displaced dextrally some 200 m along a WSW–ENE fault. Despite this appearance, no fault was detected and it appears that the dyke fissure simply made an abrupt change of course.

It is relevant here to consider the behaviour of the giant dykes in the northern (Nunarsuit–Isortoq) rift in order to gain a better perspective on the giant dykes of the southern rift (Fig. 114). Of the many Gardar dykes in the Isortoq region, the giant dykes are the youngest and, on the basis of available age data (Bangs Havn, Table l), they are approximately synchronous with those of the southern rift. Five (or more) of the Isortoq dykes are comparable to the YGDC in having (a) giant dyke dimensions with widths up to 500 m, (b) internal synformal layering, (c) possession, at least locally, of a composite character with gabbroic or syeno-gabbroic outer sheaths (or border groups) enclosing evolved central facies, typically of syenite, and (d) a remarkable propensity to exhibit pinch and swell morphologies. This last characteristic was emphasised by Bridgwater & Coe (1970) who considered it incompatible with emplacement through simple dilation, claiming that stoping must have been involved.

Bridgwater & Coe (1970) described four of these intrusions on either side of Isortoq Fjord, from north to south, as Dykes 1, 2, 3 and 4. Dykes 2, 3 and 4 only are shown in Fig. 114. Dyke 2 shows some of the most extreme behaviour, breaking up along its length into a series of rounded pods as if boudinaged. They are the youngest dyke intrusions in a terrane that had already experienced intensive intrusion by earlier doleritic dykes. Still more aberrant is the highly localised ballooning of one young Isortoq dyke from a width of c. 10 m to c. 900 m, generating the lenticular (pod-shaped) Bangs Havn intrusion with a gabbroic sheath around a syenitic and granitic core. The map (Fig. 115) also shows the sinuous, flamboyant forms of the associated dykes. Here, as with the intrusions described by Bridgwater & Coe (1970), it appears more probable that the magmas intruded highly sheared granitoids that were sufficiently hot to yield in a ductile manner in the extensional regime as mafic magma ascended.

The giant dyke shapes in the southern rift are deduced to have resulted similarly from intrusion into a hot granitoid basement but one that was at a lower ambient temperature than in the northern rift, thus resulting in less extreme diapiric behaviour. That pinch and swell features are absent in the OGDC but characterise the YGDC may then be attributed to intrusion of the former when the temperature of the crust had not yet been sufficiently raised. It is of interest that Mesoproterozoic giant dykes in Sweden exhibit comparable idiosyncrasies to these Gardar intrusions. Thus the Halleförs dyke shows a similar composite nature as well as comparable pinch-and-swell features (Krokström 1936).

The emplacement mechanism for the Klokken complex remains unexplained. If, as has been argued above, the initial gabbro at Klokken was essentially an integral part of the YGDC intrusive event, how did it acquire its ovoid form? Xenoliths of country rock granite gneiss occur within it but, in view of the densities of the latter and the inferred density of the gabbro magma (2.80 ± 0.5, Mingard 1990), the granite gneiss could not have been stoped and sunk within the magma. Whereas entry of the salic magmas into the axial cores of the composite northern and southern rift giant dykes might have taken place as these intrusions continued to dilate, the geometry of Klokken precludes this mechanism.

Figure 116 is an attempt to explain the tectono-magmatic evolution of the Narsaq and Ilímaussaq complexes. The five hypothetical maps purport to illustrate the intrusion forms as they may have been below the Eriksfjord Formation unconformity and the Narsaq lopolith.
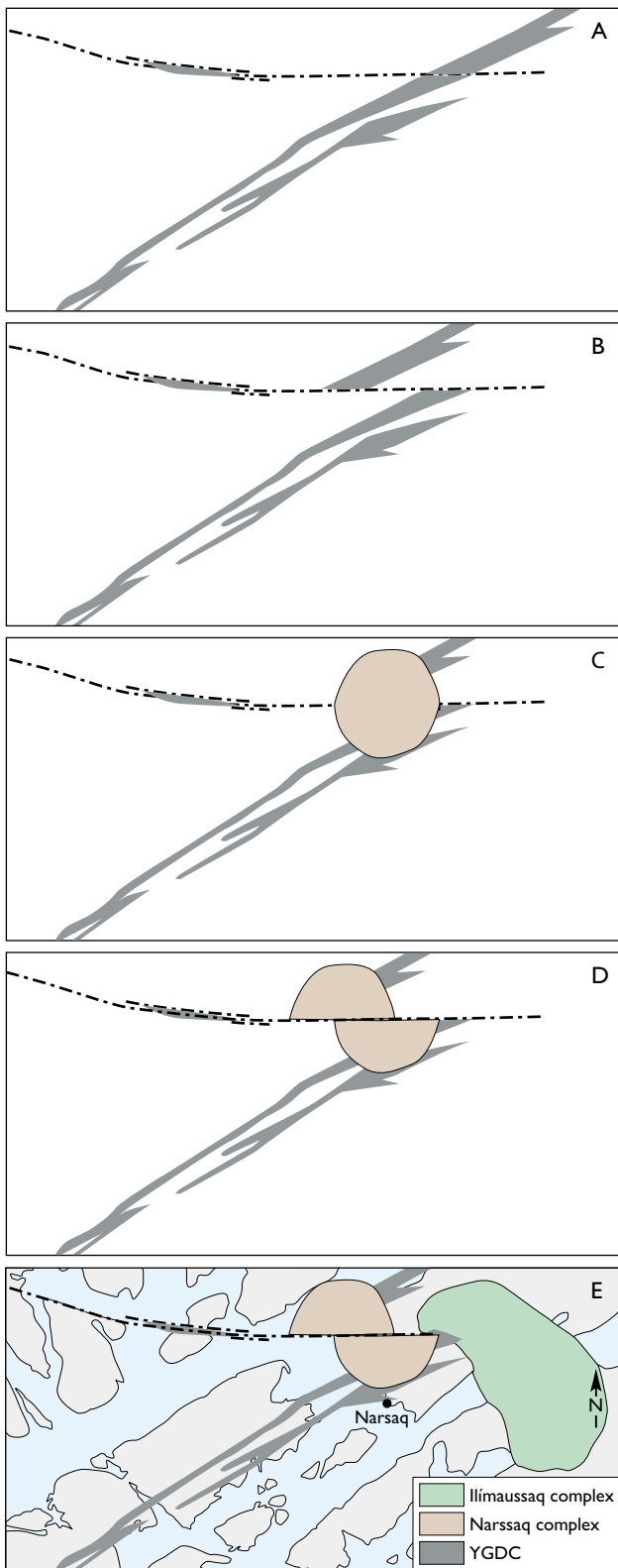
Fig. 116. Five hypothetical stages in the tectono-magmatic evolution of the Narssaq and Ilímaussaq complexes. See text for discussion.

The first (Fig. 116A) shows the YGDC as it may have been prior to faulting, with its branches on Tuttutooq widening and merging east-north-eastwards. The supposed WNW–ESE-trending contacts shown near Narsaq are based on the orientation of the contact between YGDC gabbro and Julianehåb granite on Narsaq Island. The same contact orientation is seen in the giant dyke occurring north-west of Narsaq across Tullerunat Killit and also shown on Tuttutooq west of Sejlfjord (Fig. 10). Figure 116B envisages the situation following initial left-lateral displacement along the 'Narsaq fault', whilst Fig. 116C illustrates the intrusion of the Narsaq complex and its intersection with the fault. The supposition here is that the Narsaq complex magmas exploited, as did other Gardar magmas, the lithospheric weak point caused by intersection of the fault and the rift axis fissuring. Emplacement of the Narsaq complex would have involved engulfment of substantial amounts of Eriksfjord Formation rocks, the Narsaq lopolith and giant dyke gabbros plus parts of the Julianehåb granitoids. It is supposed that magma emplacement and fault displacements were intimately associated in space and time. Figure 116D supposes further fault movement post-dating the Narsaq complex that shifted part of the YGDC towards the west, so that its outcrop now lies beneath the waters of Bredefjord, immediately north of the Ilimmasaq peninsula. Figure 116E illustrates the final situation following emplacement of the Ilímaussaq complex, the focus of which was sited one or two kilometres further east. In the terminal phases of tectonism, as strain energy was finally dissipated, the Ilímaussaq complex acquired its elliptical form and the kinked boundary on its north-western flank. Although these speculative cartoons cannot be correct in detail, they should, in overall principle, approximate the actual tectono-magmatic evolution.

Tectonics within the southern rift

There was a tendency in the Gardar Province for episodes of intrusion and faulting to alternate (Emeleus 1964; Watt 1968; Upton *et al*. 2003). Demonstration of transcurrent displacements principally along left-lateral approximately E–W faults, and right-lateral along approximately N–S faults, is readily shown in a terrain rich in steep to vertical contacts. The evidence for normal faults is unsurprisingly scarce.

Normal faulting

In a terrane affected by lithospheric extension, such as the younger Gardar southern rift zone, normal faults parallel to the rifting would be expected to be abundant, as they are e.g. in the Afar district of Ethiopia. There are many ENE–WSW-trending shear planes within the Julianehåb granite, e.g. through Tuttutooq. Whilst there is usually no evidence for lateral displacement along these, it may be suspected that many did have vertical displacement. The coastlines on either side of the 4 km wide Bredefjord north of the Tuttutooq archipelago are remarkably straight (Figs 1, 2); the glacial erosion that generated the fiord was presumably controlled by shear zones in the basement although geological mapping could prove no displacements. It is suggested that faulting through Bredefjord may have marked the northern boundary of the rift. The southern side of Bredefjord defines the north coast of the Ilimmaasaq peninsula, and along this the Eriksfjord Formation is seen in its fullest expression, *c.* 3.4 km thick, whereas on the northern side of Bredefjord the outcrop is all below the base of the Eriksfjord Formation. Large-scale vertical displacements are implied. Any such faulting was older than the Younger Gardar but whether it was pre-Older Gardar or occurred between Older and Younger Gardar times is not known.

Just as the hypothetical Bredefjord faults may represent the northern boundary of the rift, the more or less linear ENE–WSW trends of the coasts bounding the Skovfjord (Fig. 1) south of the Tuttutooq archipelago can be construed as marking the traces of normal faults along the southern boundary of the southern rift. The east-north-east extension of Skovfjord, the Tunulliarfik fjord, is regarded as the site of major faulting. downfaulting to the north, in pre-Ilímaussaq times, of at least 700 m has been postulated (Sørensen 2006). The fault for which the best data are available is the Kangerluarsuk-Lakseelv fault that transects the Ilímaussaq complex, subdividing it into a southern portion containing the floor cumulates and a larger northern portion that exposes higher structural levels (Fig. 90). It is a hinge-fault, the throw of which diminishes towards the east-north-east from at least 600 m in Kangerluarsuk, in the west-south-west, to near zero at Appat on the Tunulliarfik coast (Sørensen 2006). The northerly downthrow relates to successive movements that were: pre-Ilímaussaq and post-aegirine lujavrite and possibly also post-arfvedsonite lujavrite (Bohse *et al.* 1971; Sørensen 2006).

A minor fault on the northern margin of the YGDC at Asorutit is interpreted as a normal fault, as mentioned in the section on anorthosite xenoliths. The gabbro on the southern side is inferred to be downfaulted from a higher structural level in which the xenoliths had been concentrated by flotation. Further evidence suggests that an ENE–WSW-trending normal fault transects the southern part of the Tugtutôq central complex. Although the direction of throw is unknown, it is a reminder that some extensional faulting may have persisted until late in Younger Gardar times.

Transcurrent faulting

Figure 80 shows the pattern of transcurrent faults affecting the Gardar Province. The pattern comprises conjugate suites of ENE–WSW- to E–W-trending left-lateral faults and NNW–SSE- to NNE–SSW-trending right-lateral faults (Berthelsen & Henriksen 1975; Upton *et al.* 2003). It was, however, the left-lateral faults that were critical in the localisation of the major Gardar intrusions. These faults are known to have been intermittently active since pre-Gardar times, e.g. the 6 km displacement on the Laksenæs fault commenced in the Ketilidian and continued into late Gardar times (Fig. 80; Henriksen 1960). Lying between 60°30′ and 61°30′ and separated by distances of 20–30 km, these faults segmented the southern rift in a manner comparable to that described for the Mesoproterozoic midcontinental rift system of North America (Green 1992). Three of these fault zones are relevant to this bulletin and will be referred to as the northern, central and southern fault zones. From their effect on the YGDC components, the Younger Gardar displacements were approximately 8 km on the northern fault zone, 9 km on the central fault zone and 1.4 km on the southern fault zone that roughly bisects Tuttutooq, i.e. approximately 18.4 km in total. Thus the northern fault zone, which had been influential in the emplacement of the Older Gardar Grønnedal-Íka complex (Emeleus 1964), also controlled the clustering of both the Older and Younger Gardar members of the Igaliko syenites. Intersection of the central fault zone and the YGDC appears to have focussed emplacement of the Narsaq and Ilímaussaq complexes. Although no major intrusions occurred in conjunction with the southern fault zone crossing Tuttutooq, the fault is of interest in showing that whilst movement on the YGDC was only 1100 m, the OGDC was displaced by 1400 m. The time interval between the two giant dyke intrusions is constrained to about 20 Ma (Table 1). There is, as noted earlier, a differ-
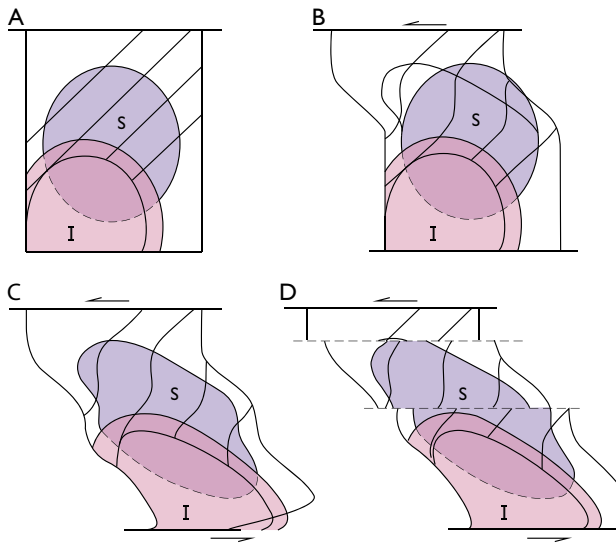
Fig. 117. Progressive deformation and faulting of the South Qôroq complex. **I**: Igdlerfigssalik complex. **S**: South Qôroq complex. Modified from Stephenson (1976b).

ence in their orientation ascribed to a change in the stress field, and a change in their palaeopole positions. Consequently, the concept that *c.* 300 m movement occurred during the time interval between the two intrusions is quite acceptable.

Some 15 km west of Narsaq the central of the three sinistral fault zones under discussion traverses the island of Tullerunnat Killit (Fig. 10). Alongside the fault, though not itself sheared, is a section of a composite giant dyke (500 m broad) that may have been a component of the broad and geometrically complex culmination of the YGDC that is suspected to have been present before its engulfment (through subsidence) by the Narsaq complex (Fig. 116C).

As noted above the Igaliko plutons tend to be elliptical in plan (long axes trending NW–SE) whilst those remote from the fault zones (e.g. Klokken and the Tugtutôq central complexes) are more circular. Stephenson (1976b) accounted for these observations by postulating a simple shear model in which the South Qôroq and Igdlerfigssalik complexes, while still hot, experienced ductile deformation that modified their supposedly initial circular plan towards that of a simple strain ellipse. The originally circular plan of the South Qôroq complex was first deformed by two sets of movement on left-lateral

faults while it remained ductile. Subsequent left-lateral movements along two further fault planes involved brittle fracture and resulted in the present plan of the centre (Fig. 117; Stephenson 1976b). Noting that similar deformation had also occurred in the Older Gardar Grønnedal-Íka complex, Stephenson (1976b) speculated that the elliptical plan of the Ilímaussaq complex may also have resulted from strain related to the central fault zone, despite the fact that significant movements along it had ceased after intrusion of the Narsaq complex and the Main dyke swarm.

West of South Qooroq, between Bredefjord and Tunulliarfik, two major faults composing the northern fault zone (Fig. 80) record a left-lateral shift of 6–6.5 km across a 4 km wide zone, all involving brittle fracturing (Emeleus & Stephenson 1970). The more northerly of this pair generated a 200 m wide crush zone in which syenites and dykes are crushed and sheared and a downthrow to the north is suspected (Emeleus & Harry 1970). The more southerly fault, well seen east of South Qooroq, has a c. 100 m wide crush zone with a sinistral displacement of c. 1 km of a contact between a syenite unit (S2) and basement granite. It also has a probable vertical throw of more than 400 m. Movement(s) on the northern fault may be later than those on its southern neighbour (Emeleus & Harry 1970). According to these authors, the age of its activity should remain open in view of some evidence that movement occurred after formation of one of the late intrusions (I6) in the Igdlerfigssalik complex.

Of the four faults investigated by Emeleus & Stephenson (1970) between Tunulliarfik and Qooroq, and east of Qooroq, vertical throws discerned from displacements in the Eriksfjord Formation strata were downwards towards both the north and south. With regard to the central fault across the Narsaq complex, a significant downthrow to the north was inferred by Hamilton (1964) and a northerly downthrow has been suggested in this work for the southerly fault across Tuttutooq in the vicinity of Itillip Saqqaa.

The southern Gardar rift was scarcely affected by the NNW–SSE to NNE–SSW dextral faults that are widespread across the province (Fig. 80). One of these faults (trending N–S) , however, is present on the east side of the Igdlerfigssalik complex, with a horizontal movement that displaces the contact between units I2 and I3 by at least 400 m (Emeleus & Harry 1970).

Evolution of the magmatic system of the younger Gardar southern rift

Parental mafic magmas

Mafic rocks ranging from basalts and dolerites to troctolitic gabbros were produced across the Gardar Province from earliest to latest Gardar times, i.e. for over 100 Ma (Table 1). Olivine dolerite dykes occur in abundance, and gabbro also participates in several Gardar plutons (Kûngnât, Nunarssuit, Klokken, South Qôroq and Igdlerfigssalik). Additionally, much of the Eriksfjord Formation consists of basaltic lavas. Analyses of lavas, dykes and chilled marginal samples from the intrusions from across the province suggest that, irrespective of place and time, the mafic magmas had a common compositional affinity (Upton 1969; Upton & Emeleus 1987; Upton *et al*. 2003). They have relatively evolved compositions with the liquids appearing rarely to have >7 wt% MgO. The analyses can be roughly subdivided into four groups: (1) Older Gardar dykes (BD_0 and early Gardar dykes from the far west of the Province), (2) Eriksfjord Formation lavas, (3) dykes and gabbros from the northern (Nunarssuit-Isortoq) rift zone, and (4) Younger Gardar dykes and gabbros of the southern rift zone.

In each group the mg* number (atomic $100Mg/(Mg + Fe^{2+})$), is <50 and olivine compositions are rarely if ever more magnesian than Fo_{70}.These basaltic compositions are typically poor in the diopside component, leaving them relatively rich in plagioclase and olivine so that they crystallise to troctolitic rocks. This characteristic is manifest in high Al_2O_3/CaO ratios in the range 1.75–2.40. All these basaltic compositions are distinctly potassic with average compositions for each group having >0.9 wt% K_2O. Virtually none are tholeiitic or typical alkali olivine basalts but are transitional olivine basalts plotting close to the ol-pl-cpx plane of critical undersaturation in the normative basalt tetrahedron (Yoder & Tilley 1962; Coombs 1963; Upton & Thomas 1980).

Geochemical characteristics of the southern rift mafic magmas

The Older Gardar basaltic lavas and dykes, and lavas and dykes from the Younger Gardar northern rift, have similar minor and trace elements ratios whereas those of the younger Gardar southern rift are markedly different. Thus the HREE/LREE and Zr/Nb ratios in the southern rift are not only significantly lower than those of the Older Gardar dykes and Eriksfjord Formation lavas but are also lower than those of the Younger Gardar northern rift (Upton & Emeleus 1987). Figure 118 is a Ce/Y vs. Zr/Nb plot of data from the four Gardar basaltic groups as well as from ultramafic lamprophyres, silicocarbonatites and carbonatites (note that these last include Gardar samples of all ages). This diagram involves ratios of two pairs of incompatible elements and in each pair one element (Ce and Nb respectively) is distinctly more incompatible than the other (Y and Zr). Ce and Y are proxies for respectively light and heavy REE. Whilst the ratios are insensitive to moderate degrees of low-pressure crystal fractionation involving mineral phases likely to crystallise from basaltic magma, they reflect differences in the degree of mantle melting and/or differences in source composition (Hardarson & Fitton 1991). The Younger Gardar mafic dykes of the southern rift (Tugtutôq–Ilímaussaq swarm in the legend) are clearly distinct from those of the Older Gardar dykes, the Eriksfjord Formation lavas and the Younger Gardar dykes of the northern (Nunarsuit–Isortoq) rift. All the southern rift data fall within the field of ocean island basalts, whereas this is true for only some of the other three basaltic groups and for some of the lamprophyre-carbonatite association. The southern rift data also fall between the fractional melting curves calculated for depleted garnet- and spinel-lherzolite mineralogies (not shown), consistent with derivation of their magmas from a melt column extending across the garnet-spinel transition zone in the mantle (Hardarson & Fitton 1991).

The southern rift basalts also have higher contents of Ba and Sr than those from elsewhere in the province, irrespective of space and time (Upton & Emeleus 1987; Fig. 119). Among the major elements, P_2O_5/TiO_2 ratios indicate relative P enrichment of the southern rift magmas (Fig. 120).

These data emphasise the broad compositional unity of Older Gardar dykes, the Eriksfjord Formation lavas and the northern rift magmas on one hand but demonstrate the distinctiveness of the southern rift mafic dykes
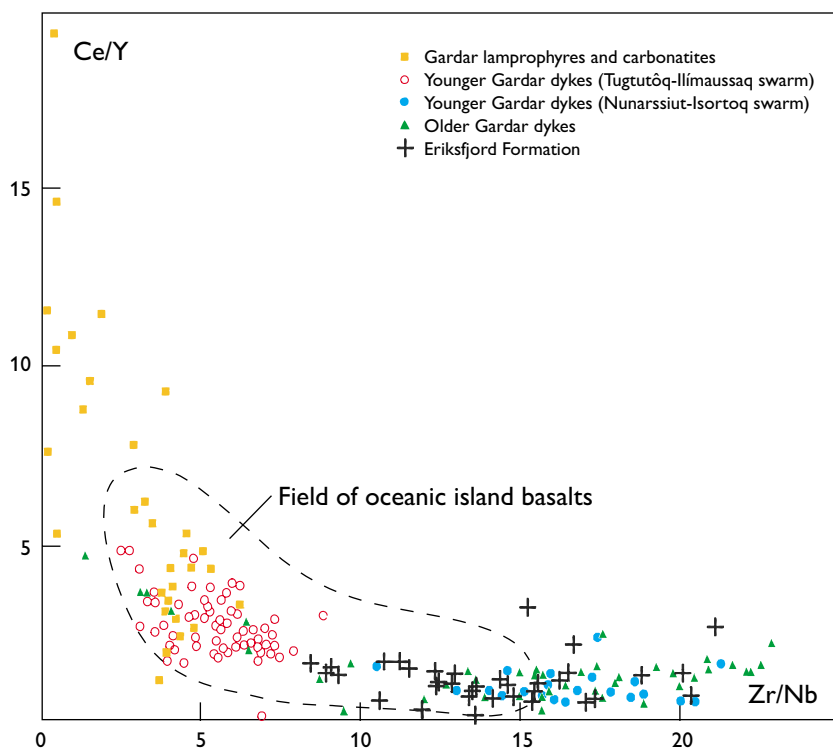
Fig. 118. Incompatible element ratios in phenocryst-poor basic Gardar dykes (4–8 wt% MgO) and Eriksfjord Formation lavas, shown together with ultramafic lamprophyres and carbonatites. Modified from Upton *et al.* (2003).

on the other hand. The relative enrichment of the latter in LREE, Nb, P, Sr and Ba might be viewed as due to a smaller degree of mantle melting than in the other three groups. However, it is not associated with variation of the silica/alkali balance as would be expected. Accordingly it is interpreted as reflecting higher concentrations of the most incompatible elements in the mantle source beneath the younger rift zone. As similar concentrations are not seen in the older Eriksfjord Formation lavas in the same area, it is suggested that the higher concentrations in the younger magmas were due to a focussed metasomatic enrichment above an asthenospheric wedge developed after eruption of the lavas but prior to the initiation of the southern rift.

Analyses of the most mafic chilled facies rocks from the southern rift zone were presented earlier in Table 2.

Magma evolution in the southern rift zone

Whilst liquid lines of descent can only be indirectly approximated from the plutonic suites, they can be authenticated through study of the smaller, fine-grained dykes that followed the giant dykes. These smaller dykes are

considered to be residues from fractional crystallisation of parental troctolitic magmas. The more primitive gabbros crystallised from melts that had either olivine alone or olivine + plagioclase on their liquidus. However, the plagioclase in these rocks is commonly seen as glomerocrysts with a radiating structure giving rise to 'snowflake' gabbros (Figs 18, 25). Such 'snowflakes' are regarded, as noted above, as products of rapid crystallisation from magma oversaturated in plagioclase; further evidence for plagioclase oversaturation comes from occurrences of 'perpendicular feldspar' crescumulates as in the YGDC (Itillip Saqqaa) described earlier (Fig. 26). The Al and Sr contents in the presumed magmas, combined with virtual absence of any negative Eu anomalies in the REE patterns (Blaxland & Upton 1978; Upton 1996), support the contention that plagioclase fractionation did not occur until the magmas reached relatively shallow crustal levels (possibly <6 km) and that, for at least part of the ascent, olivine was crystallising alone. Comparable textural and geochemical evidence for late and rapid crystallisation of plagioclase from the Gardar basaltic magmas is found elsewhere in the province, e.g. in the Eqaloqarfia dyke of the Isortoq area (Pulvertaft 1965), in the Older Gardar Kûngnât complex (Upton *et al.* 2013), as well as in all three of the principal groups of lavas of the Eriksfjord Formation (Poulsen 1964). The supposition is that
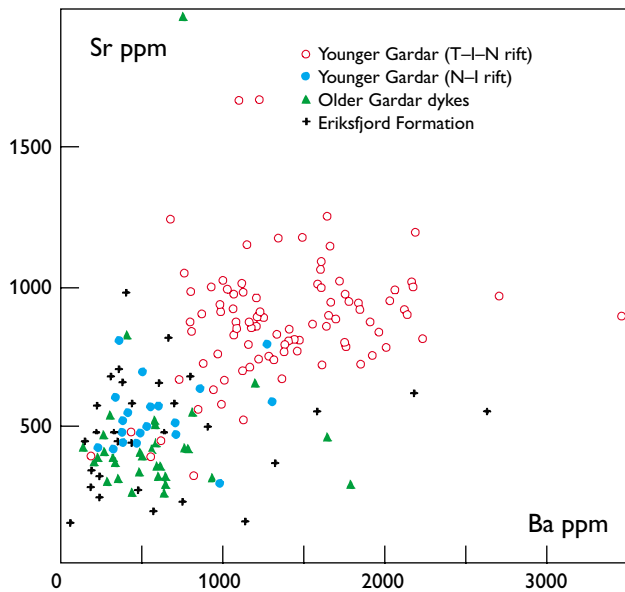
Fig. 119. Ba-Sr plot of phenocryst-poor basic Gardar dykes (4–8 wt% MgO) and Eriksfjord Formation lavas. Modified from Upton & Emeleus (1987).
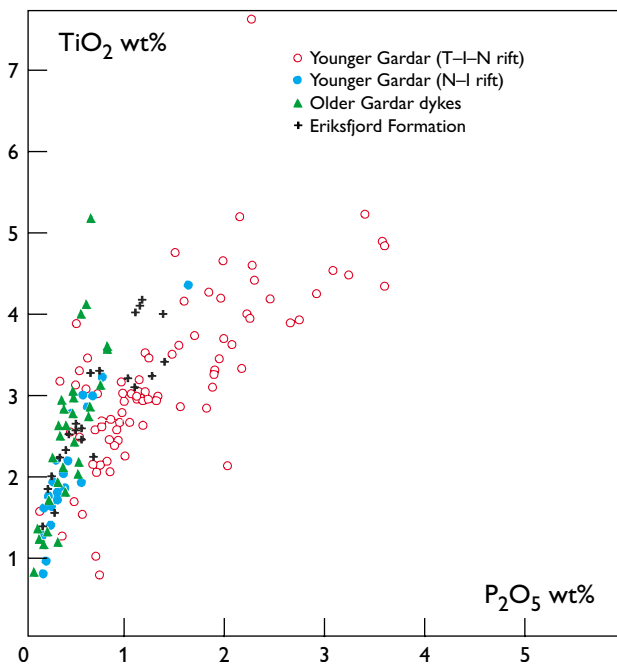

Fig. 120. P_2O_5 vs. TiO_2 in phenocryst-poor basic Gardar dykes (4–8 wt% MgO) and Eriksfjord Formation lavas. Modified from Upton et al. (2003).

had these same magmas been retained for any length of time to equilibrate in the lower crust, plagioclase crystallising from them would have gone to augment the evolv-

ing anorthosite. That this did not occur is presumably because of rapid ascent.

The anorthosite xenoliths and associated feldspar megacrysts, which are regarded as broadly cognate with the YGDC, provide contrasting evidence for higher pressure plagioclase crystallisation (Halama et al. 2002) and lack any evidence for fast growth from supersaturated melts. Since the YGDC magma arose from *beneath* the anorthosite protolith without attaining the olivine-plagioclase-liquid cotectic until it reached the upper crust, the implication is that it ascended fast, becoming increasingly plagioclase oversaturated until plagioclase nucleation commenced. Subsequently, when abundant plagioclase separation commenced, the consequent iron enrichment in the relatively reduced magmas led to generation of ferro-mugearitic melts. Prolonged fractional removal of Ca-bearing feldspars and later pyroxenes from evolving magmas at depth (inferentially in the lower crust) is considered to have caused the development of peralkalinity in the salic residues in accordance with Bowen's (1928) 'plagioclase effect', and also through the agency of 'the orthoclase effect' (Bailey & Schairer 1964) whereby the preferential entry of potassium into the feldspars helped to generate per-sodic (agpaitic) residual magmas.

The high Al/Ca ratios of the basaltic magmas were responsible for the delayed crystallisation of pyroxene. In this respect the Gardar magmas have much in common with the parental magmas of the North American Proterozoic anorthositic intrusions, e.g. that of the Kiglapait complex in Labrador (Morse 1982, 2006). A principal point of difference between the Labrador and Gardar parental magmas is the higher K content of the latter. The comparatively low silica activity and high K_2O of the Gardar magmas precluded crystallisation of low-Ca pyroxenes and dictated their evolution via hawaiites, mugearites and benmoreites to trachytes and ultimately to peralkaline rhyolites and phonolites.

The magmas also had notably high fluoride contents (Upton et al. 2003; Köhler et al. 2009). This is considered to have conferred an unusual degree of fluidity (low yield strength) facilitating convection among other things. The unusually coarse-grained nature of the Gardar plutonic rocks is attributed to depolymerisation of the magmas by fluoride ions. The F-rich character of the Gardar magmas, which are similar in this respect to the Andean volcanic rocks, provides another pointer to the mantle source having been affected by subduction-related metasomatism (Köhler et al. 2009).

In the foregoing chapters evidence has been adduced for the delicate density balance between solids, whether

these be discrete crystals (e.g. of sodalite), crystal aggregates (e.g. plagioclase-olivine 'snowflakes') and their host melts, dictating whether they sank or floated. In the remarkable BFDs (big feldspar dykes), packed with plagioclase-rich rocks and crystals, it may be surmised that melt and solid densities were closely matched. Crystal-rich slurries are judged to have descended from magma chamber sidewalls. In the case of the anorthosite roof vs. floor cumulates it was suggested that different behaviour shown in rocks of similar composition depended on density changes in the melts according to pressure. In numerous instances, the similarity of layered structures in the intrusions to those of sedimentary sequences also points to a remarkable fluidity of the magmas, whether mafic, intermediate or, as in the case of the agpaites, extreme alkaline differentiates. The apparent ease of separation of crystals from melts allowed highly effective fractional crystallisation and production of extreme lithologies.

Magmatic differentiation in the lower crust

It is inferred that great volumes of Gardar mafic magmas were underplated at or near the crust-mantle boundary and were ultimately parental to the alkaline salic plutons. In the case of the Kenya rift, to which the southern late Gardar rift may have had some resemblance, the volume of magma including underplated material has been estimated as *c.* 934 000 km³ (Latin *et al.* 1993). The Kenya rift has been magmatically active for *c.* 35 Ma whilst the activity in the younger Gardar southern rift may have covered *c.* 40 Ma (from *c.* 1180 to 1140 Ma) and the magma volumes involved may have been comparable. In the model offered here, a very large volume of magma was generated above a rising asthenospheric mantle wedge fed by rising plume material (Latin *et al.* 1993). Around 1180 Ma extensional stress culminated in lithospheric attenuation and partial melting of the metasomatised lithospheric mantle along a zone coinciding with the axis of the Julianehåb batholith, leading to extensive underplating by primitive basaltic magma. The latter was relatively Ca-poor (hence with high Al/Ca ratio) and K, Sr, Ba-rich from their inception. According to Herzberg (1995), Al/Ca of melts decreases with increasing pressure of peridotite melting and equilibration, and the high values of the Gardar basalts could signify a relatively low-pressure melting regime.

Fractional crystallisation of olivine (± pyroxene and spinel?) led to a hawaiitic magma crystallising on an olivine-plagioclase cotectic. At the deep crustal levels plagioclase crystallised and, being less dense than the magma, accreted to form a flotation cumulate while olivine sank to yield dunitic cumulates at the base. This situation is envisaged as having continued intermittently throughout the entire period of Gardar magmatism, and repetitive influx of new primitive magma batches must be assumed.

The concept for genesis of the salic magmas proposed by Bridgwater & Harry (1968) and summarised in their cartoon (Fig. 75) remains generally valid although in need of modification. The BFDs are highly instructive with respect to the petrogenesis in the rift system, providing not only the key linkage between the benmoreitic and the hawaiitic/mugearitic magmas but signalling the importance of compositionally stratified magmas at depth and indicating that these developed beneath an anorthositic lid.

When continuing extension resulted in crustal failure, the Older giant dyke was intruded. Slow crystallisation in the interior of this steep-sided tabular, half-kilometre wide intrusion led to the upward growth of its syenite suite from its residual melts. After several millions of years during which some plate rotation occurred, further build-up of transtensional stress gave rise to a second, still more dramatic crustal failure, in conjunction with a greater degree of melting of the same mantle source. After a significant amount of fractionation, a portion of the basalt magma was emplaced as the Younger giant dyke complex. Since this magma (like its OGDC predecessor) had all the characteristics of being a residue after extensive fractional crystallisation, it is assumed that these magmas were products of a far greater volume of primitive magma. Ascent of the magma disrupted part of the deep crustal anorthosite, entraining large and small masses *en route* that then accumulated by flotation at the top. Rare-earth element data (Fig. 113) indicate that the primitive magmas from which at least some of the laminated anorthosites were derived, represent smaller melt fractions of the mantle source than the parental magmas of either the YGDC or OGDC.

Residual magma retained beneath the anorthosite is envisaged as occupying one or more chambers in the lower crust, elongate parallel to the axis of the southern rift. The approximate dimensions may have been 30–50 km long, *c.* 15 km broad and perhaps a kilometre or so deep. With slow cooling these magmas then underwent compositional stratification. From the BFD evidence this appears to have comprised a hawaiitic/mugearitic lower layer overlain by salic (benmoreitic/trachytic) magma with <2 wt% MgO. Production of such stratified magma bodies

was probably repetitive. As a consequence of the extraction of plagioclase from these relatively reduced magmas during anorthosite genesis, the residual magmas became increasingly Fe-rich and correspondingly dense. This resultant density handicap incurred by iron enrichment is presumably the reason why these magmas rarely reached shallow crustal levels (cf. the Gardar 'Daly gap', Watt 1966). (The genesis of ferro-syenogabbros in the OGDC and YGDC is explained as shallow-crustal reflections of what occurred on a greater scale deep in the crust). YGDC magma, with a low density relative to these Fe-rich residual magmas, ascended through the anorthositic capping to reach shallow levels. Crustal fissuring permitted selective tapping of the stratified chamber(s) by dyke formation as rift extension continued. This process, generally but not invariably, extracted magmas from the salic top of the chamber(s). Attainment of the benmoreite composition appears to have marked an important stage in the rift's evolution, just as it was for the magmatic evolution in the Kenya rift (Macdonald 2002). Only when the residual magmas became sufficiently iron-poor (total iron as Fe_2O_3 <12 wt%) i.e. benmoreitic, did they attain low enough density to ascend through the crust, independent of dyke fissuring. It was benmoreitic magmas that were the preliminary arrivals in the Ilímaussaq, Igdlerfigssalik and Tugtutôq central complexes.

Reduction of stress energy with time is suggested by the generalised reduction in dyke widths in the Main swarm. The Igaliko swarm, introduced during the same tectonic phase as the Main swarm, may have resulted from a smaller degree of melting of contrasting mantle sources. As extensional strain energy dissipated, a changed stress regime promoting transcurrent faulting was responsible for dyke formation to become increasingly rare.

Magma chambers of the central complexes

In order to extend the model outlined above to embrace the formation of the principal salic centres, it is hypothesised that at *c.* 30 km intervals along the rift system's elongate parent chamber, foci developed where collection of buoyant salic residues was particularly concentrated. From field observations among the Gardar alkaline complexes it is surmised that ascent took place by repetitive detachments of slabs of roofing rocks, up to 100 m or so thick, that successively became underlain by lower-density magmas. The geometry of the slabs may have

been controlled by subhorizontal (thermally induced) jointing. Evidence from the Grønnedal-Íka and Kûngnât complexes (Emeleus 1964; Upton 1960; Upton *et al.* 2013) shows this behaviour where roofing consisted of high-grade gneisses. At Nunarssuit, the Tugtutôq central complex and also Kûngnât, the roofing involved supracrustal mafic volcanic cover, whilst at Klokken, Syenitknold and Ilímaussaq ascent of magma involved displacement of coeval roof sequences ('upper border groups').

By logical extrapolation from what is seen at current erosion levels to deeper levels, it may be assumed that the same mechanism by displacements between roofing slabs (intact or disintegrated) permitted ascent of the syenitic magmas through the crust. The lithospheric thickness along the southern rift axis cannot be known, but from evidence of modern rifts (e.g. the Gregory rift, East Africa) it may have been as little as 35 km and crustal thickness correspondingly reduced (Macdonald 2003). Evidence from the Kûngnât and Ilímaussaq complexes suggests that their magma chambers were situated at depths of *c.* 3 km. On this line of argument it may have needed only a limited number of such collapse events to raise the magmas from the lower crustal parent chamber to the shallow crust. In the discussion of the Ilímaussaq complex emphasis was placed on the great size of the augite syenite magma chamber required to account for the high concentration of incompatible elements in the agpaitic magmas. Such a chamber may well have had the form of an extensive accumulative benmoreitic magma in the upper parts of an elongate, compositionally stratified parent chamber as proposed above.

There is a contrast between those major salic complexes where the parent magmas at depth became increasingly evolved with time (the Tugtutôq, Narsaq and Ilímaussaq complexes) and those like South Qôroq where successive intrusions had progressively more primitive compositions. The Igdlerfigssalik complex ended with a mafic partial ring-dyke but there are as yet no data to show whether the previous six intrusions followed a comparable evolution. The closest analogue to the South Qôroq intrusive pattern is that of the Older Gardar Kûngnât complex (Upton *et al.* 2013). The first category suggests two or more admissions from a part of the salic upper layer or the 'master chamber' that was evolving through continued assimilation and fractionation (Tugtutôq and Narsaq) or through fractionation with minimal assimilation (Ilímaussaq). In the second category, repeated collapses into a stratified parent chamber may have occurred, culminating in ring-fault descent of the already crystallised (and consequently relatively dense) syenitic

components forcing the underlying hawaiitic component to high levels.

The one complex that stands alone, geographically and metaphorically, is Klokken. It differs from the Igaliko syenites (Fig. 2) in being silica-saturated, finishing with an oversaturated diorite. It differs from all the other Gardar central complexes in commencing with troctolitic gabbro, with younger units passing progressively from unlaminated syenite to the layered syenites of its centre. As has been documented above, the intrusive and crystallisation patterns at Klokken and at the differentiated YGDC pods, at Asorutit and Syenitknold were so similar as to suggest their possible contemporaneity. However, whereas emplacement in the YGDC may be explicable in terms of initial crustal dilation followed by ingrowth of sidewall cumulates and upgrowth of floor cumulates, the cylindrical geometry of Klokken is incompatible with a dilational introduction of the gabbroic magma. In starting with a mafic magma it contrasts starkly with all the other central complexes. How the initial cylindrical pluton, inferentially of mafic magma, was emplaced into granitic-gneiss country rocks remains an enigma.

Genesis of the silica-oversaturated magmas

On approaching the minimum melting point on the alkali feldspar join, the salic residues evolved either to the rhyolitic or the phonolitic minima in the Qz-Ne-Ks system (Upton 1974). The generally oversaturated Main dyke swarm and the generally undersaturated Igaliko dyke swarm can be geochemically distinguished by their Zr/Nb ratios, those of the Igaliko swarm having values <5.2 while dykes of the Main swarm have higher values. The small negative Nb anomalies in trace element patterns and higher $^{87}Sr/^{86}Sr$ values of the Main swarm dykes are attributed to greater degrees of crustal assimilation (Foland *et al*. 1993).

High-temperature fluids rich in alkalis, volatiles and incompatible trace elements, advancing ahead of rising mantle diapirs or plumes, may have a profound effect on the overlying lithospheric mantle and lower crustal rocks, causing fenitisation and varying degrees of crustal melting (Woolley 1987). Many continental A-type granites may have been generated in this manner (Martin 2006). However, whereas this hypothesis may well apply to the northern (Nunarsuit–Isortoq) rift, for which a greater degree of crustal heating has been proposed above, it has

limited applicability in the southern rift. In the latter, quartz trachyte and comendite dykes occur over much of its length but the quartz syenites and alkali granites are restricted to a 30 km long sector between the Tugtutôq and Ilímaussaq complexes. Dyke propagation probably had a very significant lateral vector, but the magmas of the central intrusions are more likely to have ascended more or less vertically from the regions in which they were generated. The crustal assimilation necessary to generate the silica-oversaturated salic melts through AFC processes may have been due to the heat of crystallisation from the deep crustal basaltic bodies affiliated to the YGDC. The greatest effects are seen around a Narsaq hot spot that is inferred to denote the principal focus of magma genesis. The tectono-magmatism cartoon (Fig. 116) shows how faulting may have distanced the Ilímaussaq intrusions from the YGDC, thus minimising crustal assimilation in its genesis. It is remarkable that the southern rift system included both the highly reduced, ultra-sodic hyperagpaites and the extremely oxidised, and potassic mela-aillikites of the Narsaq region. These petrologically polar-opposites were proximal in both space and time.

Silica-undersaturated rocks are absent from the northern (Nunarsuit–Isortoq) rift zone. This zone experienced no less than five swarms of mafic dykes during its Gardar history (Harry & Pulvertaft 1963), and high resultant geothermal gradients may have been characteristic, particularly during the Younger Gardar, modifying the mechanical properties of the crust and facilitating crustal assimilation. As outlined above, the anomalous geometries of the giant dykes of this zone may be due to hotter country rocks yielding in a more ductile fashion at the time of giant dyke intrusion. This conclusion conforms with field evidence that the contacts do not show the same degree of chilling as those of its counterparts in the southern rift.

Crystallisation histories

Whilst the intrusions along the southern rift zone involved a great number of separate magma batches these still compose broadly coherent lines of liquid descent. Whilst the overall crystallisation history of what is argued to be a single magmatic system cannot be deduced from any one part of it, it can be discerned from the collective sources of evidence. These present a remarkably complete petrogenetic narrative from simple crystal–melt equilibria exemplified by the most primitive

magmas (represented by the YGDC chilled samples) to the astonishingly complex equilibria in the Ilímaussaq agpaites. The most primitive magmas (excluding the aberrant aillikitic magmas) were slightly silica-undersaturated and their fractional crystallisation led via trachyte and phonolite to agpaitic and ultimately hyperagpaitic residuals. This undersaturated trend is regarded as the dominant one within the system as a whole, but it was interrupted by the, geographically more localised, silica-saturated/oversaturated salic magmas discussed above.

The YGDC basalt was estimated to have intruded at c. 1140°C (Upton 1971; Upton & Thomas 1980). This involved olivine + liquid, joined at shallow crustal levels by plagioclase. Titanomagnetite began precipitation at the maximum iron-enrichment stages, joined at much the same stage by apatite. Iron, Ti, Mn and P contents rose to maxima when MgO was reduced to between 2 and 3.5 wt% and the melt had attained a ferro-mugearitic composition. In tholeiitic magmas Fe and Ti contents commonly peak during the intermediate stages of differentiation which is held to be a consequence of relatively low degrees of oxidation (Fenner 1937). In the alkaline OGDC and YGDC, high Fe and Ti concentrations were similarly reached at mid-stages of magmatic evolution because the oxidation states were low, somewhat below that of the QFM buffer. Uncharacteristically for basaltic magmas, clinopyroxene (salite) only joined the crystallising assemblage at a late stage. The salite evolved to ferrosalite and from this Na-enrichment towards aegirine-augite proceeded at differing stages of Fe-enrichment according to the oxidation state. In the most extremely reduced case (Ilímaussaq) the pyroxenes attained nearly end-member hedenbergite composition before there was any significant intake of Na (Larsen 1976).

Because of the high K_2O content of the parental basalt (c. 1.4 wt%) the feldspars followed a trend from plagioclase through potassic oligoclase and anorthoclase to sanidine. Sanidine was accompanied by nepheline in the phonolites with subsequent appearance of sodalite and natrolite at lower temperatures. The feldspars crystallised under hypersolvus conditions until, with rising P_{H_2O} and falling temperature, there was a switch to subsolvus crystallisation of separate K- and Na-rich phases in the lujavrites. A continuum may have existed from temperatures >1100°C to increasingly low temperature (volatile-rich) magmas at c. 300°C before any discrete supercritical fluid phase separated.

Olivine compositions changed in the evolving melts, with the forsterite component approaching zero while the tephroite (Mn) component increased, reaching a maximum of c. 16 mol % in the South Qôroq complex (Stephenson 1974). Olivine eventually underwent reaction with melt, forming iron- and sodium-rich amphibole. Only in the kakortokite and lujavrite magmas did amphibole become a liquidus phase. Magnetite was also lost by reaction with melt, producing aenigmatite (Larsen & Steenfelt 1974; Larsen 1977). Apatite underwent continuous changes becoming increasingly rich in Sr and LREE (P.G. Hill, unpublished data) through a substitution dominated by $Ca^{2+}+P^{5+}=REE^{3+}+Si^{4+}$ with concomitant introduction of Na, until vitusite $(Na_3(Ce,La,Nd)(PO_4)_2)$ with >20 wt% REE_2O_3 crystallised in the Ilímaussaq agpaites (Rønsbo et al. 1979; Rønsbo 2008). Finally, in the hyperagpaitic magmas phosphorus became mainly accommodated in the silicate-phosphate steenstrupine. After Zr attained its maximum content in the magmas (c. 9000 ppm, Bailey et al. 1981b), a separate Zr mineral, eudialyte, joined the liquidus assemblage at the start of kakortokite crystallisation.

Thus, the magmas evolved over a crystallisation range of c. 800°C, from extremely simple, virtually mono-mineralic mineral-melt equilibria in the most primitive YGDC magma to extremely complex poly-component equilibria in the latest Ilímaussaq residua. It may be envisaged that cumulate sequences were generated beneath the southern rift system at all depths at which magma batches underwent temporary or permanent residence. To produce the large volumes of salic differentiates at high levels, huge quantities of mafic/ultramafic cumulates must have been formed at depth as envisaged beneath the Kenya rift (Macdonald 2002).

Mantle sources

There is general consensus that the Gardar magmas, and specifically those contributing to the southern rift, originated in the mantle. Crustal contamination was probably insignificant apart from the geographically and temporally restricted silica-oversaturated magma suites. Because of the close affinity between Older and Younger Gardar magmatic suites (e.g. Motzfeldt and Ilímaussaq or Kûngnât and the YGDC) that succeeded each other over a period in excess of 100 Ma, it has been argued that the magmas either originated in the lithosphere or that transient asthenospheric melts acquired lithospheric characteristics in the course of ascent (Upton & Emeleus 1987; Macdonald & Upton 1993; Upton 1996).

The relative poverty in normative diopside of the Gardar basaltic compositions could be explicable through extensive high-pressure clinopyroxene fractionation. However, as the clinopyroxene deficiency that confers the troctolitic nature to the gabbros is present in *both* Older and Younger Gardar mafic rocks it would be a remarkable coincidence if, over a time span of *c.* 140 Ma, *all* the mafic magmas had undergone similar crystallisation histories. In the case of the Nain Province (Labrador), Morse (1982) considered it possible that the source of the anorthositic rocks was an unusually iron-rich mantle poor in clinopyroxene. For the Gardar Province it has been suggested that the mantle source was a metasomatised, clinopyroxene-poor lherzolite or even harzburgite (Macdonald & Upton 1993). The strongly fractionated REE patterns of the YGDC and other Gardar basalts indicate that garnet was a residual phase during the melting processes. Trace element and isotopic studies across the Gardar Province clearly demonstrate a heterogeneous mantle source. Whilst basalts related to continental rifting (e.g. the East African rift, the basin and range province, Oslofjorden and the Carboniferous magmatism in south/central Scotland) typically have ocean island basalt type (OIB) incompatible element distributions, those of the Gardar and specifically in the southern rift system differ in their higher K, Sr, Ba, P, F and LREE contents and negative Nb-Ta anomalies, suggesting that supra-subduction zone metasomatism may have been involved, possibly dating back to Palaeoproterozoic Ketilidian events (Goodenough *et al.* 2002).

The high alkali and chlorine contents in the magmas may have resulted from interaction between carbonated peridotite and saline fluids or between peridotite and chloride-carbonate melts (Klein-BenDavid *et al.* 2009). These authors suggest that potassium may infiltrate peridotite during penetration of a saline component. The migration and focussing of such alkaline-halogen-rich fluids into the mantle wedge, supposed to have accompanied the southern Gardar rift, could have been of prime importance in the processes leading, *inter alia*, to genesis of the Ilímaussaq naujaites.

It has been suggested for the Kenya Rift magmatism that there was interaction between a plume component (similar to an OIB-source) and a heterogeneous lithospheric mantle with the qualification that the strong lithospheric signature makes identification of the plume component very difficult (Macdonald 2003 and references therein). In the case of the Eriksfjord Formation lavas, it was noted by Halama *et al.* (2002, 2004) that the trace element characteristics are comparable to those

derived from OIB-type sources. Whatever the source, the paradox of the similarities between the Older and Younger Gardar magmas remains to be resolved, despite the presumption of active asthenospheric convection during the long period separating them.

The Julianehåb batholith is considered to be of Andean type, with the implication that it was a consequence of subduction at an ocean–continent plate boundary. The Ketilidian orogeny took place at 1855–1723 Ma (Garde *et al.* 2002) and is considered to have involved oblique subduction of an oceanic plate subducting northwards beneath the craton margin (Chadwick & Garde 1996). The inferred enrichment of the sub-Gardar mantle in K, Ba, Sr, P, F and LREE, and negative Nb-Ta anomalies, was attributed to metasomatic modification by fluids or melts rising from the subducting oceanic plate (Upton & Emeleus 1987; Macdonald & Upton 1993; Goodenough *et al.* 2002; Marks *et al.* 2004; Köhler *et al.* 2009). Some of the Gardar basaltic rocks are sufficiently potassic to justify use of the term shoshonitic (Winther 1992; Köhler *et al.* 2009). Köhler *et al.* also report the high F content of Gardar doleritic dykes and note that F-enrichment is also a characteristic of Andean lavas, inferring that in both instances the element was derived from a subducting oceanic slab.

The surviving Ketilidian volcanic sequences on the craton north of the Gardar Province include tholeiitic pillow lava sequences several kilometres thick (Higgins 1970; Garde *et al.* 2002). They are characterised by low La/Yb ratios suggesting that they represent high degrees of mantle melting (M. Hamilton & B. Upton, unpublished data, 2000). The lavas are as yet undated but are presumed to have an age of *c.* 2000 Ma, and it is consequently proposed that their eruption left a restitic lithospheric mantle composed largely of refractory clinopyroxene-poor lherzolite or even harzburgite (Upton 1996). Fluids or hydrous silicic melts rising from the subducting oceanic plate may have first entered the overlying mantle wedge and, subsequently, the lithospheric mantle, or if the Ketilidian lithosphere was sufficiently thick, entered directly into the lithospheric mantle. The only mantle xenoliths known from the Gardar Province are those in an aillikitic intrusion on Illutalik, south-east of Tuttutooq (described above). Although these are severely deuterically altered, they contain glimmerite veins with high K, Rb, Ba, Sr and LREE contents (Upton 1991). It is argued that metasomatism, initially through subduction-related processes, progressively changed refractory peridotitic rocks to more fusible compositions. Accordingly a 'chemical memory', encapsulated at *c.* 1800 Ma,

was not accessed until some 500–700 Ma later when triggered during Gardar cratogenesis (Goodenough *et al.* 2002).

The Younger Gardar activity involved great quantities of parental magmas. Whilst all these were enriched, the extreme concentrations of incompatible elements at the Ilímaussaq complex demand involvement of huge volumes of the mantle. It can only be surmised that processes of fractional melting, fluid transport and fractional crystallisation were capable of scavenging and concentrating trace components of the mantle on a very large scale.

Rifting of the Columbia Supercontinent

The cratogenic Gardar tectono-magmatism commenced between 1320 and 1280 Ma. Whilst the Younger Gardar rifting occurred between 1180 and 1140 Ma, the 700 km long Great Abitibi dyke (Canada), dated at 1140 ± 2 Ma (Krogh *et al.* 1987) is approximately colinear with the YGDC in reconstructions of pre-Mesozoic Greenland and Labrador (Macdonald & Upton 1993). Although sharing numerous features with the South Greenland giant dykes, the Great Abitibi dyke has a tholeiitic composition (Ernst & Bell 1992). The ENE–WSW-trending dyke extends south-west towards Lake Superior so that, if it was associated with the YGDC, the total extent would be *c.* 2000 km (Fig. 121). From the Great Lakes south-

eastwards towards Texas, the Mid-Continental rift is traceable a further *c.* 2000 km (Hutchison *et al.* 1990). This rift, underlain by the largest Bouguer anomaly on the craton, was associated with the Keweenawan volcanism. The latter comprises a great volume of tholeiitic continental flood basalts that erupted from *c.* 1109 Ma until *c.* 1086 Ma (Davis & Paces 1990 and references therein). This volcanism has been attributed to adiabatic decompression of an asthenospheric mantle plume (Nicholson & Shirey 1990). Collectively, the Younger Gardar, Great Abitibi and Mid-Continent rift events invite the speculation that each represented a component of rifting with concomitant basaltic magmatism across the Columbia super-continent. Rift propagation towards the south-west over a distance of some 4000 km may have resulted from intermittent lithospheric failure over some 70 Ma. The Gardar activity could represent an early stage in this process.
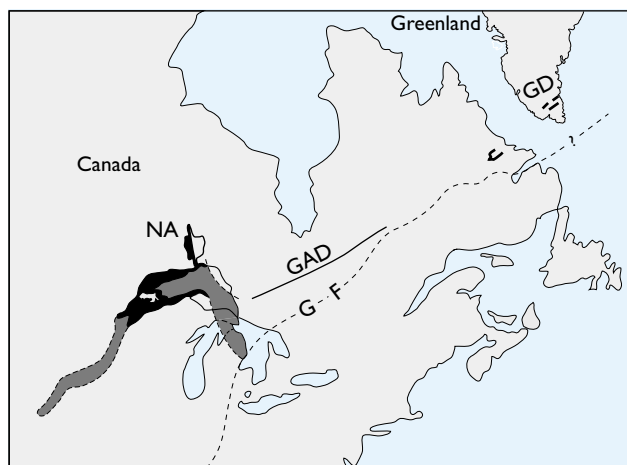
Topography of the younger Gardar southern rift

Probably not more than 4 km of supercrustal cover have been stripped off the southern rift since it was an active volcanic rift zone. With regard to the surface topography we may envisage a stark, barren volcanic landscape within the Columbia Supercontinent that may have resembled the modern terranes of the Danakil depression in Ethiopia and the Reykjanes peninsula in Iceland, with parallel crater-chains, open fissures and normal fault escarpments marking the neovolcanic zone (Fig. 122). Such a landscape is envisaged to have formerly overlain the dyke swarm and associated basement shears of eastern Tuttutooq (cf. Fig. 12). The dykes of the Main and Igaliko swarms, which certainly reached shallow crustal levels, may have erupted relatively low-viscosity salic lavas across the rift, perhaps comparable to the Kenya flood trachytes and phonolites.

Superimposed on this may have lain a chain of central volcanoes extending for some 60 km. The earliest of these, constructed above the Narssaq and South Qôroq complexes, would have been severely degraded by erosion and largely or wholly covered by younger extrusive rocks when the volcanoes over the Tugtutôq, Ilímaussaq and Igdlerfigssalik complexes were active. Possibly the Tugtutôq central complex volcano and Ilímaussaq were roughly coeval. The suggestion of an Ilímaussaq volcano is contentious because there is consensus on the closed

Fig. 121. Map of the Great Abitibi dyke (**GAD**) and its possible relationship to the Gardar giant dykes (**GD**). Nipigon arm (**NA**) of speculative triple junction. Grenville front (**GF**). Mid-continent rift and known extent of the Keweenawan lavas indicated by grey ornamentation. Modified from Ernst & Bell (1992).

Fig. 122. Lava fields of the western neovolcanic zone in south-west Iceland. Normal faults are prominent to the left. Linear features to the right include crater chains and hyaloclastite ridges. The Hengill central volcano is prominent in the far centre behind the steam columns from geothermal wells. Photo by Hjalti Franzson.

nature of the agpaitic magma chamber. The magma chamber rose high in the Eriksfjord Formation but there are no data for what might have lain above it, and it is conceivable that Ilímaussaq crystallised within its own volcanic carapace. The relationship between sinistral faulting and dyke intrusion, together with the U-Pb dating, suggests that Ilímaussaq pre-dated the late stage Igdlerfigssalik volcano.

Large linear volcanic systems such as Boina and Erta Ale in Ethiopia (Barberi *et al*. 1970; Barberi & Varet 1970) and the Harat Khabar within the Makkah-Madinah-Nafud volcanic lineament of western Saudi Arabia (Camp *et al*. 1989) could serve as approximate models for the southern rift. Erta Ale comprises an elliptical structure *c*. 100 km long and 20–30 km broad in a region of rapid crustal extension along the median axis of the Danakil depression (Fig. 123). It displays evolution from simple fissural eruptions to complex central volcanoes with a generalised volumetric decrease in time from early transitional basalts through Fe-rich intermediate compositions

to highly differentiated products (trachytes and comendites). Where silicic lavas were erupted as lava flows, the fissures are close to the central volcanoes. Some of the trachytes of Erta Ale appear to have had high fluidity (Barberi *et al*. 1970), much as is deduced for the Gardar trachyte magmas.

An evolution comparable to these Ethiopian examples occurs in Saudi Arabia in the Makkah-Madina-Nafud volcanic lineament. This extends for *c*. 600 km and has a sequence of vents that started with extensive extrusion of transitional olivine basalt that gave way to less voluminous flows including hawaiite, mugearite, benmoreite and trachyte. In the central vent area of Harrat Khaybar, the latest eruptions were of comendite (Camp *et al*. 1989). It was suggested that primary mantle melts accumulated and evolved close to the crust–mantle boundary to the stage when they were copiously erupted along the whole volcanic lineament. In at least one case, some magma batches inferred to have been arrested in crustal
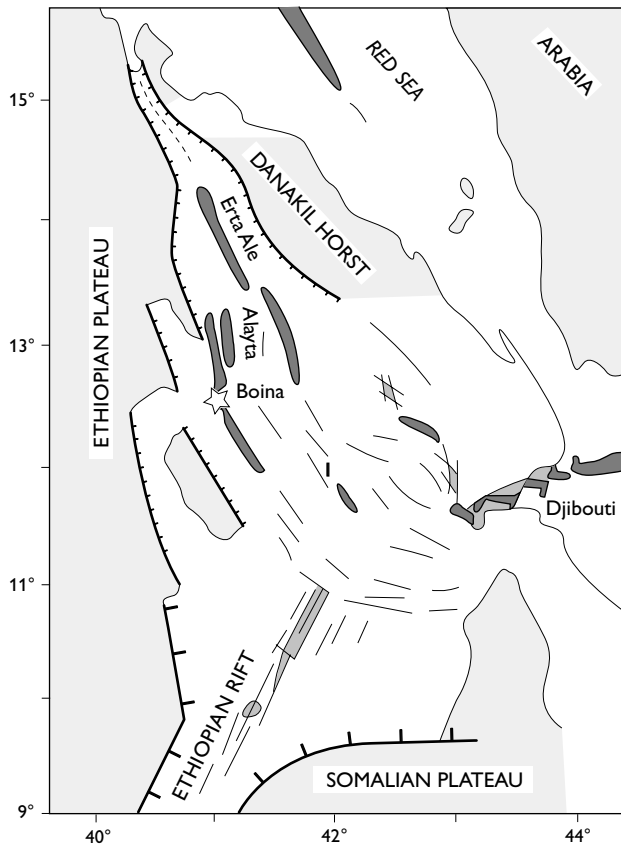
Fig. 123. Sketch map showing parts of Ethiopia, the southern Red Sea and Saudi Arabia showing trends of rift faulting, spreading centres and the linear volcanic systems of Boina and Erta Ale. Modified from Barberi *et al.* (1970).

reservoirs evolved further, resulting in comenditic residua (Camp *et al.* 1989).

Many parallels may be drawn between the rift magmatism of these Cenozoic instances and that envisaged for the younger Gardar southern rift. If fissure eruptions accompanied the emplacement of the Younger giant dyke and Main dyke swarm, an extrusive carapace may have accreted above the Tugtutôq complex, with progressively diminishing volumes of increasingly evolved lava over time in a manner comparable to these modern examples. If, as suggested, the Tugtutôq complex underlay a rift-axial volcano, this is likely to have had a superstructure of quartz trachyte and alkali rhyolite extrusives. The ring dykes of the Igdlerfigssalik complex and the central complex of Tugtutôq suggest that any overlying volcanoes bore calderas. There is close petrological affinity between the intrusions of the southern rift and those of the Kenya rift (Macdonald & Upton 1993). Kenyan volcanoes that might serve as models include e.g. Kilombe, Suswa and Longonot (Fig. 124).

Fig. 124. Longonot volcano, Kenya – a possible modern analogue for the late Gardar volcanoes postulated for the South Qôroq, Igdlerfigssalik and Tugtutôq complexes. The volcano rises *c.* 1000 m above the surrounding plains to a summit at 2776 m.

Summary

Younger Gardar (1180–1140 Ma) magmatic activity was principally manifested in two rift zones developed across the Columbia Supercontinent, viz. the northern (Nunarsuit–Isortoq) and the southern (Tuttutooq–Il-immaasaq–Narsarsuaq) rifts, in response to lithospheric extension. The tectono-magmatic evolution of the southern rift zone has been examined here. Uplift and erosion of a few kilometres of cover have revealed a sequence of intrusions ranging from gabbros to highly evolved alkali granites and peralkaline nepheline syenites including ag-paites. Many of these intrusions are considered to have been related to surface volcanism. The model presented invokes transtensional movements occurring in conjunction with lithospheric attenuation and ascent of a narrow wedge of asthenospheric mantle. Adiabatic melting of metasomatically modified lithospheric mantle within the rift zone is inferred as explanation for the unusual composition of the parental basaltic magmas. These had high Al/Ca ratios leading to crystallisation of troctolitic gabbros and anorthosites.

The intrusions may conveniently be considered under three headings, namely giant dykes, dykes and stocks and ring dykes of central complexes. The intrusions in each of these categories are remarkable, if not for their size, shape or extent, then for many of the exceptional rock types that compose them, and unique in the case of Ilímaussaq. Giant dykes 200–800 m broad and smaller dykes <50 m broad dominated the early stages of the magmatic evolution, whilst central complexes characterised the later stages. The giant dykes and central complexes are largely composed of coarse-grained cumulates; the smaller dykes provide valuable petrographic and compositional data on magma types.

Lithospheric rupturing and emplacement of the Older giant dyke complex (OGDC) marked the onset of activity. This intrusion comprises a near-complete spectrum of rock types from alkali gabbro via ferro-syenogabbros to syenites and peralkaline foyaites. After a time lapse of some tens of millions of years, a second and greater rift-axial rupturing event occurred, accompanied by intrusion of transitional basalt magma, to form the Younger giant dyke complex (YGDC). This is considered to have arisen from a much more voluminous body of mafic magma most of which was retained in an underplated parental chamber near the Moho. It is inferred to have resulted from a larger mantle melt fraction than that which had previously given rise to the OGDC and to have marked the acme of energy release and magma genesis related to the southern rift system. The YGDC fed an overlying lopolith at the unconformity between the Palaeoproterozoic granites and the early Gardar supracrustal strata. Only relics of this now remain. Layered cumulate pods developed along the c. 145 km length of the YGDC may denote sites where vigorous convection was established. Whilst most of the YGDC is composed of troctolite, differentiated products include peridotite, ferro-syenogabbro, syenite and both foyaite and quartz syenite to alkali granite. The closely related gabbroic to syenitic Klokken complex to the south-east of the YGDC may be coeval and comagmatic with the YGDC.

Following the YGDC event, extensional energy was slowly dissipated, with intrusion of two remarkable dyke swarms. With time these show a tendency to diminish in width (and volume?) whilst increasing in degree of differentiation. Dykes of the rift-axial Main swarm are dominantly of hawaiite leading to trachyte and comendite. So-called big feldspar dykes (BFDs) are important early components of the swarm and provide evidence of a deep crustal, compositionally stratified parental chamber in which hawaiitic magma became serially overlain by magma with compositions leading to quarz trachyte and comendite. The subsidiary Igaliko dyke swarm, occurring to the south and east of the Main dyke swarm, may have originated from smaller melt fractions of the mantle source. In this swarm phonolitic dykes are dominant amongst the salic members.

Anorthosite xenoliths in the troctolitic gabbros of the YGDC and Klokken, in the doleritic component of the BFDs, and elsewhere in the Gardar Province, indicate the presence of a large anorthositic body at depth. This body is considered to be cogenetic with the Gardar alkaline magmas. The salic magmas of the province, including those of the southern rift magmatic system, are inferred to have been generated in a lower crustal chamber beneath a capping of anorthosite flotation cumulate. Despite many features in common with the North American mid-Proterozoic anorthosites, the Gardar troctolites and anorthosites differ in being more potassic. In consequence, residual magmas followed alkaline lines of liquid descent.

Decline of fissuring and concomitant dyke intrusion coincided with rejuvenation of transcurrent (transform?)

fault systems oriented transverse to the rift. These, spaced *c*. 20–30 km apart, segment the rift zone with a total left-lateral offset of >18 km. Weak spots provided by intersection of the faults and the rift axis offered potential access routes for magmas rising from the lower crust to shallow levels. These magmas are inferred to have arisen from the salic upper portions (grown, through maturation with time) of the stratified chambers mentioned above in relation to the BFDs. The iron-rich, ferro-mugearitic magmas, inferentially generated at depth by massive plagioclase fractionation from relatively reduced melts, rarely, if ever, reached the shallow crust because of their high density. As the Fe content of the magmas decreased through titanomagnetite fractionation, the benmoreite residues attained densities low enough for them to ascend by overhead stoping.

Benmoreitic magmas were the earliest to intrude at the Ilímaussaq, Tugtutôq and Igdlerfigssalik complexes and were important in supplying dykes of the Main swarm. The crustal weaknesses at the rift and fault intersections localised four of the central complexes of the southern rift. The two earliest of these, the Narssaq and South Qôroq complexes, were built up by successive magma batches ascending while the left-lateral faulting was still active. The Narssaq complex consists of quartz syenite and alkali granite; the South Qôroq complex consists of silica-undersaturated products. Since each intrusion at the South Qôroq complex was of increasingly primitive magma, it provides confirmation for the presence of the compositionally stratified chamber inferred from the BFD evidence. As crustal equilibration took place following the slow demise of both fissuring and transcurrent faulting, late magma batches exploited the fault-controlled conduits to form the Ilímaussaq and Igdlerfigssalik complexes. Location of the nearly contemporaneous Tugtutôq central complex may have been dictated by the proximity of the Older and Younger giant dykes.

Whereas magma evolution primarily occurred along silica-undersaturated lines of descent there was exception to this in the central sector of the southern rift where benmoreite/trachyte residues evolved towards silica-oversaturated products. For a distance of *c*. 30 km, quartz syenites and alkali granites predominate in the Tugtutôq central complex, the Asorutit sector of the YGDC, the Narssaq complex and the Main dyke swarm. The occurrence of silica-oversaturated salic dykes beyond this sector is explicable by their lateral propagation. These more siliceous magmas probably originated from crustal contamination of their more mafic forerunners, brought about through further heating of the crust by hot fluids arising from the underlying mantle or by crystallisation of the underplated basaltic magma. Despite the plethora of disparate and apparently unrelated rock types within the rift, a simple unitary genetic system is discernible, involving a bunch of closely related liquid lines of descent.

The only magma types unrelated to this principal theme are those of the mela-aillikite–carbonatite association. It is suggested that these aberrant magmas resulted from rheomorphism of fusible masses of metasomites rich in diopside-phlogopite-apatite-calcite in the lithospheric mantle.

The postulate of a mainly lithospheric mantle origin for all the Gardar magmas is made to account for the close similarities between the Older and Younger Gardar magmas. In view of the age difference of more than 100 Ma between them, this precludes a purely asthenospheric origin.

Although the world shows examples of a great many linear magmatic systems, the younger Gardar southern rift system is unique with regard to its exposures, degree of preservation, layering features, and extreme and well-documented compositional variations.

References

Allaart, J.H. 1969: The chronology and petrography of the Gardar dykes between Igaliko Fjord and Redekammen, South Greenland. Rapport Grønlands Geologiske Undersøgelse **25**, 26 pp.

Andersen, S., Bohse, H. & Steenfelt, A. 1981a: A geological section through the southern part of the Ilímaussaq intrusion. Rapport Grønlands Geologiske Undersøgelse **103**, 39–42.

Andersen, S., Bailey, J.C. & Bohse, H. 1981b: Zr-Y-U stratigraphy of the kakortokite-lujavrite-sequence, southern Ilímaussaq intrusion. Rapport Grønlands Geologiske Undersøgelse **103**, 69–76.

Andersen, S., Bohse, H. & Steenfelt, A. 1988: The southern part of the Ilímaussaq complex, South Greenland 1: 20 000. Copenhagen: Geological Survey of Greenland.

Andersen, T. 1997: Age and petrogenesis of the Qassiarsuk carbonatite-alkaline silicate volcanic complex in the Gardar rift, South Greenland. Mineralogical Magazine **61**, 499–513.

Andersen, T. 2008: Coexisting silicate and carbonatitic magmas in the Qassiarsuk complex, Gardar Rift, Southwest Greenland. Canadian Mineralogist **46**, 933–950.

Andersen, T. & Sørensen, H. 2005: Stability of naujakasite in hyperagpaitic melts and the petrology of naujakasite lujavrite in the Ilímaussaq alkaline complex, South Greenland. Mineralogical Magazine **69**, 125–136.

Ashwal, L.D. 1993: Anorthosites, 422 pp. Berlin: Springer-Verlag.

Bailey, D.K. & Schairer, J.F. 1964: Feldspar-liquid equilibria in peralkaline liquids – the orthoclase effect. American Journal of Science **262**, 1198–1208.

Bailey, J.C. 1995: Cryptorhythmic and macrorhythmic layering in aegirine lujavrite, Ilímaussaq alkaline intrusion, South Greenland. Bulletin of the Geological Society of Denmark **42**, 1–16.

Bailey, J.C. 2006: Geochemistry of boron in the Ilímaussaq alkaline complex, South Greenland. Lithos **91**, 319–330.

Bailey, J.C. & Gwodz, R. 1994: Li distribution in aegirine lujavrite, Ilímaussaq alkaline intrusion, South Greenland: role of cumulus and post-cumulus processes. Lithos **31**, 207–225.

Bailey, J.C., Rose-Hansen, J., Løvborg, L. & Sørensen, H. 1981a: Evolution of Th and U whole-rock contents in the Ilímaussaq intrusion. In: Bailey, J.C., Larsen, L.M. & Sørensen, H. (eds): The Ilímaussaq intrusion, South Greenland. A progress report on geology, mineralogy, geochemistry and economic geology. Rapport Grønlands Geologiske Undersøgelse **103**, 87–98.

Bailey, J.C., Bohse, H. & Demina, A. 1981b: Extension of Zr-REE-Nb resource at Kangerdluarssuk, Ilímaussaq intrusion. In: Bailey, J.C., Larsen, L.M. & Sørensen, H. (eds): The Ilímaussaq intrusion, South Greenland. A progress report on geology, mineralogy, geochemistry and economic geology. Rapport Grønlands Geologiske Undersøgelse **103**, 63–67.

Bailey, J.C., Gwordz, R., Rose-Hansen, J. & Sørensen, H. 2001: Geochemical overview of the Ilímaussaq complex, South Greenland. In: Sørensen, H. (ed.): The Ilímaussaq alkaline complex, South Greenland: status of mineralogical research with new results. Geology of Greenland Survey Bulletin **190**, 35–53.

Bailey, J.C., Sørensen, H., Andersen, T., Kogarko, L.N. & Rose-Hansen, J. 2006: On the origin of microrhythmic layering in arfvedsonite lujavrite from the Ilímaussaq alkaline complex, South Greenland. Lithos **91**, 301–308.

Barberi, F. & Varet, J. 1970: The Erta Ale volcanic range (Danakil Depression, northern Afar, Ethiopia). Bulletin of Volcanology **34**, 848–917.

Barberi, F., Borsi, S., Ferrara, G., Marinelli, G. & Varet, J. 1970: Relations between tectonics and magmatology in the northern Danakil Depression (Ethiopia). Philosophical Transactions of the Royal Society of London **A267**, 293–311.

Bédard, J.H. 2001: Parental magmas of the Nain Plutonic Suite anorthosites and mafic cumulates: a trace element modelling approach. Contributions to Mineralogy and Petrology **141**, 747–771.

Berg, J.H. 1980: Snowflake troctolite in the Hetasch Intrusion, Labrador: evidence for magma-mixing and supercooling in a plutonic environment. Contributions to Mineralogy and Petrology **72**, 339–351.

Berthelsen, A. & Noe-Nygaard, A. 1965: The Precambrian of Greenland. In: Rankama, K. (ed.): The Precambrian **2**, 113–262. New York: Interscience Publishers.

Berthelsen, A. & Henriksen, N. 1975: Geological map of Greenland, 1:100 000, Ivigtut 61 V.1 Syd. Descriptive text, 169 pp., 8 plates. Copenhagen: Geological Survey of Greenland. (Also Meddelelser om Grønland **186,** 169 pp.)

Blaxland, A.B. & Parsons, I. 1975: Age and origin of the Klokken gabbro-syenite intrusion, South Greenland: Rb-Sr study. Bulletin of the Geological Society of Denmark **24**, 27–32.

Blaxland, A.B. & Upton, B.G.J. 1978: Rare-earth distribution in the Tugtutôq younger giant dyke complex: evidence bearing on alkaline magma genesis in South Greenland. Lithos **11**, 288–299.

Blaxland, A.B., van Breemen O., Emeleus, C.H. & Anderson, J.G. 1978: Age and origin of the major syenite centers in the Gardar Province of South Greenland: Rb-Sr studies. Geological Society of America Bulletin **89**, 231–244.

Blundell, D.J. 1978: A gravity survey across the Gardar Igneous Province, SW Greenland. Journal of the Geological Society (London) **135**, 545–554.

Bøggild, O.B. & Winther, C. 1899: On some minerals from the nepheline syenite at Julianehaab, Greenland (epistolite, britholite, schizolite and steenstrupine) collected by G. Flink. Meddelelser om Grønland **24**, 181–213.

Bohse, H. & Andersen, S. 1981: Review of the stratigraphic divisions of the kakortokite and lujavrite in southern Ilímaussaq. In: Bailey, J.C., Larsen, L.M. & Sørensen, H.: The Ilímaussaq intrusion, South Greenland. A progress report on geology, mineralogy, geochemistry and economic geology. Rapport Grønlands Geologiske Undersøgelse **103**, 53–62.

Bohse, H., Brooks, C.K. & Kunzendorf, H. 1971: Field observations on the kakortokites of the Ilímaussaq intrusion, South Greenland,

including mapping and analyses by portable X-ray fluorescence equipment for zirconium and niobium. Rapport Grønlands Geologiske Undersøgelse **38**, 43 pp.

Bohse, H., Rose-Hansen, J., Sørensen, H., Steenfelt, A., Løvborg, L. & Kunzendorf, H. 1974: On the behaviour of uranium during crystallization of magmas – with special emphasis on alkaline magmas, 49–60. In: Formation of uranium ore deposits, 748 pp. Proceedings of a symposium in Athens, Greece, 6–10 May 1974. Organiser: International Atomic Energy Agency, Vienna.

Bondam, J. 1955: Petrography of a group of alkali-trachyte dykes from the Julianehaab district, South Greenland. Meddelelser om Grønland **135**(2), 1–31.

Bowen, N.L. 1928: The evolution of the igneous rocks, 334 pp. Princeton: Princeton University Press.

Bridgwater, D. 1967: Feldspathic inclusions in the Gardar igneous rocks and their relevance to the formation of major anorthosites in the Canadian shield. Canadian Journal of Earth Sciences **4**, 995–1014.

Bridgwater, D. & Coe, K. 1970: The role of stoping in the emplacement of the giant dykes of Isortoq, South Greenland. Geological Journal Special Issue **2**, 67–78.

Bridgwater, D. & Harry, W.T. 1968: Anorthosite xenoliths and plagioclase megacrysts in Precambrian intrusions of South Greenland. Bulletin Grønlands Geologiske Undersøgelse **77**, 243 pp., 6 plates (also Meddelelser om Grønland **185**).

Brown, W.L., Becker, S.M. & Parsons, I. 1983: Cryptoperthites and cooling rate in a layered syenite pluton: a chemical and TEM study. Contributions to Mineralogy and Petrology **82**, 13–25.

Buchan, K.L., Ernst, R.E., Hamilton, M.A., Mertanen, S., Pesonen, L.J. & Elming, S-A. 2001: Rodinia: the evidence from integrated palaeomagnetism and U-Pb geochronology. Precambrian Research **110**, 9–32.

Camp, V.E., Roobol, M.J. & Hooper, P.R. 1989: Intraplate alkaline volcanism and magmatic processes along the 600 km Makkah–Madinah–Nafud volcanic line, western Saudi Arabia. General Assembly on Continental Magmatism Abstracts **39**, 39 only. Santa Fe, New Mexico: International Association of Volcanology and Chemistry of the Earth's Interior (IAVCEI)

Chadwick, B. & Garde, A.A. 1996: Palaeoproterozoic oblique plate convergence in South Greenland: a reappraisal of the Ketilidian orogen. In: Brewer, T.S. & Atkin, B.P. (eds): Precambrian crustal evolution in the North Atlantic region. Geological Society Special Publication (London) **112**, 179–196.

Charlier, B., Duchesne, J.-C., Auwera, J.V., Storme, J.-Y., Maquil, R. & Longhi, J. 2010: Polybaric fractional crystallisation of high-alumina basalt parental magmas in the Egersund–Ogna massif-type anorthosite (Rogaland, SW Norway) constrained by plagioclase and high-alumina orthopyroxene megacrysts. Journal of Petrology **51**, 2515–2546.

Chase, C.G. & Gilmer, T.H. 1973: Precambrian plate tectonics: the mid-continent gravity high. Earth and Planetary Science Letters **21,** 70–78.

Coombs, D.S.1963: Trends and affinities of basaltic magmas and pyroxenes as illustrated on the diopside-olivine-silica diagram. Mineralogical Society of America Special Paper **1**, 227–250.

Coulson, I.M., Goodenough, K.M., Pearce, N.J.G. & Leng, M.J. 2003: Carbonatites and lamprophyres of the Gardar Province – a 'window' to the sub-Gardar mantle? Mineralogical Magazine **67**, 855–872.

Craven, J.A. 1985: The petrogenesis of some ultramafic rocks from the Gardar Province, S.W. Greenland. Unpublished PhD thesis, University of Edinburgh, UK.

Dahl-Jensen, T., Thybo, H., Hopper, J., and Rosing, M. 1998. Crustal structure at the SE Greenland margin from wide-angle and normal incidence seismic data. Tectonophysics, **288**: 191–198.

Davis, D.W. & Paces, J.B. 1990: Time resolution of geologic events on the Keweenaw Peninsula and implications for development of the Midcontinent Rift system. Earth and Planetary Science Letters **97**, 54–64.

Duchesne, J.C., Liégois, J.P., Auwera, J.V. & Longhi, J. 1999: The crustal tongue melting model and the origin of massive anorthosites. Terra Nova **11**, 100–105.

Emeleus, C.H. 1964: The Grønnedal–Ika alkaline complex, South Greenland. Bulletin Grønlands Geologiske Undersøgelse **45**, 75 pp. (also Meddelelser om Grønland **172**(3).

Emeleus, C.H. & Harry, W.T. 1970: The Igaliko nepheline syenite complex. General description. Bulletin Grønlands Geologiske Undersøgelse **85**, 115 pp., 4 plates (also Meddelelser om Grønland **186**).

Emeleus C.H. & Stephenson, D. 1970: Field-work between Tunugdliarfik and Tasiussaq. Rapport Grønlands Geologiske Undersøgelse **28**, 30–32.

Emeleus, C.J. & Upton, B.G.J. 1976: The Gardar period in southern Greenland. In: Escher, A. & Watt, W.S. (eds): Geology of Greenland, 152–181. Copenhagen: Geological Survey of Greenland.

Emslie, R.F. 1965: The Michikamau anorthositic intrusion, Labrador. Canadian Journal of Earth Science **2**, 385–390.

Emslie, R.F. 1970: The geology of the Michikamau Intrusion, Labrador (131,231). Geological Survey of Canada Paper **68-57**, 85 pp.

Emslie, R.F. 1977: Anorthosite massifs, Rapakivi granites, and late Proterozoic rifting in North America. Precambrian Research **7,** 61–98.

Engell, J. 1973: A closed system crystal fractionation model for the agpaitic Ilímaussaq intrusion, South Greenland, with special reference to the lujavrites. Bulletin of the Geological Society of Denmark **22**, 334–362.

Engell J. & Pedersen, S. 1974: Rubidium-strontium whole-rock isochron age determination from the Bangs Havn intrusion, South Greenland. Bulletin of the Geological Society of Denmark **23**, 130–133.

Engell, J., Hansen, J., Jensen, M., Kunzendorf, H. & Lovberg, L. 1971: Beryllium mineralization in the Ilímaussaq intrusion, South Greenland, with description of a field beryllometer and chemical methods. Rapport Grønlands Geologiske Undersøgelse **33**, 40 pp.

Ernst, R.E. & Bell, K. 1992: Petrology of the Great Abitibi Dyke, Superior Province, Canada. Journal of Petrology **33**, 423–469.

Fairhead, J.D. 1976: The structure of the lithosphere beneath the Eastern Rift, East Africa, deduced from gravity studies. Tectonophysics **30**, 269–298.

Fenner, C.N. 1937: The crystallisation of basalts. American Journal of

Science **18**, 225–253.

Ferguson, J. 1964: Geology of the Ilímaussaq alkaline intrusion, South Greenland: description of map and structure. Meddelelser om Grønland **172**(4), 1–82.

Ferguson, J. 1970a: The significance of the kakortokite in the evolution of the Ilímaussaq intrusion, South Greenland. Meddelelser om Grønland **190**(1), 193 pp.

Ferguson, J. 1970b: The differentiation of agpaitic magmas: the Ilímaussaq intrusion, South Greenland. Canadian Mineralogist **10**, 335–349.

Ferguson, J. 1970c: On the schistose structures of some lujavrites. Bulletin of the Geological Society of Denmark **20**, 67–68.

Ferguson, J. & Pulvertaft, T.C.R. 1963: Contrasted styles of igneous layering in the Gardar Province of South Greenland. Mineralogical Society of America Special Publication **1**, 10–21.

Finch, A.A. 1995: Metasomatic overprinting by juvenile igneous fluids, Igdlerfigsalik, South Greenland. Contributions to Mineralogy and Petrology **122**, 11–24.

Finch, A.A. & Walker, F.D.L. 1991: Cathodoluminescence and microporosity in alkali feldspars from the Blå Måne Sø perthosite, South Greenland. Mineralogical Magazine **55**, 583–589.

Finch, A.A., Mansfield, J. & Andersen, T. 2001a: U-Pb radiometric age of Nunarssuit pegmatite, Greenland: constraints on the timing of Gardar magmatism. Bulletin of the Geological Society of Denmark **48**, 1–7.

Finch, A., Goodenough, K., Salmon, H.M. & Andersen, T. 2001b: The petrology and petrogenesis of the North Motzfeldt Centre, Gardar Province, South Greenland. Mineralogical Magazine **65**, 759–774.

Flink, G. 1901: On the minerals from Narsarsuk on the Firth of Tunugdliarfik in southern Greenland, Meddelelser om Grønland **24**(1), 213 pp.

Foland, K.A., Landoll, J.D., Henerson, C.M.B. & Joanfeng, C. 1993: Formation of cogenetic quartz and nepheline syenites. Geochimica et Cosmochimica Acta **57**, 697–704.

Forsberg, R. & Rasmussen, K.L. 1978: Gravity and rock densities in the Ilímaussaq area, South Greenland. Rapport Grønlands Geologiske Undersøgelse **90**, 81–84.

Galimov, E.M. & Petersilie, L.A. 1968: Carbon isotope composition of bitumens from igneous and metamorphic rocks. Doklady Akademii Nauk USSR **182**, 186–189.

Garde, A.A., Hamilton, M.A., Chadwick, B., Grocott, J. & McCaffrey, K.J.W. 2002: The Ketilidian orogen of South Greenland: geochronology, tectonics, magmatism and fore-arc accretion during Palaeoproterozoic oblique convergence. Canadian Journal of Earth Sciences **39**, 765–793.

Gerasimovsky, V.L. & Kuznetsova, S.Ya. 1967: On the petrochemistry of the Ilimaussaq intrusion, South Greenland. Geokimiya **1967**(3), 274–283 (in Russian). (Translation: Geochemistry International **4**, 236–246.)

Giesecke, K.L. 1910: Mineralogisch Reisejournal über Grönland 1806–1813. 2te Vollständige Ausgabe. Meddelelser om Grønland **35**, 478 pp.

Gleissner, P., Druppel, K. & Taubald, H. 2010: Magmatic evolution of anorthosites of the Kunene intrusive complex, NW Namibia.

Evidence from oxygen isotope data and trace element zoning. Journal of Petrology **51**, 897–919.

Goodenough, K.M., Upton, B.G.J. & Ellam, R.M. 2002: Long-term memory of subduction processes in the lithospheric mantle. Evidence from the geochemistry of basic dykes in the Gardar Province of South Greenland. Journal of the Geological Society (London) **159**, 1–10.

Gordon, S.G. 1924: Minerals obtained in Greenland on the Second Vaux-Academy Expedition, 1923. Proceedings of the Academy of Natural Science, Philadelphia **76**, 249–268.

Green, J.C. 1992: Proterozoic rifts. In: Condie, K.C. (ed.): Proterozoic crustal evolution. Developments in Precambrian Geology **10**, 97–149.

Halama, R., Waight, T. & Markl, G. 2002: Geochemical and isotopic zoning patterns of plagioclase megacrysts in gabbroic dykes from the Gardar Province, South Greenland: implications for crystallisation processes in anorthositic magmas. Contributions to Mineralogy and Petrology **144**, 109–127.

Halama, R., Marks, M., Brügmann, G., Siebel, W., Wenzel, T. & Markl, G. 2004: Crustal contamination of mafic magmas: evidence from a petrological and Sr-Nd-Os-O isotopic study of the Proterozoic Isortoq dike swarm, South Greenland. Lithos **74**, 199–232.

Hamilton, E.I. 1964: The geochemistry of the northern part of the Ilímaussaq intrusion, S.W. Greenland. Bulletin Grønlands Geologiske Undersøgelse **42**, 104 pp. (also Meddelelser om Grønland **162**(10)).

Hardarson, B.S. & Fitton, J.G. 1991: Increased mantle melting beneath Snaefellsjökull volcano during Late Pleistocene deglaciation. Nature **353**, 61–64.

Harper, C.L. 1988: On the nature of time in cosmological perspective. Unpublished PhD thesis, University of Oxford.

Harry, W.T. & Pulvertaft, T.C.R. 1963: The Nunarssuit intrusive complex, South Greenland **1**: General description. Bulletin Grønlands Geologiske Undersøgelse **36**, 136 pp., 3 plates (also Meddelelser om Grønland **162**(9).

Henriksen, N. 1960: Structural analysis of a fault in South-West Greenland. Bulletin Grønlands Geologiske Undersøgelse **26**, 40 pp. (also Meddelelser om Grønland **162**(9).

Herzberg, C. 1995: Generation of plume magmas through time; an experimental perspective. Chemical Geology **126**, 1–16.

Higgins, A.K. 1970: The stratigraphy and structure of Ketilidian rocks of Midternæs, South-West Greenland. Bulletin Grønlands Geologiske Undersøgelse **87**, 96 pp. (also Meddelelser om Grønland **189**(2).

Humphreys, M.C.S. & Holness, M.B. 2010: Melt-rich segregations in the Skaergaard Marginal Border Series: tearing of a vertical silicate mush. Lithos **119**, 181–192.

Hutchison, D.R., White, R.S., Connon, W. F. & Schulze, K.J. 1990: Keweenaw hot-spot: geophysical evidence for a 1.1 Ga mantle plume beneath the Midcontinent Rift System. Journal of Geophysical Research **95**, 10869–10884.

Irvine, T.N. 1987: Glossary of terms for layered intrusions. In: Parsons I. (ed.): Origins of igneous layering, 641–647. Dordrecht: D. Reidel, Dordrecht.

Irvine, T.N. & Baragar, W.R.A. 1972: The Muskox Intrusion and

Coppermine River lavas, Northwest Territories, Canada. 24th International Geological Congress, Montreal. Field Excursion **A 29**, Guidebook, 70 pp.

Jones, A.P. & Larsen, L.M. 1985: Geochemistry and REE minerals of nepheline syenites from the Motzfeldt Centre, South Greenland. American Mineralogist **70**, 1087–1100.

Kalsbeek, F. & Taylor, P.N. 1985. Isotopic and chemical variation in granites across a Proterozoic continental margin - the Ketilidian mobile belt of South Greenland. Earth and Planetary Science Letters, **73**: 65–80.

Karup-Møller, S. 1978: The ore minerals of the Ilímaussaq intrusion: their mode of occurrence and their conditions of formation. Bulletin Grønlands Geologiske Undersøgelse **127**, 51 pp.

Khomyakov, A.P., Sørensen, H., Petersen, O.V. & Bailey, J.C. 2001: Naujakasite from the Ilímaussaq alkaline complex, South Greenland, and the Lovozero alkaline complex, Kola Peninsula, Russia: a comparison. In: Sørensen, H. (ed.): The Ilímaussaq alkaline complex, South Greenland: status of mineralogical research with new results. Geology of Greenland Survey Bulletin **190**, 95–108.

Klein-BenDavid, O., Logvinova, A.M., Schrauder, M., Spetius, Z.V., Weiss, Y., Hauri, E.H., Kaminsky, F.V., Sobolev, N.V. & Navon, O. 2009: High-Mg carbonatitic microinclusions in some Yakutian diamonds – a new type of diamond-forming fluid. Lithos **112**, 648–659.

Köhler, J., Schönenberger, J., Upton, B.G.J. & Markl, G. 2009: Halogen and trace element geochemistry in the magmatic Gardar Province, South Greenland: evidence for subduction-related mantle metasomatism and fluid exsolution processes from alkaline melts. Lithos **113**, 731–747.

Konnerup-Madsen, J., Larsen, E. & Rose-Hansen, J. 1979: Hydrocarbon-rich fluid inclusions in minerals from the alkaline Ilímaussaq intrusion, South Greenland. Bulletin de Minéralogie **102**, 642–653.

Konnerup-Madsen, J. 2001: A review of the composition and evolution of hydrocarbon gases during solidification of the Ilímaussaq alkaline complex, South Greenland. Geology of Greenland Survey Bulletin **190**, 159–166.

Konnerup-Madsen, J. & Rose-Hansen, J. 1982: Volatiles associated with alkaline igneous rift activity and fluid inclusions: the Ilímaussaq intrusion and the Gardar granite complexes (South Greenland). Chemical Geology **37**, 79–93.

Konnerup-Madsen, J. Kreulen, R. & Rose-Hansen, J. 1988: Stable isotope characteristics of hydrocarbon gases in the alkaline Ilímaussaq intrusion, South Greenland. Bulletin de . Minéralogie, **111**, 567–576.

Krogh, T.E., Corfu, F., Davis, D.W., Dunning, G.R., Heaman, L.M., Kamo, S.L., Machado, N., Greenough, J.D. & Nakamura, E. 1987: Precise U-Pb isotopic ages of diabase dykes and mafic to ultramafic rocks via trace amounts of baddeleyite and zircon. In: Halls, H.C. &. Fahrig, W.F. (eds): North American dyke swarms. Geological Association of Canada Special Paper **34**, 147–152.

Krokström, T. 1936: The Halleförs dyke. Bulletin of the Geological Institute Uppsala **26**, 113–263.

Krumrei, T.V., Villa, I.M., Marks, M.A.W. & Markl, G. 2006: A $^{40}Ar/^{39}Ar$ and U/Pb study of the Ilímaussaq complex, South Greenland: implication for ^{40}K decay constant and for the duration of magmatic activity in a peralkaline complex. Chemical Geology **227**, 258–273.

Krumrei, T.V., Pernicka, E., Kaliwoda, M. & Markl, G. 2007: Volatiles in a peralkaline system: abiogenic hydrocarbons and F-Cl-Br systematics in the naujaite of the Ilímaussaq intrusion, South Greenland. Lithos **95,** 298–314.

Kushiro, I. 1980: Viscosity, density, and structure of silicate melts at high pressures, and their petrological applications. In: Hargreaves, R.B. (ed.): Physics of magmatic processes, 93–120. Princeton, N.J.: Princeton University Press.

Kushiro, I. & Fuji, T. 1977: Flotation of plagioclase in magma at high pressure and its bearing on the origin of anorthosite. Proceedings of the Japanese Academy, Series B **53**, 262–266.

Laier, T. & Nytoft, H.P. 1995: Isotopically heavy hydrocarbon gases and bitumen in the Precambrian Ilímaussaq intrusion. In: Grimalt J.O & Dorronsoro, C. (eds): Organic geochemistry developments and applications to energy, climate, environment and human history. 17th International Meeting on Organic Geochemistry, San Sebastian, 4–8 September 1995, 1109–1111.

Laier, T. & Nytoft, H.P. 2012: Bitumen biomarkers in the Mid-Proterozoic Ilímaussaq intrusion, Southwest Greenland – a challenge to the mantle gas theory. Marine and Petroleum Geology **30**, 50–65.

Larsen, J.G. 1974: Stratigrafi, geokemi og petrologi i den øvre vulkanske del af Eriksfjord Formationen, Gardar-provinsen, Sydgrønland **1**, **2**, 134 pp., 47 pp. Unpublished cand. scient. thesis, Københavns Universitet, Danmark.

Larsen, J.G. 1977: Petrology of the late lavas of the Eriksfjord Formation, Gardar province, South Greenland. Bulletin Grønlands Geologiske Undersøgelse **125**, 31 pp.

Larsen, L.M. 1976: Clinopyroxenes and coexisting mafic minerals from the alkaline Ilímaussaq intrusion, South Greenland. Journal of Petrology **17**, 258–290.

Larsen, L.M. 1977: Aenigmatites from the Ilímaussaq intrusion, South Greenland: chemistry and petrological implications. Lithos **10**, 257–270.

Larsen, L.M. 1979: Distribution of REE and other trace elements between phenocrysts and peralkaline undersaturated magmas, exemplified by rocks from the Gardar igneous province, South Greenland. Lithos **12**, 303–315.

Larsen, L.M. 1981: Chemistry of feldspars in the Ilímaussaq augite syenite with additional data on some other minerals. Rapport Grønlands Geologiske Undersøgelse **103**, 31–38.

Larsen, L.M. 2006: Mesozoic to Palaeogene dyke swarms in West Greenland and their significance for the formation of the Labrador Sea and the Davis Strait. Danmarks og Grønlands Geologiske Undersøgelse Rapport **2006/34**, 69 pp. + appendices.

Larsen, L.M. & Sørensen, H. 1987: The Ilímaussaq intrusion – progressive crystallisation and formation of layering in an agpaitic magma. Geological Society Special Publication (London) **30**, 473–488.

Larsen, L.M. & Steenfelt, A. 1974: Alkali loss and retention in an iron-rich peralkaline phonolite dyke from the Gardar province, South Greenland. Lithos **7**, 81–90.

Latin, D., Norry, M.J. & Tarney, R.J.E. 1993: Magmatism in the

Gregory Rift, East Africa: evidence for melt generation by plume. Journal of Petrology **34**, 1007–1027.

Lindhuber, M. 2011: The igneous layering of the Ilímaussaq alkaline complex, Greenland. Unpublished Diplomarbeit, Eberhard Karls University, Tübingen, Germany.

McCreath, J.A., Finch, A.A., Simonsen, S.L., Donaldson, C.H. & Armour-Brown, A. 2012: Independent ages of magmatic and hydrothermal activity in alkaline igneous rocks: the Motzfeldt Centre, Gardar Province, South Greenland. Contributions to Mineralogy and Petrology **163**, 967–982.

Macdonald, R. 1969: The petrology of alkaline dykes from the Tugtutoq area, South Greenland. Bulletin of the Geological Society of Denmark **19**, 257–282 (also Grønlands Geologiske Undersøgelse Miscellaneous Papers **72**).

Macdonald, R. 1970: Mid-Gardar feldspathoidal dykes in the Tugtutoq region, South Greenland. Bulletin of the Geological Society of Denmark **20**, 64–66.

Macdonald, R. 2003: Magmatism of the Kenya Rift Valley: a review. Transactions of the Royal Society of Edinburgh: Earth Sciences **93**, 239–253.

Macdonald, R. & Edge, R.A. 1970: Trace element distribution in alkaline dykes from the Tugtutoq region, South Greenland. Bulletin of the Geological Society of Denmark **20**, 38–58.

Macdonald, R. & Parker, A. 1970: Zirconium in alkaline dykes from the Tugtutoq region, South Greenland. Bulletin of the Geological Society of Denmark **20**, 59–63.

Macdonald, R. & Smith, R.L. 1988: Relationships between silicic plutonism and volcanism: geochemical evidence. Transactions of the Royal Society of Edinburgh, Earth Science **79**, 257–263.

Macdonald, R. & Upton, B.G.J. 1993: The Proterozoic Gardar rift zone, South Greenland: comparisons with the East African Rift System. Geological Society Special Publication (London) **76**, 427–442.

Macdonald, R., Bagiński, B., Upton, B.G.J., Dzierzanowski, P. & Marshall-Roberts, W. 2009: The Palaeogene Eskdalemuir dyke, Scotland: long distance lateral travel of rhyolitic magma is a mixed-magma intrusion. Mineralogical Magazine **73**, 285–300.

Macdonald, R., Bagiński, B., Upton, B.G.J., Pinkerton, H., McInnes, D.A. & MacGilivray, J.C. 2010: The Mull Palaeogene dyke swarm: insights into the evolution of the Mull igneous centre and dyke emplacement mechanisms. Mineralogical Magazine **74**, 601–622.

Markl, G., Marks, M., Schwinn, G. & Sommer, H. 2001: Phase equilibrium constraints on intensive crystallisation parameters of the Ilímaussaq Complex, South Greenland. Journal of Petrology **42**, 2231–2258.

Marks, M. & Markl, G. 2001: Fractionation and assimilation processes in the alkaline augite syenite unit of the Ilímaussaq Intrusion, South Greenland, as deduced from phase equilibria. Journal of Petrology **42,** 1947–1969.

Marks, M. & Markl, G. 2003: Ilímaussaq 'en miniature'; closed-system fractionation in an agpaitic dyke rock from the Gardar Province, South Greenland (contribution to the mineralogy of Ilímaussaq number 117). Mineralogical Magazine **67**, 893–919.

Marks M.A.W. and Markl G. in press: The Ilímaussaq alkaline complex, South Greenland. In: Charlier B., Namur O., Latypov R., Teg-

ner C. (eds), Layered Intrusions, Springer, Dordrecht.

Marks, M., Vennemann, T., Siebel, W. & Markl, G. 2003: Quantification of magmatic and hydrothermal processes in a peralkaline syenite-alkali granite complex based on textures, phase-equilibria,and stable and radiogenic isotopes. Journal of Petrology **44**, 1247–1280.

Marks, M., Vennemann, T., Siebel, W. & Markl, G. 2004: Nd-, O-, and H-isotopic evidence for complex, closed-system fluid evolution of the peralkaline Ilímaussaq intrusion, South Greenland. Geochimica et Cosmochimica Acta **68**, 3379–3395.

Marks, M., Rudnick, R., McCammon, C., Vennemann, T. & Markl, G. 2007: Arrested kinetic Li isotope fractionation at the margin of the Ilímaussaq complex, South Greenland: evidence for open-system processes during final cooling of peralkaline igneous rocks. Chemical Geology **246**, 207–230.

Martin, A.R. 1985: The evolution of the Tugtutôq–Ilímaussaq dyke swarm, southwest Greenland. Unpublished PhD thesis, University of Edinburgh, UK.

Martin, R.F. 2006: A-type granites of crustal origin ultimately result from open-system fenitization-type reactions in an extensional environment. Lithos **91**, 125–136.

Meade, F.C., Chew, D.M., Troll, V.R., Ellam, R.M. & Page, L.M. 2009: Magma ascent along a major terrane boundary: crustal contamination and magma mixing at the Drumadoon intrusive complex, Isle of Arran, Scotland. Journal of Petrology **50**, 2345–2374.

Mingard, S.C. 1990: Crystallisation processes in giant dykes of the Tugtutoq rift, South Greenland. Unpublished PhD thesis, University of Edinburgh, UK.

Mitchell, J.N., Scoates, J.S. & Frost, C.D. 1995: High-Al gabbros in the Laramie anorthosite complex, Wyoming: implications for the composition of melts parental to Proterozoic anorthosite. Contributions to Mineralogy and Petrology **119**, 166–180.

Morse, S.A. 1973: The plagioclase/magma density paradox re-examined and the crystallisation of Proterozoic anorthosites. In: Morse, S.A. (ed.): The Nain Anorthosite Project, Labrador Field Report 1972, 113–116. Amherst MA: University of Massachusetts at Amherst,.

Morse, S.A. 1982: A partisan review of Proterozoic anorthosites. American Mineralogist **67**, 1087–1100.

Morse, S.A. 2006: Labrador massif anorthosites: chasing the liquids and their sources. Lithos **89**, 202–221.

Nicholson, S.W. & Shirey, S.B. 1990: Midcontinent rift volcanism in the Lake Superior region: Sr, Nd and Pb isotopic evidence for a mantle plume origin. Journal of Geophysical Research **95**, 10851–10868.

Nielsen, B.K & Steenfelt, A. 1979: Intrusive events at Kvanefeld in the Ilímaussaq igneous complex. Bulletin of the Geological Society of Denmark **27**, 143–155.

Ocola, L.C. & Meyer, R.P. 1973: Central North American Rift System l. Structure of the axial zone from seismic and gravimetric data. Journal of Geophysical Research **78**, 5173–5194.

Olsen, D. 1977: Geological mapping in the Narssaq intrusion, South Greenland. Rapport Grønlands Geologiske Undersøgelse **85**, 73 only.

Olsen, D. 1982: Struktur, mineralogi og geokemi i den nordlige del

af Narssaq intrusionen, Sydgrønland. Unpublished Master's thesis, Københavns Universitet, Danmark.

Osborn, E.F. & Tait, D.B. 1952: The system diopside-forsterite-anorthite. American Journal of Science, Bowen vol., 413–433.

Parsons, I. 1972: Petrology of the Puklen syenite-alkali granite complex, Nunarssuit, South Greenland. Meddelelser om Grønland **195**, 73 pp.

Parsons, I. 1979: The Klokken gabbro-syenite complex, South Greenland: cryptic variation and origin of inversely graded layering. Journal of Petrology **20**, 653–694.

Parsons, I. 2012: Full-stop for Mother Earth. Parting shots. Elements **8**(5), 396–398.

Parsons, I. & Becker, S.M. 1986: High-temperature fluid-rock interactions in a layered syenite pluton. Nature **321**(6072), 764–769.

Parsons, I. & Brown, W.L. 1988: Sidewall crystallisation in the Klokken intrusion: zoned ternary feldspars and coexisting minerals. Contributions to Mineralogy and Petrology **98**, 431–443.

Parsons, I., Rex, D.C., Guise, P. & Halliday, A.N. 1988: Argon-loss by alkali feldspars. Geochimica et Cosmochimica Acta **52**, 1097–1112.

Paslick, C.R., Halliday, A.N., Davies, G.R., Mezger, K. & Upton, B.G.J. 1993: Timing of Proterozoic magmatism in the Gardar Province, southern Greenland. Geological Society of America Bulletin **105**, 272–278.

Patchett, P.J., Hutchison, J., Blaxland, A.B. & Upton, B.G. J. 1976: Origin of anorthosites, gabbros and potassic ultramafic rocks from the Gardar Province, South Greenland: Sr isotopic ratio studies. Bulletin of the Geological. Society of Denmark **25**, 79–84.

Patchett, P.J., Bylund, G. & Upton, B.G.J. 1978: Palaeomagnetism and the Grenville orogeny: new Rb-Sr ages for dolerites in Canada and Greenland. Earth and Planetary Science Letters **40**, 349–364.

Pearce, N.J.G. 1988: The petrology and geochemistry of the Igaliko dyke swarm, South Greenland. Unpublished PhD thesis, University of Durham, UK.

Pearce. N.J.G. & Leng, M.J. 1996: The origin of carbonatites and related rocks from the Igaliko Dyke Swarm, Gardar Province, South Greenland: field, geochemical and C-O-Sr-Nd isotope evidence. Lithos **39**, 21–40.

Petersilie, I.A. & Sørensen, H. 1970: Hydrocarbon gases and bituminous substances in rocks from the alkaline Ilímaussaq intrusion, South Greenland. Lithos **3**, 59–76.

Pfaff, K., Krumrei, T., Marks, M., Wenzel, T., Rudolf, T. & Markl, G. 2008: Chemical and physical evolution of the 'lower layered sequence' from the nepheline syenitic Ilímaussaq intrusion, South Greenland: implications for the origin of magmatic layering in peralkaline felsic liquids. Lithos **106**, 280–296.

Piper, J.D.A. 1976: Palaeomagnetism of the giant dykes of Tugtutoq and Narssaq gabbro, Gardar Igneous Province, South Greenland. Bulletin of the Geological Society of Denmark **26**, 85–94.

Piper, J.D.A. 1992: The palaeomagnetism of major (Middle Proterozoic) igneous complexes. South Greenland and the Gardar apparent polar wander track. Precambrian Research **54**, 153–172.

Piper, J.D.A. 1995: The palaeomagnetism of middle Proterozoic dyke swarms of the Gardar Province and Mesozoic dykes in Greenland. Geophysical Journal International **120**, 339–355.

Poulsen, V. 1964: The sandstones of the PreCambrian Eriksfjord Formation in South Greenland. Rapport Grønlands Geologiske Undersøgelse **2**, 16 pp.

Powell, M. 1978: Crystallisation history of Igdlerfigssalik nepheline syenite intrusion, Greenland. Lithos **11**, 99–120.

Pulvertaft, T.C.R. 1961: The Puklen intrusion, Nunarssuit, SW Greenland. Meddelelser om Grønland **123**(6), 50 pp.

Pulvertaft, T.C.R. 1965: The Eqaloqarfia layered dyke, Nunarssuit, South Greenland. Bulletin Grønlands Geologiske Undersøgelse **55**, 39 pp. (also Meddelelser om Grønland **169**(10).

Pulvertaft, T.C.R. 1967: Geological map of Greenland, 1:100 000, Nunarssuit 60 V.1 Nord. Copenhagen: Geological Survey of Greenland.

Ramberg, I.B. 1972: Crustal structure across the Permian Oslo Graben from gravity measurements. Nature Physical Science **240**, 149–153.

Ratschbacher, B., Marks, M., Pfaff, K. & Markl, G. 2011: Mineral compositions indicate recharge processes in the Ilímaussaq complex, Greenland. Abstract. Peralkaline & Carbonatite Workshop, Tübingen, June 2011.

Ridolfi, F., Upton, B.G.J. & Renzulli, A. 2006a: Mineralogy of quartz syenites from the Tugtutoq Central Complex (Gardar Province, southern Greenland): unravelling late-magmatic vs. metasomatic processes. GAC-MAC Montreal, Canada, 15–17 May 2006.

Ridolfi, F., Renzulli, A., Macdonald, R. & Upton, B.G.J. 2006b: Peralkaline syenite autoliths from Kilombe volcano, Kenya Rift Valley; evidence for subvolcanic interaction with carbonatitic fluids. Lithos **91**, 373–392.

Rock, N.M.S. 1986: The nature and origin of ultramafic lamprophyre, alnöite and related rocks. Journal of Petrology **27**, 155–196.

Rock, N.M.S. 1991: Lamprophyres, 285 pp. Glasgow: Blackie and Son.

Rock, N.M.S., 1997: The nature and origin of lamprophyres. In: Fitton, J.G. & Upton, B.G.J. (eds): Alkaline igneous rocks. Geological Society Special Publication (London) **30**, 191–226.

Rogers, J.W. & Santosh, M. 2002: Configuration of Columbia, a Mesoproterozoic supercontinent. Gondwana Research **5**, 5–22.

Rønsbo, J.G. 2008: Apatite in the Ilímaussaq alkaline complex: occurrence, zonation and compositional variation. Lithos **106**, 71–82.

Rønsbo, J.G., Khomyakov, A.P., Semenov, E.I., Vorokov, A.A. & Garanin, V.K. 1979: Vitusite – a new phosphate of sodium and rare earths from the Lovozero alkaline massif, Kola, and the Ilímaussaq alkaline intrusion, South Greenland. Neues Jarhbuch für Mineralogie Abhandlungen **137**, 42–53.

Rose-Hansen, J. & Sørensen, H. 2001: Minor intrusions of peralkaline microsyenites in the Ilímaussaq alkaline complex, South Greenland. Bulletin of the Geological Society of Denmark **48**, 9–12.

Rose-Hansen, J. & Sørensen, H. 2002: Geology of lujavrites from the Ilímaussaq alkaline complex, South Greenland with information from seven boreholes. Meddelelser om Grønland Geoscience **40**, 58 pp.

Salmon, H. 2013: The Mineralogy and Petrology of Satellitic Intrusions within the Igaliku Complex, South Greenland, 300 pp. Unpublished PhD thesis, Birkbeck, University of London, UK.

Sass, J.H., Nielsen, B.L., Wollanberg, H.A. & Monroe, R.J. 1972: Heat flow and surface radioactivity at two sites in southern Greenland. Journal of Geophysical Research **77**, 6435–6444.

Scoates, J.S. 2000: The plagioclase-magma density paradox re-examined and the crystallisation of Proterozoic anorthosites. Journal of Petrology **41**, 627–649.

Simpson, E.S.W. & Otto, J.D.T. 1960: On the Pre-Cambrian anorthosite mass of southern Angola. Report of the International Geological Congress, 21st session, Norden, pt. **8**, 216–217.

Sørensen, H. 1958: The Ilímaussaq batholith. A review and discussion. Bulletin Grønlands Geologiske Undersøgelse **19**, 48 pp. (also Meddelelser om Grønland **162**(3)).

Sørensen, H. 1960: On the agpaitic rocks. Report of the International Geological Congress, XXl Session, Norden, part **13** (also Grønlands Geologiske Undersøgelse Miscellaneous Papers **29**, 319–327).

Sørensen, H. 1967: On the history of exploration of the Ilímaussaq alkaline intrusion, South Greenland. Meddelelser om Grønland **181**(3), 32 pp.

Sørensen, H. 1969: Rhythmic igneous layering in peralkaline intrusions; an essay review on Ilimaussaq and Lovozero. Lithos **2**, 261–283.

Sørensen, H. 1978: The position of the augite syenite and pulaskite in the Ilímaussaq intrusion, South Greenland. Bulletin of the Geological Society of Denmark **27**, 15–23.

Sørensen, H. 1997: The agpaitic rocks – an overview. Mineralogical Magazine **61**, 485–498.

Sørensen, H. 2001: Brief introduction to the geology of Ilímaussaq alkaline complex, South Greenland and its exploration history.Geology of Greenland Survey Bulletin **190**, 7–24.

Sørensen, H. 2006: The Ilímaussaq alkaline complex, South Greenland – an overview of 200 years of research and an outlook. Meddelelser om Grønland Geoscience **45**, 70 pp.

Sørensen, H. & Larsen, L.M. 1987: Layering in the Ilímaussaq alkaline intrusion, South Greenland. In: Parsons, I (ed.): Origins of igneous layering, 1–28. Dordrecht: D. Reidel.

Sørensen, H. & Larsen, L.M. 2001: The hyper-agpaitic stage in the evolution of the Ilímaussaq alkaline complex, South Greenland. Geology of Greenland Survey Bulletin **190**, 83–94.

Sørensen, H., Hansen, J. & Bondam, J. 1969: Preliminary account of the geology of the Kvanefjeld area of the Ilímaussaq intrusion, South Greenland. Rapport Grønlands Geologiske Undersøgelse **18**, 1–40.

Sørensen, H., Rose-Hansen, J., Nielsen, B.K.L., Løvberg, L., Sørensen, E. & Lundgaard, T. 1974: The uranium deposit at Kvanefjeld, the Ilímaussaq intrusion, South Greenland. Geology reserves and beneficiation. Rapport Grønlands Geologiske Undersøgelse **60**, 54 pp.

Sørensen, H., Bailey, J.C., Kogarko, L.N., Rose-Hansen, J. & Karup Møller, S. 2003: Spheroidal structures in arfvedsonite lujavrite, Ilímaussaq alkaline complex, South Greenland – an example of macro-scale liquid immiscibility. Lithos **70**, 1–20.

Sørensen, H., Bohse, H. & Bailey, J.C. 2006: The origin and mode of emplacement of lujavrites in the Ilímaussaq alkaline complex, South Greenland. Lithos **91**, 286–300.

Sørensen, H., Bailey, J.C. & Rose-Hansen, J. 2011: The emplacement and crystallisation of the U-Th-REE-rich agpaitic and hyperagpaitic lujavrites at Kvanefjeld, Ilímaussaq alkaline complex, South Greenland. Bulletin of the Geological Society of Denmark **3**, 10–28.

Steenfelt, A. 1981: Field relations in the roof zone of the Ilímaussaq intrusion with special reference to the position of the alkali acid rocks. In: Bailey, J.C..Larsen, L.M. & Sørensen, H. (eds): The Ilímaussaq intrusion, South Greenland. A progress report on geology, mineralogy, geochemistry and economic geology. Rapport Grønlands Geologiske Undersøgelse **103**, 43–52.

Steenfelt, A. & Bohse, H. 1975: Variations in the content of uranium in eudialyte from the differentiated alkaline Ilímaussaq intrusion, South Greenland. Lithos **8**, 39–45.

Steenstrup, K.J.V. 1910: Geologiske og antikvariske Iagttagelser i Julianehaabs Distrikt. Meddelelser om Grønland **34**, 115–154.

Steenstrup, K.J.V. & Kornerup, A. 1881: Beretning om Expeditionen til Julianehaabs Distrikt, 1874. Meddelelser om Grønland **2**, 1–26.

Steiger, R.H. & Jäger, E. 1977. Subcommission on geochronology: convention on the use of decay constants in geo- and cosmochronology. Earth and Planetary Science Letters **36**, 359–362.

Stephenson, D. 1972: Alkali pyroxenes from nepheline syenites of the South Qôroq Centre, South Greenland. Lithos **5**, 187–201.

Stephenson, D. 1974: Mn and Ca enriched olivines from nepheline syenites of the South Qôroq Centre, South Greenland. Lithos **7**, 35–41.

Stephenson, D.1976a: The South Qôroq Centre nepheline syenites, South Greenland. Bulletin Grønlands Geologiske Undersøgelse **118**. 55 pp.

Stephenson, D.1976b: A simple-shear model for the ductile deformation of high-level intrusions in South Greenland. Journal of the Geological Society (London) **132**, 307–318.

Stephenson, D. & Upton, B.G.J. 1982: Ferromagnesian silicates in a differentiated alkaline complex: Kûngnât Fjeld, South Greenland. Mineralogical Magazine **46**, 283–300.

Stevenson, R., Upton, B.G.J. & Steenfelt, A. 1997: Crust-mantle interaction in the evolution of the Ilímaussaq Complex, South Greenland: Nd isotopic studies. Lithos **40**, 189–202.

Stewart, J.W. 1964: The earlier Gardar igneous rocks of the Ilímaussaq area, South Greenland. Unpublished PhD thesis, University of Durham, UK.

Stewart, J.W. 1970: Precambrian alkaline ultramafic-carbonatite volcanism at Qagssiarssuk, South Greenland. Bulletin Grønlands Geologiske Undersøgelse **84**, 70 pp. (also Meddelelser om Grønland **186**(4).

Tappe, S., Foley, S.F., Jenner, G.A. & Kjarsgaard, B.A. 2005: Integrating ultramafic lamprophyres into the USGS classification of igneous rocks: rationale and implications. Journal of Petrology **46**, 1893–1900.

Taylor, H.P. & Forrester, R.W. 1979: An oxygen and hydrogen isotope study of the Skaergaard Intrusion and its country rocks: a description of a 55-m.y. old fossil hydrothermal system. Journal of Petrology **20**, 355–419.

Taylor, P.N. & Upton, B.G.J. 1993: Contrasting Pb isotopic compositions in two intrusive complexes of the Gardar magmatic province of South Greenland. Chemical Geology Isotope Geoscience **104**,

261–268.

Upton, B.G.J. 1960: The alkaline igneous complex of Kûngnât Fjeld, South Greenland. Meddelelser om Grønland **123**(4), 145 pp.

Upton, B.G.J. 1961: Textural features of some contrasted cumulates from South Greenland. Meddelelser om Grønland **123**(6), 29 pp.

Upton, B.G.J. 1962: The geology of Tugtutôq and neighbouring islands, South Greenland. Part 1. Meddelelser om Grønland **169**(8) 1–59.

Upton, B.G.J. 1964a: The geology of Tugtutôq and neighbouring islands, South Greenland. Part II. Nordmarkitic syenites and related rocks. Meddelelser om Grønland **169**(2), 1–62.

Upton, B.G.J. 1964b: The geology of Tugtutôq and neighbouring islands, South Greenland. Part III. Olivine gabbros, syeno-gabbros and anorthosites. Meddelelser om Grønland **169**(2), 1–45.

Upton, B.G.J. 1964c: The geology of Tugtutôq and neighbouring islands, South Greenland. Part IV. The nepheline syenite of the Hviddal composite dyke. Meddelelser om Grønland **169**(2), 49–80.

Upton, B.G.J. 1966: Ultrabasic intrusives from Narssaq and Tugtutôq. Rapport Grønlands Geologiske Undersøgelse **11**, 41–44.

Upton, B.G.J. 1969: Basic rocks of the Gardar igneous province. Rapport Grønlands Geologiske Undersøgelse **28,** 27–29.

Upton, B.G.J. 1971: Melting experiments on chilled gabbros and syenogabbros. Carnegie Institute of Washington Yearbook **70**, 112–118.

Upton, B.G.J. 1974: The alkaline province of South-West Greenland. In: Sørensen, H. (ed.): The alkaline rocks, 221–238. Interscience.

Upton, B.G.J. 1987: Gabbroic, syenogabbroic and syenitic cumulates of the Tugtutôq Younger Giant Dyke Complex, South Greenland. In: Parsons, I. (ed.): Origins of igneous layering, 93–123. Dordrecht: D. Reidel.

Upton, B.G.J. 1991: Gardar-age mantle xenoliths: Igdlutalik, S. Greenland. Rapport Grønlands Geologiske Undersøgelse **150**, 37–43.

Upton, B.G.J. 1996: Anorthosites and troctolites of the Gardar magmatic province. In: Demaiffe, D. (ed.): Petrology and Geochemistry of Magmatic suites of rocks in the continental and oceanic crusts, 19–34. A volume dedicated to Professor Jean Michot. Université Libre de Bruxelles, Royal Museum for Central Africa (Tevuren).

Upton, B.G.J. & Blundell, D.J. 1978: The Gardar Igneous Province: evidence for Proterozoic continental .rifting. In: Neumann, E.R. & Ramberg, I.B. (eds): Petrology and geochemistry of continental rifts, 163–172. Dordrecht: Reidel.

Upton, B.G.J. & Emeleus, C.H. 1987: Mid-Proterozoic alkaline magmatism in southern Greenland. In: Fitton, J.G. & Upton, B.G.J. (eds): Alkaline igneous rocks', 449–471. Oxford: Blackwell Scientific Publications.

Upton, B.G.J. & Fitton, J.G. 1985: Gardar dykes north of the Igaliko Syenite Complex, southern Greenland. Rapport Grønlands Geologiske Undersøgelse **127**, 24 pp.

Upton, B.G.J. & Thomas, J.E. 1973: Precambrian potassic ultramafic rocks in South Greenland. Journal of Petrology **14**, 509–534.

Upton, B.G.J. & Yoder, H.S. 1971: Melting experiments on chiled gabbros and syenogabbros. Yearbook of the Carnegie Institution of Washington **70**, 112–118.

Upton, B.G.J. & Thomas, J.E. 1980: The Tugtutôq Younger Giant Dyke Complex, South Greenland: fractional crystallisation of a transitional olivine basalt magma. Journal of Petrology **21**, 167–198.

Upton, B.G.J., Macdonald, R., Hill, P.G., Jeffries, B. & Ford, C.E. 1976: Narsarsukite, a new occurrence in peralkaline trachyte, South Greenland. Mineralogical Magazine **40**, 737–746.

Upton, B.G.J., Hill, P.G., Jonsen. O. & Petersen, O.V. 1978: Emeleusite: a new LiNaFe111 silicate from South Greenland. Mineralogical Magazine **42**, 31–34.

Upton, B.G.J., Stephenson, D. & Martin, A.R. 1985: The Tugtutôq Older Giant Dyke Complex: mineralogy and geochemistry of an alkali-gabbro-augite-syenite-foyaite association in the Gardar Province of South Greenland. Mineralogical Magazine **49**, 623–642.

Upton, B.G.J., Martin, A.R. & Stephenson, D. 1990: Evolution of the Tugtutôq Central Complex, South Greenland: a high-level, rift-axial, late Gardar centre. Journal of Volcanology and Geothermal Research **43**, 195–214.

Upton, B.G.J., Parsons, I., Emeleus, C.H. & Hodson, M.E. 1996: Layered alkaline igneous rocks of the Gardar Province, South Greenland. In: Cawthorn, C.G. (ed.): Layered intrusions, 331–363. Elsevier Science B.V.

Upton, B.G.J., Emeleus, C.H., Heaman, L.M., Goodenough, K.M. & Finch, A. 2003: Magmatism of the mid-Proterozoic Gardar Province, South Greenland: chronology, petrogenesis and geological setting. Lithos **68**, 43–65.

Upton, B.G.J., Craven, J.A. & Kirstein, L.A. 2006: Crystallisation of mela-aillikites of the Narsaq region, Gardar alkaline province, South Greenland and relationships to other aillikitic-carbonatitic associations in the province. Lithos **92**, 300–319.

Upton, B.G.J., Macdonald, R., Odling, N., Rämö T. & Bagiński, B. 2013: Kûngnât revisited. A review of five decades research into an alkaline complex in South Greenland, with new trace element analyses and Nd isotopic data. Mineralogical Magazine **77**, 523–550.

Ussing, N.V. 1912: Geology of the country around Julianehaab, Greenland. Meddelelser om Grønland **38**, V–XI and 1–376.

Wager, L.R. & Brown, G.M. 1968: Layered igneous rocks, 588 pp. Edinburgh: Oliver & Boyd Ltd.

Wager, L.R. & Deer, 1939: Geological investigations in East Greenland. Part III. The Petrology of the Skaergaard Intrusion, Kangerdlugssuak. Meddelelser om Grønland **105**(4), 352 pp.

Wager, L.R., Brown, G.M. & Wadsworth, W.J. 1960: Types of igneous cumulates. Journal of Petrology **1**, 73–85.

Waight, T., Baker, J. & Willigers, B. 2002: Rb isotope dilution analyses by MC-ICPMS using Zr to correct for mass fractionation: towards improved Rb-Sr geochronology? Chemical Geology **186**, 99–116.

Walker, G.P.L. 1993: Basaltic-volcano systems. In: Prichard, H.M. *et al.* (eds): Magmatic processes and plate tectonics. Geological Society Special Publication (London) **76**, 7–38.

Walton, B.J. 1965: Sanerutian appinitic rocks and Gardar dykes and diatremes north of Narssarssuaq, South Greenland. Bulletin Grønlands Geologiske Undersøgelse **57**, 66 pp. (also Meddelelser om Grønland **179**).

Watt, W.S. 1966: Chemical analyses from the Gardar Igneous Province, South Greenland. Rapport Grønlands Gelogiske Under-

søgelse **6**, 92 pp.

Watt, W.S. 1968: Petrology and geology of the Precambrian Gardar dykes on Qaersuarsuk, South Greenland. Rapport Grønlands Geologiske Undersøgelse **14,** 51 pp.

Wegman, C.E. 1938: Geological investigations in southern Greenland. Part 1. On the structural divisions of southern Greenland. Meddelelser om Grønland **113**, 148 pp.

Wiebe, R.A. 1992: Proterozoic anorthosite complexes. In: Condie, K.C. (ed.): Proterozoic crustal evolution, 215–261. Amsterdam: Elsevier.

Winther, K.T. 1992: Feldspar megacryst and anorthosite xenolith-bearing dykes in the Narssarssuaq area, South Greenland. Rapport Grønlands Geologiske Undersøgelse **154**, 49–59.

Woolley, A.R. 1987: Lithosphere metasomatism and the petrogenesis of alkaline igneous rocks and carbonatites, Malawi. Journal of African Earth Science **6**, 891–898.

Yoder, H.S. & Tilley, C.E. 1962: Origin of basalt magma: an experimental study of natural and synthetic rock systems. Journal of Petrology **3**, 342–532.

The series *Geological Survey of Denmark and Greenland Bulletin* started in 2003 and replaced the two former bulletin series of the Survey, viz. *Geology of Greenland Survey Bulletin* and *Geology of Denmark Survey Bulletin*. Some of the twenty-one volumes published since 1997 in those two series are listed on the facing page. The present series, together with *Geological Survey of Denmark and Greenland Map Series*, now form the peer-reviewed scientific series of the Survey.

Geological Survey of Denmark and Greenland Bulletin

26	Review of Survey activities 2011, 88 pp. (21 articles), 2012. *Edited by* O. Bennike, A.A. Garde & W.S. Watt.	200.00
27	Neoglacial and historical glacier changes around Kangersuneq fjord in southern West Greenland, 68 pp., 2012. *By* A. Weidick, O. Bennike, M. Citterio & N. Nørgaard-Pedersen.	200.00
28	Review of Survey activities 2012, 76 pp. (17 articles), 2013. *Edited by* O. Bennike, A.A. Garde & W.S. Watt.	200.00
29	Tectono-magmatic evolution of the younger Gardar southern rift, South Greenland, 124 pp., 2013. *By* B.G.J. Upton.	240.00

Geological Survey of Denmark and Greenland Map Series

1	Explanatory notes to the Geological map of Greenland, 1:500 000, Humboldt Gletscher, Sheet 6, 48 pp. + map, 2004. *By* P.R. Dawes.	280.00
2	Explanatory notes to the Geological map of Greenland, 1:500 000, Thule, Sheet 5 (1991), 97 pp. + map, 2006. *By* P.R. Dawes.	300.00
3	Explanatory notes to the Geological map of Greenland, 1:100 000, Ussuit 67 V.2 Nord, 40 pp. + map, 2007. *By* J.A.M. van Gool & M. Marker.	280.00
4	Descriptive text to the Geological map of Greenland, 1:500 000, Dove Bugt, Sheet 10, 32 pp. + map, 2009. *By* N. Henriksen & A.K. Higgins.	240.00
5	Descriptive text to the Geological map of Greenland, 1:100 000, Kangaatsiaq 68 V.1 Syd and Ikamiut 68 V.1 Nord, 41 pp. + 2 maps, 2010. *By* A.A. Garde & J.A. Hollis.	280.00

Geology of Greenland Survey Bulletin (173–191; discontinued)

181	Precambrian geology of the Disko Bugt region, West Greenland, 179 pp. (15 articles), 1999. *Edited by* F. Kalsbeek.	240.00
182	Vertebrate remains from Upper Silurian – Lower Devonian beds of Hall Land, North Greenland, 80 pp., 1999. *By* H. Blom.	120.00
183	Review of Greenland activities 1998, 81 pp. (10 articles), 1999. *Edited by* A.K. Higgins & W.S. Watt.	200.00
184	Collected research papers: palaeontology, geochronology, geochemistry, 62 pp. (6 articles), 1999.	150.00
185	Greenland from Archaean to Quaternary. Descriptive text to the Geological map of Greenland, 1:2 500 000, 93 pp., 2000. *By* N. Henriksen, A.K. Higgins, F. Kalsbeek & T.C.R. Pulvertaft.	225.00
186	Review of Greenland activities 1999, 105 pp. (13 articles), 2000. *Edited by* P.R. Dawes & A.K. Higgins.	225.00
187	Palynology and deposition in the Wandel Sea Basin, eastern North Greenland, 101 pp. (6 articles), 2000. *Edited by* L. Stemmerik.	160.00
188	The structure of the Cretaceous–Palaeogene sedimentary-volcanic area of Svartenhuk Halvø, central West Greenland, 40 pp., 2000. *By* J. Gutzon Larsen & T.C.R. Pulvertaft.	130.00
189	Review of Greenland activities 2000, 131 pp. (17 articles), 2001. *Edited by* A.K. Higgins & K. Secher.	160.00
190	The Ilímaussaq alkaline complex, South Greenland: status of mineralogical research with new results, 167 pp. (19 articles), 2001. *Edited by* H. Sørensen.	160.00
191	Review of Greenland activities 2001, 161 pp. (20 articles), 2002. *Edited by* A.K. Higgins, K. Secher & M. Sønderholm.	200.00

Geology of Denmark Survey Bulletin (36–37; discontinued)

| 36 | Petroleum potential and depositional environments of Middle Jurassic coals and non-marine deposits, Danish Central Graben, with special reference to the Søgne Basin, 78 pp., 1998. *By* H.I. Petersen, J. Andsbjerg, J.A. Bojesen-Koefoed, H.P. Nytoft & P. Rosenberg. | 250.00 |
| 37 | The Selandian (Paleocene) mollusc fauna from Copenhagen, Denmark: the Poul Harder 1920 collection, 85 pp., 2001. *By* K.I. Schnetler. | 150.00 |

Prices are in Danish kroner exclusive of local taxes, postage and handling

Note that information on the publications of the former Geological Survey of Denmark and the former Geological Survey of Greenland (amalgamated in 1995 to form the present Geological Survey of Denmark and Greenland) can be found on *www.geus.dk*